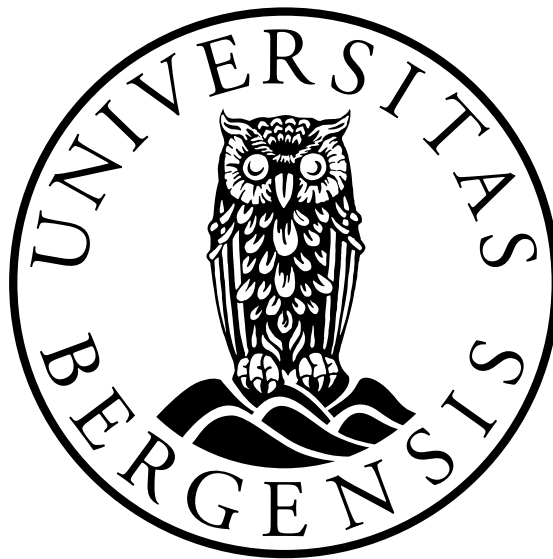


# General Slit Stochastic Löwner Evolution and Conformal Field Theory

Alexey Tochin



Dissertation for the degree of Philosophiae Doctor (PhD)

Department of Mathematics  
University of Bergen

September 2015



# Acknowledgements

I would like to express my sincere gratitude to all those who helped me on the way to this thesis. During my journey I was lucky to have an excellent guidance and noteworthy support.

First of all I am especially grateful to my supervisor, **Alexander Vasil'ev**. My study mathematics at the University of Bergen would not possible without him. I also thank Alexander for all generous help and support I received. He was always ready to read my early drafts with a bunch of misprints and technical mistakes.

The second important person is my co-author, **Georgy Ivanov**, with whom we had numerous of lively discussions. Let me also mark the contribution from **Bruno Carneiro da Cunha** and **Tiago Anselmo**, and valuable discussions with them during my stay in Brazil.

A special thanks goes to my colleagues and friends, who read the text in the final stage and corrected numerous of grammar and language mistakes. This hard work was done by **Anastasia Frolova**, **Valentin Krasontovitsch**, **Daulet Moldabayev**, and again **Alexander Vasil'ev**.

I also want to thank various people at the Mathematical Institute, including **Irina Markina**, **Bjørn Ian Dundas**, **Henrik Kalisch**, **Mauricio Godoy Molina**, **Erlend Grong**, **Christian Autenried**, **Mirjam Solberg**, **Sergey Alyaev**, **Viktor Kiselev**, **Anna Varzina**, **Anna Kvashchuk**, **Lina Astrakova**, and many others.



# Contents

<b>Acknowledgements</b>	<b>i</b>
<b>Introduction</b>	<b>1</b>
<b>1 Slit Löwner equation and its stochastic version</b>	<b>3</b>
1.1 Preliminaries . . . . .	4
1.2 $(\delta, \sigma)$ -Löwner chain (slit holomorphic Löwner chain) . . . . .	9
1.2.1 Definition and basic properties . . . . .	9
1.2.2 General properties of $(\delta, \sigma)$ -Löwner chain . . . . .	13
1.2.3 Equivalence and normalization of $(\delta, \sigma)$ -Löwner chains . . . . .	19
1.3 Slit holomorphic stochastic flow or $(\delta, \sigma)$ -SLE . . . . .	24
1.3.1 Definition and basic properties . . . . .	24
1.3.2 Equivalence and normalization of $(\delta, \sigma)$ -SLE . . . . .	28
1.3.3 Relations between essentially different $(\delta, \sigma)$ -SLEs . . . . .	29
1.3.4 Domain Markov property and conformal invariance of random laws on planar curves . . . . .	33
<b>2 Numerical Simulation</b>	<b>37</b>
2.1 Approximation of $(\delta, \sigma)$ -Löwner chain . . . . .	37
2.1.1 The zipper method . . . . .	37
2.1.2 Choice of the step map $\tilde{G}_n$ . . . . .	39
2.1.3 Choice of the partition . . . . .	41
2.2 Simulation of $(\delta, \sigma)$ -SLE . . . . .	42
2.3 Simulation of $(\delta, \sigma)$ -Löwner equation driven by a stable Levy process . . . . .	45
2.3.1 Stable Levy process . . . . .	48
2.3.2 Simulation method for Levy process . . . . .	50
<b>3 <math>(\delta, \sigma)</math>-Löwner equation from the algebraic point of view</b>	<b>53</b>
3.1 Algebraic classification and normalization . . . . .	53
3.2 $(\delta, \sigma)$ -Löwner equation and representation theory . . . . .	55
<b>4 Gaussian Free Field or probabilistic approach to Euclidean Conformal Field Theory</b>	<b>63</b>
Introduction . . . . .	63
4.1 Test functions . . . . .	64
4.2 Pre-pre-Schwarzian . . . . .	66
4.3 Linear functionals and change of coordinates . . . . .	68

4.4	Fundamental solution to the Laplace-Beltrami equation . . . . .	70
4.5	Gaussian free field . . . . .	73
4.6	The Schwinger functionals . . . . .	75
4.7	Gaussian Hilbert space . . . . .	77
4.8	Stress tensor and the conformal Ward identity . . . . .	79
4.9	Vertex operators . . . . .	84
<b>5</b>	<b>Coupling of <math>(\delta, \sigma)</math>-SLE and the GFF</b>	<b>87</b>
5.1	Some technical propositions . . . . .	90
5.2	Coupling between SLE and GFF . . . . .	95
5.3	Coupling in the case of the Dirichlet and Neumann boundary conditions	103
5.4	Alternative definition of $G_t^{-1} * \eta[f]$ . . . . .	107
<b>6</b>	<b>Important spacial cases</b>	<b>111</b>
6.1	Chordal case . . . . .	111
6.1.1	Chordal Löwner equation . . . . .	111
6.1.2	Coupling of forward chordal SLE and Dirichlet GFF . . . . .	114
6.1.3	Coupling of reverse chordal SLE and Neumann GFF . . . . .	114
6.2	Dipolar Case . . . . .	115
6.2.1	Dipolar Löwner equation . . . . .	115
6.2.2	Coupling of forward dipolar SLE and Dirichlet GFF . . . . .	118
6.2.3	Coupling of reverse dipolar SLE and Neumann GFF . . . . .	119
6.2.4	Coupling of forward dipolar SLE and combined Dirichlet- Neumann GFF . . . . .	119
6.3	Radial Case . . . . .	121
6.3.1	Radial Löwner equation . . . . .	121
6.3.2	Coupling of forward radial SLE and Dirichlet GFF . . . . .	124
6.3.3	Coupling of reverse radial SLE and Neumann GFF . . . . .	125
6.3.4	Coupling with twisted GFF . . . . .	126
6.4	Chordal case with a fix time change . . . . .	128
6.5	The case with one fixed point . . . . .	130
6.6	Degenerate case . . . . .	132
<b>A</b>	<b>Some relations from stochastic calculus</b>	<b>135</b>

# Introduction

The thesis is presented in the style of a monograph and is dedicated to a generalization of the Löwner equation in its stochastic form known as the Schramm-Löwner equation, and to its coupling with the Gaussian free field, ultimately aiming at the construction of a boundary conformal field theory with one free scalar<sup>1</sup> bosonic field. This study is presented in line with a systematic, and hopefully concise, presentation and generalization of known elements of the theory of Löwner evolution. This topic is closely related with lattice models of statistical physics in their scaling limit. However, we deal only with continuous models, focusing in particular, on domain Markov properties, on the Gaussian free field, etc. Numerical simulations are given in Chapter 2.

The main results are in the proof of the basic properties of  $(\delta, \sigma)$ -SLE and general necessary and sufficient conditions for the coupling. We also introduce a machinery that possesses to consider all Löwner equations and known types of the coupling as different manifestations of the same thing.

The thesis is split into six chapters each of which contains a short introductory part providing general ideas and a list of main results. Chapter 1 (deterministic and stochastic Löwner equation) and Chapter 4 (Gaussian free field and conformal field theory) are self-contained and can be studied independently. The coupling with the Gaussian free field/CFT is considered in Chapter 5, where the results collected in Chapters 1 and 4 merge together. Another aspect of the same connection to conformal field theory related to the representation of the Virasoro algebra is discussed in Chapter 3. Important special cases of the general slit stochastic Löwner evolution and its possible couplings with CFT are collected in Chapter 6.

---

<sup>1</sup>pre-precise, to be more precise, see Section 4.2.





# Chapter 1

## Slit Löwner equation and its stochastic version

This chapter mostly repeats [ITV14]. Here, we use a different manner, in particular, we focus on working in generic domain rather than the unit disk. We also present some additional results such as Theorem 1.3 and discuss the **domain Markov property** in details.

The Löwner theory was introduced in 1923 by Karl Löwner (Charles Loewner) [Loe], and was later developed by Kufarev [Kuf43] and Pommerenke [Pom75]. The Löwner differential equation became one of the most powerful tools for solving extremal problems in the theory of univalent function. In the modern period, Löwner theory has again attracted a lot of interest due to the discovery of the Stochastic (Schramm)-Löwner Evolution (SLE), a stochastic process that has made it possible to describe analytically scaling limits of several 2-dimensional lattice models in statistical physics, see [LSW01a] and [Sch00]. SLE theory focuses on describing probability measures on families of curves which possess the property of **conformal invariance** and the **domain Markov property**. The second property, in its turn, is related to the diffusion form of SLE. So far, the following types of SLE have been studied: the **chordal** SLE [LSW01a, RS05, Sch00], the **dipolar** SLE [BBH04], the **radial** SLE [Law08, LSW01a],  $SLE(\kappa, \rho)$  [Dub05], and multiple SLE [Dub07].

In this thesis we address the following questions. What are other possible diffusion equations with holomorphic coefficients that generate random families of curves? How similar are the properties of these families of curves to the properties of known SLE curves?

We start by introducing notations and basic concepts. In the second section, we introduce  $(\delta, \sigma)$ -**Löwner chains** (or **slit Löwner chains**) and their stochastic versions are given in the third section. This construction includes the **chordal**, **dipolar**, and **radial** Löwner equations as special cases.  $SLE(\kappa, \rho)$  and multiple SLE exceed the framework of this thesis because it can not be formulated as a single (not a system of) diffusion equation. In particular,  $SLE(\kappa, \rho)$  measure of curves do not possess a domain Markov property defined in terms of slits only because the conditional random law depends not only on the fixed part of the curve but on some additional parameters.

We try to keep the presentation as self-sufficient as possible avoiding, however, any length introduction referring to, e.g. [Law08] instead. The stochastic calculus, the Itô and Stratonovich differentiation are assumed to be familiar to the reader. Some additional facts are given in Appendix A.

## 1.1 Preliminaries

Each of the versions of the Löwner equations, and more generally, of holomorphic stochastic flows, is usually associated with a certain canonical domain  $D \subset \mathbb{C}$  in the complex plane, e.g., the upper half-plane (in the case of the chordal SLE) or the unit disk (in the case of the radial SLE), etc. Focusing on conformal invariant properties we avoid this specific choice and map the canonical domains one to another if necessary. For example, the number of fixed points of the flow or the algebraic properties of vector fields that define the flow are presented in this invariant way. The invariance is achieved by considering a general hyperbolic simply connected domain, or a chart, from the very beginning. It is also natural to go further and work with a simply connected hyperbolic Riemann surface  $\mathcal{D}$  (with a boundary  $\partial \mathcal{D}$ ). Below,  $\mathcal{D}$  is understood as a generic domain with a well-defined boundary as well as a Riemann surface. A simply connected hyperbolic Riemann surface with a boundary is denoted by  $\tilde{\mathcal{D}} = \mathcal{D} \cup \partial \mathcal{D}$ , where  $\partial \mathcal{D}$  is the boundary and  $\mathcal{D}$  is the open interior. We will mostly use global chart maps  $\psi: \mathcal{D} \rightarrow D^\psi \subset \mathbb{C}$  from  $\mathcal{D}$  to a domain of the complex plane, writing  $\psi$  for a chart  $(D, \psi)$  for simplicity. For any other chart  $\tilde{\psi}: \mathcal{D} \rightarrow D^{\tilde{\psi}} \subset \mathbb{C}$  the transition map is denoted by

$$\tau^{\psi, \tilde{\psi}} := \psi \circ \tilde{\psi}^{-1}: D^{\tilde{\psi}} \rightarrow D^\psi. \quad (1.1)$$

For example, we will often use the half-plane chart map  $\psi_{\mathbb{H}}: \mathcal{D} \rightarrow \mathbb{H}$ ,

$$\mathbb{H} := \{z \in \mathbb{C} : \text{Im}(z) > 0\}. \quad (1.2)$$

Another example is the unit disk chart map  $\psi_{\mathbb{D}}: \mathcal{D} \rightarrow \mathbb{D}$ , where

$$\mathbb{D} := \{z \in \mathbb{C} : |z| < 1\}. \quad (1.3)$$

These charts are related by the transition map

$$\tau^{\mathbb{H}, \mathbb{D}}(z) := \psi^{\mathbb{H}} \circ \left(\psi^{\mathbb{D}}\right)^{-1} = i \frac{1-z}{1+z}: \mathbb{D} \rightarrow \mathbb{H}, \quad . \quad (1.4)$$

Thus, the point  $z = 1$  in the unit disk chart corresponds to the origin in the half-plane chart and the point  $z = -1$  corresponds to infinity. We will also use a non global multivalued chart  $\psi^{\mathbb{L}}: \mathcal{D} \rightarrow \mathbb{H}$  in Section 6.3.

Consider now a holomorphic vector field  $v$  on  $\mathcal{D}$ , that is a holomorphic section of the complexified tangent bundle. We also can define it as a map  $\psi \mapsto v^\psi$  from the set of all possible global charts  $\psi: \mathcal{D} \rightarrow D^\psi$  to the set of holomorphic functions  $v^\psi: D^\psi \rightarrow \mathbb{C}$  defined on  $D^\psi := \psi(\mathcal{D})$ . For the vector fields, the following coordinate change holds. Any chart map  $\tilde{\psi}: \mathcal{D} \rightarrow D^{\tilde{\psi}}$  induces the transition

$$v^{\tilde{\psi}}(\tilde{z}) = v^{\tau^{-1} \circ \psi}(\tilde{z}) = \frac{1}{\tau'(\tilde{z})} v^\psi(\tau(\tilde{z})), \quad \tau := \psi \circ \tilde{\psi}^{-1}: D^{\tilde{\psi}} \rightarrow D^\psi, \quad (1.5)$$

If  $v$  is defined for one chart, then it is automatically defined on all other charts. A vector field also can be called a  $(-1, 0)$ -differential.

Consider now a conformal map  $F: \mathcal{D} \rightarrow \tilde{\mathcal{D}}$  between two hyperbolic simply connected Riemann surfaces (or generic domains)  $\mathcal{D}$  and  $\tilde{\mathcal{D}}$ , and let  $\psi: \mathcal{D} \rightarrow D^\psi \subset \mathbb{C}$ , and let  $\tilde{\psi}: \tilde{\mathcal{D}} \rightarrow \tilde{D}^{\tilde{\psi}} \subset \mathbb{C}$  be the chart map. Define

$$F^{\tilde{\psi}, \psi} := \tilde{\psi} \circ F \circ \psi^{-1}: D^\psi \rightarrow \tilde{D}^{\tilde{\psi}}, \quad (1.6)$$

consequently,

$$(F^{\tilde{\Psi}, \Psi})^{-1} = (F^{-1})^{\Psi, \tilde{\Psi}} = \Psi \circ F^{-1} \circ \tilde{\Psi}^{-1} : \tilde{D}^{\tilde{\Psi}} \rightarrow D^{\Psi}. \quad (1.7)$$

The pushforward  $F_* : \nu^{\Psi} \mapsto \tilde{\nu}^{\tilde{\Psi}}$  is defined by the rule

$$\begin{aligned} \nu^{\Psi}(z) \rightarrow \tilde{\nu}^{\tilde{\Psi}}(\tilde{z}) &= (F_* \nu)^{\tilde{\Psi}}(\tilde{z}) := \nu^{\tilde{\Psi} \circ F}(\tilde{z}) = \nu^{\tilde{\Psi} \circ F \circ \Psi^{-1} \circ \Psi}(\tilde{z}) = \nu^{F^{\tilde{\Psi}, \Psi} \circ \Psi}(\tilde{z}) = \\ &= \frac{1}{\left( (F^{\tilde{\Psi}, \Psi})^{-1} \right)'(\tilde{z})} \nu^{\Psi} \left( \left( (F^{\tilde{\Psi}, \Psi})^{-1} \right)(\tilde{z}) \right), \quad \tilde{z} \in \tilde{D}^{\tilde{\Psi}}, \end{aligned} \quad (1.8)$$

because  $(F^{\tilde{\Psi}, \Psi})^{-1}$  plays the same role as  $\tau$  in (1.5).

Let now  $F$  be an endomorphism of  $\mathcal{D}$ , namely,  $F(\mathcal{D}) = \tilde{\mathcal{D}} = \mathcal{D} \setminus \mathcal{K}$  for some compact subset  $\mathcal{K}$ ,  $\tilde{\Psi} \equiv \Psi|_{\mathcal{D} \setminus \mathcal{K}}$ , and  $F^{\Psi} := F^{\Psi, \Psi}$ . Then,

$$\begin{aligned} F_* \nu^{\Psi}(z) &= \nu^{\Psi \circ F}(z) = \frac{1}{\left( (F^{\Psi})^{-1} \right)'(z)} \nu^{\Psi} \left( \left( (F^{\Psi})^{-1} \right)(z) \right), \\ z \in \Psi(\tilde{\mathcal{D}}) &= \Psi(\mathcal{D} \setminus \mathcal{K}) \subset D^{\Psi}, \end{aligned} \quad (1.9)$$

is a vector field defined in  $\mathcal{D} \setminus \mathcal{K}$ . For the inverse map  $F^{-1} : \mathcal{D} \setminus \mathcal{K} \rightarrow \mathcal{D}$  the vector field  $F_*^{-1} \nu^{\Psi}$  is defined in entire  $\mathcal{D}$  but the values of  $\nu$  in  $\mathcal{K}$  are not taken into account. It is also easy to see that

$$\tilde{F}_* F_* = (F \circ \tilde{F})_* . \quad (1.10)$$

The pushforward  $F_*$  also can be understood as a bundle map between corresponding tangent bundles induced by  $F$ . We stick the way above because it can be extended to more general transformations with respect to the change of charts such as the **pre-pre-Schwarzian**, see Section 4.2. We will use the notation  $X^{\mathbb{H}} := X^{\Psi^{\mathbb{H}}}$  if  $X$  is a vector field, conformal map or pre-pre-Schwarzian (defined below) in  $\mathcal{D}$  as well as  $X^{\mathbb{D}} := X^{\Psi^{\mathbb{D}}}$  for the unit disk chart, and similarly, for other standard charts.

It will be also convenient to use a basis of holomorphic vector fields given by holomorphic functions as

$$\ell_n^{\mathbb{H}}(z) := z^{n+1}, \quad z \in \mathbb{H} \quad (1.11)$$

in the half-plane chart. In the unit disk chart they admit the form

$$\ell_n^{\mathbb{D}}(z) = -\frac{i^n}{2} (1-z)^{1+n} (1+z)^{1-n} \quad (1.12)$$

according to (1.4) and (1.5). We remark that  $\ell_n$  are holomorphic in  $\mathcal{D}$ , tangent at the boundary except two points, which are the origin and infinity in the half-plane chart or  $z = \pm 1$  in the unit disk chart. In these points  $\ell_n$  has critical points of order  $1+n$  and  $1-n$  correspondingly, which are zeros for positive order and poles for negative order.

A holomorphic vector field  $\sigma$  in  $\mathcal{D}$  is called **complete** if the solution  $H_t[\sigma]^{\Psi}(z)$  of the initial value problem

$$\dot{H}_t[\sigma]^{\Psi}(z) = \sigma^{\Psi}(H_t[\sigma]^{\Psi}(z)), \quad H_0[\sigma]^{\Psi}(z) = z, \quad z \in D^{\Psi} \quad (1.13)$$

is defined for  $t \in (-\infty, \infty)$  as a conformal automorphism  $H_t[\sigma]^{\Psi} : D^{\Psi} \rightarrow D^{\Psi}$ . Here and below, we denote the partial derivative with respect to  $t$  (called **time** henceforth) as

$\dot{H}_t := \frac{\partial}{\partial t} H_t$ . It is straightforward to see that the differential equation has the same form in any chart  $\psi$ . That is why it is reasonable to drop the index  $\psi$  and the argument  $z$  as

$$\dot{H}_t[\sigma] = \sigma \circ H_t[\sigma], \quad H_0[\sigma] = \text{id}. \quad (1.14)$$

We will use notation ‘ $\circ$ ’ in what follows. The advantage is the explicit independence of the choice of a chart.

The collection  $\{H_t[\sigma]\}_{t \in \mathbb{R}}$  forms a one-parameter group:

$$H_t[\sigma] \circ H_s[\sigma] = H_{t+s}[\sigma], \quad H_t^{-1}[\sigma] = H_{-t}[\sigma], \quad , \quad t, s \in (-\infty, +\infty). \quad (1.15)$$

Besides, for any complete vector field  $\sigma$  we have

$$H_t[\sigma]_* \sigma = \sigma, \quad t \in (-\infty, +\infty). \quad (1.16)$$

It is possible to show, see [Sho01], that a complete vector field  $\sigma$  is a linear combination of  $\ell_{-1}$ ,  $\ell_0$ , and  $\ell_1$  with real coefficients

$$\sigma = \sigma_{-1}\ell_{-1} + \sigma_0\ell_0 + \sigma_1\ell_1, \quad \sigma_{-1}, \sigma_0, \sigma_1 \in \mathbb{R}. \quad (1.17)$$

In the half-plane chart this relation looks as

$$\sigma^{\mathbb{H}}(z) = \sigma_{-1} + \sigma_0 z + \sigma_1 z^2, \quad z \in \mathbb{H}, \quad \sigma_{-1}, \sigma_0, \sigma_1 \in \mathbb{R} \quad (1.18)$$

due to (1.12). It is also true that a holomorphic vector field is complete if and only if it is holomorphic and tangent at the boundary.

Define the parameter

$$\Delta_2 := \sigma_0^2 - \sigma_1\sigma_{-1}. \quad (1.19)$$

It is invariant with respect to choice of basis  $\ell_n$ , or equivalently, Möbius automorphisms of  $\mathcal{D}$ . We distinguish 3 cases:

1.  $\Delta_2 = 0$ . We call this case **parabolic**. The vector field  $\sigma$  has one zero at the boundary of order 2.
2.  $\Delta_2 > 0$ . We call this case **hyperbolic**. The vector field  $\sigma$  has two zeros at the boundary of order 1.
3.  $\Delta_2 < 0$ . We call this case **elliptic**. The vector field  $\sigma$  has one zeros inside of  $\mathcal{D}$ .

We illustrate each type in the Fig. 1.1. We notice that any complete vector field can be reduced to a one from the Fig. 1.1 up to a constant with the Möbius transform. We remark that  $H_t[\sigma]$  is periodic with respect to  $t$  if and only if  $\sigma$  is elliptic.

A holomorphic vector field  $\delta$  is called **semicomplete** if the initial value problem (1.14) with  $\delta$  at the place of  $\sigma$  has a solution  $H_t[\delta]$ , which is a conformal map  $H_t[\delta] : \mathcal{D} \rightarrow \mathcal{D} \setminus K_t$  for all  $t \in [0, +\infty)$  and for some family  $\{\mathcal{K}_t\}_{t \geq 0}$  of subsets  $\mathcal{K}_t \subset \mathcal{D}$ . The equation (1.14) also has a solution for  $t \in (-\infty, 0]$  but  $\{H_t[\delta]\}_{t \leq 0}$  is the family of inverse endomorphisms  $H_t[\delta] : \mathcal{D} \setminus \mathcal{K}_t \rightarrow \mathcal{D}$ .

**Antisemicomplete** vector fields can be defined as just minus semicompletes fields.

Thus,  $-\delta$  is an antisemicomplete vector field if and only if  $\delta$  is a semicomplete field, and vice versa. Equivalently, we can define an antisemicomplete vector field by

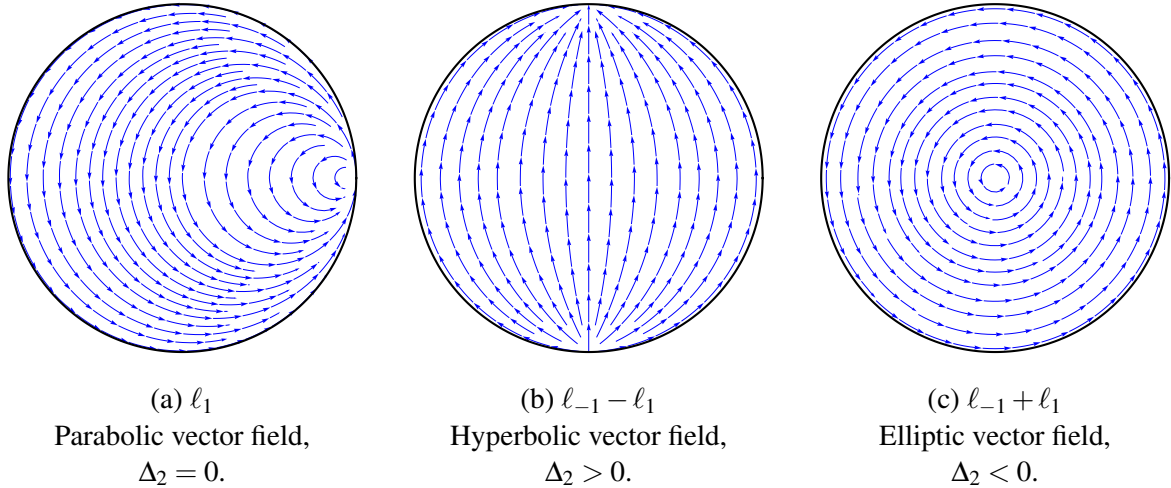


Figure 1.1: Examples of three types of complete vector field in the unit disk chart.

assumption that  $\{H_t[\delta]\}_{t \leq 0}$  is a collection of endomorphisms or, which is the same,  $\{H_t[\delta]\}_{t \geq 0}$  is a collection of inverse endomorphisms. A complete field is, in particular, semicomplete and anticomplete at the same time.

The collection  $\{H_t[\delta]\}_{t \geq 0}$  for semicomplete  $\delta$  is a one-parameter semigroup of endomorphisms with respect to composition. Analogously, for an anticomplete  $\delta$  the collection  $\{H_t[\delta]\}_{t \geq 0}$  is also a one-parameter semigroup of inverse endomorphisms with respect to composition.

**Proposition 1.1.** (*Berkson-Porta representation*) [BP78]

A vector field  $\delta$  is semicomplete if and only if

$$\delta^{\mathbb{D}}(z) = (z - \tau)(\bar{\tau}z - 1)p(z), \quad \tau \in \bar{\mathbb{D}}, \quad \operatorname{Re} p(z) \geq 0, \quad z \in \bar{\mathbb{D}}, \quad (1.20)$$

in the unit disk chart for some holomorphic  $p : \bar{\mathbb{D}} \rightarrow \mathbb{C}$ .

The space of all semicomplete fields is essentially bigger than the space of complete fields and it is infinite-dimensional. We restrict ourselves to the case of fields which are holomorphic in  $\mathcal{D}$  and tangent at the boundary except one point  $a \in \partial \mathcal{D}$  that is called **source** below.

**Proposition 1.2.** A semicomplete vector field  $\delta$  is holomorphic in  $\mathcal{D}$  and tangent at the boundary except one point  $a \in \partial \mathcal{D}$  if and only if it is of the form

$$\delta = \delta_{-2}\ell_{-2} + \delta_{-1}\ell_{-1} + \delta_0\ell_0 + \delta_1\ell_1, \quad \delta_{-1}, \delta_0, \delta_1 \in \mathbb{R}, \quad \delta_{-2} \leq 0. \quad (1.21)$$

*Proof.* Without loss of generality assume that  $\tau = 1$  and  $p(1) = 0$  under the conditions of Proposition 1.1, that can be achieved by adding an appropriate complete field.

Consider now a chart

$$\psi^{\mathbb{H}} := -\frac{1}{\psi^{\mathbb{H}}} : \mathcal{D} \rightarrow \mathbb{H}, \quad (1.22)$$

which is similar to  $\psi^{\mathbb{H}}$  defined above, but it maps the source point  $a$  to infinity  $\psi^{\mathbb{H}}(a) = \infty$ . The function  $\delta^{\mathbb{H}}(z)$  can be expressed as

$$\delta^{\mathbb{H}}(z) = 2iz^2 p\left(\frac{i-z}{i+z}\right), \quad z \in \mathbb{H}. \quad (1.23)$$

On the other hand,  $\delta^{\mathbb{H}}(z)$  is an entire function after the Schwartz reflection to the lower half-plane. The Taylor series of  $\delta^{\mathbb{H}}(z)$  and of  $ip\left(\frac{i-z}{i+z}\right)$  about  $z=0$  have real coefficients because  $\delta$  is tangent at the boundary. The conditions  $\operatorname{Re}\left(p\left(\frac{i-z}{i+z}\right)\right) \geq 0$  and  $p(1) = 0$  leave a unique possibility:

$$ip\left(\frac{i-z}{i+z}\right) = cz, \quad c > 0. \quad (1.24)$$

We conclude that

$$\delta^{\mathbb{H}}(z) = 2cz^3, \quad c > 0. \quad (1.25)$$

After the coordinate change  $z \mapsto 1/z$  to the standard half-plane chart and adding a generic complete part we obtain (1.26).  $\square$

In the half-plane chart, we have

$$\delta^{\mathbb{H}}(z) = \frac{\delta_{-2}}{z} + \delta_{-1} + \delta_0 z + \delta_1 z^2, \quad z \in \mathbb{H}, \quad \delta_{-1}, \delta_0, \delta_1 \in \mathbb{R}, \quad \delta_{-2} \leq 0. \quad (1.26)$$

Thus,  $\delta$  has a simple pole at  $a$  with a non-positive residue. The sum of the last three terms is just a complete field.

We notice that, if a vector field  $v$  has a zero at  $z_0$ , then the parameter  $v^{\psi'}(z_0)$  does not depend on the choice of chart. We call a zero of a vector field **attracting** if  $\operatorname{Re} v^{\psi'}(z_0) > 0$ .

Analogous to the complete field define the parameter

$$\Delta_3 := 18\delta_{-1}\delta_0\delta_1 - 4\delta_0^3 + \frac{\delta_{-1}^2\delta_0^2}{\delta_{-2}} - 4\frac{\delta_{-1}^3\delta_1}{\delta_{-2}} - 27\delta_{-2}\delta_1^2 \quad (1.27)$$

As well, it is invariant with respect to choice of basis  $\ell_n$ , or equivalently, Möbius automorphisms of  $\mathcal{D}$  preserving the pole position. We distinguish 3 cases:

1.  $\Delta_3 = 0$ . We call this case **parabolic**. The vector field  $\delta$  has either one zero at the boundary of order 2 and one zero of order 1 at another point at the boundary or one zero at the boundary of order 3.
2.  $\Delta_3 > 0$ . We call this case **hyperbolic**. The vector field  $\delta$  has three different zeros at the boundary of order 1 each. The one between is attracting.
3.  $\Delta_3 < 0$ . We call this case **elliptic**. The vector field  $\delta$  has one attracting zeros inside of  $\mathcal{D}$  of order 1 and one zero at the boundary of order 1.

We illustrate each type in the Fig. 1.2.

The solution  $H_t[\delta]$  of (1.14) with  $\delta$  from (1.26) is a conformal endomorphism  $H_t[\delta]: \mathcal{D} \rightarrow \mathcal{D} \setminus \gamma_t$ . Here,  $\{\gamma_t\}_{t \in [0, +\infty)}$  is a family of curves such as  $\gamma_t \subset \gamma_s$ ,  $t < s$  and  $\gamma_0 = \emptyset$ . The curves starts form  $a$ , lie along the flow line of  $\delta$  and tend to the attracting (or degenerate) zero when  $t \rightarrow +\infty$ . We call such family  $\{\gamma_t\}_{t \in [0, +\infty)}$  a **growing curve**.

Let  $v_t$  and  $\tilde{v}_t$  be two holomorphic vector fields depending on time continuously such as the following differential equations has continuously differentiable solutions  $F_t$  and  $\tilde{F}_t$  in some time interval

$$\begin{aligned} \dot{F}_t &= v_t \circ F_t, \\ \dot{\tilde{F}}_t &= \tilde{v}_t \circ \tilde{F}_t. \end{aligned} \quad (1.28)$$

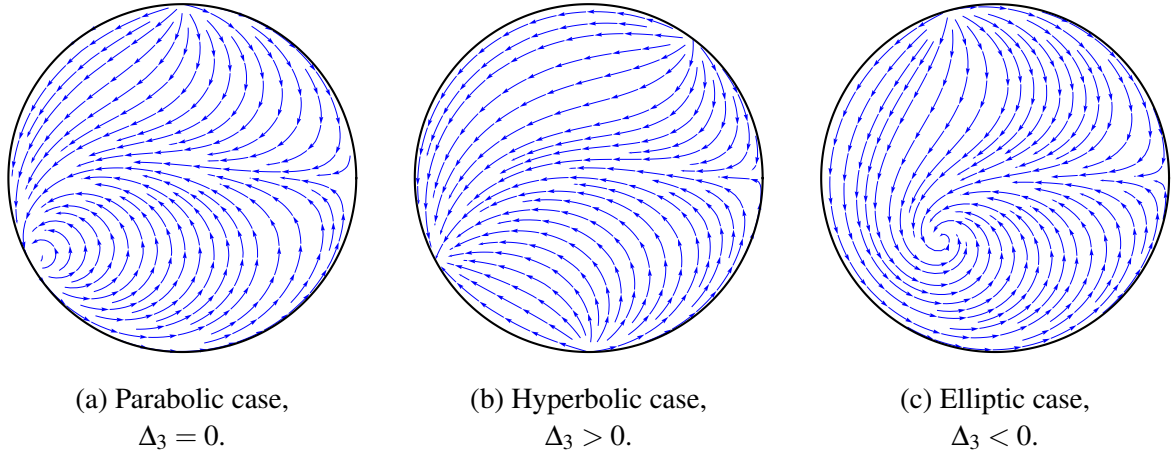


Figure 1.2: Examples of three types of vector field  $\delta$  defined by (1.26) in the unit disk chart. Each field has a simple pole at  $\psi^{\mathbb{D}}(a) = 1$ . The attracting zeros of order one correspond to singular points with divergent arrows.

Then, we can conclude that

$$\frac{\partial}{\partial t}(F_t \circ \tilde{F}_t) = (v_t + F_{t*} \tilde{v}_t) \circ F_t \circ \tilde{F}_t \quad (1.29)$$

$$\dot{F}_t^{-1} = -(F_t^{-1} v_t) \circ F_t^{-1}. \quad (1.30)$$

in the same interval and in the region of  $\mathcal{D}$  where  $F_t$  and  $\tilde{F}_t$  are defined. The latter relation can be reformulated in a fixed chart  $\psi$  as

$$F_t^{-1} \dot{\psi}(z) = -\left((F_t^{-1})'\right)'(z) v_t^\psi(z). \quad (1.31)$$

## 1.2 $(\delta, \sigma)$ -Löwner chain (slit holomorphic Löwner chain)

### 1.2.1 Definition and basic properties

Consider the autonomous initial value problem

$$\dot{G}_t = \delta \circ G_t + \dot{u}_t \sigma \circ G_t, \quad G_0 = \text{id}, \quad t \in [0, +\infty), \quad (1.32)$$

for a conformal map  $G_t$  defined for a complete vector field  $\sigma$ , for semicomplete or anticomplete vector field  $\delta$ , and for a continuously differentiable function  $u_t : [0, +\infty) \rightarrow \mathbb{R}$ .

Avoid now the requirement of differentiability of  $u_t$  by using the following method. Define first a conformal map

$$g_t := H_{u_t}[\sigma]^{-1} \circ G_t, \quad (1.33)$$

where  $H[\sigma]$  is defined by (1.14). Thanks to (1.29) the map  $g_t$  satisfies

$$\dot{g}_t = (H_{u_t}[\sigma]_*^{-1} \delta) \circ g_t, \quad g_0 = \text{id}. \quad (1.34)$$

The inverse is also true: (1.32) can be obtained from (1.34). But ((1.34) is defined for a more general set of driving functions, not necessarily continuously differentiable. Thus, we can define

$$G_t := H_{u_t}[\sigma] \circ g_t \quad (1.35)$$

for non-differentiable driving functions  $u_t$ . The use of  $g_t$  is technically less convenient than  $G_t$ , however, the advantage is the possibility to consider not differentiable driving functions. This motivates the definition as follows.

**Definition 1.1.** *Let  $\delta$  and  $\sigma$  be holomorphic vector fields of the form*

$$\begin{aligned} \delta &= \delta_{-2}\ell_{-2} + \delta_{-1}\ell_{-1} + \delta_0\ell_0 + \delta_1\ell_1, & \delta_{-2}, \delta_{-1}, \delta_0, \delta_1 &\in \mathbb{R}, & \delta_{-2} &\neq 0 \\ \sigma &= \sigma_{-1}\ell_{-1} + \sigma_0\ell_0 + \sigma_1\ell_1, & \sigma_{-1}, \sigma_0, \sigma_1 &\in \mathbb{R}, & \sigma_{-1} &\neq 0, \end{aligned} \quad (1.36)$$

and let  $u_t$  be a continuous function  $u : [0, \infty) \rightarrow \mathbb{R}$ . Then the initial value problem (1.34) is called the  $(\delta, \sigma)$ -Löwner equation, or equivalently, the *slit holomorphic Löwner equation*, and its solution  $\{g_t\}_{t \in [0, +\infty)}$  given by

$$\{u_t\}_{t \in [0, +\infty)} \mapsto \{g_t\}_{t \in [0, +\infty)} \quad (1.37)$$

or  $\{G_t\}_{t \in [0, +\infty)}$  given by

$$\{u_t\}_{t \in [0, +\infty)} \mapsto \{G_t := H_{u_t}[\sigma] \circ g_t\}_{t \in [0, +\infty)} \quad (1.38)$$

is called the  $(\delta, \sigma)$ -Löwner chain, or equivalently, the *slit holomorphic Löwner chain*. The chain is called **forward** if  $\delta$  is antisemicomplete ( $\delta_{-2} > 0$ ), and it is called **reverse** if  $\delta$  is semicomplete ( $\delta_{-2} < 0$ ).

We do not consider the degenerate cases when  $\delta_{-2} = 0$  or  $\sigma_{-1} = 0$ , because the most of the proposition below are not satisfied. If  $\delta_{-2} = 0$ , then we have just Möbius automorphisms. The case  $\sigma_{-1} = 0$  is considered in Section 6.6. Henceforth, we always assume, that  $\delta$  and  $\sigma$  are of the form (1.36).

The well-known chordal, radial, and dipolar equations are special cases of (1.34). We summarize them in Table 1.1.

Equation type	$\delta$	$\sigma$
Chordal	$2\ell_{-2}$	$-\ell_2$
Dipolar	$\frac{1}{2}\ell_{-2} - \frac{1}{2}\ell_0$	$-\frac{1}{2}\ell_{-1} + \frac{1}{2}\ell_1$
Radial	$\frac{1}{2}\ell_{-2} + \frac{1}{2}\ell_0$	$-\frac{1}{2}\ell_{-1} - \frac{1}{2}\ell_1$
ABP, see [IV12]	$\frac{1}{2}\ell_{-2}$	$-\frac{1}{2}\ell_{-1} - \frac{1}{2}\ell_1$

Table 1.1: Known cases of forward  $(\delta, \sigma)$ -Löwner chains.

We call first three cases in the table **classical** and discuss each of them in the corresponding sections of Chapter 6. Each of the three classical cases are combinations of  $\delta$  and  $\sigma$  of the same type and with the identical positions of zeros. This leads to simple restrictions for corresponding maps  $G_t$  and  $g_t$  that we call **normalization**.



We apply the general theory of Löwner chains to solve the initial value problem (1.34). According to the terminology from [CDMG11] the vector field  $(H_{u_t}[\sigma]_*^{-1} \delta)^\mathbb{D}$  in the unit disc chart is Herglotz in the reverse case and minus Herglotz in the forward case. We conclude that the solution  $\{g_t\}_{t \in [0, +\infty)}$  exists, is unique, and is given by the conformal maps  $g_t: \mathbb{D} \rightarrow \mathbb{D} \setminus \mathcal{K}_t$  in the reverse case and by the conformal maps  $g_t: \mathbb{D} \setminus \mathcal{K}_t \rightarrow \mathbb{D}$  in the forward case for some collection  $\{\mathcal{K}_t\}_{t \in [0, +\infty)}$  of subsets  $\mathcal{K}_t \subset \mathbb{C}$ . Moreover, in the forward case, the collection  $\{\mathcal{K}_t\}_{t \in [0, +\infty)}$  is strictly growing  $\mathcal{K}_s \subset \mathcal{K}_t$ ,  $s < t$ . In the Fig. 1.3, we show how a typical map  $G_t$  acts in the unit disc chart. Table 1.2 shows the limit  $t \rightarrow +\infty$  of the hull  $\mathcal{K}_t$  (which is a curve in these cases) for some fixed choice of the driving function and for various choices of  $\delta$  and  $\sigma$ . Some exact solution of the Chordal Löwner equation are considered in [KNK04].

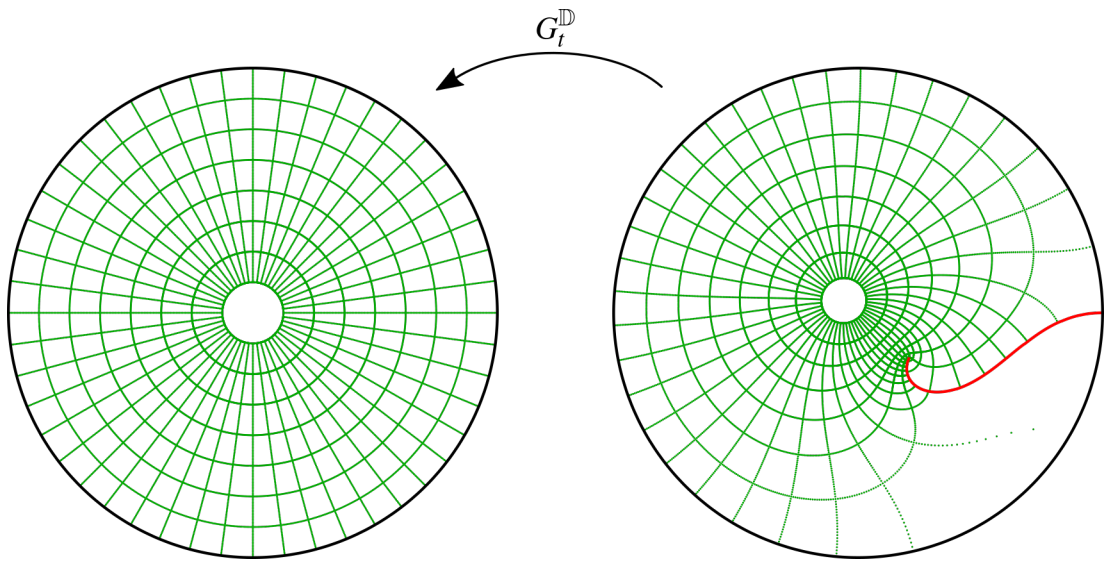


Figure 1.3: This is how a typical conformal map  $G_t$  acts in the unit disc chart  $\mathbb{D}$  for some choice of  $\delta$ ,  $\sigma$ , the driving function  $u$ , and  $t$  in the forward case. The red line is the hull  $\mathcal{K}_t$ , which is a simple curve (slit) in this case. In the reverse case, the map  $G_t$  acts in the opposite direction, see Proposition 1.3.

Let  $G_{t,s}$  be the solution of (1.34) and (1.35) for  $t \in [0, +\infty)$  parametrized by  $s \in [0, +\infty)$  with the initial condition  $G_{s,s} = \text{id}$ . Hence,  $\{G_{t,s}\}_{t \in [s, +\infty)}$  is a  $(\delta, \sigma)$ -Löwner chain with the driving function

$$u_{t,s} := u_t - u_s, \quad t \in [s, +\infty). \quad (1.39)$$

In particular,  $G_{t,0} = G_t$ ,  $t \in [0, +\infty)$ . We see that  $G_{t+s,s}$  is also defined for negative values of  $t$  ( $t \in [-s, 0]$ ,  $s \geq 0$ ) and

$$G_{t,s} = G_t \circ G_s^{-1}, \quad t, s \geq 0 \quad (1.40)$$

Besides,

$$G_{t,s} = G_{t,r} \circ G_{r,s}, \quad t, s, r \geq 0. \quad (1.41)$$

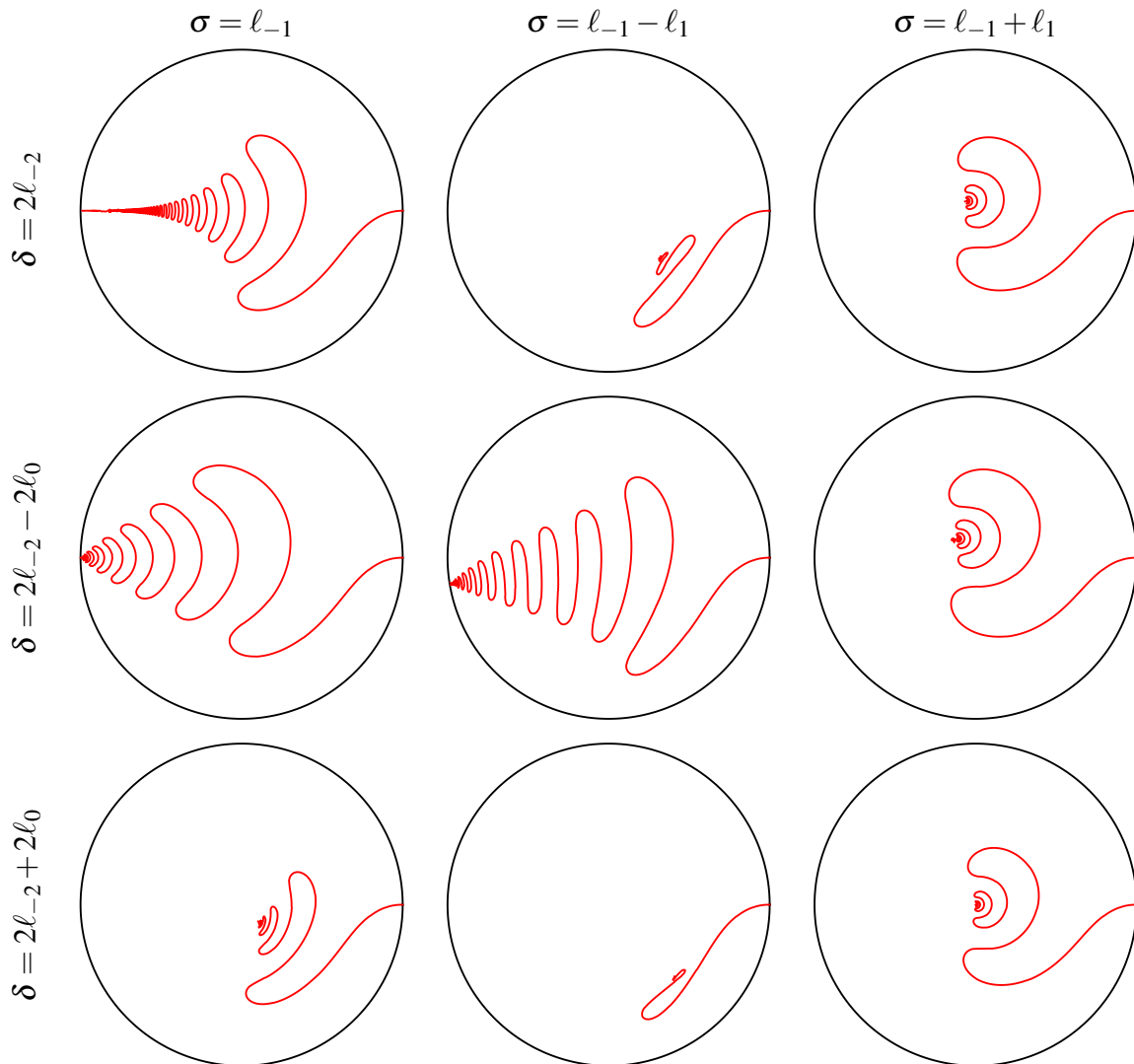


Table 1.2: Slits of  $(\delta, \sigma)$ -Löwner chains ( $t \rightarrow +\infty$ ) in the unit disk chart driven by  $u_t = \sin 20t$ . We fix the choice of  $\delta$  row-wise, and we fix the choice of  $\sigma$  column-wise. So, the three cases on the diagonal are classical.

In particular,

$$G_t = G_{t,s} \circ G_s, \quad s, t \geq 0, \quad (1.42)$$

and

$$G_{t,s} = G_{s,t}^{-1}, \quad s, t \geq 0. \quad (1.43)$$

Analogous relations are valid for the differentiable version of the chain  $g_{s,t}$

$$g_{t,s} = g_{t,r} \circ g_{r,s}, \quad g_{t,s} = g_{s,t}^{-1}, \quad g_{t,s} := g_t \circ g_s^{-1}, \quad t, s, r \geq 0. \quad (1.44)$$

The collection  $\{g_{t,s}^{\mathbb{D}}\}_{0 \leq s \leq t < +\infty}$  is known as an ‘evolution family’.

The inverse maps  $G_t^{-1}$  and  $g_t^{-1}$  satisfy the partial differential equations:

$$\dot{G}_t^{-1} = -G_t^{-1} * (\delta + \sigma \dot{u}_t) \circ G_t^{-1} \quad (1.45)$$

for continuously differentiable  $u_t$ , and

$$\dot{g}_t^{-1} = - (g_t^{-1} *_H u_t[\sigma]_* \delta) \circ g_t^{-1} \quad (1.46)$$

for continuous  $u_t$ .

**Proposition 1.3.** *Fix  $T \geq 0$ . Let  $\{G_t\}_{t \in [0, T]}$  be a forward  $(\delta, \sigma)$ -Löwner chain driven by  $\{u_t\}_{t \in [0, T]}$ , and let  $\{\tilde{G}_t\}_{t \in [0, T]}$  be a reverse  $(-\delta, \sigma)$ -Löwner chain driven by*

$$\tilde{u}_t := u_{T-t} - u_T, \quad t \in [0, T]. \quad (1.47)$$

Thus,

$$\tilde{G}_T = G_T^{-1}, \quad (1.48)$$

and

$$\tilde{g}_T = H_{u_T}[\sigma] \circ g_T^{-1} \circ H_{u_T}[\sigma]^{-1}. \quad (1.49)$$

*Proof.* Set

$$\hat{g}_t := H_{u_T}[\sigma] \circ g_{T-t, T} \circ H_{u_T}[\sigma]^{-1}, \quad t \in [0, T], \quad (1.50)$$

and observe that  $\hat{g}_T = \tilde{g}_T$  because they are the solutions of the same initial value problem. Indeed,

$$\begin{aligned} \frac{\partial}{\partial t} \hat{g}_t &= \frac{\partial}{\partial t} (H_{u_T}[\sigma] \circ g_{T-t} \circ g_T^{-1} \circ H_{u_T}[\sigma]^{-1}) = \\ &= - (H_{u_T}[\sigma] *_H u_{T-t}[\sigma]_*^{-1} \delta) \circ H_{u_T}[\sigma] \circ g_{T-t} \circ g_T^{-1} \circ H_{u_T}[\sigma]^{-1} = \\ &= (H_{u_{T-t} - u_T}[\sigma]_*^{-1} (-\delta)) \circ \hat{g}_t, \quad t \in [0, T]. \end{aligned} \quad (1.51)$$

and  $\hat{g}_0 = \text{id}$ . Putting  $t = T$  we obtain (1.49) and (1.48).  $\square$

Given a pair of  $\delta$  and  $\sigma$ , we denote by  $\mathcal{G}[\delta, \sigma] \subset \mathcal{G}$  the collection of all endomorphisms and inverse endomorphisms  $G_t$  of  $\mathcal{D}$  from all possible  $(\delta, \sigma)$ -Löwner chains for all possible continuous driving functions  $u$  and  $t \in [0, +\infty)$ .

Proposition 1.3, in particular, states that the collection  $\mathcal{G}[\delta, \sigma]$  coincides with  $\mathcal{G}[-\delta, \sigma]$  up to inversion. We will consider mostly forward chains below. The advantage of the forward case is that the hulls are growing  $\mathcal{K}_s \subset \mathcal{K}_t, s < t$ .

The equation (1.34) together with (1.35) induce a surjective map  $C^0[0, T] \rightarrow \mathcal{G}[\delta, \sigma]$  ( $T \in [0, +\infty)$ ) acting as  $\{u_t\}_{t \in [0, T]} \mapsto G_T \in \mathcal{G}[\delta, \sigma]$ , where  $C^0[0, T]$  is the set of all continuous functions  $u: [0, T] \rightarrow \mathbb{R}$  in the interval  $[0, T]$ , and such that  $u_0 = 0$ .

## 1.2.2 General properties of $(\delta, \sigma)$ -Löwner chain

Relations (1.39) - (1.51) are valid for arbitrary semicomplete or anticomplete vector fields  $\delta$ , not necessarily of the form (1.36). But, the theorem below uses essentially that  $\delta$  has only one simple pole, and that is tangent at other points of the boundary. The result of the theorem motivates the term ‘slit Löwner chain’.

**Theorem 1.1.** *Let  $\{g_t\}_{t \in [0, +\infty)}$  be a forward  $(\delta, \sigma)$ -Löwner chain with a driving function  $\{u_t\}_{t \in [0, +\infty)}$  and with the hulls  $\{\mathcal{K}_t\}_{t \in [0, +\infty)}$ . Let also  $\tilde{\delta}$  and  $\tilde{\sigma}$  be as in (1.36) with  $\tilde{\delta}_{-2} > 0$ . Then the following statements hold:*

1. There exists a  $(\tilde{\delta}, \tilde{\sigma})$ -Löwner chain  $\{\tilde{g}_t\}_{t \in [0, \tilde{T})}$  for some maximal  $\tilde{T} \in (0, +\infty]$  driven by a function  $\{\tilde{u}_t\}_{t \in [0, \tilde{T})}$  such that its hulls are

$$\tilde{\mathcal{K}}_t = \mathcal{K}_{\lambda_t^{-1}}, \quad t \in [0, \tilde{T}) \quad (1.52)$$

for a continuous time reparametrization  $\lambda : [0, T) \rightarrow [0, \tilde{T})$  defined for some  $T \in (0, \infty]$ .

2. If the  $(\tilde{\delta}, \tilde{\sigma})$ -Löwner chain, as in item 1, exists until  $\tilde{T} \in [0, +\infty)$ , then it is unique.
3. The time reparametrization  $\lambda_t$  is continuously differentiable.
4. The Löwner chains  $\{g_t\}_{t \in [0, \infty)}$  and  $\{\tilde{g}_t\}_{t \in [0, \tilde{T})}$  are related by a family of Möbious automorphisms

$$M_t := \tilde{g}_{\lambda_t} \circ g_t^{-1}, \quad t \in [0, T) \quad (1.53)$$

that satisfy (1.54) for  $t \in [0, T)$ .

5. The functions  $\lambda_t$  and  $\tilde{u}_t$  are defined by (1.65) and by (1.66) correspondingly.
6. Let  $b \in \mathcal{D}$  (or  $b \in \partial \mathcal{D}$ ) be a point such that  $b \notin \tilde{\mathcal{K}}_t$  for  $t \in [0, +\infty)$  (where  $\tilde{\mathcal{K}} \subset \bar{\mathcal{D}}$  is the closure of  $\mathcal{K}$  in  $\bar{\mathcal{D}}$ ). Assume that  $\tilde{\delta}$  and  $\tilde{\sigma}$  are radial (see Table 1.1 and Section 6.3) with the common zero at  $b \in \mathcal{D}$  or chordal (see Section 6.1) with the common zero at  $b \in \partial \mathcal{D}$ . Then  $T = +\infty$ .

*Proof.* Assume first that there exists a  $(\tilde{\delta}, \tilde{\sigma})$ -Löwner chain  $\{\tilde{g}_t\}_{t \in [0, \tilde{T})}$  ( $\tilde{T} \in (0, +\infty]$ ), a collection of hulls  $\{\tilde{\mathcal{K}}_t\}_{t \in [0, \tilde{T})}$  constructed as a reparametrization of  $\{\mathcal{K}_t\}_{t \in [0, T)}$  with some  $T \in (0, +\infty]$ , and a continuous strictly increasing  $\lambda : [0, T) \rightarrow [0, \tilde{T})$ . Such function  $\lambda$  is invertible and differentiable a.e. in  $[0, T)$ . Then define  $M_t$  by the relation (1.53) and conclude that it is also differentiable with respect to  $t$  a.e. due to the differentiability of  $g_t$  and  $\tilde{g}_t$ . Moreover, according to (1.29) and (1.33) we have

$$\dot{M}_t = \left( \dot{\lambda}_t H_{\tilde{u}_{\lambda_t}}[\tilde{\sigma}]_*^{-1} \tilde{\delta} - M_{t*} H_{u_t}[\sigma]_*^{-1} \delta \right) \circ M_t, \quad M_0 = \text{id}. \quad (1.54)$$

a.e. in  $[0, T)$ . From the fact that  $M_t$  is a Möbious automorphism it follows that the expression above in the parenthesis is a complete vector field for a.a.  $t$ .

We study now the conditions of completeness. Define the vector field

$$m(M, x, y, c) := c H_y[\tilde{\sigma}]_*^{-1} \tilde{\delta} - M_* H_x[\sigma]_*^{-1} \delta, \quad x, y \in \mathbb{R}, \quad c > 0, \quad M : \mathcal{D} \rightarrow \mathcal{D}. \quad (1.55)$$

It is complete if and only if the field

$$H_y[\tilde{\sigma}]_* m(M, x, y, c) = c \tilde{\delta} - \hat{M}_* \delta \quad (1.56)$$

is complete, where

$$\hat{M} := H_y[\tilde{\sigma}] \circ M \circ H_x[\sigma]^{-1}. \quad (1.57)$$

In general, it contains the sum of two poles at  $a \in \mathcal{D}$  of opposite signs because of the structure of  $\tilde{\delta}$  and  $\delta$ . Let us obtain the necessary and sufficient conditions for the pole

cancellation for  $M$ ,  $x$ ,  $y$ , and  $c$ . The positions of the poles must coincide as well as absolute values of the residues must be equal (for example, it is clear in the half-plane chart). These conditions are

$$\hat{M}(a) = a, \quad (1.58)$$

and

$$\begin{aligned} c \operatorname{res}_a \tilde{\delta} &= \operatorname{res}_a (\tilde{M} \delta) \quad \Leftrightarrow \\ c \tilde{\delta}_{-2} &= \delta_{-2} \left( (\tilde{M}^\psi)'(a) \right)^2 \quad \Leftrightarrow \\ c &= \frac{\delta_{-2}}{\tilde{\delta}_{-2}} \left( (\tilde{M}^\psi)'(a) \right)^2. \end{aligned} \quad (1.59)$$

Remark that  $(\tilde{M}^\psi)'(a) > 0$  does not depend on the choice of the chart  $\psi$  as well as the ratio  $\frac{\delta_{-2}}{\tilde{\delta}_{-2}}$ .

The first condition (1.58) holds uniquely as an implicit solution to  $y = y(x, M)$  (see (1.57)) due to the condition  $\tilde{\sigma}(a) \neq 0$ , at least for sufficiently small  $|x|$ ,  $|y|$ , and  $M$  close enough to the identity map. In the case of an elliptic  $\tilde{\sigma}$ , the function  $y(x, M)$  is unique up to the transform  $y \rightarrow y + kd$ ,  $k \in \mathbb{Z}$ , where  $d > 0$  is a minimal number such that  $H_d[\tilde{\sigma}] = \operatorname{id}$ .

Assume now

$$M = M_t, \quad x = u_t, \quad y = \tilde{u}_{\lambda_t}, \quad c = \dot{\lambda}_t, \quad (1.60)$$

which leads to

$$\hat{M} = \hat{M}_t = H_{\tilde{u}_{\lambda_t}}[\tilde{\sigma}] \circ M_t \circ H_{u_t}[\sigma]^{-1} \quad (1.61)$$

and

$$m(M_t, u_t, \tilde{u}_{\lambda_t}, \dot{\lambda}_t) = \dot{\lambda}_t H_{\tilde{u}_{\lambda_t}}[\tilde{\sigma}]_*^{-1} \tilde{\delta} - M_t \circ H_{u_t}[\sigma]_*^{-1} \delta, \quad (1.62)$$

which is exactly the vector field form (1.54). The condition (1.59) gives

$$\dot{\lambda}_t = \frac{\delta_{-2}}{\tilde{\delta}_{-2}} \left( (\hat{M}_t)'(a) \right)^2 \quad (1.63)$$

for a.a  $t \in [0, T)$ . On the other hand, the continuity of  $M_t'(a)$  follows from (1.53). This and (1.63) in their turn implies that  $\lambda_t$  is continuously differentiable in  $[0, T)$ , and that (1.63) holds for all  $t \in [0, T)$ , and not only a.e. Due to the property  $M_t'(a) > 0$  of the Möbius maps we also conclude that the inverse function  $\lambda^{-1}$  is continuously differentiable in  $[0, \tilde{T})$ .

Conditions (1.58) and (1.57) give

$$\tilde{u}_{\lambda_t} = y(M_t, u_t), \quad t \in [0, T), \quad (1.64)$$

Here we decrease the value of  $T$  according to the set of definition of  $y(M_t, u_t)$ . For an elliptic  $\tilde{\sigma}$  we impose the continuity condition and  $\tilde{u}_0 = 0$ . This fixes the mentioned above arbitrariness uniquely.

So, we have found  $\lambda_t$  as an integral functional of  $\{M_t\}_{t \in [0, T]}$  and  $\{u_t\}_{t \in [0, T]}$ :

$$\begin{aligned}
\lambda_t &= \frac{\delta_{-2}}{\bar{\delta}_{-2}} \int_0^t \left( (\hat{M}_\tau)'(a) \right)^2 d\tau = \\
&= \frac{\delta_{-2}}{\bar{\delta}_{-2}} \int_0^t \left( \left( H_{\tilde{u}_\tau}[\tilde{\sigma}] \circ M_\tau \circ H_{u_{\lambda_\tau}}[\sigma]^{-1} \right)'(a) \right)^2 d\tau = \\
&= \frac{\delta_{-2}}{\bar{\delta}_{-2}} \int_0^t \left( \left( H_{y(M_\tau, u_\tau)}[\tilde{\sigma}] \circ M_\tau \circ H_{u_\tau}[\sigma]^{-1} \right)'(a) \right)^2 d\tau, \\
&t \in [0, T),
\end{aligned} \tag{1.65}$$

where we have used (1.61) and (1.64).

The driving function  $\tilde{u}_{\tilde{t}}$  can be expressed now as

$$\tilde{u}_{\tilde{t}} = y(M_{\lambda_{\tilde{t}}^{-1}}, u_{\lambda_{\tilde{t}}^{-1}}), \quad \tilde{t} \in [0, \lambda_T^{-1}). \tag{1.66}$$

Substituting now (1.61), (1.64) and (1.63) in (1.54) gives the initial value problem

$$\begin{aligned}
\dot{M}_t &= \left( \frac{\delta_{-2}}{\bar{\delta}_{-2}} \left( \left( H_{y(M_t, u_t)}[\tilde{\sigma}] \circ M_t \circ H_{u_t}[\sigma]^{-1} \right)'(a) \right)^2 H_{y(M_t, u_t)}[\tilde{\sigma}]_*^{-1} \tilde{\delta} - \right. \\
&\quad \left. - M_t \circ H_{u_t}[\sigma]_*^{-1} \delta \right) \circ M_t,
\end{aligned} \tag{1.67}$$

$$M_0 = \text{id}.$$

which is defined by the driving function  $\{u_t\}_{t \in [0, T]}$  only. By the construction, it is a partial differential equation for  $M$  in  $[0, T) \times \mathcal{D}$  because it contains the derivatives of  $M_t^\psi(z)$  with respect to  $z$ . However, the family of Möbius automorphisms is 3-parametric. For example, in the half-plane chart, we have

$$M_t^{\mathbb{H}}(z) = \frac{a_t z + b_t}{c_t z + d_t}, \quad z \in \mathbb{H}, \quad a_t d_t - b_t c_t = 1 \tag{1.68}$$

(an explicit relations in the unit-disk chart are presented in [ITV14]). Thus, (1.67) is actually a system of 3 ordinary differential equations with continuous coefficients. Its solution always exists and is unique at least until some  $T_1 > 0$ . Moreover, if the chain  $\{\tilde{g}_t\}_{t \in [0, \tilde{T})}$  exists it is unique due to the uniqueness of the solution of (1.67) and due to the arguments above about the differentiability of  $\lambda_t$  and  $M_t$ .

In order to show the item 6, we construct the second chain  $\{\tilde{g}_{\tilde{t}}\}_{\tilde{t} \in [0, +\infty)}$ . Let us define  $\{\hat{M}_t\}_{t \in [0, \infty)}$  by condition (1.58) and

$$\hat{M}_t \circ G_t(b) = b. \tag{1.69}$$

If  $b \in \partial \mathcal{D}$ , then we can assume a chart  $\psi$  such that the boundary of  $D^\psi := \psi(\mathcal{D})$  is a straight line segment in a neighborhood of  $\psi(b)$  and we require in addition

$$(\hat{M}_t \circ G_t)'(b) = 1. \tag{1.70}$$

The derivative  $(G_t^\psi)'(\psi(b))$  is defined because  $b \notin \tilde{\mathcal{K}}_t$ ,  $t \in [0, +\infty)$ . Thus, the function  $\hat{M}_t$  is continuous in  $t \in [0, +\infty)$ . Define the time reparametrisation  $\{\lambda_t\}_{t \in [0, +\infty)}$  by the first line of (1.65), which is possible for  $t \in [0, +\infty)$  due to the continuity of  $(\hat{M}_t)'(a)$ . From another side, the properties of the radial and chordal Löwner equations ensure that  $\tilde{g}_t$  and  $\tilde{G}_t$  is defined for any collection of hulls such that  $b \notin \mathcal{K}_t$  until with some driving function  $\tilde{u}$ , and  $\tilde{G}_t = \hat{M}_{\lambda_t^{-1}} \circ G_{\lambda_t^{-1}}$ ,  $t \in [0, +\infty)$ . We use it now to define  $M_t$  for  $t \in [0, +\infty)$ .  $\square$

We remark that if the original chain  $\{g_t\}_{t \in [0, +\infty)}$  is defined only until some  $T' \in (0, +\infty)$  then the modification of the theorem is straightforward. The same is true for the reverse Löwner chains.

With the aid of this theorem we can extend the properties of the classical Löwner equation to general  $(\delta, \sigma)$ -Löwner chains. Following [Law08] we give define:

**Definition 1.2.** *We say that a collection of hulls  $\{\mathcal{K}_t\}_{t \in [0, \infty)}$  ( $\mathcal{K}_0 = \emptyset$ ) is **continuously increasing** if*

1. *The set*

$$U_t := \bigcap_{\varepsilon > 0} \mathcal{K}_{t+\varepsilon, t}, \quad t \in [0, +\infty) \quad (1.71)$$

*is a point at the boundary  $\partial \mathcal{D}$ , where*

$$\mathcal{K}_{t,s} := \mathcal{D} \setminus g_{t,s}(\mathcal{D}); \quad (1.72)$$

2. *The function  $U : [0, +\infty) \rightarrow \partial \mathcal{D}$  is continuous;*

3. *There exists a continuously differentiable time reparametrization*

$$\lambda : [0, +\infty) \rightarrow [0, +\infty)$$

*such that the family of hulls  $\{\mathcal{K}_{\lambda_t}\}_{t \in [0, +\infty)}$  is induced by some radial or chordal Löwner chain.*

**Proposition 1.4.** *The hulls induced by the radial or chordal Löwner equations are continuously increasing.*

*Proof.* This follows from the results of [Law08, Chapter 4] and from the formulation in the unit disk chart  $(\psi^{\mathbb{D}}(b) = 0)$  for the radial case and in the half-plane chart  $(\psi^{\mathbb{H}}(b) = \infty, \text{res}_a \tilde{\delta}^{\mathbb{H}} = 2)$  for the chordal case.  $\square$

**Corollary 1.1.** *Any continuously increasing collection of hulls  $\{\mathcal{K}_t\}_{t \in [0, +\infty)}$  can be induced by any  $(\delta, \sigma)$ -Löwner equation up to a continuously differentiable time reparametrisation at least until some maximal time  $T \in (0, +\infty]$ . The inverse is also true: a collection of hulls induced by a  $(\delta, \sigma)$ -Löwner equation is continuously increasing for  $t \in [0, +\infty)$ .*

*Proof.* It follows from Proposition 1.4 and Theorem 1.1.  $\square$

We call the point

$$z_t := g_t(U_t) \quad (1.73)$$

**tip** of the hull  $\mathcal{K}_t$ . Due to (1.58),  $\hat{M} = \tilde{G}_{\lambda_t} \circ G_t^{-1}$ , and the property of forward chordal or radial chains to map the tip to the source point (see [Law08]) we conclude that the same is true for general case of  $(\delta, \sigma)$ -Löwner chain

$$\begin{aligned} G_t(z_t) &= a, & t \in [0, +\infty), & \text{ in the forward case,} \\ G_t(a) &= z_t, & t \in [0, +\infty), & \text{ in the reverse case.} \end{aligned} \quad (1.74)$$

Besides, for the map  $g_t$  we have

$$\begin{aligned} g_t(z_t) &= H_{u_t}^{-1}[\sigma](a), & t \in [0, +\infty), & \text{ in the forward case,} \\ g_t \circ H_{u_t}^{-1}[\sigma](a) &= z_t, & t \in [0, +\infty), & \text{ in the reverse case.} \end{aligned} \quad (1.75)$$

We have studied how to construct a  $(\delta, \sigma)$ -Löwner chain for a given family of hulls. Consider now a fixed hull  $\mathcal{K} \subset \mathcal{D}$ . In general, for given  $\delta, \sigma$ , and  $\mathcal{K} \subset \mathbb{C}$  a  $(\delta, \sigma)$ -Löwner chain such that  $\mathcal{K} = \mathcal{K}_T$  for some  $(T \in [0, \infty))$  may not exist or can be not unique. For example, the radial chain does not exist if  $b \in \mathcal{K}$ . However, if  $\mathcal{K}$  is a simple curve we can state the following.

We will consider only simple curves that start from the source point  $a \in \partial \mathcal{D}$  and that are parametrized in an open interval. Namely, let  $\gamma: (0, T) \rightarrow \mathcal{D}$  (for some  $T \in (0, \infty]$ ) is an endomorphism such that  $\lim_{t \rightarrow +0} \gamma(t) = a$  and the limit  $\lim_{t \rightarrow -T} \gamma(t)$  may not exist. Let  $\mathcal{G}_{\mathcal{D}, a}$  be the space of all such curves up to a continuous reparametrization  $\lambda: [0, T) \rightarrow [0, \tilde{T})$  ( $\tilde{T} \in (0, \infty]$ ).

**Theorem 1.2.** *For any curve from  $\mathcal{G}_{\mathcal{D}, a}$  there exists a parametrization  $\gamma: (0, T) \rightarrow \mathcal{D}$ ,  $T \in (0, +\infty]$ , such that  $\{\gamma_{(0, t]}\}_{t \in [0, T)}$  is a continuously increasing family of hulls. In particular, for any pair of  $\delta$  and  $\sigma$  any simple curve contains a subcurve started from  $a \in \partial \mathcal{D}$  that can be induced by  $(\delta, \sigma)$ -Löwner chain for given  $\delta$  and  $\sigma$ , and a such chain is uniquely defined.*

*Proof.* This follows from the results in [Law08, Chapter 3, Chapter 4], in particular, from Remark 4.4.  $\square$

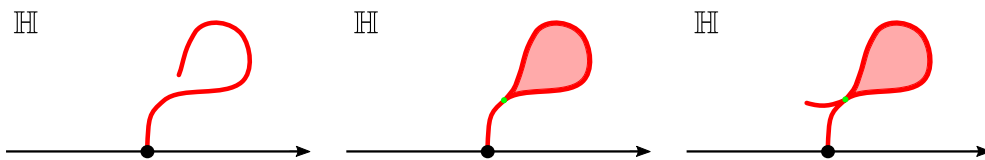


Figure 1.4: This figure illustrates how a slit curve  $\gamma_t$  (the red line) generates a hull  $\mathcal{K}_t$  (the red line and the pink interior) which is not a curve. The time  $t$  increases from left to right. The slit touches itself at the green point and swallows up the pink connected component of  $\mathbb{H} \setminus \gamma_t$ .

We remark that if the slit is not a simple curve but curve parametrized as  $\gamma(t) = G^{-1}(a)$  for the forward chain  $\{G_t\}_{t \in [0, +\infty)}$ , then The hull  $\mathcal{K}_t$  consist of the curve and all subsets of  $\mathcal{D}$  swallowed by the curve except one, where the map  $G_t$  is defined, see Fig. 1.4. In the classical cases, It is the connected component of  $\mathcal{D} \setminus \gamma_t$  that contains the



fixed points (see Sections 6.1.1, 6.2.1, and 6.3.1). In the general case of  $(\delta, \sigma)$ -Löwner chain, it is an interesting problem which of the components is swallowed.

It is important, but more difficult, to establish analogous results for curves that touch themselves or the boundary  $\partial \mathcal{D}$ . We do not discuss this problem here. However, if there is a simple normalization for the  $(\delta, \sigma)$ -Löwner chain maps such as for the classical cases, see (6.10), (6.46), and (6.87), then the existence is guaranteed by the Riemann mapping theorem and the uniqueness can be shown by Corollary 1.1.

It is also an interesting but not solved yet problem to specify the collection of hulls induced by  $(\delta, \sigma)$ -Löwner chain for arbitrary  $\delta$  and  $\sigma$  as we did for the classical cases discussed in Chapter 6. It would be also important to prove the following conjecture.

**Conjecture 1.1.** *For any pair of  $\delta$  and  $\sigma$  and for any hull  $\mathcal{K} \subset \mathcal{D}$  there exists at most one  $T \in [0, \infty)$  and at most one map  $G \in \mathcal{G}[\delta, \sigma]$  such that  $\mathcal{K} = \mathcal{D} \setminus G(\mathcal{D})$  for the forward case,  $\mathcal{K} = \mathcal{D} \setminus G^{-1}(\mathcal{D})$  for the reverse case, and  $G = G_T$  for some possible non-unique  $(\delta, \sigma)$ -Löwner chain  $\{G_t\}_{t \in [0, T]}$ .*

In other words, the chain  $\{G_t\}_{t \in [0, T]}$  may not be unique, but the value  $T \in [0, \infty)$  is unique (which is an interesting conformal invariant characteristic of the set  $\mathcal{K}$ ), besides, the final map  $G_T$  is also a unique possible. The proof of the conjecture is straightforward for the classical cases thanks to the simple normalization conditions. The parameter  $T$  is just related to the conformal radius for the radial case and the half-plane capacity for chordal case. However, for a general choice of  $\delta$  and  $\sigma$  the problem is still unsolved.

### 1.2.3 Equivalence and normalization of $(\delta, \sigma)$ -Löwner chains

A slit Löwner chain is determined by a triple  $(\delta, \sigma, u_t)$ . This correspondence, however, is not one-to-one. It may happen that different combinations of  $\delta$ ,  $\sigma$  and  $u_t$  produce the same Löwner chain  $\{g_t\}_{t \geq 0}$ . It may also happen that the resulting chains can be transformed one to another by means of a simple transformation, for instance, by a linear time reparameterization.

In this section, we define precisely what we mean by a ‘simple’, or **elementary transformation** of a triple  $(\delta, \sigma, u_t)$ . If two slit Löwner chains are determined by triples that can be transformed one into another by means of elementary transformations, we call such chains **essentially equivalent**.

In particular, we show that we can always find a representative in the equivalence class of triples so that the conditions

$$\delta_{-2} = \pm 2, \tag{1.76}$$

and

$$\sigma_{-1} = -1 \tag{1.77}$$

are satisfied.

If the vector fields  $\delta$  and  $\sigma$  are of the form (1.76) and (1.77), then we say that a general slit Löwner chain driven by  $\delta$  and  $\sigma$  is a **normalized slit Löwner chain**.

Below we list the transformations that we regard as elementary. We use the following notations  $\mathcal{V}_c$ ,  $\mathcal{I}_c$ ,  $\mathcal{D}_c$ ,  $\mathcal{R}_c$ , and  $\mathcal{S}_c$  with the index  $c$  for these transforms parametrized by  $c \in \mathbb{R}$  and the same letters without the index for the corresponding one-parametric

groups for automorphisms on the triples  $(\delta, \sigma, u_t)$ . We summarize the properties of the transformations described above in Table 1.3 together with a special combination of them

$$\mathcal{P}_c := \mathcal{V}_{e^c} \circ \mathcal{T}_{2^c} \circ \mathcal{I}_c. \quad (1.78)$$

that will be used in Section 1.3.2

#### Dilation of the driving function $\mathcal{V}$ .

Let  $c \in \mathbb{R} \setminus \{0\}$ . Then we define the transformation  $\mathcal{V}_c$  by the formula

$$\mathcal{V}_c : (\delta, \sigma, u_t) \mapsto (\delta, c\sigma, c^{-1}u_t). \quad (1.79)$$

The triple  $(\delta, \tilde{\sigma}, \tilde{u}_t) = (\delta, c\sigma, c^{-1}u_t)$  produces the same Löwner chain as the triple  $(\delta, \sigma, u_t)$ . In order to see this, note that the flow  $\{\tilde{H}_t[\tilde{\sigma}]\}_{t \in \mathbb{R}}$  differs from the flow of  $\{H_t[\sigma]\}_{t \in \mathbb{R}}$  only by time reparameterization,  $H_t[\tilde{\sigma}] = H_{ct}[\sigma]$ , so that

$$H_{\tilde{u}_t}[\tilde{\sigma}]_*^{-1} \delta = H_{u_t}[\sigma]_*^{-1} \delta. \quad (1.80)$$

#### Time dilation $\mathcal{T}$

For a constant  $c > 0$  we can consider the time reparameterized chain  $\{\tilde{g}_t\}_{t \geq 0}$ , where  $\tilde{g}_t = g_{ct}$ , and note that  $\{\tilde{g}_t\}_{t \geq 0}$  is generated by the triple  $(c\delta, \sigma, u_{ct})$ . Indeed,

$$\frac{\partial}{\partial t} \tilde{g}_t = (H_{u_{ct}}[\sigma]_*^{-1}(c\delta)) \circ \tilde{g}_t \quad (1.81)$$

This motivates us to define the transformation  $\mathcal{T}_c$

$$\mathcal{T}_c : (\delta, \sigma, u_t) \mapsto (c\delta, \sigma, u_{ct}), \quad c > 0. \quad (1.82)$$

The transformations  $\mathcal{V}_c$  and  $\mathcal{T}_c$  are sufficient for imposing the normalization conditions (1.76) and (1.77). Indeed, due to the fact that  $\sigma_{-1} \neq 0$ , we can apply  $\mathcal{V}_{1/\sigma_{-1}}$  and the transform  $(\delta, \sigma, u_t) \mapsto (\delta, \frac{\sigma}{\sigma_{-1}}, \sigma_{-1}u_t)$ , so that the vector field

$$\frac{\sigma}{\sigma_{-1}} = \ell_{-1} + \frac{\sigma_0}{\sigma_{-1}} \ell_0 + \frac{\sigma_1}{\sigma_{-1}} \ell_1 \quad (1.83)$$

has coefficient 1 at  $\ell_{-1}$ .

Then, since  $\delta_{-2} > 0$ , we apply  $\mathcal{T}_{2/\delta_{-2}}$ , so that the triple  $(\delta, \frac{\sigma}{\sigma_{-1}}, \sigma_{-1}u_t)$  is further transformed to

$$(\tilde{\delta}, \tilde{\sigma}, \tilde{u}_t) = \left( \frac{2\delta}{\delta_{-2}}, \frac{\sigma}{\sigma_{-1}}, \sigma_{-1}u_{\frac{2}{\delta_{-2}}t} \right) \quad (1.84)$$

and the vector field  $\tilde{\delta}$  has the coefficient 2 at  $\ell_{-2}$ .

**Drift  $\mathcal{D}$** 

We add a linear drift to the driving function  $u_t$  and simultaneously modify the field  $\delta$ :

$$\mathcal{D}_c : (\delta, \sigma, u_t) \mapsto (\delta - c\sigma, \sigma, u_t + ct), \quad c \in \mathbb{R}. \quad (1.85)$$

The new slit Löwner chain  $\{\tilde{g}_t\}_{t \geq 0}$  can be expressed as

$$\tilde{g}_t = H_{-ct}[\sigma] \circ g_t. \quad (1.86)$$

Indeed, due to (1.29) and (1.16),

$$\begin{aligned} \dot{\tilde{g}}_t &= \frac{\partial}{\partial t} H_{-ct}[\sigma] \circ g_t = (-c\sigma + H_{-ct}[\sigma]_* H_{u_t}[\sigma]_*^{-1} \delta) \circ H_{-ct}[\sigma] \circ g_t = \\ &= H_{u_t+ct}[\sigma]_*^{-1} (\delta - c\sigma) \circ \tilde{g}_t. \end{aligned} \quad (1.87)$$

For a differentiable  $u_t$  this is straightforward from (1.32).

We can apply  $\mathcal{D}_c$  with  $c = \frac{\frac{3}{2}\delta_{-2}\sigma_0 - \delta_{-1}}{\sigma_{-1}}$ , so that the coefficients in the normalized fields  $\tilde{\delta}$  and  $\tilde{\sigma}$  satisfy the following normalization condition

$$2 \frac{\delta_{-1}}{\delta_{-2}} - 3 \frac{\sigma_0}{\sigma_{-1}} = 0. \quad (1.88)$$

This particular choice is motivated by the stochastic equation that we consider below. In particular, this restriction appears in Theorem 1.3, Section 3.1, the end of Section 3.2, and Theorem 5.3.

**Parabolic Möbius transform  $\mathcal{R}$** 

This elementary transform is related to a homomorphic automorphism  $H_c[\ell_1] : \mathcal{D} \rightarrow \mathcal{D}$ ,  $c \in \mathbb{R}$  of  $\mathcal{D}$  induced by the vector field  $\ell_1^{\mathbb{H}}(z) = z^2$  which has a double zero at the point  $a$ . The map  $H_c[\ell_1]_*$  preserves the form (1.36) of  $\delta$  and  $\sigma$ . In the half-plane chart we have

$$H_c[\ell_1]^{\mathbb{H}} = \frac{z}{1 - cz}, \quad c \in \mathbb{R}. \quad (1.89)$$

The transformation  $\mathcal{R}_c$  is defined by

$$\mathcal{R}_c : (\delta, \sigma, u_t) \mapsto (H_c[\ell_1]_* \delta, H_c[\ell_1]_* \sigma, u_t), \quad c \in \mathbb{R}. \quad (1.90)$$

The new chain  $\{\tilde{g}_t\}_{t \geq 0}$  can be related to the original chain by  $\tilde{g}_t = H_c[\ell_1] \circ g_t \circ H_c[\ell_1]^{-1}$  with the aid of (1.29). This transform changes the hull as  $K_t \rightarrow \tilde{K}_t = H_c[\ell_1](K_t)$ .

We present how the components  $\delta_n, \sigma_n$  of the fields  $\delta$  and  $\sigma$  are transformed under the action of  $H_c[\ell_1]_*$  in the table 1.3.

Application of  $\mathcal{R}_c$  preserves the normalization conditions (1.76), (1.77) and (1.88).

**Hyperbolic Möbius transform  $\mathcal{S}$  (space dilation)**

The transformation  $\mathcal{S}_c$  ( $c \in \mathbb{R}$ ) is analogous to  $\mathcal{R}_c$ , except for the fact that we use the holomorphic automorphisms  $H_c[\ell_0]$  generated by  $\ell_0$  in this case. The vector field

$\ell_0(z) = z$  has a simple zero at the source point  $a$ . the map  $H_c[\ell_0]_*$ , as well as  $H_c[\ell_1]_*$ , preserves the form (1.36) of  $\delta$  and  $\sigma$ .

In the half-plane chart  $H_c[\ell_0]$  is simply the multiplication by the real constant  $e^{-c}$ , i.e.,

$$H_c[\ell_0]^{\mathbb{H}}(z) = e^c z. \quad (1.91)$$

This motivates the term ‘space dilation’. In the unit disk chart,

$$H_c[\ell_0]^{\mathbb{D}}(z) = \tau_{\mathbb{D},\mathbb{H}} \circ H_c[\ell_0]^{\mathbb{H}} \circ \tau_{\mathbb{H},\mathbb{D}} = \frac{e^{-\frac{c}{2}}(1+z) - e^{\frac{c}{2}}(1-z)}{e^{-\frac{c}{2}}(1+z) + e^{\frac{c}{2}}(1-z)} \quad (1.92)$$

is a Möbius automorphism of  $\mathbb{D}$  that keeps the points  $z = \pm 1$  fixed

The transformation  $\mathcal{S}\mathcal{R}_c$  is defined by

$$\mathcal{S}_c : (\delta, \sigma, u_t) \mapsto (H_c[\ell_0]_* \delta, H_c[\ell_0]_* \sigma, u_t), \quad c \in \mathbb{R}. \quad (1.93)$$

The new chain  $\{\tilde{g}_t\}_{t \geq 0}$  can be related to the original chain by  $\tilde{g}_t = H_c[\ell_0] \circ g_t \circ H_c[\ell_0]^{-1}$  with the aid of (1.29). This transform changes the hull as  $K_t \rightarrow \tilde{K}_t = H_c[\ell_t](K_t)$ .

We present how the components  $\delta_n, \sigma_n$  of the fields  $\delta$  and  $\sigma$  are transformed under the action of  $H_c[\ell_0]_*$  in Table 1.3.

Application of  $\mathcal{S}_c$  keeps the normalization conditions (1.76), (1.77) and (1.88) unchanged.

### The structure of the family of essentially different $(\delta, \sigma)$ -Löwner chains

The collection of the slit Löwner chains given by  $\delta$  and  $\sigma$  as in (1.36) can be considered as a 7-parametric space  $\mathbb{R}^{\times 5} \times (\mathbb{R} \setminus \{0\})^2$ , where one term  $(\mathbb{R} \setminus \{0\})$  corresponds to  $\delta_{-2} \neq 0$  and  $\mathbb{R} \setminus \{0\}$  corresponds to  $\sigma_{-1} \neq 0$ . The group  $\mathcal{G}$  generated by 5 elementary transforms introduced above forms equivalence classes of **essentially equivalent** Löwner chains. Thus, the family of essentially different forward chains can be represented by the factor space  $\mathbb{R}^{\times 5} \times \mathbb{R}^+ \times (\mathbb{R} \setminus \{0\})/\mathcal{G}$ . The classical chordal, dipolar and radial chains are represented by three single points in this 2-dimensional space.

To specify this factorized collection of Löwner chains we have already introduced 3 normalization conditions (1.76), (1.77) and (1.88) above. Using the last two transforms  $\mathcal{R}$  and  $\mathcal{S}$ , 2 more parameters can be fixed, but it is not reasonable to introduce such restriction in this text.

Action of the transformation							
	$\delta \mapsto$	$\delta_n$	$\sigma \mapsto$	$\sigma_n$	$u_t \mapsto$	$g_t \mapsto$	$K_t \mapsto$
$\mathcal{V}_c$	$\delta$	$\delta_n \rightarrow \delta_n$	$c\sigma$	$\sigma_n \rightarrow c\sigma_n$	$c^{-1}u_t$	$g_t$	$K_t$
$\mathcal{T}_c$	$c\delta$	$\delta_n \mapsto c\delta_n$	$\sigma$	$\sigma_n \mapsto \sigma_n$	$u_{ct}$	$g_{ct}$	$K_{ct}$
$\mathcal{D}_c$	$\delta - c\sigma$	$\delta_{-2} \mapsto \delta_{-2}$ $\delta_{-1} \mapsto \delta_{-1} - c\sigma_{-1}$ $\delta_0 \mapsto \delta_0 - c\sigma_0$ $\delta_1 \mapsto \delta_1 - c\sigma_1$	$\sigma$	$\sigma_n \mapsto \sigma_n$	$u_t + ct$	$H_{-ct}[\sigma] \circ g_t$	$K_t$
$\mathcal{R}_c$	$H_c[\ell_1]_* \delta$	$\delta_{-2} \mapsto \delta_{-2}$ $\delta_{-1} \mapsto \delta_{-1} - 3c\delta_{-2}$ $\delta_0 \mapsto \delta_0 - 2c\delta_{-1} + 3c^2\delta_{-2}$ $\delta_1 \mapsto \delta_1 - c\delta_0 + c^2\delta_{-1} - c^3\delta_{-2}$	$H_c[\ell_1]_* \sigma$	$\sigma_{-1} \mapsto \sigma_{-1}$ $\sigma_0 \mapsto \sigma_0 - 2c\sigma_{-1}$ $\sigma_1 \mapsto \sigma_1 - c\sigma_0 + c^2\sigma_{-1}$	$u_t$	$H_c[\ell_1] \circ g_t \circ H_c[\ell_1]^{-1}$	$H_c[\ell_1](K_t)$
$\mathcal{S}_c$	$H_c[\ell_0]_* \delta$	$\delta_n \mapsto e^{nc} \delta_n$	$H_c[\ell_0]_* \sigma$	$\sigma_n \mapsto e^{nc} \sigma_n$	$u_t$	$H_c[\ell_0] \circ g_t \circ H_c[\ell_0]^{-1}$	$H_c[\ell_0](K_t)$
$\mathcal{P}_c$	$e^{2c} H_c[\ell_0] \delta$	$\delta_{-2} \mapsto \delta_{-2}$ $\delta_{-1} \mapsto e^c \delta_{-1}$ $\delta_0 \mapsto e^{2c} \delta_0$ $\delta_1 \mapsto e^{3c} \delta_1$	$e^c H_c[\ell_0]_* \sigma$	$\sigma_{-1} \mapsto \sigma_{-1}$ $\sigma_0 \mapsto e^c \sigma_0$ $\sigma_1 \mapsto e^{2c} \sigma_1$	$e^{-c} u_{e^{2c}t}$	$H_c[\ell_0] \circ g_{e^{2c}t} \circ H_c[\ell_0]^{-1}$	$H_c[\ell_0](K_{e^{2c}t})$

Table 1.3: Elementary transformations of slit Löwner chains. The last transform  $\mathcal{P}_c$  is just the composition  $\mathcal{P}_c := \mathcal{V}_{e^c} \circ \mathcal{T}_{e^{2c}} \circ \mathcal{S}_c$ , see the text for the motivation.

### 1.3 Slit holomorphic stochastic flow or $(\delta, \sigma)$ -SLE

This section is dedicated to the central object of this monograph called the slit holomorphic stochastic flow or  $(\delta, \sigma)$ -SLE. The author prefers the second name to highlight that it is a version of the Schramm-Löwner evolution.

#### 1.3.1 Definition and basic properties

Let  $(\Omega, \mathcal{F}, P)$  be a probability, space and let  $A$  and  $B$  be two random variables taking values in a measurable space  $S$ . We denote by  $\text{Law}[A]$  the induced measure on  $S$ . We say that the laws of  $A$  and  $B$  are **identical** (equivalently,  $A$  and  $B$  **agree in law**):

$$\text{Law}[A] = \text{Law}[B] \quad (1.94)$$

if the following expectations are equal

$$\mathbb{E}[f(A)] = \mathbb{E}[f(B)] \quad (1.95)$$

for any bounded measurable functions  $f : S \rightarrow \mathbb{R}$ . More generally, an equality of conditional random laws

$$\text{Law}[A \mid \mathcal{F}_1] = \text{Law}[B \mid \mathcal{F}_2] \quad (1.96)$$

is, by definition, the identity

$$\mathbb{E}[f(A) \mid \mathcal{F}_1](\omega) = \mathbb{E}[f(B) \mid \mathcal{F}_2](\omega) \quad \text{a.s.} \quad (1.97)$$

for any bounded  $\mathcal{F}$ -measurable functions  $f : S \rightarrow \mathbb{R}$ . One can understand a conditional law as a law parametrized by  $\omega$ .

Let  $\{B_t\}_{t \in [0, +\infty)}$  be the standard Brownian motion naturally adapted to a filtration  $\{\mathcal{F}_t\}_{t \in [0, +\infty)}$  of a filtered probability space

$$(\Omega^B, \{\mathcal{F}_t^B\}_{t \in [0, +\infty)}, P^B). \quad (1.98)$$

Define

$$\mathcal{F}_T := \{B \in \mathcal{F}^B : B \cap \{t \leq T\} \in \mathcal{F}_t^B, \forall t \in [0, +\infty)\}. \quad (1.99)$$

The following statement is known as the **strong Markov property of the Brownian motion**

$$\text{Law}[\{B_{s+T} - B_T\}_{s \in [0, +\infty)}] = \text{Law}[\{B_s\}_{s \in [0, \infty)}] \quad (1.100)$$

and  $\{B_{s+T} - B_T\}_{s \in [0, \infty)}$  is independent of  $\mathcal{F}_T$  for any stopping time  $T < +\infty$  a.s. We consider  $\{B_s\}_{s \in [0, \infty)}$  as a random variable taking values in the space  $C_{[0, +\infty)}^0$  of the continuous functions  $B : [0, +\infty) \rightarrow \mathbb{R}$  such that  $B_0 = 0$ .

One of the consequences of the strong Markov property is

$$\text{Law}[B_s \mid \mathcal{F}_T] = \text{Law}[B_s \mid B_T], \quad s \in [0, \infty) \quad (1.101)$$

for any stopping time  $T < +\infty$  a.s. In particular, we have

$$\text{Law}[B_s \mid \mathcal{F}_t^B] = \text{Law}[B_s \mid B_t], \quad t, s \in [0, \infty), \quad (1.102)$$

which is known as the **simple Markov property** of  $\{B_t\}_{t \in [0, +\infty)}$ . Here and below, under a conditional expectation (or conditional law) with respect to a random variable  $X$  we mean the expectation (or the law) with respect to the sigma-algebra  $\mathcal{F}_X$  generated by  $X$ .

We are ready now to discuss a stochastic version of the  $(\delta, \sigma)$ -Löwner equation. We just equip the driving function  $u_t$  with the Brownian measure

$$u_t := B_t, \quad t \geq 0. \quad (1.103)$$

Equivalently, we formulate the following definition.

**Definition 1.3.** *Let  $\delta$  and  $\sigma$  be as in (1.36), and let  $\{B_t\}_{t \geq 0}$  be the standard Brownian motion. Then the solution to the stochastic differential equation in the Stratonovich form*

$$d^S G_t = \delta \circ G_t dt + \sigma \circ G_t d^S B_t, \quad G_0 = \text{id}, \quad (1.104)$$

*is called a forward (reverse) slit holomorphic stochastic flow or forward (reverse)  $(\delta, \sigma)$ -SLE.*

The stochastic differential equation (1.104) is a convenient form to write down the Stratonovich integral equation.

$$\int_0^t G_\tau d^S B_\tau = \int_0^t \delta \circ G_\tau d\tau + \int_0^t \sigma \circ G_\tau d^S B_\tau. \quad (1.105)$$

We use the notation ‘ $d^S$ ’ ( $d^{\text{It}\hat{o}}$ ) to mark that the integral are taken in the Stratonovich ( $\text{It}\hat{o}$ ) sense. The relation between these two integrals are given in, e.g. [Gar82, Section 4.3.6] and in Appendix A.

The Stratonovich form is more convenient in our setup than a more frequently used  $\text{It}\hat{o}$  form. The equation (1.104) in the  $\text{It}\hat{o}$  form is

$$\begin{aligned} d^{\text{It}\hat{o}} G_t^\psi(z) &= \left( \delta^\psi + \frac{1}{2} \sigma^\psi \sigma^{\psi'} \right) \circ G_t^\psi(z) dt + \sigma^\psi \circ G_t^\psi(z) d^{\text{It}\hat{o}} B_t, \\ G_0^\psi(z) &= z, \end{aligned} \quad (1.106)$$

choosing some chart  $\psi$ . A disadvantage of the  $\text{It}\hat{o}$  form is that the expression in parenthesis of (1.106) transforms from chart to chart in a complicated manner, whereas the functions  $\delta$  and  $\sigma$  in the Stratonovich form (1.104) transform as vector fields.

An equivalent definition of  $(\delta, \sigma)$ -SLE can be given in terms of  $\{g_t\}_{t \in [0, +\infty)}$  and equation (1.34) if we equip the set of driving function  $\{u_t\}_{t \in [0, +\infty)}$  with the Brownian measure by

$$u_t := B_t, \quad t \in [0, +\infty). \quad (1.107)$$

The existence and uniqueness of the solution to (1.104) can be directly obtained from the existence and uniqueness of the solution to (1.34) for each sample of  $u_t = B_t$ . An alternative approach is to use a general theory of stochastic differential equations and flows, see, for instance, [Pro04]. The main difficulty of this way is that the function  $\delta^\psi(z)$  does not possess the Lipschitz condition.

Since there is at most one driving function for a given chain, we have the following one-to-one correspondence

$$\{B_t\}_{t \in [0, \infty)} \longleftrightarrow \{G_t\}_{t \in [0, \infty)} \quad (1.108)$$

for each fixed pair  $(\delta, \sigma)$ . Thereby, the  $(\delta, \sigma)$ -Löwner chain  $\{G_t\}_{t \in [0, +\infty)}$  is a random variable on the same probability space (1.98) as the Brownian motion  $B_t$ . Moreover, the chain  $\{G_s\}_{s \in [0, t]}$  is a  $\mathcal{F}_t^B$ -measurable random variable defined by the one-to-one correspondence

$$\{B_s\}_{s \in [0, t]} \longleftrightarrow \{G_s\}_{s \in [0, t]}. \quad (1.109)$$

Using the map

$$\{G_s\}_{s \in [0, t]} \mapsto G_t \quad (1.110)$$

we can define a stochastic process  $\{G_t\}_{t \in [0, +\infty)}$  taking values in  $\mathcal{G}[\delta, \sigma]$  adopted to the filtration  $\{\mathcal{F}_t^B\}_{t \in [0, +\infty)}$ .

From the strong Markov property of the Brownian motion (1.100) and (1.108) we conclude that

$$\text{Law}[\{G_{t+T} \circ G_T^{-1}\}_{t \in [0, +\infty)}] = \text{Law}[\{G_t\}_{t \in [0, \infty)}] \quad (1.111)$$

and independent of  $\mathcal{F}_T$  for any stopping time  $T < +\infty$  a.s. This property of the random law of the Löwner chains  $\{G_t\}_{t \in [0, +\infty)}$  can be called the **strong Markov property of  $(\delta, \sigma)$ -SLE**. From the properties of  $\{B_t\}_{t \in [0, +\infty)}$  and from the relation (1.42) it follows that the process  $\{G_t\}_{t \in [0, +\infty)}$  possesses also the simple Markov property:

$$\text{Law}[G_{t+s} \mid \mathcal{F}_t] = \text{Law}[G_{t+s} \mid G_t], \quad s, t \geq 0. \quad (1.112)$$

Equivalently,

$$\mathbb{E}[f(G_{t+s}) \mid \mathcal{F}_t](\omega) = \mathbb{E}[f(G_{t+s}) \mid \mathcal{F}_{G_t}](\omega), \quad \text{a.s.}, \quad s, t \geq 0 \quad (1.113)$$

for any bounded measurable function  $f: \mathcal{G}[\delta, \sigma] \rightarrow \mathbb{R}$  which is bounded and measurable with respect to the sigma-algebra on  $\mathcal{G}[\delta, \sigma]$  generated by  $\{B_\tau\}_{\tau \in [0, t+s]}$ . We denote by  $\mathcal{F}_{G_t}$  the sigma-algebra on  $\Omega_B$  induced by the random variable  $G_t$ . Moreover, the random conformal maps  $G_{t+s, s} := G_{t-s} \circ G_t^{-1}$  and  $G_s$  are independent for  $t, s \geq 0$ . More generally, for any finite collection of times  $t_1 > t_2 > t_3 > \dots > t_n \geq 0$  the random variables  $G_{t_1, t_2}, G_{t_2, t_3}, \dots, G_{t_{n-1}, t_n}$  are independent thanks to the independence of  $B_{t_1} - B_{t_2}, B_{t_2} - B_{t_3}, \dots, B_{t_{n-1}} - B_{t_n}$  and (1.41). If we take into account that  $\mathcal{G}[\delta, \sigma]$  is a semigroup with respect to the composition, the last property can be interpreted as the ‘independence of semigroup increments’.

Thanks to the map

$$G_t \mapsto \mathcal{K}_t = \mathcal{D} \setminus G_t(\mathcal{D}) \quad (1.114)$$

there is a  $\mathcal{F}_t^B$ -process on the subsets of  $\mathcal{D}$ . The strong Markov property of random maps  $G_t$  can be extended to the random law on the subsets  $\mathcal{K}_t$  if the Conjecture 1.1 is true:

$$\text{Law}[\{G_T(\mathcal{K}_{t+T} \setminus \mathcal{K}_T)\}_{t \in [0, +\infty)}] = \text{Law}[\{\mathcal{K}_t\}_{t \in [0, +\infty)}]. \quad (1.115)$$

According to the results of Section 1.2 this is true at least for the classical cases (due to the normalization conditions), and when  $\mathcal{K}_t$  is a simple curve a.s. (due to Theorem 1.2). We study when  $\mathcal{K}_t$  is a simple curve in Section 1.3.3.



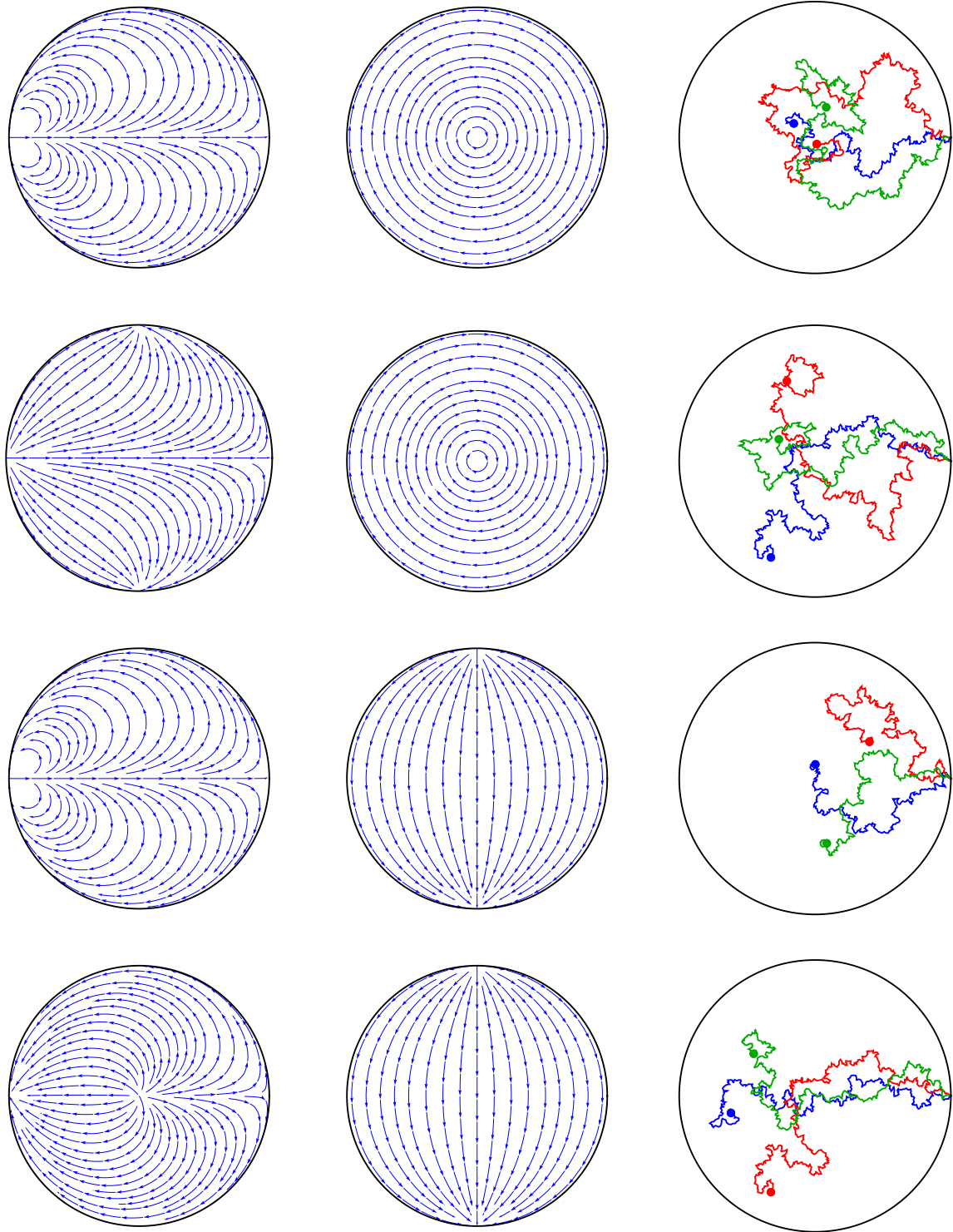


Figure 1.5: Samples of the  $(\delta, \sigma)$ -SLE slits (in the right column) for different choices of  $\delta$  (the left column) and  $\sigma$  (the central column). We use the normalization from Section 1.3.2 and  $\kappa = 2$ . Each of the four strings corresponds to some choice of  $\delta$  and  $\sigma$ . We pick these four combinations just for illustration, they do not have any special properties. Some other combinations are studied in Chapter 6.

### 1.3.2 Equivalence and normalization of $(\delta, \sigma)$ -SLE

We now use the results of Section 1.2.3 to study how the elementary transformations change the random law on the driving function  $u_t = B_t$ . We remark that the transforms  $\mathcal{V}$ ,  $\mathcal{T}$ , and  $\mathcal{D}$  change the random law as follows:

$$\mathcal{V}_c : B_t \mapsto c^{-1}B_t, \quad (1.116)$$

$$\mathcal{T}_c : B_t \mapsto B_{ct} = c^{\frac{1}{2}}\tilde{B}_t, \quad (1.117)$$

$$\mathcal{D}_c : B_t \mapsto B_t + ct, \quad (1.118)$$

where  $\tilde{B}_t$  is a another sample of the standard Brownian motion. The transforms  $\mathcal{R}$  and  $\mathcal{S}$  do not change the law of  $B_t$ .

Using the transform

$$\mathcal{T}_{c^2} \circ \mathcal{V}_c \quad (1.119)$$

with  $c = 2/\delta_{-2}$  we can impose the normalisation condition (1.76) keeping the random law of the deriving function unchanged. The equation (1.104) takes the form

$$d^S G_t = \underline{\delta} \circ G_t dt + \underline{\sigma} \circ G_t \sqrt{\kappa} d^S B_t, \quad G_0 = \text{id}, \quad (1.120)$$

where we defined a parameter

$$\kappa := \frac{2\sigma_{-1}^2}{\delta_{-2}} \quad (1.121)$$

and denote the normalized  $\delta$  and  $\sigma$  with the underline:

$$\begin{aligned} \underline{\delta} &= \pm (2\ell_{-2} + \underline{\delta}_{-1}\ell_{-1} + \underline{\delta}_0\ell_0 + \underline{\delta}_1\ell_1) \\ \underline{\sigma} &= -\ell_{-1} + \underline{\sigma}_0\ell_0 + \underline{\sigma}_1\ell_1 \end{aligned} \quad (1.122)$$

This definition of  $\kappa$  agrees with its analog from the classical chordal, dipolar, and radial cases. It will be clear below that the parameter  $\kappa$  defined this way is responsible for the local geometric properties of the hull  $\mathcal{K}_t$  in general case as well. We will often assume below that  $\delta$  and  $\sigma$  are normalized and drop the underline.

The transform  $\mathcal{R}$  keeps the form of (1.120) unchanged because it has no influence on the driving function  $B_t$  and on the normalizations (1.76) and (1.77). The transform  $\mathcal{P}$  introduced at the end of Section 1.2.3 acts on the driving function as

$$\mathcal{P}_c : B_t \mapsto e^{-c}B_{e^{2c}t} =: \tilde{B}_t \quad (1.123)$$

and does not change the random law of the Brownian motion. On the other hand,  $\mathcal{P}$  does not change normalisation conditions (1.76) and (1.77) introduced above.

In addition, we can use the transform  $\mathcal{D}$  to impose (1.88). After that, we have

$$d^S G_t = \underline{\delta} \circ G_t dt + \underline{\sigma} \circ G_t (\sqrt{\kappa} d^S B_t + \nu dt), \quad G_0 = \text{id}, \quad (1.124)$$

where the parameter  $\nu$  is chosen such that the additional (drift) normalization condition

$$\underline{\delta}_{-1} + 3\underline{\sigma}_0 = 0 \quad (1.125)$$

is satisfied.

The parameter  $\nu$  can be defined by

$$\nu := \frac{\sqrt{2}\delta_{-1}}{\sqrt{\delta_{-2}}} - \frac{3\sqrt{\delta_{-2}}\sigma_0}{\sqrt{2}\sigma_{-1}}. \quad (1.126)$$

The transform  $\mathcal{P}$  preserves  $\kappa$ , but changes  $\nu$  as

$$\mathcal{P}_c: \nu \mapsto e^c \nu. \quad (1.127)$$

Thereby, there are 3 nonequivalent cases:  $\nu = 0$ ,  $\nu > 0$ , and  $\nu < 0$ . Each case is invariant with respect to  $\mathcal{P}$ . The case  $\nu = 0$  we call **driftless**. The last two cases are the mirror images of each other.

The relations (1.125) and (1.126) will be motivated below (in Theorems 1.3 and 5.3). For now we just remark that (1.125) is invariant with respect to  $\mathcal{R}$  and  $\mathcal{P}$ . The right-hand side of (1.126) is invariant with respect to  $\mathcal{S}$  and  $\mathcal{R}$ . In particular,  $\nu$  does not depend on the choice of the basis vectors  $\ell_n$  if one of the poles is placed at the source point  $a \in \partial \mathcal{D}$ .

From above we conclude that the family of **essentially different**  $(\delta, \sigma)$ -SLEs is two-parametric ( $7 - 2 - 1 - 2 = 2$ ) and each  $(\delta, \sigma)$ -SLE is in addition parametrized by  $\kappa > 0$  and  $\nu \in \mathbb{R}$ . The classical chordal, radial and dipolar equations are just elements of this 2-parametric set. We emphasise that both of  $\kappa$  and  $\nu$  are parameters related to the stochastic version of the Löwner equation only. In the deterministic case they can always be absorbed by the driving function after the transforms  $\mathcal{V}$  and  $\mathcal{D}$ .

### 1.3.3 Relations between essentially different $(\delta, \sigma)$ -SLEs

In Section 1.2.2, we showed that any  $(\delta, \sigma)$ -Löwner chain  $\{G_t\}_{t \in [0, +\infty)}$  after the transform

$$\tilde{G}_{\tilde{t}} = \hat{M}_{\tilde{t}} \circ G_{\lambda_{\tilde{t}}}, \quad \tilde{t} \in [0, \tilde{T}) \quad (1.128)$$

is a  $(\tilde{\delta}, \tilde{\sigma})$ -Löwner chain for a given pair of  $\tilde{\delta}$  and  $\tilde{\sigma}$  and some properly chosen  $\{\hat{M}_{\tilde{t}}\}_{\tilde{t} \in [0, \tilde{T})}$  and  $\{\lambda_{\tilde{t}}\}_{\tilde{t} \in [0, \tilde{T})}$ . It will be convenient in this setup to parametrize the map  $M$  by  $\tilde{t}$  but not  $t$  and to define the time reparametrization in the inverse way  $\lambda: [0, \tilde{T}) \rightarrow [0, T)$ . In this subsection, we consider a stochastic analogous of this proposition. Namely, we ask how the random law on the driving functions changes under this transform. We establish that, in general case, the initial Brownian random law on the driving functions  $\{u_t\}_{t \in [0, +\infty)}$  of  $\{G_t\}_{t \in [0, +\infty)}$  and the transformed random law on  $\{\tilde{u}_{\tilde{t}}\}_{\tilde{t} \in [0, +\infty)}$  of  $\{\tilde{G}_{\tilde{t}}\}_{\tilde{t} \in [0, +\infty)}$  are absolutely continuous with respect to each other. This has far reaching consequences for the local properties of  $\mathcal{K}_t$ . Moreover, in some cases, the law of  $\{\tilde{u}_{\tilde{t}}\}_{\tilde{t} \in [0, \tilde{T})}$  is also Brownian. A special case of this for the chordal and radial SLEs was considered before in [SW05].

**Theorem 1.3.** *The random laws on  $\{\mathcal{K}_t\}_{t \in [0, \infty)}$  and  $\{\tilde{\mathcal{K}}_{\tilde{t}}\}_{\tilde{t} \in [0, \infty)}$  generated by a forward  $(\delta, \sigma)$ -SLE and the forward  $(\tilde{\delta}, \tilde{\sigma})$ -SLE correspondingly with the same  $\kappa$  are locally equivalent until some stopping time  $T > 0$  modulo some random strictly increasing time change  $\lambda: [0, \tilde{T}) \rightarrow [0, T)$ . Moreover, if  $\kappa = 6$  and if both SLEs are driftless, then the random laws of  $\tilde{\mathcal{K}}_{\lambda_{\tilde{t}}}$  and  $\tilde{\mathcal{K}}_{\tilde{t}}$  are identical for  $\tilde{t} \in [0, \tilde{T})$ .*

‘Locally’ means that the equivalence is valid until each stopping time  $T_n > 0$  from some collection  $\{T_n\}_{n=1,2,3,\dots}$  such as  $T_n \geq T_m$  if  $n > m$  and  $T_n \rightarrow T$  a.s. when  $n \rightarrow \infty$ .

*Proof.* We use the results of the proof of Theorem 1.1. Assume  $u_t$  and  $\tilde{u}_{\tilde{t}}$  are some continuous Itô processes, Then the stochastic version of formula (1.54) is

$$d^S \hat{M}_{\tilde{t}} \circ \hat{M}_{\tilde{t}}^{-1} = \left( \tilde{\delta} d\tilde{t} + \tilde{\sigma} d^S \tilde{u}_{\tilde{t}} \right) - \dot{\lambda}_{\tilde{t}} \hat{M}_{\tilde{t}*} (\delta d\tilde{t} + \sigma d^S u_{\lambda_{\tilde{t}}}) \quad (1.129)$$

It will be convenient to consider this relation in the half-plane chart. The expression for  $\hat{M}_{\tilde{t}}^{\mathbb{H}}: \mathbb{H} \rightarrow \mathbb{H}$  is

$$\hat{M}_{\tilde{t}}^{\mathbb{H}}(z) = \frac{\alpha_{\tilde{t}} z}{1 + \beta_{\tilde{t}} z}, \quad z \in \mathbb{H}, \quad (1.130)$$

for some real-valued stochastic processes  $\{\alpha_{\tilde{t}}\}_{\tilde{t} \in [0, \tilde{T}]}$  and  $\{\beta_{\tilde{t}}\}_{\tilde{t} \in [0, \tilde{T}]}$ . Since  $G_0 = \tilde{G}_0 = \text{id}$  we impose the initial conditions

$$\alpha_0 = 1, \quad \beta_0 = 0. \quad (1.131)$$

For  $(\hat{M}_{\tilde{t}*} \nu)^{\mathbb{H}}(z)$  we have

$$(\hat{M}_{\tilde{t}*} \nu)^{\mathbb{H}}(z) = \frac{(\alpha_{\tilde{t}} - \beta_{\tilde{t}} z)^2}{\alpha_{\tilde{t}}} \nu^{\mathbb{H}} \left( \frac{z}{\alpha_{\tilde{t}} - \beta_{\tilde{t}} z} \right), \quad z \in \mathbb{H}. \quad (1.132)$$

Expand both sides of the identity (1.129) into the Laurent series with respect to  $z$  and impose the normalization (1.122). The coefficients at  $z^{-1}$  give

$$0 = 2 - 2 \alpha_{\tilde{t}}^2 \dot{\lambda}_{\tilde{t}} \Leftrightarrow \alpha_{\tilde{t}} = \frac{1}{\sqrt{\dot{\lambda}_{\tilde{t}}}}, \quad (1.133)$$

We remind that  $\dot{\lambda}_{\tilde{t}} > 0$ ,  $\tilde{t} \in [0, \tilde{T})$  a.s.

The coefficients at  $z^0$  give

$$0 = \tilde{\delta}_{-1} d\tilde{t} - d^S \tilde{u}_{\tilde{t}} + 6 \dot{\lambda}_{\tilde{t}} \alpha_{\tilde{t}} \beta_{\tilde{t}} d\tilde{t} - \dot{\lambda}_{\tilde{t}} \alpha_{\tilde{t}} \delta_{-1} d\tilde{t} + \dot{\lambda}_{\tilde{t}} \alpha_{\tilde{t}} d^S u_{\lambda_{\tilde{t}}}, \quad (1.134)$$

and we conclude that

$$d^S \tilde{u}_{\tilde{t}} = \left( 6 \dot{\lambda}_{\tilde{t}}^{\frac{1}{2}} \beta_{\tilde{t}} + \tilde{\delta}_{-1} - \dot{\lambda}_{\tilde{t}}^{\frac{1}{2}} \delta_{-1} \right) d\tilde{t} + \dot{\lambda}_{\tilde{t}}^{\frac{1}{2}} d^S u_{\lambda_{\tilde{t}}}. \quad (1.135)$$

If we assume that the driving function  $u_t$  is a Brownian motion  $u_t = \sqrt{\kappa} B_t$  the last formula is an analogue of the relation from Proposition 4.2 in [LSW01b]. We apply the same argumentation and item 6 from Theorem 1.1 to conclude the first theorem statement.

In order to obtain the second statement we consider the coefficient at  $z^1$  in the identity (1.129)

$$\begin{aligned} \frac{d^S \alpha_{\tilde{t}}}{\alpha_{\tilde{t}}} &= \tilde{\delta}_0 d\tilde{t} + \tilde{\sigma}_0 d^S \tilde{u}_{\tilde{t}} - 6 \beta_{\tilde{t}}^2 \dot{\lambda}_{\tilde{t}} d\tilde{t} - \\ &- 2 \beta_{\tilde{t}} \dot{\lambda}_{\tilde{t}} d^S u_{\lambda_{\tilde{t}}} + 2 \dot{\lambda}_{\tilde{t}} \beta_{\tilde{t}} \delta_{-1} d\tilde{t} - \dot{\lambda}_{\tilde{t}} \delta_0 d\tilde{t} - \dot{\lambda}_{\tilde{t}} \sigma_0 d^S u_{\lambda_{\tilde{t}}}. \end{aligned} \quad (1.136)$$

we use this formula and (1.133) to obtain  $d^S \dot{\lambda}_{\tilde{t}}$

$$d^S \dot{\lambda}_{\tilde{t}} = -2\dot{\lambda}_{\tilde{t}} \frac{d^S \alpha_{\tilde{t}}}{\alpha_{\tilde{t}}} = (\dots) d\tilde{t} - 2\dot{\lambda}_{\tilde{t}} \left( -2\dot{\lambda}_{\tilde{t}}^{\frac{1}{2}} \beta_{\tilde{t}} + \tilde{\sigma}_0 - \dot{\lambda}_{\tilde{t}}^{\frac{1}{2}} \sigma_0 \right) d^S \tilde{u}_{\tilde{t}}. \quad (1.137)$$

Assume now that  $\tilde{u}_{\tilde{t}}$  is a Brownian motion,  $\tilde{u}_{\tilde{t}} = \sqrt{\tilde{\kappa}} \tilde{B}_{\tilde{t}}$ ,  $\tilde{t} \in [0, \tilde{T}]$ . We can apply (A.10) and (A.12) to conclude

$$\sqrt{\kappa} d^{\text{It}\hat{\circ}} \tilde{B}_{\tilde{t}} = \left( (6 - \kappa) \dot{\lambda}_{\tilde{t}}^{\frac{1}{2}} \beta_{\tilde{t}} + \left( \tilde{\delta}_{-1} + \frac{\kappa}{2} \tilde{\sigma}_0 \right) - \dot{\lambda}_{\tilde{t}}^{\frac{1}{2}} \left( \delta_{-1} + \frac{\kappa}{2} \sigma_0 \right) \right) d\tilde{t} + \dot{\lambda}_{\tilde{t}}^{\frac{1}{2}} d^{\text{It}\hat{\circ}} u_{\lambda_{\tilde{t}}} \quad (1.138)$$

Analogously to [SW05] the SLEs are locally equivalent if and only if the  $u_t = \sqrt{\kappa} \tilde{B}_t$  is a Brownian motion with  $\kappa = \tilde{\kappa}$ .

If  $\kappa = 6$  and  $\tilde{\delta}_{-1} + 3\tilde{\sigma}_0 = \delta_{-1} + 3\sigma_0 = 0$ , then the random laws on  $\{u_t\}_{t \in [0, T]}$  is also Brownian times  $\sqrt{\kappa}$ .  $\square$

With the aid of this theorem we can extend various properties of the well-studied chordal SLE to the general case of  $(\delta, \sigma)$ -SLE. In particular, we can prove the following.

**Corollary 1.2.** *For  $\delta$  and  $\sigma$  as in (1.122) the random family of hulls  $\{\mathcal{K}_t\}_{t \in [0, \infty)}$  possesses the following properties:*

1.  $\{\mathcal{K}_t\}_{t \in [0, \infty)}$  is a curve generated set a.s. Namely, there exists a parametrised random curve  $\gamma: [0, \infty) \rightarrow \bar{\mathcal{D}}$  (not necessarily simple), started from the source point  $\lim_{t \rightarrow +0} \gamma_t = a$ , such that  $G_t^{-1}(\mathcal{D}) \subset \mathcal{D}$  is a connected component of  $\mathcal{D} \setminus \gamma_{[0, t]}$  for the forward case.
2.
  - $0 < \kappa \leq 4$ :  $\gamma$  is a simple curve in the interior of  $\mathcal{D}$ ;
  - $4 < \kappa < 8$ :  $\gamma$  touches itself and the boundary  $\partial \mathcal{D}$ ;
  - $8 \leq \kappa$ :  $\gamma$  is a space filling curve.

See fig. 1.6 for a qualitative illustration and 2.3, 2.4 for numerical simulation for  $\kappa = 4$  and  $\kappa = 7$  correspondingly.

3. The Hausdorff dimension of  $\gamma$  is equal to  $\min\{2, 1 + \kappa/8\}$ .

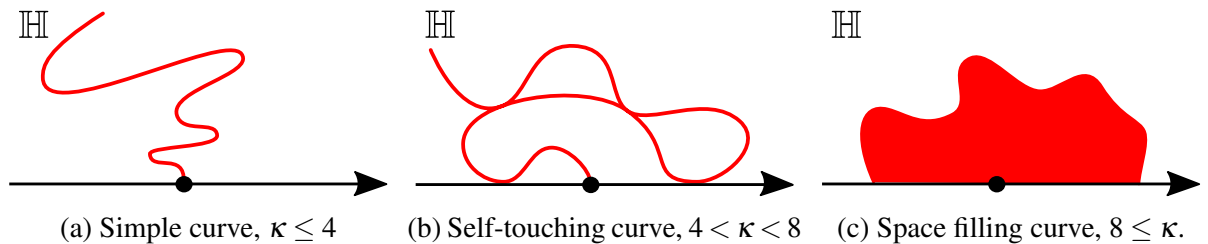


Figure 1.6: Schematic illustration of the qualitative behaviour of the SLE slit for different values of  $\kappa$  in the half-plane chart.

*Proof.* Let  $\{\tilde{G}_{\tilde{t}}\}_{\tilde{t} \in [0, +\infty)}$  be the radial SLE, see Section 6.3.1, and let  $b \in \partial \mathcal{D}$  be the common zero of  $\tilde{\delta}$  and  $\tilde{\sigma}$ . Let also  $T_1$  be the first stopping time from the collection and let  $\lambda$  be the time reparametrization from Theorem 1.3. Then the law of  $\{\mathcal{K}_t\}_{t \in [0, T_1]}$  stopped at  $T_1 > 0$  is equivalent to the chordal law  $\{\tilde{\mathcal{K}}_{\tilde{t}}\}_{\tilde{t} \in [0, \lambda_{T_1}]}$  stopped at  $\lambda_{T_1} > 0$ . In particular,  $\{\mathcal{K}_t\}_{t \in [0, T_1]}$  is curve generated a.s.

In order to extend this property for  $t \in [0, \infty)$ , observe that the law of  $\{G_{t+T_1} \circ G_{T_1}^{-1}\}_{t \in [0, +\infty)}$  coincides with the law of  $\{G_t\}_{t \in [0, +\infty)}$ , which is the strong Markov property. Thus, application of Theorem 1.3 again to the pair of  $(\delta, \sigma)$ -SLE  $G_{t+T_1} \circ G_{T_1}^{-1}$  and to the chordal SLE with the same zero point  $b$  gives that  $\mathcal{K}_t$  is curve generated until  $T_1 + T'_1$ , where  $T'_1$  has the same law as  $T_1$ . Continuing by induction we conclude that the hull is generated by curve until a countable sum of independent equally distributed positive stopping times. Such sum diverges a.s.

The second two items can be proved similarly.  $\square$

Thanks to Corollary 1.2, the hull  $\mathcal{K}_t$  is a simple curve a.s. if  $\kappa \leq 4$ . Moreover, due to Theorem 1.2 there is at most one sample of the Brownian motion for any curve. On the other hand, the sigma-algebra and the measure on curves can be defined by methods not related to conformal maps. For example, we can consider a scaling limit of a lattice path. In particular, the self-avoiding walk and the loop-erased random walk are constructed this way. Another approach is to define the curve as an interface in various two-dimensional models from statistical physics such as the Ising model or percolation.

Last decades, the relation between measures constructed in such two different ways was established, see for example [LSW01a] and [Sch00], for classical SLEs. We restrict our consideration by remarking that Theorem 1.3 might be a key tool in this direction.

We established before that the random law of the Brownian motion is preserved under transition from one pair of  $\delta$  and  $\sigma$  to another if  $\kappa = 6$  and  $\nu = 0$  for both pairs. Consider now such two essentially different  $(\delta, \sigma)$ -SLEs that the random law is kept unchanged under transition from one to another for any  $\kappa > 0$ . This question is motivated by the Theorems 5.3 and 5.4. The case when one of the SLEs is chordal is the subject of the following theorem.

**Theorem 1.4.** *Let  $\{G_t\}_{t \in [0, +\infty)}$  be a forward  $(\delta, \sigma)$ -SLE, and let its transform by (1.128) be a forward chordal SLE  $\{\tilde{G}_{\tilde{t}}\}_{\tilde{t} \in [0, +\infty)}$  for some  $\{\lambda_{\tilde{t}}\}_{\tilde{t} \in [0, +\infty)}$ , and  $\{\hat{M}_{\tilde{t}}\}_{\tilde{t} \in [0, \tilde{T}]}$ . Then, the  $(\delta, \sigma)$ -SLE  $\{G_t\}_{t \in [0, +\infty)}$  is one of the following*

1. Chordal;
2. The case described in Section 6.4;
3. The case described in Section 6.5.

*Proof.* We use the proof of Theorem 1.3. The term in the parentheses of (1.138) is identically zero if and only if  $\beta_{\tilde{t}}$  is a constant because  $\dot{\lambda}_{\tilde{t}} \neq 0$ . Due to (1.131)

$$\beta_{\tilde{t}} \equiv 0. \tag{1.139}$$

Hence,  $\hat{M}^{\mathbb{H}}(z) = \alpha_{\tilde{t}} z = e^{-c_{\tilde{t}}} z$  for some real valued function  $c_{\tilde{t}}$ , and

$$\tilde{G}_{\tilde{t}}^{\mathbb{H}}(z) = e^{-c_{\tilde{t}}} G_{\lambda_{\tilde{t}}}^{\mathbb{H}}(z). \quad (1.140)$$

The Stratonovich differential of  $\tilde{G}_{\tilde{t}}^{\mathbb{H}}(z)$  is

$$\begin{aligned} d^S \tilde{G}_{\tilde{t}}^{\mathbb{H}}(z) &= (d^S e^{-c_{\tilde{t}}}) G_{\lambda_{\tilde{t}}}^{\mathbb{H}}(z) + e^{-c_{\tilde{t}}} d^S G_{\lambda_{\tilde{t}}}^{\mathbb{H}}(z) = \\ &= (d^S e^{-c_{\tilde{t}}}) G_{\lambda_{\tilde{t}}}^{\mathbb{H}}(z) + e^{-c_{\tilde{t}}} \dot{\lambda}_{\tilde{t}} \left( \frac{2}{G_{\lambda_{\tilde{t}}}^{\mathbb{H}}(z)} d\tilde{t} - \sqrt{\kappa} d^S B_{\lambda_{\tilde{t}}} \right) \end{aligned} \quad (1.141)$$

Due to (1.133), we have

$$e^{-c_{\tilde{t}}} = \dot{\lambda}_{\tilde{t}}^{-\frac{1}{2}}, \quad (1.142)$$

and consequently,

$$d^S e^{-c_{\tilde{t}}} = -\frac{1}{2} e^{-3c_{\tilde{t}}} x_{\tilde{t}} d\tilde{t} - \frac{1}{2} e^{-3c_{\tilde{t}}} y_{\tilde{t}} d^S \tilde{B}_{\tilde{t}}, \quad (1.143)$$

where we used (A.10). Thus, we conclude that

$$\begin{aligned} d^S \tilde{G}_{\tilde{t}}^{\mathbb{H}}(z) &= \left( -\frac{1}{2} e^{-3c_{\tilde{t}}} x_{\tilde{t}} d\tilde{t} - \frac{1}{2} e^{-3c_{\tilde{t}}} y_{\tilde{t}} d^S \tilde{B}_{\tilde{t}} \right) e^{c_{\tilde{t}}} \tilde{G}_{\tilde{t}}^{\mathbb{H}}(z) + \\ &+ \frac{2}{\tilde{G}_{\tilde{t}}^{\mathbb{H}}(z)} d\tilde{t} - \sqrt{\kappa} d^S \tilde{B}_{\tilde{t}} + \frac{1}{4} \sqrt{\kappa} e^{-2c_{\tilde{t}}} y_{\tilde{t}} d\tilde{t}. \end{aligned} \quad (1.144)$$

In order to have time independent coefficients we assume that  $x_{\tilde{t}}$  and  $y_{\tilde{t}}$  are proportional to  $e^{2c_{\tilde{t}}}$ . Hence, define  $\xi \in \mathbb{R}$  by

$$x_{\tilde{t}} = -4\xi e^{2c_{\tilde{t}}}. \quad (1.145)$$

Without loss of generality, we can assume that  $y_{\tilde{t}}$  is one of three possible forms

1.  $y_{\tilde{t}} = 0$ ,
2.  $y_{\tilde{t}} = 4\sqrt{\kappa} e^{2c_{\tilde{t}}}$ ,
3.  $y_{\tilde{t}} = -4\sqrt{\kappa} e^{2c_{\tilde{t}}}$ ,

because all other choices can be reduced to these three with the transform  $\mathcal{S}$ . The first case is considered in Section 6.4. Other two cases are discussed in Section 6.5.  $\square$

### 1.3.4 Domain Markov property and conformal invariance of random laws on planar curves

In this section, we consider the property of random laws on planar curves that are defined as above, not necessary as the complement of images of conformal maps.

Let  $\mathcal{G}_{D,a}$  be the set of all simple open curves  $\gamma$  in a domain  $D \subset \mathbb{C}$ . All curves start from some point  $a \in \partial D$  in a smooth piece of the boundary. Let  $(\mathcal{G}_{D,a}, \mathcal{F}_{D,a}, P_{D,a})$  be a probability space.

Let  $\tau : \tilde{D} \rightarrow D$  be a conformal map that can be continuously extended to the boundary near the point  $a$  and let  $\tilde{a} := \tau(a) \in \partial \tilde{D}$ . Let  $(\mathcal{G}_{\tilde{D}, \tilde{a}}, \tilde{\mathcal{F}}_{\tilde{D}, \tilde{a}}, \tilde{P}_{\tilde{D}, \tilde{a}})$  be the probability space induced by the map  $G$ . We will use the notation

$$(\tau_* P)(\tilde{B}) := P(G(\tilde{B})), \quad \tilde{B} \in \tilde{\mathcal{F}}. \quad (1.146)$$

For example,  $\tau_* P_{D,a} = \tilde{P}_{\tilde{D}, \tilde{a}}$ .

On the other hand, a measure on  $\mathcal{G}_{\tilde{D}, \tilde{a}}$  can be defined independently, regardless of the conformal mapping. For example, self-avoiding and loop-erased random walks are usually defined on a lattice grid embedded to arbitrary domain. Then we can consider a limiting measure as the mesh size tends to zero. If such laws are related with (1.146) then the limiting measure is called **conformally invariant**. It arises in the scaling limit and possesses only some special random law on the lattice paths like mentioned above. We emphasize that, if the measure  $P_{D,a}$  is designed with the aid of  $(\delta, \sigma)$ -SLE like in the present text, the conformal invariance is straightforward from the very definition formulated in terms of  $\mathcal{D}$ .

In Section 1.3.3, we define a  $\mathcal{F}_t$ -random law on hulls  $\mathcal{K}_t$  for  $t \in [0, +\infty)$  and for any pair of  $\delta$  and  $\sigma$ . In particular, for  $\kappa \leq 4$ , and for any given domain  $D$ . This gives a random law on planar curves as above with  $\mathcal{F}_{D,a}$  induced by  $\mathcal{F}_t^B$  and  $P_{D,a}$  given by  $P^B$ .

**Remark 1.1.** *It is an interesting problem to study the relation between the sigma-algebra  $\mathcal{F}_{D,a}$  as above and the sigma-algebra induced by the Hausdorff distance on  $\mathcal{G}_{D,a}$ .*

Let us discuss now another (and independent) property of a family of measures on planar curves called the domain Markov property. It is related to the strong Markov property of  $G_t$  considered above but it is formulated for a general not necessary conformally invariant random law on curves.

Let  $\mathcal{G}_{D,a}[\gamma | \tilde{\gamma}]$  be a conditional law on curves  $\gamma \in \mathcal{G}_{D,a}$ . The condition is such that  $\gamma_{\sim} \subset \gamma$  is a fixed subcurve also started from the point  $a$  and ended at  $a_{\sim} \in \gamma$ . Assume that a random law on  $\mathcal{G}_{D \setminus \gamma_{\sim}, a_{\sim}}$  is given for some curve  $\gamma_{\sim}$ . The **domain Markov property** is usually defined as

$$\text{Law}_{D,a}[\gamma | \gamma_{\sim}] = \text{Law}_{D \setminus \gamma_{\sim}, a_{\sim}}[\gamma \setminus \gamma_{\sim}]. \quad (1.147)$$

The conditional law on the left-hand side can be understood heuristically or defined as below.

Consider first the case of discrete measures, for example, self-avoiding or loop-erased random walks defined on a finite lattice grid. The conditional law of their continuous versions (scaling limits) can be understood as the limit law. For more detail we refer, for example, to [Sch00]. However, if the law is defined on a continuous set of curves (and the conditional expectation is taken with respect to an event of probability zero) from the very beginning like we did using  $(\delta, \sigma)$ -SLE, then we need the following constructions for a mathematically rigorous definition.

Consider a quotient space  $(\mathcal{G}_{D,a})_{\sim}$  of  $\mathcal{G}_{D,a}$  with the following property. For each equivalence class there exists a maximal curve  $\gamma_{\sim} \in \mathcal{G}_{D,a}$  which is strictly contained in each of the curve from this class and all curves with this subcurve are in this class. Thus, each element of  $(\mathcal{G}_{D,a})_{\sim}$  is represented by  $\gamma_{\sim} \in \mathcal{G}_{D,a}$ . We use the letter  $\gamma_{\sim}$  for both: the equivalence class and the common part of curves it represents. We denote by



$a_\sim$  the end of the curve  $\gamma_\sim$  which differs from  $a$ . Let  $\mathcal{F}_\sim$  be the sigma-subalgebra of  $\mathcal{F}$  generated by this factor space. Namely, each subset from  $\mathcal{F}_\sim$  is a preimage of the quotient map of some set of  $\mathcal{F}$ . Remark that  $\gamma_\sim$  is a  $\mathcal{F}_\sim$ -random variable.

Let  $\mathcal{F}_{D \setminus \gamma_\sim, a_\sim}$  be the sigma-algebra on  $\mathcal{G}_{D \setminus \gamma_\sim, a_\sim}$  consisting of all sets from  $\mathcal{F}_{D, a}$  that are subsets of the equivalence class given by  $\gamma_\sim$ . Assume now that for a.a.  $\gamma_\sim$  a  $\mathcal{F}_{D \setminus \gamma_\sim, a_\sim}$ -random law on  $\mathcal{G}_{D \setminus \gamma_\sim, a_\sim}$  is given. Hence, for any bounded  $\mathcal{F}_{D, a}$ -measurable function  $f : \mathcal{G}_{D, a} \rightarrow \mathbb{R}$ , the function  $f(\cdot \cup \gamma_\sim) : \mathcal{G}_{D \setminus \gamma_\sim, a_\sim} \rightarrow \mathbb{R}$  is bounded and  $\mathcal{F}_{D \setminus \gamma_\sim, a_\sim}$ -measurable. We are now ready to give meaning to (1.147):

$$\mathbb{E}_{D, a} [f(\gamma) | \mathcal{F}_\sim] (\omega) = \mathbb{E}_{D \setminus \gamma_\sim(\omega), a_\sim(\omega)} [f(\gamma \cup \gamma_\sim(\omega))] \quad a.s. \quad (1.148)$$

for any bounded  $\mathcal{F}_{D, a}$ -measurable function  $f$ .

Thus, to formulate the domain Markov property we have to specify not only random laws for each  $\gamma_\sim$  on  $D \setminus \gamma_\sim$ , but also the collection of curves  $\gamma_\sim$ . For example, in the case of curves on finite lattice grid, we can consider the set of all curves of fixed length. In the case of  $(\delta, \sigma)$ -SLE generated curve, we can pick up any stopping time  $0 < T < +\infty$  and consider the set of curves  $\gamma_\sim$  generated by the random map  $G_T$ . We use Theorem 1.2 and denote by  $G[\gamma_\sim]$  the unique map which corresponds to the curve  $\gamma_\sim$ . We can now formulate what we mean by the **domain Markov property of  $(\delta, \sigma)$ -SLE**, see also Fig. 1.7.

**Proposition 1.5.** *Let  $\{G_t\}_{t \in [0, +\infty)}$  be a  $(\delta, \sigma)$ -SLE with  $\kappa \leq 4$ . Choose some chart  $\psi : \mathcal{D} \rightarrow D^\Psi$ . For a positive stopping time  $T < +\infty$  a.s., let  $\mathcal{F}_\sim := \mathcal{F}_T^B$ , and let us define*

$$P_{D \setminus \gamma_\sim, a_\sim}(\tilde{B}) := (G[\gamma_\sim]^\Psi)_* P_{D, a}(\tilde{B}), \quad \tilde{B} \in \mathcal{F}_\sim. \quad (1.149)$$

*The domain Markov property is satisfied with respect to  $\mathcal{F}_\sim$ .*

*Proof.* This follows from the strong Markov property of  $(\delta, \sigma)$ -SLE and from the construction above.  $\square$

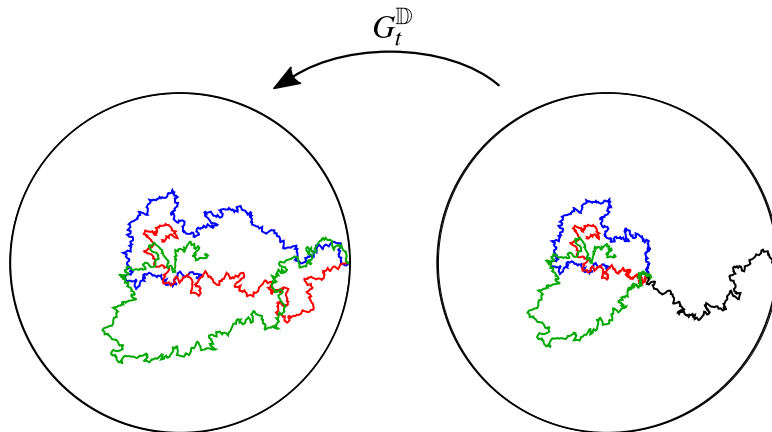


Figure 1.7: This is an illustration of the domain Markov property of  $(\delta, \sigma)$ -SLE. The three color lines on the left-hand side are samples of the  $(\delta, \sigma)$ -SLE slit  $\gamma$ . The corresponding color lines on the right-hand side are the preimages with respect to an independently sampled forward  $(\delta, \sigma)$ -SLE map  $G_t$ , which has the slit denoted by the black line  $\gamma_\sim$ . The domain Markov property states that the union of the black line and any of the color lines has the same law as the  $(\delta, \sigma)$ -SLE slit. For this figure we made the slit simulation for  $\delta = 2\ell_{-2}$  and  $\sigma = -\sqrt{2}(\ell_{-1} + \ell_1)$ . in the unit disk chart

The domain Markov property can also be considered for continuously growing hulls that are not curves. This can be done for the classical cases, but for other cases we would need to prove the Conjecture 1.1.

## Conclusions and perspectives

1. It is important to prove Conjecture 1.1 and obtain which normalization conditions are satisfied for the general case of  $(\delta, \sigma)$ -SLE analogous to the classical cases.
2. We considered only holomorphic vector fields and conformal maps. This restriction can be relaxed as follows. Let  $\delta$  and  $\sigma$  are tangent at the boundary (except the point  $a$  for  $\delta$ ) and holomorphic only on some neighborhood of the boundary of  $\mathcal{D} \setminus \mathcal{K}_t$ . On the rest part of  $\mathcal{D}$  the vector fields can be smooth and such that the initial value problem (1.34) has a unique solution  $\{G_t\}_{t \in [0, +\infty)}$  that is a family of endomorphisms. Such map  $G_t$  is holomorphic only on some neighborhood of the boundary and smooth inside. On the other hand, the local behaviour of the hull is the same as for holomorphic  $\delta$  and  $\sigma$ . This provides a more general random law on curves with the SLE local behaviour.
3. The generalisation of the SLE to multiply-connected Riemann surfaces (genuses with boundaries) is not straightforward because the amount of complete and semicomplete vector fields tangent at the boundaries is hardly restricted by the Riemann-Roch theorem. The approach from the previous item is a possible way to avoid this difficulty.

# Chapter 2

## Numerical Simulation

### Introduction

This chapter is dedicated to methods of numerical solution of forward  $(\delta, \sigma)$ -Löwner chains and simulation of the forward  $(\delta, \sigma)$ -SLE. A general method for the approximation of conformal maps was introduced in [MR07]. Its application to the chordal Löwner equation is considered in [Ken09] together with some technical details.

Numerical simulation of the  $(\delta, \sigma)$ -SLE was developed and implemented independently by the author using Wolfram Mathematica software. All figures with  $(\delta, \sigma)$ -SLE samples in this monograph, except Fig. 2.2, are made with this program. Here we describe the applied method together with some technical difficulties, which motivates the structure of the program. The correctness (convergence) in the deterministic case is actually proved in [MR07]. The analogous statement for the stochastic case is more difficult, see [Tra14] for details. We avoid the consideration of this problem in the present text.

We organize this chapter as follows. In the first section we study how to approximate  $(\delta, \sigma)$ -Löwner chains with given driving function. If the driving function is a sample of the Brownian motion, there are additional technical difficulties that are considered in the second section. The third part of the chapter is actually a conclusion/perspective section. We discuss how to extend these methods to non-continuous stochastic processes such as the stable Levy process.

## 2.1 Approximation of $(\delta, \sigma)$ -Löwner chain

### 2.1.1 The zipper method

Let  $G_t$  be a conformal map from a forward Löwner chain  $\{G_s\}_{s \in [0, t]}$  with driving function  $\{u_s\}_{s \in [0, t]}$ ,  $t \in [0, +\infty)$ . Our purpose is to obtain a reasonable approximation map  $\bar{G}_t$  ( $\bar{G}_t \approx G_t$ ). Namely, for a given chart  $\psi$  and a large integer  $N$  we define a conformal map  $\bar{G}_t^N$  and claim

$$(\bar{G}_t^N)^\psi(z) \xrightarrow{N \rightarrow \infty} G_t^\psi(z) \quad \text{uniformly on } \psi(\mathcal{D}). \quad (2.1)$$

To this end, consider a finite partition of the interval  $[0, t]$  given by a collection

$\{t_0, t_1, t_2, \dots, t_N\}$  such that

$$0 = t_0 < t_1 < t_2 < \dots < t_{N-1} < t_N = t < \infty. \quad (2.2)$$

For example, one can use the uniform partition

$$t_n := \frac{n}{N}t, \quad n = 1, 2, \dots, N. \quad (2.3)$$

We use the results of Section 1.2.1 to split  $G_t$  into the composition

$$G_t = G_{t_N, t_{N-1}} \circ G_{t_{N-1}, t_{N-2}} \circ \dots \circ G_{t_3, t_2} \circ G_{t_2, t_1} \circ G_{t_1, t_0}. \quad (2.4)$$

Each function  $G_{t_n, t_{n-1}}$  ( $n = 1, 2, \dots, N$ ) is a Löwner map  $\tilde{G}_{t_n - t_{n-1}}$  obtained with the driving function  $\{\tilde{u}_s := u_{s+t_{n-1}} - u_{t_{n-1}}\}_{s \in [0, t_n - t_{n-1}]}$ . Let  $\bar{G}_n$  ( $n = 1, 2, \dots, N$ ) be some approximation of  $G_{t_n, t_{n-1}}$ . We call  $\bar{G}_n$  the **step map**. We choose the partition (2.2) such that

$$\max_{n=1, 2, \dots, N} (t_n - t_{n-1}) \xrightarrow{N \rightarrow \infty} 0, \quad (2.5)$$

and define the approximation  $\bar{G}_t^N$  by

$$\bar{G}_t^N := \bar{G}_N \circ \bar{G}_{N-1} \circ \dots \circ \bar{G}_2 \circ \bar{G}_1, \quad N = 1, 2, \dots. \quad (2.6)$$

Our main purpose is to approximate the curve  $\gamma_t$  that generates the hull

$$\mathcal{K}_t = \mathcal{D} \setminus G_t^{-1}(\mathcal{D}). \quad (2.7)$$

We assume first that  $\mathcal{K}_t = \gamma_t$  is a simple curve. Then the curve

$$\tilde{\gamma}_t^N := \mathcal{D} \setminus (\bar{G}_t^N)^{-1}(\mathcal{D}) \quad (2.8)$$

is such that

$$\psi(\tilde{\gamma}_t^N) \xrightarrow{N \rightarrow \infty} \psi(\gamma_t) \quad (2.9)$$

due to (2.1).

We notice that  $\tilde{\gamma}_t^N$  consists of arcs such that the first one is  $\mathcal{D} \setminus \bar{G}_1^{-1}(\mathcal{D})$ , the second one is the image of  $\mathcal{D} \setminus \bar{G}_2^{-1}(\mathcal{D})$  with respect to  $\bar{G}_1^{-1}$ , the third one is the image of  $\mathcal{D} \setminus \bar{G}_3^{-1}(\mathcal{D})$  with respect to  $\bar{G}_1^{-1} \circ \bar{G}_2^{-1}$ , and so on.

Consider the **joint points**  $\tilde{\gamma}_{n,a}^N \in \tilde{\gamma}_t^N$  defined by

$$\tilde{\gamma}_{n,a}^N := \bar{G}_1^{-1} \circ \bar{G}_2^{-1} \circ \dots \circ \bar{G}_n^{-1}(a), \quad n = 1, 2, \dots, N, \quad (2.10)$$

where  $a \in \partial \mathcal{D}$  is the source point. In the limit  $N \rightarrow \infty$ , the distance between them tends to zero:

$$\max_{n=1, 2, \dots, N} |\psi(\tilde{\gamma}_{n,a}^N) - \psi(\tilde{\gamma}_{n-1,a}^N)| \xrightarrow{N \rightarrow \infty} 0, \quad (2.11)$$

and the arcs tends to straight line segments due to the continuity of the driving function  $\{u_s\}_{s \in [0, t]}$ . Thereby, to approximate the curve  $\gamma_t$  in chart  $\psi$  we can just find all joined points  $\tilde{\gamma}_{n,a}^N$  with large enough  $N$  and proper partition (2.2). The joint points  $\{\tilde{\gamma}_{n,a}^N\}_{n=1, 2, \dots, N}$  can then be connected by straight line segments in the chart  $\psi$ .

To find each point  $\tilde{\gamma}_{n,a}^N$  we need to make  $n$  iterations (calculate the map  $\bar{G}_i$  for different values of  $i$ ,  $n$  times). Hence, the time of the calculation of  $\tilde{\gamma}_t^N$  grows as  $O(N^2)$ . A faster method of approximation is considered in [Ken07]. We do not implement it here.

Below, we discuss how to choose the step map and the partition (2.2).

### 2.1.2 Choice of the step map $\bar{G}_n$

One of the possible choices of the approximation function  $\bar{G}_n$  for the chordal case is made, e.g., in [Ken09]. The map  $\bar{G}_n$  is chosen such that the slit  $\bar{\gamma} := \mathcal{D} \setminus \bar{G}_n^{-1}(\mathcal{D})$  is a straight line segment in the half-plane chart from  $a$  to some point inside the domain. See [Ken09] for exact formulas.

An alternative can be given by the solution of the equation

$$\dot{G}_s = \delta \circ G_s + \frac{u_{t_n} - u_{t_{n-1}}}{t_n - t_{n-1}} \sigma \circ G_s, \quad G_0 = \text{id}, \quad s \in [0, t_n - t_{n-1}], \quad (2.12)$$

which is  $H_s \left[ \delta + \frac{u_{t_n} - u_{t_{n-1}}}{t_n - t_{n-1}} \sigma \right]$ . With such a step map the full approximation  $\bar{G}_t^N$  is a Löwner chain with driving function  $\{\bar{u}_s^N\}_{s \in [0, t]}$  obtained as a piecewise linear continuous approximation of  $\{u_s\}_{s \in [0, t]}$  such that  $\bar{u}_{t_n}^N = u_{t_n}$ ,  $n = 0, 1, 2, \dots, N$  at each joint point of  $\bar{u}_t^N$ .

The third alternative considered here corresponds to the approximation of  $\{u_s\}_{s \in [0, t]}$  by a piecewise constant function  $\{\bar{u}_s^N\}_{s \in [0, t]}$  such that

$$\bar{u}_s^N = u_{t_n}, \quad s \in [t_n, t_{n+1}), \quad n = 0, 1, 2, \dots, N. \quad (2.13)$$

Thus,  $\{\bar{u}_s^N\}_{s \in [0, t]}$  is not continuous, and the step function is a composition

$$\bar{G}_n = H_{u_{t_n} - u_{t_{n-1}}}[\sigma] \circ H_{t_n - t_{n-1}}[\delta], \quad n = 1, 2, \dots, N. \quad (2.14)$$

The term  $H_{t_n - t_{n-1}}[\delta]$  corresponds to the interval  $[t_{n-1}, t_n)$ , where  $\bar{u}_t^N$  is constant. The curve  $\bar{\gamma} := \mathcal{D} \setminus H_s[\delta]^{-1}(\mathcal{D})$  is a flow line of  $\delta$  that starts at  $a$  and tends to the attracting (or degenerate) zero of  $\delta$  when  $s \rightarrow +\infty$ . Meanwhile,  $H_{t_n - t_{n-1}}[\delta]$  maps the tip of  $\bar{\gamma}$  to  $a$  and both sides of the slit  $\bar{\gamma}$  to the boundary  $\partial \mathcal{D}$  of  $\mathcal{D}$ .

The second term  $H_{u_{t_n} - u_{t_{n-1}}}[\sigma]$  in (2.12) is a Möbius automorphism that moves the point  $a$  along the boundary of  $\mathcal{D}$ . The length of the move is defined by the jump of  $\bar{u}_s^N$  at  $s = t_n$ , which is  $u_{t_n} - u_{t_{n-1}}$ . Hence, the inverse step map  $\bar{G}_n^{-1}$  produces a slit  $\bar{\gamma}$  which starts at the source  $a$ , but maps  $a$  to the boundary of  $\mathcal{D} \setminus \bar{\gamma}$ , which is either a side of  $\bar{\gamma}$  or the boundary  $\partial \mathcal{D}$ , if the jump is big enough. It is that point from which the next piece of  $\bar{\gamma}^N$  starts.

Thereby, in the chain (2.10), each next part of the slit  $\bar{\gamma}_t^N$  grows not from the tip of the previous one, but from a moved point on a side of the slit. Thus,  $\bar{\gamma}_t^N$  is not a curve, but a tree with the property that in the limit (2.5) the source of each arc of  $\bar{\gamma}^N$  tends to the tip of the previous arc, see Fig. 2.1. This is a consequence of the continuity of the driving function  $\{u_s\}_{s \in [0, t]}$ , see Fig. 2.1.

The choice (2.14) has the disadvantage that the map  $H_s[\delta]$  cannot be expressed in terms of elementary functions. This increases the time of numerical calculations. To handle this we combine the second (2.12) and the third (2.14) approach as follows. Assume the normalization (1.76) and consider the semicomplete vector field

$$\delta + \frac{u_{t_n} - u_{t_{n-1}}}{t_n - t_{n-1}} \sigma \quad (2.15)$$

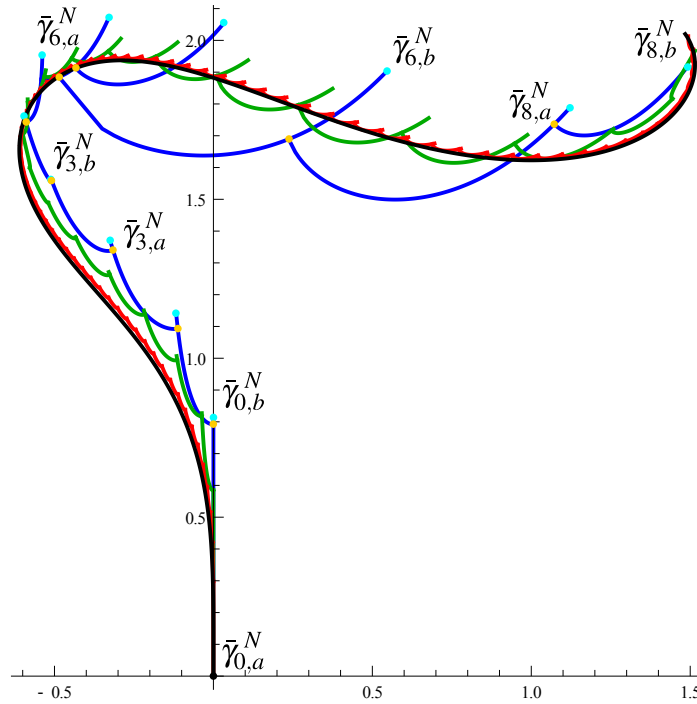


Figure 2.1: We show the slit (the blue line) of the approximation map  $\bar{G}_t^N$ . We denote the points  $\bar{\gamma}_{i,a}^N$  with yellow color and the points  $\bar{\gamma}_{i,b}^N$  with blue color. We also demonstrate the convergence of  $\bar{\gamma}_t^N$  to  $\gamma_t$  when  $N \rightarrow +\infty$ . This figure shows how the slit  $\bar{\gamma}_t^N$  of  $\bar{G}_t^N$  looks for different values of  $N$ . For illustration we consider the chordal case, half-plane chart, the driving function  $u_s := -4s^2(s-1)(s-2)$ ,  $t = 1.8$ , and use the partition (2.3). The black line is the exact slit  $\gamma_t$ , the blue, green, and red lines are the slits  $\bar{\gamma}_t^N$  for  $N = 10, N = 20$ , and  $N = 80$  correspondingly.

from (2.12). Now we apply the classification from Section 1.1 and Fig.1.2 to define a vector field  $\bar{\delta}_n$ .

1. If (2.15) is parabolic, then  $\bar{\delta}_n$  is chordal (see Section 6.1.1) with triple zero at the same point where (2.15) has the double zero.
2. If (2.15) is hyperbolic, let  $b_1, b_2 \in \partial \mathcal{D}$  be the non-attracting zeros of (2.15). Assume  $\bar{\delta}_n$  is dipolar (see Section 6.2.1) with non-attracting zeros at  $b_1$  and  $b_2$ .
3. If (2.15) is elliptic, then  $\bar{\delta}_n$  is radial (see Section 6.3.1) with zero at the position of the attracting zero of (2.15).

We also define a complete vector field  $\bar{\sigma}_n$  by

$$\bar{\sigma}_n := \delta + \frac{u_{t_n} - u_{t_{n-1}}}{t_n - t_{n-1}} \sigma - \bar{\delta}_n \quad (2.16)$$

and the step function by

$$\bar{G}_n = H_{t_n - t_{n-1}}[\bar{\sigma}_n] \circ H_{t_n - t_{n-1}}[\bar{\delta}_n], \quad n = 1, 2, \dots, N. \quad (2.17)$$

Thereby, the slit  $\bar{\gamma}$  obtained with  $\bar{G}_n$  tends to the attracting zero of 2.15 in the chordal and radial cases. The map  $\bar{G}_n$  is given by the solution of driftless chordal, dipolar, or

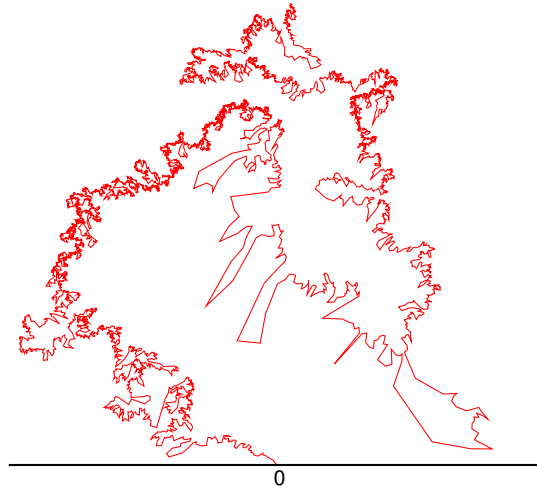


Figure 2.2: An approximation of the slit of a chordal Löwner chain with the driving function given by a sample of Brownian motion (SLE slit) in the half-plane chart. The partition of the time interval is uniform. The parameters are chosen to be  $\kappa = 6$  and  $N = 10000$ . ([Ken09])

radial equations with a piecewise constant driving function. In fact, this method is a version of (2.14) after some drift transform  $\mathcal{D}_c$  of the tripple

$$\left( \delta, \sigma, \left\{ \frac{u_{t_n} - u_{t_{n-1}}}{t_n - t_{n-1}} s \right\}_{s=[0, t_n - t_{n-1}]} \right) \quad (2.18)$$

of (2.12).

### 2.1.3 Choice of the partition

The simplest choice of partition (2.2) is the uniform one (2.3). A critical disadvantage of this approach is discussed in [Ken09]. The difficulty is that the distance between the joint points  $\bar{\gamma}_n^N$  is far from being homogenous in this case. Define the distance

$$d(z_2, z_1) := |\psi(z_2) - \psi(z_1)|, \quad z_1, z_2 \in \mathcal{D} \quad (2.19)$$

for a given chart  $\psi$ . For a fixed driving function  $\{u_s\}_{s \in [0, s]}$  and a fixed integer  $N$  the distance  $d(\bar{\gamma}_n^N, \bar{\gamma}_{n-1}^N)$  may vary from numerically very large to very small, see Fig. 2.2. Thus, the curve  $\gamma$  is approximated with too high accuracy in some regions and with too low accuracy in other regions. As an illustration we present a simulation of a chordal Löwner chain with a driving function obtained as a sample of Brownian motion (a sample of chordal SLE), see fig. 2.2. The thin straight lines correspond to regions of time where  $d(\bar{\gamma}_{n,a}^N, \bar{\gamma}_{n-1,a}^N)$  is much bigger than the resolution of the picture. On the other hand, in other regions, where the curve is bold, the distance  $d(\bar{\gamma}_{n,a}^N, \bar{\gamma}_{n-1,a}^N)$  is overabundantly small.

To avoid this unpleasant situation it is enough to take each next  $t_n$  not uniformly as above, but such that  $d_{\min} < d(\bar{\gamma}_n^N, \bar{\gamma}_{n-1,a}^N) < d_{\max}$  for some parameters  $d_{\min}, d_{\max} > 0$  that correspond to the desired degree of resolution. Thus, the choice of partition strongly

depends on the driving function  $u_t$ . We remark that such a partition also depends on the choice of chart  $\psi$  also, as the Lebesgue distance  $d(\cdot, \cdot)$  does.

If the driving function  $\{u_s\}_{s \in [0, t]}$  is given analytically for all values of  $s \in [0, t]$ , than the implementation of this method is straightforward. Once we have found  $\{\bar{\gamma}_i^N\}_{i=1,2,\dots,n}$  for some  $n < N$ , we can just take some  $t_{n+1} > t_n$ , calculate  $\bar{\gamma}_{n+1,a}^N$ , and increase or decrease the value of  $t_{n+1}$  depending on the calculated value of  $d(\bar{\gamma}_{n+1,a}^N, \bar{\gamma}_{n,a}^N)$ . Only after obtaining an optimal  $\bar{\gamma}_{n+1,a}^N$  we add such  $\bar{\gamma}_{n+1,a}^N$  to the collection  $\{\bar{\gamma}_i^N\}_{i=1,2,\dots,n}$ . One can also use the distance

$$d(\bar{\gamma}_{n+1,a}^N, \bar{\gamma}_{n,b}^N) + d(\bar{\gamma}_{n,b}^N, \bar{\gamma}_{n,a}^N) \quad (2.20)$$

instead of  $d(\bar{\gamma}_{n+1,a}^N, \bar{\gamma}_{n,a}^N)$ .

## 2.2 Simulation of $(\delta, \sigma)$ -SLE

Above we considered a method of numerical simulation for  $(\delta, \sigma)$ -Löwner chains. The problem becomes more complicated when the driving function is a sample of a random process such as the Brownian motion  $\{B_t\}_{t \in [0, +\infty)}$ . This is due to the fact that we have to sample the process during the simulation. We prefer to avoid sampling of  $B_t$  beforehand, because we do not know the partition in advance (the required amount of floating-point operations and memory is incredibly big if we just take the smallest possible mesh  $t_n - t_{n-1}$  and sample  $B_{t_n}$  uniformly, in all points  $t_n$ ), see also the caption to Fig. 2.5.

On the other hand, if we have sampled  $B_t$  at  $t = t_n$  and have concluded that  $\bar{\gamma}_{n,a}$  is too close to or too far away from  $\bar{\gamma}_{n-1,a}$  we cannot ignore the value of  $B_{t_n}$  in the future sampling of  $B_t$  for other values of  $t$  (say,  $\tilde{t}_n$ ) as we did above for a not random driving function, as  $B_{\tilde{t}_n}$  and  $B_{t_n}$  are not independent random variables. This motivates the following method (algorithm) for the  $(\delta, \sigma)$ -SLE simulation. The scheme (see Fig. 2.1) presented below is motivated by the discussion above and the experience of the author. We do not present any proof of correctness.

We consider a routine  $R(\bar{\gamma}_{x,a}, \{t_x, B_x\}, \{t_y, B_y\})$  that should obtain all points  $\bar{\gamma}_n$  that correspond to a given time interval  $[t_x, t_y]$ . It also samples all necessary values of  $B_t$  inside  $[t_x, t_y]$ . The values of  $B_t$  for  $t = t_x$  and  $t = t_y$  are assumed to be given as  $B_x$  and  $B_y$ . All points  $\bar{\gamma}_{i,a} \in \mathcal{D}\}_{i=1,2,\dots,n}$  for the interval  $[0, t_x]$  are assumed to be obtained during the previous steps. The last joint point  $\bar{\gamma}_{n,a} \in \mathcal{D}$ , which corresponds to  $t = t_x$  and is denoted by  $\bar{\gamma}_{x,a}$ , is the first argument of the routine  $R$ . The algorithm is recursive, as the routine  $R$  calls itself to obtain  $\bar{\gamma}_{n,a}$  on subintervals of  $[t_x, t_y]$ .

In the very beginning of the simulation, we pick some  $T > 0$ , sample  $B_T$ , and set  $\bar{\gamma}_{0,a} := a$ . Then we call the routine  $R$  for the first time with the arguments  $R(\bar{\gamma}_{0,a}, (0, 0), (T, B_T))$ , which initiates the simulation.

The points  $\bar{\gamma}_{n,a}$ ,  $n = 1, 2, \dots$ , are obtained sequentially in different execution instance of  $R$ . There is also a global Boolean parameter ‘additional point’ that is equal to ‘false’ by default and is equal to ‘true’ if the last sampled point  $\bar{\gamma}_{n+1,a}$  is too close to  $\bar{\gamma}_{n,a}$ , see details below.

The design of the routine  $R$  is presented in Fig. 2.1 as a block scheme. First of all the routine calculates the point  $\bar{\gamma}_{y,a}$  by an application of the step map  $\bar{G}_{n+1}$  with given time



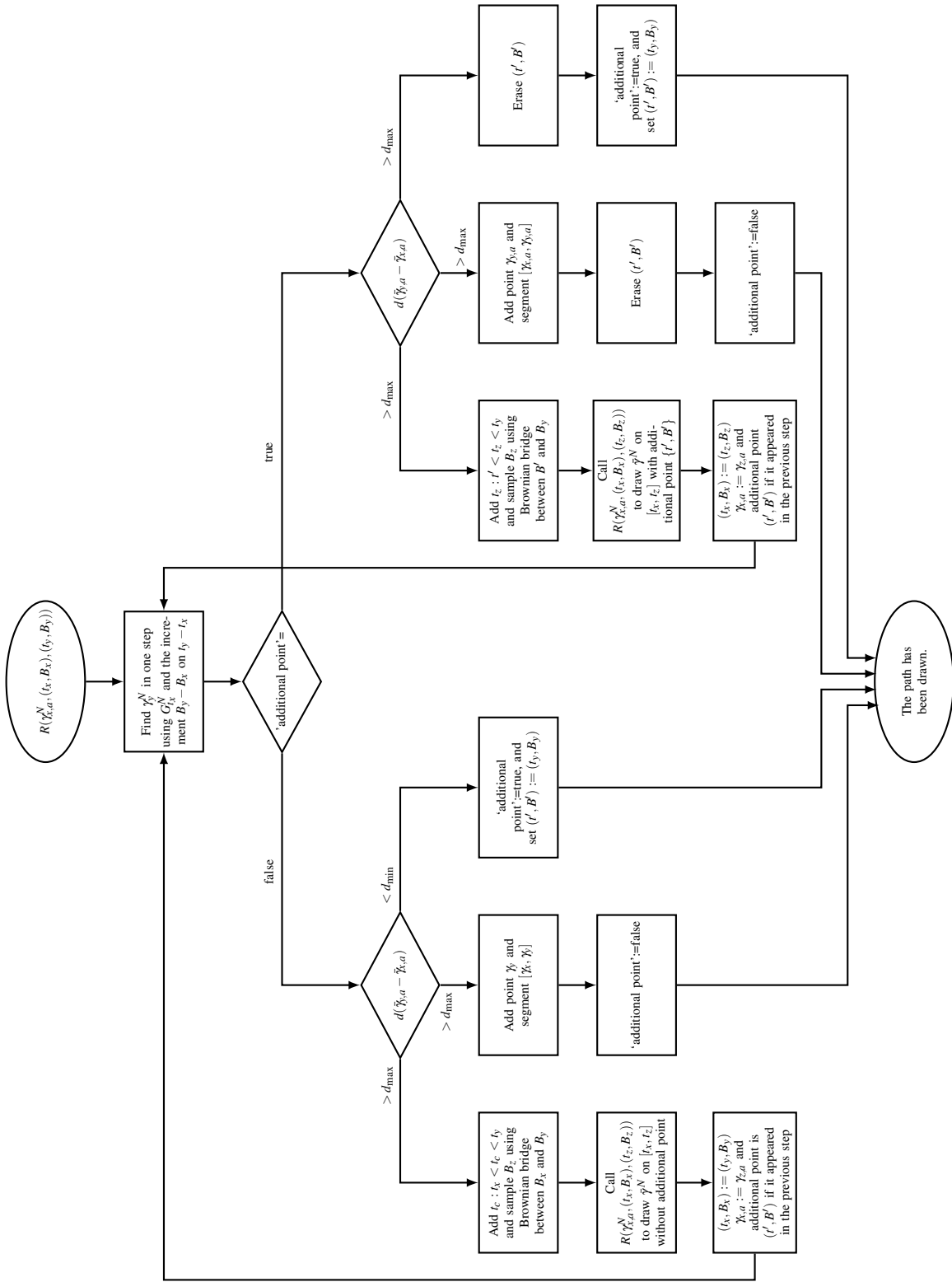


Table 2.1: Block scheme for the routine  $R$ .

interval  $t_y - t_x$  and jump  $B_y - B_x$  (the top rectangle on 2.1). The method is described in Section 2.1.2. The next decision (the diamond below the rectangle) will be discussed below. For now assume that there is no additional point and go left. Afterwards there are three alternatives related to the value of the distance  $d(\bar{\gamma}_{y,a}, \bar{\gamma}_{x,a})$ .

1.  $d(\bar{\gamma}_{y,a}, \bar{\gamma}_{x,a})$  is too big. In this case, we pick up some point  $t_z \in (t_x, t_y)$ , sample  $B_z := B_{t_z}$ , and call the routine  $R$  for the interval  $[t_x, t_z]$ . Afterwards we return to the beginning but with a changed left boundary of the time interval  $t_x := t_z$  (or smaller, see below for details) and new  $\bar{\gamma}_{x,a}$ , which corresponds to the new value of  $t_x$ .
2.  $d(\bar{\gamma}_{y,a}, \bar{\gamma}_{x,a})$  is neither too big, nor too small. This means that the point  $\bar{\gamma}_{y,a}$  obtained before can be added to the collection  $\{\bar{\gamma}_{i,a}\}_{i=0,1,2,\dots,n}$  of the joint points. Hence, the task of the routine is complete and we finish it with attribute ‘additional point’=‘false’.
3.  $d(\bar{\gamma}_{y,a}, \bar{\gamma}_{x,a})$  is too small. This means that the point  $\bar{\gamma}_{y,a}$  is too close to  $\bar{\gamma}_{x,a}$  and it is not reasonable to add it to the collection of the joint points because this uselessly increases the number of iterations in (2.10). We finish the routine but with the attribute ‘additional point’=‘true’. We also register the pair  $(t', B') := (t_y, B_y)$  for future needs.

Thus, we finish the consideration of the first left half of the block scheme that corresponds to the option ‘additional point’=‘false’. The alternative happens when the last considered point  $\bar{\gamma}_{n+1,a}$  is too close to the last point added to the collection  $\{\bar{\gamma}_i\}_{i=0,1,2,\dots,n}$  as in item 3 above. So, if after the calculation of  $\bar{\gamma}_{y,a}$  in the upper rectangle the global attribute ‘additional point’=‘true’, we go right from the diamond. In addition, the pair  $(t', B')$  is given and it is known that it corresponds to a point too closed to  $\bar{\gamma}_{x,a}$ . The right half of the algorithm is analogous to the left half. We have the same three alternatives after the calculation of the distance  $d(\bar{\gamma}_{y,a}, \bar{\gamma}_{x,a})$ .

1.  $d(\bar{\gamma}_{y,a}, \bar{\gamma}_{x,a})$  is too big. In this case we pick some point  $t_z \in (t', t_y)$ , sample  $B_z := B_{t_z}$ , and call the routine  $R$  for the interval  $[t_x, t_z]$  with option ‘Additional point’=‘True’. Afterwards we return to the beginning, but the value of  $t_x$  can be increased and the point  $\gamma_{x,a}$  can be changed to another one as in item 1 above. The global attribute ‘additional point’ depends on the results of the called routine for the interval  $[t_x, t_z]$ . We recall that it equals to ‘false’ if the point  $\bar{\gamma}_{z,a}$  for  $(t_z, B_z)$  is added to the collection, and it equals to ‘true’ if  $\bar{\gamma}_{z,a}$  for  $(t_z, B_z)$  is too close to the last point  $\bar{\gamma}_n$  added to the collection. In the second case, the pair  $\{t_z, B_z\}$  is registered as  $(t', B')$  and  $\{t_x, B_x\}$  corresponds to the last point  $\bar{\gamma}_{n,a}$  added to the collection.
2.  $d(\bar{\gamma}_{y,a}, \bar{\gamma}_{x,a})$  is neither too big, nor not too small. This means that the point  $\bar{\gamma}_{y,a}$  obtained before can be added to the collection  $\{\bar{\gamma}_{i,a}\}_{i=0,1,2,\dots,n}$  of the joint points. The pair  $(t', B')$  can be erased, as it has no influence on values of  $B_t$  if  $t > t_y > t'$ . The task of the routine is complete after that, and we finish it with the attribute ‘additional point’=‘false’.
3.  $d(\bar{\gamma}_{y,a}, \bar{\gamma}_{x,a})$  is too small. This means that the point  $\bar{\gamma}_{y,a}$  is also too close to  $\bar{\gamma}_{x,a}$ . Just as in the previous alternative we no longer need  $(t', B')$  and we exchange  $(t', B') := (t_y, B_y)$ . We finish the routine with the attribute ‘additional point’=‘true’.

That is the functionality of the program. The routine  $R$  calls itself for smaller and smaller intervals of time until the distance between the points  $\tilde{\gamma}_{n,a}$  is small enough. The choice of point  $t_z$  in the first alternatives of both halves of the block scheme can be prescribed by the time interval between the two previously added points.

The simulation can be stopped when the first call of the routine for  $[0, T]$  finishes. If the time intervals between the last added points are of the same order of magnitude as  $T$ , the last point  $B_T$  may be interpreted as the limit point  $t \rightarrow +\infty$  of the slit  $\gamma_t$ . The value  $T = 10^8$  was used in all simulations. This choice is motivated by some technical characteristics of numerical calculations in Wolfram Mathematica.

The limit point of the slit can be observed in all simulations in Chapter 6. In some situations, however, such as a chordal SLE in the half-plane chart, the limit points were not observed (this is in accordance with the analytic theory, which states that the limit point is the infinity). In this case, the simulation can be stopped when the number  $n$  of the joint points achieves some maximal value  $N$ .

Here we present two examples with high resolution for a sample of the chordal SLE slit in the half-plane chart, see fig. 2.3 and 2.4. In most other figures with slit samples from this monograph the number of points  $N$  is approximately equal to several hundreds and  $d_{\max} = 0.02$ ,  $d_{\min} = 0.01$ . The figure (2.5) is dedicated to demonstrate the importance of dynamical choice of the partition of time.

## 2.3 Simulation of $(\delta, \sigma)$ -Löwner equation driven by a stable Levy process

Substituting a stochastic process in the place of the driving function is a convenient instrument to study the structure of  $(\delta, \sigma)$ -Löwner chain. Fig. 1.5 shows that a  $(\delta, \sigma)$ -Löwner chain driven by a sample the Brownian motion  $((\delta, \sigma)$ -SLE) does not allow one to distinguish one choice of  $\delta$  and  $\sigma$  from another. In the general case, the curves have identical local behaviour and tend to a random point inside the disk.

To make such figures more representative one may consider a more general stochastic process than the Brownian motion. One of the most natural choices is the stable Levy process. This version of the stochastic chordal Löwner equation is considered in [ROKG06, ORGK08, CR09]. The point is that the usage of a discontinuous but piecewise continuous driving function gives a tree slit, not just a single curve. Each of the intervals of continuity of the driving function corresponds to a curve that is a branch of the tree. And each branch tends to a different random point. Thus, for each choice of  $\delta$  and  $\sigma$  we expect to have a unique characteristic pattern of a random tree.

The problem of a correct numerical simulation of a  $(\delta, \sigma)$ -Löwner equation driven by a stable Levy process has not been completely solved in the present work. The technical difficulty will be described below. However, we present some intermediate results and a picture that is somehow close to be correct. The author is not aware which method was used in the cited above papers. The most important step is the choice of partition of the time interval.

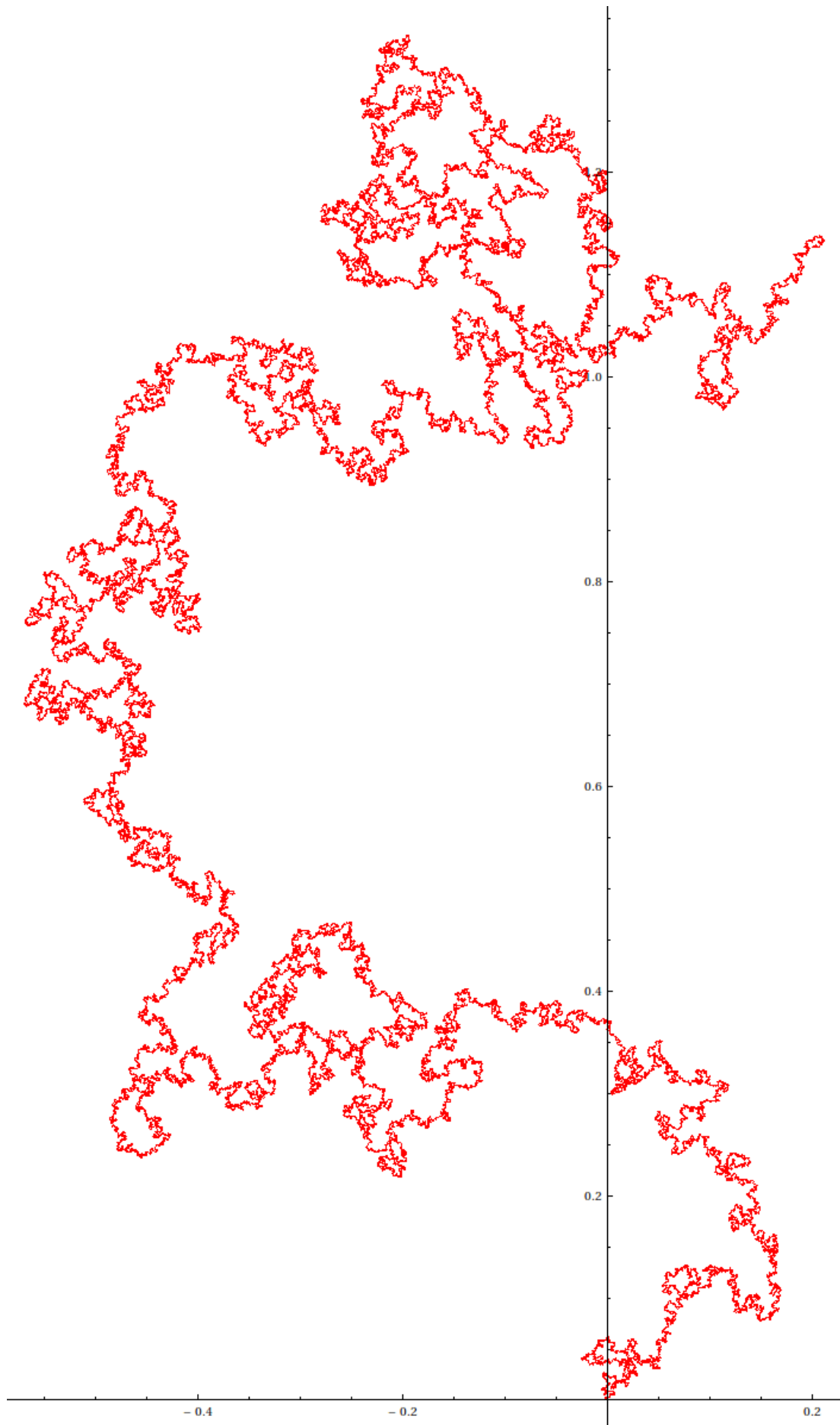


Figure 2.3: Simulation of chordal SLE slit in the half-plane chart for  $\kappa = 4$  ( $10^5$  points,  $d_{\max} = 10^{-3}$ , and  $d_{\min} = 0.5 \cdot 10^{-3}$ ).

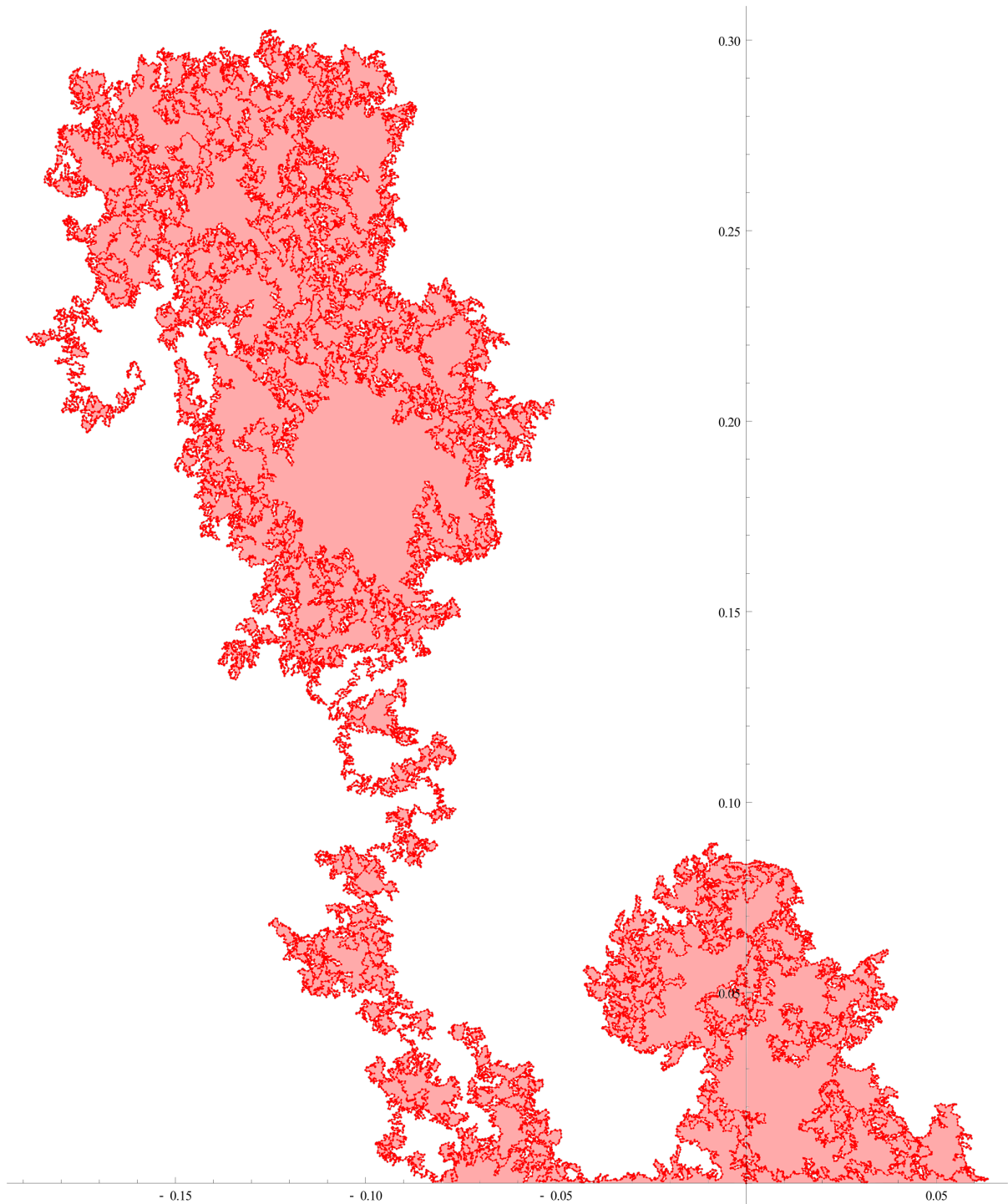


Figure 2.4: Simulation of the chordal SLE slit for  $\kappa = 7$  in the half-plane chart (38793 points),  $d_{\max} = 10^{-3}$ , and  $d_{\min} = 0.5 \cdot 10^{-3}$ . The method gives only an approximation of the curve that generates the hull  $\mathcal{K}_t$ . This approximate curve  $\tilde{\gamma}_t^N$  never touches itself, but passes close to itself. We fill the regions that are numerically close to be bounded by the curve with pink color by hand in a graphics editor.

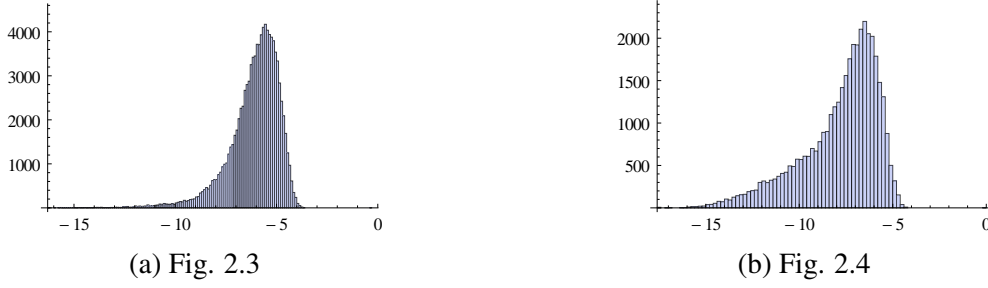


Figure 2.5: The histograms illustrate the distribution of the length of the intervals  $t_n - t_{n-1}$ ,  $n = 1, 2, \dots, N$  in the partitions of time that are used for the simulations in Fig.2.3 and 2.3. We used the logarithmic scale on the horizontal axis. The left histogram demonstrates that the length of the time intervals varies from  $10^{-12}$  to  $10^{-4}$ , which corresponds to a difference of eight orders of magnitude between the typical smallest and typical biggest time interval. The right histogram demonstrates the same variation, but from  $10^{-15}$  to  $10^{-5}$ .

### 2.3.1 Stable Levy process

In this section, we give the definition and consider some basic properties of the stable Levy process. For more details we refer to [App09].

**Definition 2.1.** *The stable Levy process (symmetric  $\alpha$ -stable Levy process) is an  $\mathbb{R}$ -valued stochastic process  $\{L_t^\alpha\}_{t \in [0, \infty)}$  ( $L_0 = 0$ ) with independent increments. The distribution law of the increments are defined by the following characteristic function*

$$\mathbb{E} \left[ e^{i(L_{t-s}^\alpha - L_s) \theta} \right] = e^{-s|\theta|^\alpha}, \quad \theta \in \mathbb{R}, \quad t, s \in [0, +\infty). \quad (2.21)$$

for some fixed  $0 < \alpha \leq 2$ .

The process  $\{L_t^\alpha\}_{t \in [0, \infty)}$  possesses the following properties:

1.  $\{L_t^\alpha\}_{t \in [0, \infty)}$  is time homogeneous;
2.  $\{L_t^\alpha\}_{t \in [0, \infty)}$  is strong Markov;
3.  $\{L_t^\alpha\}_{t \in [0, \infty)}$  is self-similar (scale covariant):

$$\text{Law}[L_{ct}^\alpha] = \text{Law}[c^{\frac{1}{\alpha}} L_t], \quad c > 0, \quad t \in [0, +\infty); \quad (2.22)$$

4.  $\{L_t^\alpha\}_{t \in [0, \infty)}$  is stochastically continuous, i.e.,

$$\lim_{t \rightarrow s} P^{L^\alpha} [ |L_{t+s}^\alpha| > a ] = 0, \quad a > 0, \quad s \in [0, +\infty); \quad (2.23)$$

5.  $\{L_t^\alpha\}_{t \in [0, \infty)}$  is right-continuous with left limits a.s.;
6. For  $\alpha < 2$ ,  $\{L_t^\alpha\}_{t \in [0, \infty)}$  is piecewise continuous, in the sense that on each finite time interval it is represented by a continuous function with a finite number of jumps of size bigger then  $\varepsilon > 0$  and a countable number of jumps smaller then  $\varepsilon$  a.s.;
7. For  $\alpha = 2$ ,  $\{L_t^\alpha\}_{t \in [0, \infty)}$  is the Brownian motion  $\{B_t\}_{t \in [0, +\infty)}$ .

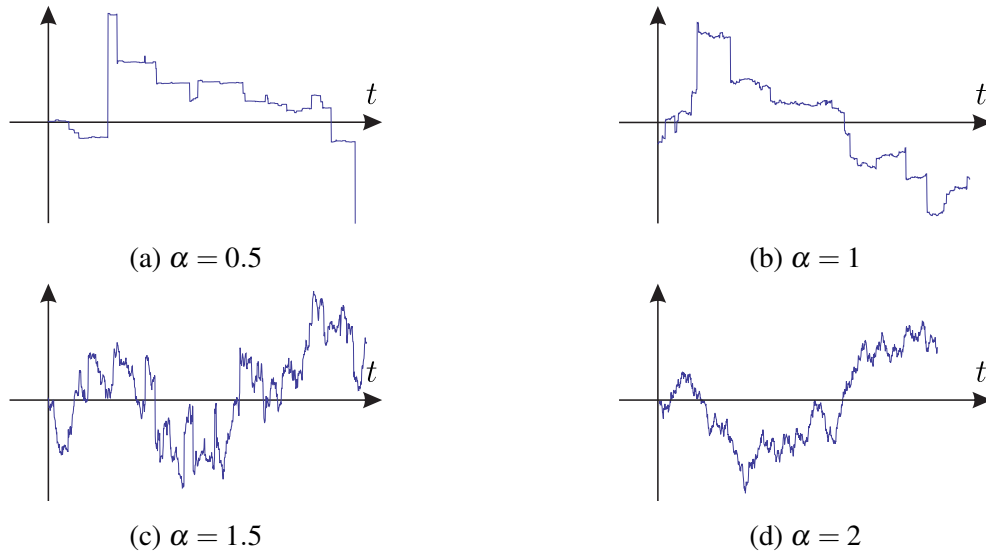


Figure 2.6: Samples of the stable Levy process  $\{L_t^\alpha\}_{t \in [0, +\infty)}$  for different values of  $\alpha$ .

Figure 2.6 illustrates samples of  $\{L_t^\alpha\}_{t \in [0, +\infty)}$  for different values of  $\alpha$ . We can see that smaller values of  $\alpha$  correspond to bigger but rarer jumps and more continuously looking behaviour between jumps. When  $\alpha$  tends to 2, the number of jumps increases, but they are smaller. In the limit we have the Brownian motion, which has no jumps a.s.

We use the following method of numerical sampling of  $\{L_t^\alpha\}_{t \in [0, \infty)}$ . Represent  $L_t$  as a composition

$$L_t = B_{Y_t^\alpha}, \quad t \in [0, +\infty) \quad (2.24)$$

of the Brownian motion  $\{B_s\}_{s \in [0, +\infty)}$  and an independent positive-valued strictly increasing stochastic process  $\{Y_t^\alpha\}_{t \in [0, \infty)}$  called **Levy subordinator**. The value of  $Y_t^\alpha$  may be sampled with the aid of the formula

$$Y_t^\alpha = \frac{t^{\frac{2}{\alpha}} \sin\left(\left(x + \frac{\pi}{2}\right) \frac{\alpha}{2}\right) \left(\frac{\cos\left(x - \frac{\pi}{2}\right) \frac{\alpha}{2}}{y}\right)^{\frac{2}{\alpha} - 1}}{\cos^{\frac{2}{\alpha}}(x)}, \quad t \in [0, +\infty), \quad (2.25)$$

where  $x$  is a random variable homogeneously distributed on the interval  $[-\pi/2, \pi/2]$  and  $y$  is an independent positive random variable with the probability density function  $p_y = e^{-y}$ ,  $y \geq 0$ . It can be shown<sup>1</sup> that a third independent Gaussian random variable with variance  $Y_t$  has characteristic function  $e^{-s|\theta|^\alpha}$ . Furthermore, the process  $\{Y_t\}_{t \in [0, +\infty)}$  defined by (2.25) is time-homogeneous.

For the Löwner slits simulation we also need a method to sample the Levy bridge. It is a stable Levy process, conditioned  $L_T^\alpha = X$  for some fixed  $X \in \mathbb{R}$  and  $T > 0$ , and denoted by  $\{L_{t;T,X}^\alpha\}_{t \in [0, t]}$ . This can be done by the following method. Let  $\{B_{t;T,X}\}_{t \in [0, t]}$  be the Brownian bridge, namely, the Brownian motion conditioned  $B_T = X$ . Then

$$L_{t;T,X}^\alpha = B_{Y_t^\alpha; Y_t^\alpha + \tilde{Y}_{T-t}^\alpha, X}, \quad t \in [0, t], \quad (2.26)$$

where  $Y_t^\alpha$  and  $\tilde{Y}_{T-t}^\alpha$  are two independently sampled subordinators as above.

<sup>1</sup>Unfortunately the author lost the reference to the book the formula (2.25) is from.

### 2.3.2 Simulation method for Levy process

Due to the strong Markov property of  $\{L_t^\alpha\}_{t \in [0, +\infty)}$  the stochastic process  $G_t$  driven by  $u_t = L_t$  is also strong Markov by the same argumentation as in Section 1.3.4. Thus, we can use the same representation (2.6) as before.

Each jump of the driving function corresponds to a new brunch of the tree slit. Hence, instead of connecting of the points  $\{\tilde{\gamma}_{n,a}^N\}_{n=1,2,\dots}$  by straight line segments, we apply the following method. We define a second sort of joint points:

$$\begin{aligned} \tilde{\gamma}_{n,b}^N &:= \bar{G}_1^{-1} \circ \bar{G}_2^{-1} \circ \dots \circ \bar{G}_n^{-1} \circ H_{t_{n+1}-t_n}^{-1}[\delta](a), \\ n &= 0, 1, 2, \dots, N-1 \end{aligned} \quad (2.27)$$

denoted with the index ‘ $b$ ’, see also the Fig. 2.1. Let

$$\bar{l}_n^N := \{\bar{G}_1^{-1} \circ \bar{G}_2^{-1} \circ \dots \circ \bar{G}_n^{-1} \circ H_s^{-1}[\delta](a) \in \mathcal{D}, \quad s \in [0, t_{n+1} - t_n]\} \quad (2.28)$$

be an arc that connects  $\tilde{\gamma}_{n,a}^N$  and  $\tilde{\gamma}_{n,b}^N$ . We approximate the tree hull  $\mathcal{K}_t$  by the union  $\bar{\mathcal{K}}_t^N := \bigcup_{n=0,1,\dots,N} \bar{l}_n^N$ . If we apply this for a continuous driving function, than the end  $\tilde{\gamma}_{n,b}^N$  of each arc  $\bar{l}_n^N$  would be close to the beginning point  $\tilde{\gamma}_{n+1,a}^N$  of the next arc  $\bar{l}_{n+1}^N$ . Thus, the tree  $\bar{\mathcal{K}}_t^N$  would tend to a simple curve. On the other hand, if the driving function has a jump  $\Delta u$  at  $t = t'$ ,  $t' \in (t_n, t_{n+1})$  the points  $\tilde{\gamma}_{n+1,a}^N$  and  $\tilde{\gamma}_{n+1,b}^N$  do not tend to each other because the distance between them is defined by the map  $H_{B_{t_{n+1}} - B_{t_n}}[\sigma]$  that tends to  $H_{\Delta u}[\sigma]$ , when  $t_n \rightarrow t' -$  and  $t_{n+1} \rightarrow t' +$ .

We can force to extend the method considered in the previous section to this situation by the substituting the distance  $d(\tilde{\gamma}_{n,a}^N, \tilde{\gamma}_{n-1,a}^N)$  by the distance  $d(\tilde{\gamma}_{n,b}^N, \tilde{\gamma}_{n,a}^N)$ . However, it turns out that  $\bar{\mathcal{K}}_t^N$  is not close to  $\mathcal{K}_t$  in this case. This happens for the following reason. The method of sampling of the stable Levi process  $\{L_t^\alpha\}_{t \in [0, +\infty)}$  allows to know the value of  $L_t^\alpha$  in some finite number of points, but not the positions of jumps. We obtain each visible branch of  $\bar{\mathcal{K}}_t^N$  just because of a relatively high value of  $L_{t_{n+1}}^\alpha - L_{t_n}^\alpha$  with respect to  $t_{n+1} - t_n$ . If the length of the arc  $\bar{l}_{n+1}^N$  after the ‘jump’ is not too big or small, the program continues the simulation for  $t > t_{n+1}$ . However, it may occur, and numerical tests confirm this, that the behaviour of  $L_t^\alpha$  between  $t_{n+1}$  and  $t_n$  is important. Namely, the jump between  $t_{n+1}$  and  $t_n$  may consists of two jumps and a small time interval between them may correspond to a numerically big subtree of  $\mathcal{K}_t$  that is lost. In the case of Brownian motion the probability of such a phenomenon was suppressed due to the continuity of the driving function (absence of jumps). In case of the Levy process, a numerical test showed that this regularly happens. In other words, the method of simulation proposed above does not give all the branches, but only some of them.

Nevertheless, we force this method. The result for chordal SLE and  $\alpha = 1.9$  is presented in fig. 2.2. The application for other types of  $(\delta, \sigma)$ -SLE in the unit disk chart does not give the expected result with the characteristic pattern because too many branches of the tree are lost. It would be promising to modify the discussed method in order to solve this problem.



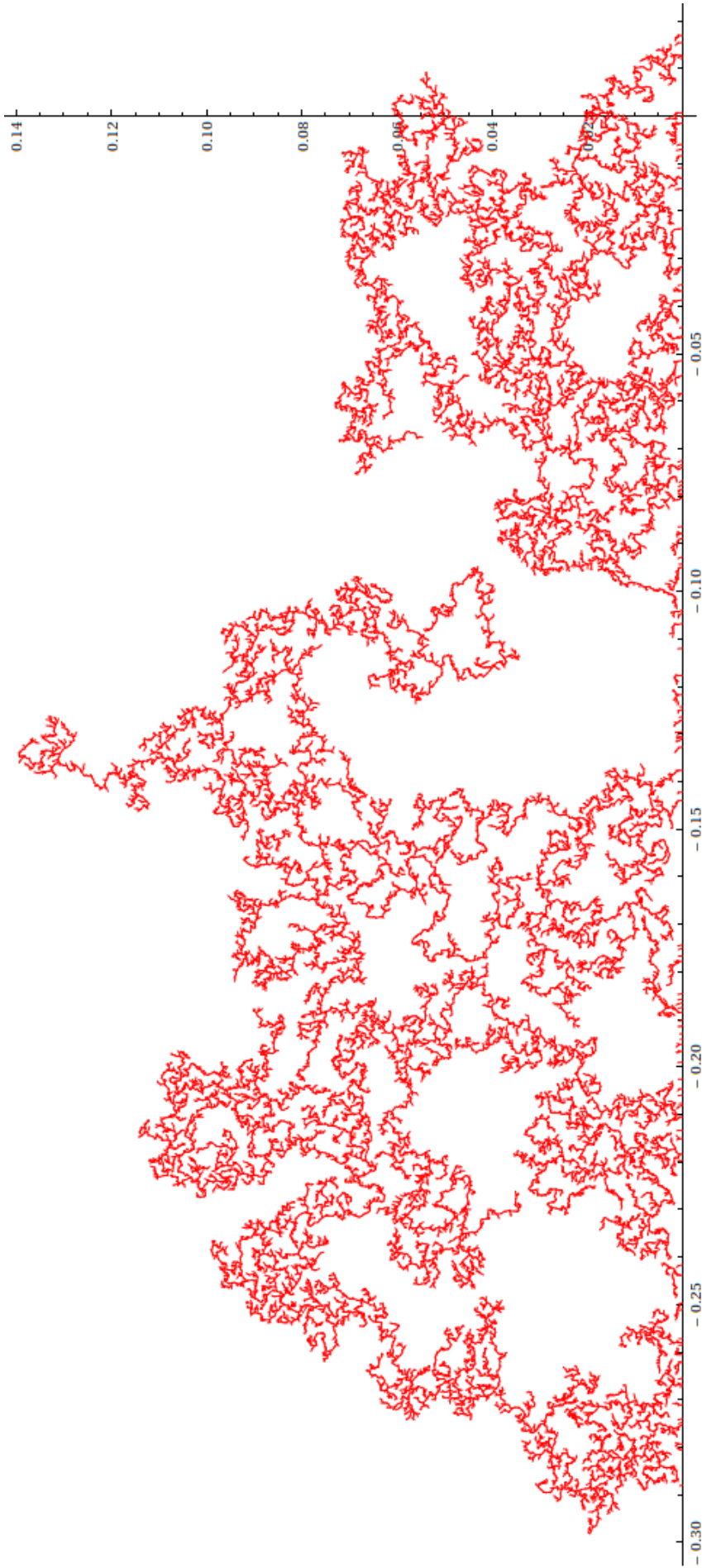


Table 2.2: Simulation of chordal SLE slit driven by stable Levy process ( $\mu_t := L_t^\alpha$ ) with the method described in the text ( $3 \cdot 10^4$  points). The parameters are  $\alpha = 1.9$  and  $T = 8 \cdot 10^{-3}$ . The slit is a sample of a random tree.



# Chapter 3

## $(\delta, \sigma)$ -Löwner equation from the algebraic point of view

### Introduction

In this chapter, we study the  $(\delta, \sigma)$ -Löwner equations from the point of view of the Lie algebras they are related to. In the first section, we reconsider the  $(\delta, \sigma)$ -SLE classification problem. The second one is dedicated to a generalization of the results of Roland Friedrich, Michel Bauer, and Denis Bernard about the SLE/CFT relation from the classical SLEs to the general case of  $(\delta, \sigma)$ -SLE.

### 3.1 Algebraic classification and normalization

In Section 1.2.3, we explained what we mean by essentially different Löwner chains and introduced normalization conditions in terms of coefficients  $\{\delta_i\}_{i=-2,-1,0,1}$  and  $\{\sigma_i\}_{i=-1,0,1}$ . Here, we study the family of essentially different  $(\delta, \sigma)$ -Löwner equations from a different point of view. We avoid using the basis (1.12) and parametrization (1.36). Instead, we consider purely algebraic properties of vector fields  $\delta$  and  $\sigma$  and their possible linear combinations and commutators. Such objects are invariant with respect to the transforms  $\mathcal{R}$  and  $\mathcal{S}$  by the construction.

Define a commutator of holomorphic vector two fields  $v$  and  $w$  by

$$[v, w]^\Psi(z) := v^\Psi(z) (w^\Psi)'(z) - w^\Psi(z) (v^\Psi)'(z) \quad (3.1)$$

It is straightforward to check that the right-hand side transforms as a vector field, according to the rule (1.5). Thus, we assume that  $[v, w]$  is also a vector field and the definition above is chart independent. For the basis vectors (1.12) this commutator takes the form

$$[\ell_n, \ell_m] = (m - n)\ell_{n+m}. \quad (3.2)$$

Define an infinite dimensional Lie algebra of holomorphic vector fields on  $\mathcal{D}$  that are tangent at the boundary except the point  $a \in \partial \mathcal{D}$ , where a finite order pole is allowed. The algebra is a real linear space

$$\mathcal{U}_{\leq 1} := \text{span}\{\ell_n \mid n = 1, 0, -1, -2, \dots\} \quad (3.3)$$

equipped with the Lie operation \$[\cdot, \cdot]\$. The algebra \$N\_{\leq 1}\$ is a subalgebra of a more frequently used Witt algebra

$$\text{Witt} := \text{span}\{\ell_n \mid n = \dots, -2, 1, 0, -1, -2, \dots\}. \quad (3.4)$$

Consider the Lie hull

$$\mathcal{U}[\delta, \sigma] := \text{span}\{\delta, \sigma, [\delta, \sigma], [[\delta, \sigma], \sigma], \dots\}, \quad (3.5)$$

where \$\delta\$ and \$\sigma\$ are given by (1.36). It is a subalgebra of \$\mathcal{U}\_{\leq 1}\$. Since we only consider such vector fields that \$\delta\_{-2} \neq 0\$ and \$\sigma\_{-1} \neq 0\$, the Lie algebra \$\mathcal{U}[\delta, \sigma]\$ is always infinite dimensional. For example, in the chordal \$\delta\$ and \$\sigma\$ case, see Section 6.1.1, we have

$$\mathcal{U}[2\ell_{-2}, \ell_{-1}] = \text{span}\{\ell_n \mid n = -1, -2, \dots\}. \quad (3.6)$$

It is remarkable that the transformations \$\mathcal{V}\$, \$\mathcal{T}\$ and \$\mathcal{D}\$ act on \$\delta\$ and \$\sigma\$ linearly and preserve the 2-dimensional subspace \$\text{span}\{\delta, \sigma\}\$. In particular, they leave the Lie hull \$\mathcal{U}[\delta, \sigma]\$ invariant. The transformations \$\mathcal{R}\$ and \$\mathcal{S}\$ do change \$\text{span}\{\delta, \sigma\}\$ and \$\mathcal{U}[\delta, \sigma]\$ (as a subset of \$\mathcal{U}\_{\leq 1}\$), but preserve the Lie algebra structure. Namely, the transforms \$\mathcal{R}\$ and \$\mathcal{S}\$ induce isomorphisms of subalgebras of \$\mathcal{U}\_{\leq 1}\$. Thus, in particular, essentially equivalent \$(\delta, \sigma)\$-SLEs correspond to isomorphic Lie algebras.

We also mention that the algebra corresponding to the chordal Löwner equation is represented by vector fields with a second order zero at the boundary point; the Lie algebra corresponding to the radial Löwner equations consists of vector fields vanishing at an interior point of the disk; and the Lie algebra corresponding to the dipolar Löwner equation consists of vector fields vanishing at two boundary points, see also the corresponding sections in Chapter 6. In other words, the Lie algebras corresponding to these essentially different Löwner equations are not isomorphic. It is a more difficult question whether or not the Lie hulls are isomorphic as algebras for essentially different equations. The investigation how the algebraic properties of \$\delta\$ and \$\sigma\$ influence the geometric properties of \$(\delta, \sigma)\$-Löwner chains seems very promising.

A possible way to classify the Löwner equations is to consider the following identity, which is the simplest nontrivial commutation relation between \$\delta\$ and \$\sigma\$.

$$[[\delta, \sigma], \delta] = x_5[[[\delta, \sigma], \sigma], \sigma] + x_4[[\delta, \sigma], \sigma] + x_3[\delta, \sigma] + x_2\delta + x_1\sigma + w, \quad (3.7)$$

where \$w\$ is a holomorphic vector field vanishing at the source point \$a\$. The coefficients \$x\_i\$, \$i = 1, 2, 3, 4, 5\$ are obviously invariant with respect to the transformations \$\mathcal{R}\$ and \$\mathcal{S}\$. With the aid of the transforms \$\mathcal{T}\$ and \$\mathcal{D}\$ it is always possible to fix

$$x_5 = \frac{1}{3}, \quad x_4 = 0 \quad (3.8)$$

(\$x\_5 = -\frac{1}{3}\$ for the reverse case). The transform

$$\mathcal{T}_c^2 \circ \mathcal{V}_c, \quad c \in \mathbb{R} \setminus \{0\} \quad (3.9)$$

keeps the above conditions unchanged. On other parameters it acts as

$$\begin{aligned} x_3 &\mapsto c^2 x_3, \\ x_2 &\mapsto c^3 x_2, \\ x_1 &\mapsto c^4 x_1, \end{aligned} \quad (3.10)$$

The collection of three real parameters  $\{x_3, x_2, x_1\}$  up to the transform (3.10), can be identified with the collection of all essentially different  $(\delta, \sigma)$ -Löwner chains. For example, in the normalization 1.76 and 1.77, for the forward dipolar equation  $x_3 = 8/3$  and  $x_2 = x_1 = 0$  and for the forward radial case  $x_3 = -8/3$  and  $x_2 = x_1 = 0$ . The value  $8/3$  can be replaced by an arbitrary positive constant due to (3.10). The case considered in [IV12] corresponds to  $x_3 = 32/3$ ,  $x_2 = 0$ , and  $x_1 = -60$  for the normalization (3.8).

The chordal case is special because  $x_1 = x_2 = x_3 = 0$ . All other cases can be understood as points on a 2-dimensional real manifold obtained as a quotient of  $\{x_3, x_2, x_1\}/$  by the transform (3.10), which is homeomorphic to a disk. The dipolar, radial, and [IV12] cases correspond to different points on the boundary of this manifold.

Essential difference in the stochastic case can be studied analogously. The investigation into how the algebraic properties of  $\delta$  and  $\sigma$  influence the random law of the  $(\delta, \sigma)$ -SLE seems to be very promising; in particular, in effects on the properties of the highest weight representation of  $\mathcal{U}[\delta, \sigma]$ , which plays an important role in the SLE/CFT connection discussed in Section 5.2.

We use the transform (1.119) to fix

$$x_5 = \frac{1}{3\kappa}, \quad x_4 = \frac{\nu}{\kappa^2} \quad (3.11)$$

according to definitions (1.121) and (1.126). The remaining part of the classification of essentially different  $(\delta, \sigma)$ -SLEs is the same as in Section 1.2.3. We just remark that there is one more special property of the chordal case: the chordal stochastic equation is the only one invariant with respect to  $\mathcal{P}$ .

## 3.2 $(\delta, \sigma)$ -Löwner equation and representation theory

In the theory of the Lie group-algebra correspondence and their representations (see, e.g. [Kna02]), the following construction is considered. Let  $\mathcal{M}$  be a manifold and  $\{v^i\}_{i=1,2,\dots,n}$  be a collection of vector fields on it such that the initial value problem

$$\dot{H}_t[v^i] = v^i \circ G_t, \quad G_0 = \text{id} \quad (3.12)$$

induces flows of automorphisms  $H_t[v^i] : \mathcal{M} \rightarrow \mathcal{M}$  for  $t \in (-\infty, +\infty)$ . Consider the Lie algebra  $\mathcal{U}\{v^1, v^2, \dots, v^n\}$  induced by the collection of vector fields  $\{v^i\}_{i=1,2,\dots,n}$  with respect to the commutator  $[\cdot, \cdot]$ . The linear space of this algebra consists of all linear combinations of  $v^1, v^2, \dots, v^n$  and all possible commutators. It is a subspace of the space of all vector fields on  $\mathcal{M}$ . Consider also the Lie group generated by all automorphisms  $H_t[v^i]$ ,  $t \in (-\infty, +\infty)$  with respect to composition. The Lie group-algebra theory establishes a connection between this group and algebra. As a linear space,  $\mathcal{U}\{v^1, v^2, \dots, v^n\}$  can be finite or infinite dimensional.

The Lie algebra  $\mathcal{U}[\delta, \sigma]$  and the semigroup of endomorphisms or inverse endomorphisms  $\mathcal{G}[\delta, \sigma]$  on  $\mathcal{D}$  introduced in Chapter 1 can be considered in the spirit of Lie theory. The author is not aware of any Lie semi-group analogous to this theory, and we avoid the construction of such a theory here.

The Lie algebra  $\mathcal{U}_{\leq 1}$  (see (3.3)) can be associated with the semi-group  $\mathcal{G}$  of all conformal endomorphisms of  $\mathcal{D}$ . We notice that any semigroup  $\mathcal{G}[\delta, \sigma]$  is a subsemigroup

of  $\mathcal{G}$ , as any algebra  $\mathcal{U}[\delta, \sigma]$  is a subalgebra of  $\mathcal{U}_{\leq 1}$ . Just as in the Lie group unitary representation theory we can expect that for a Lie algebra representation there is a corresponding group representation connected with the exponential map.

We notice that the algebra  $\mathcal{U}_{\leq 1}$  is a subalgebra of the **Virasoro algebra**. On the other hand, a Virasoro algebra representation is one of the key ingredients of the CFT. This is one of two approaches considered in this monograph to see the SLE/CFT relation.

A peculiar property of the classical cases is that the map  $G_t$  has fixed points. One can consider the Taylor expansion of  $G_t^\Psi(z)$  at these points, and define a group of germs instead of the semigroup. Michel Bauer and Denis Bernard used this in their series of papers (see, for example, [BB04b]) and considered an infinite dimensional group representation, see also [Kyt07]. We generalize this construction slightly by the consideration of non classical SLEs and the semigroups.

Consider the universal enveloping algebra (see e.g., [Kna02])  $\widehat{\mathcal{U}}_{\leq 1}$  of  $\mathcal{U}_{\leq 1}$ . According to the Poincaré–Birkhoff–Witt theorem it is a span of finite formal ordered products of the vectors in  $\mathcal{U}_{\leq 1}$

$$\mathcal{U}_{\leq 1} = \text{span}\{\ell_{-N}^{n-N} \dots \hat{\ell}_{-2}^{n-2} \hat{\ell}_{-1}^{n-1} \hat{\ell}_0^{n_0} \hat{\ell}_1^{n_1} \mid$$

$$\mid n_1, n_0, n_{-1}, n_{-2}, \dots, n_{-N+1} = 0, 1, 2, \dots, \quad n_{-N} = 1, 2, \dots, \quad N = 0, 1, 2, \dots\}, \quad (3.13)$$

where each  $\hat{\ell}_n \in \widehat{\mathcal{U}}_{\leq 1}$  corresponds to a basis vector of  $\mathcal{U}_{\leq 1}$ . We use the hat ‘ $\widehat{\phantom{x}}$ ’ to distinguish vector fields on  $\mathcal{D}$  and elements of the universal enveloping algebra as well as for the corresponding algebras. Following physics terminology we call elements of the universal enveloping algebra **operators** because they correspond to linear maps on  $\widehat{\mathcal{U}}$ . The formal product of operators  $\hat{\ell}_n$  possesses the property

$$\hat{\ell}_n \hat{\ell}_m - \hat{\ell}_m \hat{\ell}_n = (m - n) \hat{\ell}_{n+m} \quad (3.14)$$

due to (3.2).

Our purpose is to construct a representation of the semigroup  $\mathcal{G}[\delta, \sigma]$ . To this end we have to consider infinite linear combinations in (3.13), but not finite as above. We denote by  $\widetilde{\mathcal{U}}_{\leq 1}$  the linear space of formal infinite linear combinations of the basis vectors from  $\widehat{\mathcal{U}}_{\leq 1}$ . However, the algebraic structure of  $\widehat{\mathcal{U}}_{\leq 1}$  cannot be extended to  $\widetilde{\mathcal{U}}_{\leq 1}$  because infinite divergent sums appears near basis vectors after multiplications. For example, the square of

$$\hat{\ell}_{-1} \hat{\ell}_1 + \hat{\ell}_{-1}^2 \hat{\ell}_1^2 + \hat{\ell}_{-1}^3 \hat{\ell}_1^3 + \dots \in \widetilde{\mathcal{U}}_{\leq 1} \quad (3.15)$$

is not well defined because, in the formal series for the square, the coefficient near  $\hat{\ell}_0$  is an infinite divergent sum.

However, in some cases, like  $\text{Lie}\{\ell_{-2}, \ell_{-1}\}$ , it is possible due to the grading property. Let  $\widehat{\mathcal{U}}_{\leq 1}^n$ ,  $n \in \mathbb{Z}$  be a subset of  $\widehat{\mathcal{U}}_{\leq 1}$  defined by

$$\widehat{\mathcal{U}}_{\leq 1}^n := \text{span}\{\ell_{-N}^{n-N} \dots \hat{\ell}_{-2}^{n-2} \hat{\ell}_{-1}^{n-1} \hat{\ell}_0^{n_0} \hat{\ell}_1^{n_1} \mid$$

$$\mid n_1, n_0, n_{-1}, n_{-2}, \dots, n_{-N} = 0, 1, 2, \dots, \quad n_{-N} = 1, 2, \dots \wedge$$

$$\wedge n_1 + n_0 + n_{-1} + n_{-2} + \dots + n_{-N} = n, \quad N = 0, 1, 2, \dots\}. \quad (3.16)$$

Thus,

$$\widehat{u}_{\leq 1} = \bigcup_{n \in \mathbb{Z}} \widehat{u}_{\leq 1}^n \quad (3.17)$$

and

$$[\widehat{u}_{\leq 1}^n, \widehat{u}_{\leq 1}^m] = \widehat{u}_{\leq 1}^{n+m}, \quad n, m \in \mathbb{Z}. \quad (3.18)$$

We remark now that the restriction of  $\widehat{u}_{\leq 1}^n$  to  $\widehat{u}[\ell_{-2}, \ell_{-1}]$  is a finite dimensional space for  $n \leq -1$  and a zero dimensional space for  $n \geq 0$ . Hence the product in  $\widehat{u}[\ell_{-2}, \ell_{-1}]$  (formal infinite linear combinations of basis vectors from  $\widehat{u}[\ell_{-2}, \ell_{-1}]$ ) is well-defined because each coefficient in the product is given by an at most finite sum.

This case coincides with the chordal case because  $\mathcal{U}[\ell_{-2}, \ell_{-1}] = \mathcal{U}[\delta_c, \sigma_c]$ , see Section 6.1.1. The grading property can be generalized for the dipolar and the radial cases as well. To this end we can consider the basis of  $\mathcal{U}[\delta_d, \sigma_d]$  for the dipolar case, see Section 6.2.1, defined by

$$\ell_{d,n} := \ell_n - \ell_{n+2}, \quad n = -1, -2, -3, \dots, \quad (3.19)$$

and use the decomposition

$$\widehat{u}[\delta_d, \sigma_d] = \bigcup_{n=-1, -2, \dots} \widehat{u}_d^n \quad (3.20)$$

into finite dimensional subspaces

$$\begin{aligned} \widehat{u}_d^n := & \text{span} \{ \ell_{d, -N}^{n-N} \dots \ell_{d, -2}^{n-2} \ell_{d, -1}^{n-1} \ell_{d, 0}^{n_0} \ell_{d, 1}^{n_1} \mid \\ & | n_1, n_0, n_{-1}, n_{-2}, \dots, n_{-N} = 0, 1, 2, \dots \wedge n_1 + n_0 + n_{-1} + n_{-2} + \dots + n_{-N} = n, \\ & N = 0, 1, 2, \dots \}. \end{aligned} \quad (3.21)$$

They satisfy a weaker version of (3.18), namely,

$$[\widehat{u}_d^n, \widehat{u}_d^m] \subset \bigcup_{i=-1, -2, \dots, n+m} \widehat{u}_d^i. \quad (3.22)$$

For the radial case, see Section 6.3.1, we can apply an analogous method and obtain the basis

$$\ell_{r,n} := \ell_n + \ell_{n+2}, \quad n = -1, -2, -3, \dots. \quad (3.23)$$

Let the operators  $\widehat{\delta}$  and  $\widehat{\sigma}$  be the images of vector fields  $\delta$  and  $\sigma$  in  $\widehat{u}_{\leq 1}$ :

$$\begin{aligned} \widehat{\delta} &:= \delta_{-2} \widehat{\ell}_{-2} + \delta_{-1} \widehat{\ell}_{-1} + \delta_0 \widehat{\ell}_0 + \delta_1 \widehat{\ell}_1, \\ \widehat{\sigma} &:= \sigma_{-1} \widehat{\ell}_{-1} + \sigma_0 \widehat{\ell}_0 + \sigma_1 \widehat{\ell}_1 \end{aligned} \quad (3.24)$$

according to (1.36). Consider the initial value problem

$$\dot{\widehat{G}}_t = \widehat{G}_t \widehat{\delta} + \widehat{G}_t \widehat{\sigma} \dot{u}_t, \quad \widehat{G}_0 = \widehat{I}, \quad t \in [0, +\infty), \quad \widehat{G}_t \in \widehat{\mathcal{U}}[\delta, \sigma] \quad (3.25)$$

for some given  $\widehat{\delta}$  and  $\widehat{\sigma}$  and for any continuously differentiable function  $u_t$ . We denote by  $\widehat{I}$  the identity in  $\widehat{\mathcal{U}}$ . The vectors  $\widehat{\delta}$  and  $\widehat{\sigma}$  are placed on the right-hand side of  $\widehat{G}_t$  to be

in agreement with [BB04b] and traditional notation from quantum physics. The grading property ensures the existence and uniqueness of the solution because the system can be reduced to a countable collection of finite linear subsystems. For general  $(\delta, \sigma)$ -SLEs the existence is a more difficult problem. We assume the following conjecture henceforth.

**Conjecture 3.1.** *For any  $\delta$  and  $\sigma$  as in (1.36) and any continuously differentiable function  $\{u_t\}_{t \in [0, +\infty)}$  there exist a unique solution (3.25).*

If we denote the solution with the initial condition  $\hat{G}_0 = \hat{I}$  by  $\hat{G}_t$  we obtain the same properties as for  $G_t$  from section (1.2.1) as well as an analogue of Proposition 1.3. Thus, we obtained a map

$$\{u_t\}_{t \in [0, +\infty)} \mapsto \{\hat{G}_t\}_{t \in [0, +\infty)} \quad (3.26)$$

analogous to (1.38). Thereby, the product  $\hat{G}_t \hat{G}_\tau$  of two solutions  $\hat{G}_t$  and  $\hat{G}_\tau$  of (3.25) is well-defined, and it is the solution with driving function

$$\tilde{u}_s = \begin{cases} u_s & \text{if } s \in [0, t] \\ \tilde{u}_{s-t} + u_t & \text{if } s \in (t, +\infty). \end{cases} \quad (3.27)$$

We remark that it may be not true in general (for not classical cases) that for given  $G_t$  in  $\mathcal{G}[\delta, \sigma]$  there is a unique  $\hat{G}_t$  in  $\widehat{\mathcal{U}}[\delta, \sigma]$ , see the discussion in Section 1.2.2. This is because the map  $G_t$  depends only on the hull  $\mathcal{K}_t$ , while the vector  $\hat{G}_t$  ‘contains information’ of how the hull was generated. However, if  $\mathcal{K}_t = \gamma_t$  is a simple curve, we have the representation

$$\mathcal{G}[\delta, \sigma] \rightarrow \widehat{\mathcal{U}}[\delta, \sigma], \quad t \in [0, T]. \quad (3.28)$$

of the semigroup  $\mathcal{G}[\delta, \sigma]$ .

It is straightforward to define the stochastic process  $\{\hat{G}_t\}_{t \in [0, +\infty)}$  by

$$d^S \hat{G}_t = \hat{G}_t \hat{\delta} dt + \hat{G}_t \hat{\sigma} d^S B_t, \quad \hat{G}_0 = 1, \quad t \in [0, +\infty). \quad (3.29)$$

The existence of the solution is related to the Conjecture 3.1.

**Theorem 3.1.** *The Itô form for  $\hat{G}_t$  is*

$$d^{\text{Itô}} \hat{G}_t = \hat{G}_t \left( \hat{\delta} + \frac{1}{2} \hat{\sigma}^2 \right) dt + \hat{G}_t \hat{\sigma} d^{\text{Itô}} B_t, \quad \hat{G}_0 = 1, \quad t \in [0, +\infty). \quad (3.30)$$

*Proof.* We use that the Itô form of a vector valued stochastic process (5.17) is

$$d^{\text{Itô}} X_t^i = \left( \alpha^i(X_t) + \frac{1}{2} \beta^j(X_t) \frac{\partial \beta^i(X_t)}{\partial X_t^j} \right) dt + \beta^i(X_t) d^{\text{Itô}} B_t. \quad (3.31)$$

Let  $\{\hat{U}_i\}_{i=1,2,\dots}$  be the basis of  $\widehat{\mathcal{U}}[\delta, \sigma]$  and let  $X_t^i$  be the corresponding components of  $\hat{G}_t$  such as

$$\hat{G}_t = \sum_{i=1,2,\dots} X_t^i \hat{U}_i. \quad (3.32)$$



Thus,

$$\hat{G}_t \hat{\delta} = \sum_{i=1,2,\dots} \alpha^i(X_t) \hat{U}_i, \quad \hat{G}_t \hat{\sigma} = \sum_{i=1,2,\dots} \beta^i(X_t) \hat{U}_i, \quad (3.33)$$

and the matrix  $\frac{\partial}{\partial X_t^j} \beta^i(X_t)$  is represented by right multiplication with  $\hat{\sigma}$ . Thereby, we conclude (3.30) from (3.31).  $\square$

We define an operator in  $\widehat{\mathcal{U}}[\delta, \sigma]$ , which is an analogue of the diffusion differential operator  $\mathcal{A}$  (defined below by (5.14)) for the differential equation (1.104),

$$\hat{A} := \hat{\delta} + \frac{1}{2} \hat{\sigma}^2. \quad (3.34)$$

Let now  $\mathcal{V}[\delta, \sigma]$  be a representation space of the algebra  $\mathcal{U}[\delta, \sigma]$  and denote by  $|\rangle \in \mathcal{V}[\delta, \sigma]$  a vector such that

$$\hat{A}|\rangle = 0. \quad (3.35)$$

Then

$$d^{\text{It}\hat{\delta}} \hat{G}_t |\rangle = \hat{G}_t \hat{\sigma} |\rangle d^{\text{It}\hat{\delta}} B_t, \quad (3.36)$$

which means that  $\hat{G}_t |\rangle$  is a  $\widehat{\mathcal{U}}[\delta, \sigma]$ -valued local martingale. Now we consider a possible way to define such a space.

Let  $\text{Vir}$  be the Virasoro algebra, which is the only nontrivial central extension of the Witt algebra (3.4). We use the basis  $\{L_n, I\}_{n \in \mathbb{Z}}$ , in which the Lie brackets are

$$[L_n, L_m] = (m - n)L_{n+m} + \frac{1}{12}(n^3 - n)\delta_{n+m}I, \quad [L_n, I] = 0, \quad n, m \in \mathbb{Z}, \quad (3.37)$$

where  $\delta_{n+m}$  is the Kronecker delta ( $\delta_0 = 1$  and  $\delta_n = 0$ ,  $n \neq 0$ ). We used a non-standard choice of the sign of the basis elements  $L_n$  to be compatible with (1.12).

It is straightforward that  $\mathcal{U}_{\leq 1} \subset \text{Vir}$ , hence any representation of  $\text{Vir}$  is also a representation of  $\mathcal{U}_{\leq 1}$ . For the Virasoro algebra there is a well-studied representation theory. In particular, there is an infinite dimensional highest weight representation  $\mathcal{V}_{h,c}$ , for  $h, c \in \mathbb{R}$

$$\begin{aligned} \hat{L}_n |\rangle &= 0, \quad n = 1, 2, \dots \\ \hat{L}_0 |\rangle &= -h |\rangle, \\ \hat{I} |\rangle &= c |\rangle. \end{aligned} \quad (3.38)$$

Thereby, the collection

$$\begin{aligned} &\hat{L}_{-N}^{n-N} \dots \hat{L}_{-3}^{n-3} \hat{L}_{-2}^{n-2} \hat{L}_{-1}^{n-1} |\rangle, \\ &n_{-1}, n_{-2}, n_{-3}, \dots, n_{-N+1} = 0, 1, 2, \dots, \quad n_{-N} = 1, 2, \dots, \quad N = 0, 1, 2, \dots \end{aligned} \quad (3.39)$$

is a basis of  $\mathcal{V}_{h,c}$  and  $\mathcal{V}_{h,c} \approx \mathcal{U}[\ell_{-2}, \ell_{-1}]$  as linear spaces.

We denote the vectors from the space dual to  $\mathcal{V}_{h,c}$  by  $\langle \alpha |$ . In this notation,  $\langle |$  is a vector from the dual basis that corresponds to  $|\rangle$ , namely,

$$\begin{aligned} \langle || &= 1, \\ \langle |\hat{L}_{-N}^{n-N} \dots \hat{L}_{-3}^{n-3} \hat{L}_{-2}^{n-2} \hat{L}_{-1}^{n-1} |\rangle &= 0, \\ n_{-1}, n_{-2}, n_{-3}, \dots, n_{-N+1} &= 0, 1, 2, \dots, \quad n_{-N} = 1, 2, \dots, \quad N = 1, 2, \dots \end{aligned} \quad (3.40)$$

The parameters  $h$  and  $c$  can be chosen such that

$$\hat{L}_n \left( 2\hat{L}_{-2} \pm \frac{\kappa}{2} \hat{L}_{-1}^2 \right) |\rangle = 0, \quad n = 1, 2, \dots, \quad (3.41)$$

for given  $\kappa > 0$ . The necessary and sufficient conditions are

$$h = -\frac{\pm\kappa - 6}{\pm 2\kappa}, \quad c = h(\pm 3\kappa - 8). \quad (3.42)$$

This can be obtained with elementary calculations using (3.37) and (3.38), see [BB03a] for details. The condition (3.41) implies that the quotient space

$$\mathcal{V}_{h,c} |_{(2L_{-2} \pm \frac{\kappa}{2} L_{-1}^2) |\rangle \sim 0} \quad (3.43)$$

is a representation of  $\text{Vir}$  with the property (3.35), if we assume the upper sign in the ‘ $\pm$ ’ pairs for the forward case and the lower one for the reverse case.

If in addition  $\hat{L}_{-1} |\rangle = 0$ , the representation is trivial,  $\hat{L}_n |\rangle = 0$ ,  $n \in \mathbb{Z}$ . This is why we assume

$$\hat{L}_{-1} |\rangle \neq 0. \quad (3.44)$$

It can be shown (see [KR87]) that, in this case, the space (3.43) is a non-trivial irreducible infinite-dimensional representation of  $\text{Vir}$ , and consequently,  $\mathcal{U}_{\leq 1}$ .

Thereby, to obtain the space of local martingales, we extend the algebra  $\mathcal{U}[\delta, \sigma]$  to the algebra  $\text{Vir}$  and consider the vector space  $\mathcal{V}_{h,c}$ . From (3.24) and the rules (3.37) and (3.38) we conclude that

$$\begin{aligned} \hat{A} |\rangle = & \left[ \delta_{-2} \hat{L}_{-2} + \frac{\sigma_{-1}^2}{2} \hat{L}_{-1}^2 + \left( \delta_{-1} - \sigma_{-1} \sigma_0 \left( h + \frac{1}{2} \right) \right) \hat{L}_{-1} + \right. \\ & \left. + h \left( -\delta_0 + \sigma_{-1} \sigma_1 + \frac{1}{2} h \sigma_0^2 \right) \right] |\rangle \end{aligned} \quad (3.45)$$

Now we use the normalization from Section (1.3.2), (3.42), and (1.126) to obtain

$$\begin{aligned} \hat{A} |\rangle = & \\ = & \left( \pm 2\hat{L}_{-2} + \frac{\kappa}{2} \hat{L}_{-1}^2 \pm (\delta_{-1} + 3\sigma_0) \hat{L}_{-1} + \frac{(\kappa \mp 6) (\pm 4\delta_0 + (\mp 6 + \kappa) \sigma_0^2 + 4\kappa \sigma_1)}{8\kappa} \right) |\rangle = \\ = & \pm \left( 2\hat{L}_{-2} + \frac{\pm\kappa}{2} \hat{L}_{-1}^2 + \nu \hat{L}_{-1} + \frac{(\pm\kappa - 6) (4\delta_0 + (\pm\kappa - 6) \sigma_0^2 \pm 4\kappa \sigma_1)}{\pm 8\kappa} \right) |\rangle \end{aligned} \quad (3.46)$$

It is convenient to formally assume  $\kappa \rightarrow -\kappa$  for the reverse  $(\delta, \sigma)$ -SLE.

We conclude that  $\hat{G}_t |\rangle$  is a local martingale taking values in the quotient space (3.43) for the forward and reverse cases if and only if  $\nu = 0$  (or equivalently, (1.125)). This property does not depend on the choice of the basis  $\ell_n$ , however, the last coefficient in (3.46) does. We have proved the following theorem

**Theorem 3.2.** *Assume that for given  $\delta$  and  $\sigma$  the solution  $\hat{G}_t$  of 3.30 exists in the highest weight representation space of the Virasoro algebra. Then,  $\hat{G}_t |\rangle$  is a local martingale if and only if (3.42) is satisfied and  $\nu = 0$ .*

## Conclusions and Perspectives

1. We introduced the parameters  $x_1$ ,  $x_2$ , and  $x_3$  to classify  $(\delta, \sigma)$ -SLEs that are not essentially equivalent and the corresponding algebras  $\mathcal{U}[\delta, \sigma]$ . Does a better way to parametrize exist and what is possible to say about the properties of a  $(\delta, \sigma)$ -SLE, given  $\mathcal{U}[\delta, \sigma]$ , and vice versa?
2. It is important to prove Conjecture 3.1
3. We showed that the SLE/CFT connection in the sense of the existence of the related singular highest weight Virasoro algebra representation is only possible if  $\nu = 0$ . On the other hand, as we see in Chapter 5, there is no difficulty to relate SLEs with  $\nu \neq 0$  to the Gaussian free field. It is essential to obtain a possible generalization of the above approach to include the case  $\nu \neq 0$  as well as to understand the relation between the Gaussian free field and representation of the Virasoro algebra. For example, a more general approach from [Kyt09] may help.



# Chapter 4

## Gaussian Free Field or probabilistic approach to Euclidean Conformal Field Theory

### Introduction

This chapter is a kind of preface to the next one. Here, we introduce the **Gaussian free field (GFF)** and explain what we mean by **Conformal field theory (CFT)**. The author does not pretend to present new results in this chapter, however, he is not aware of direct analogues of some of the calculations and approaches. For example, the usage of derivational functional technique is frequently used in quantum field theory (see, for instance, [Vas98]) and in the probability theory, but not in mathematically strict application to CFT. The **Ward identity** in the form (4.123) is also not frequently used in literature.

We give some historical remarks now. Belavin, Polyakov, and Zamolodchikov (BPZ) [BPZ84] defined in 1984 a class of conformal theories ‘minimal models’, which described some discrete models (Ising, Potts, etc.) at criticality. Central theme is universality, i.e., the properties of a system close to the critical point are independent of its microscopic realization. Universal classes are characterized by a special parameter, central charge. A characteristic property of such model is the invariance with respect to a change of scale. In two dimensions this usually implies invariance with respect to arbitrary conformal change of coordinates. The ‘group’ of these transforms is infinite-dimensional and is called conformal group. This motivates the term Conformal field theory. The classical references are [FMS97, BP09, MS89], see also [Sch08] as an introduction for mathematicians.

CFT includes several ingredients such as correlation functions, operator-valued distributions, the highest weight representation of the Virasoro algebra, symmetry with respect to infinitesimal conformal maps, the Ward identities, the operator product expansion (OPE), and the vertex algebras. However, there is still no mathematically complete formulation that covers all of the aspects at the same time. See [Sum12] for an overview about the current status. The axiomatic approach to CFT grew up from the Hilbert sixth problem, and the Euclidean axioms were suggested by Osterwalder and Schrader [OS75]. BPZ conjectured that the behaviour of the system at criticality should be described by critical exponents identified as the highest weights of degenerate rep-

representations of infinite-dimensional Lie algebras, Virasoro in our case. The boundary version of this approach BCFT, i.e., CFT on domains with boundary, was developed by Cardy, [Car06].

Our approach to CFT, in this chapter, is mathematically complete and the reader does not need to have any background in this area. However, we consider here only aspects of CFT that we need to define its relation to  $(\delta, \sigma)$ -SLE. We restrict ourselves to the consideration of only Euclidean CFT with one free scalar (**pre-pre-Schwarzian**) bosonic field on a simply connected 2-dimensional domain (BCFT). It is because we couple only these models to SLE in the next chapter. The generalization is straightforward if one starts to consider a more general version of the coupling. The only important restriction is that the theory is supposed to be Euclidean, 2-dimensional, and bosonic.

In Section 4.5 we define GFF, which is a random law on the space of distributions over a domain in the complex plane that is invariant with respect to conformal transformation. The moments of this random variable can be interpreted as the correlation functions  $S_n$  and the analogue of the tress tensor and Ward identities are considered in Section 4.8. The operator product expansion can also be derived with this approach. To define the Hilbert space of states one can apply the so-called Wick rotation and the field reconstruction theorem, see [Sch08], to the correlation functions. The last step requires an additional element which is an anticonformal isomorphism denoted by  $*$  in [Sch08].

This is what we imply under CFT in this monograph. A similar approach is used in [Sim04, Nel73] for generic Euclidean field theory and in [SJSS] for the string theory and the Liouville theory.

## 4.1 Test functions

We will define the Schwinger functions  $S_n$  and the Gaussian free field  $\Phi$  in terms of linear functionals over some space of smooth test functions defined in what follows.

Let  $\mathcal{H}_s^\Psi$  be a linear space of real-valued smooth functions  $f: D^\Psi \rightarrow \mathbb{R}$  in the domain  $D^\Psi := \psi(\mathcal{D}) \subset \mathbb{C}$  with compact support equipped with the topology of homogeneous convergence of all derivatives on the corresponding compact, namely, the topology is generated by following collection of neighborhoods of the zero function

$$U_K^\Psi := \bigcap_{n,m=0,1,2,\dots} \{f(z) \in C^\infty(D) : \text{supp } f \subseteq K \wedge |\partial^n \bar{\partial}^m f^\Psi(z)| < \varepsilon_{n,m}, \quad z \in K\},$$

$$\varepsilon_{n,m} > 0, \quad n, m = 0, 1, 2, \dots,$$
(4.1)

where  $K \subset D^\Psi$  is any compact subset of  $D^\Psi$ .

We call  $f^\Psi \in \mathcal{H}_s^\Psi$  the **test functions** and assume that they are  $(1, 1)$ -differentials

$$f^{\tilde{\Psi}}(\tilde{z}) = \tau'(\tilde{z}) \overline{\tau'(\tilde{z})} f^\Psi(\tau(\tilde{z})), \quad \tau := \psi \circ \tilde{\psi}^{-1},$$
(4.2)

It is straightforward to check that any transition map  $\tau$  induces a homeomorphism between  $\mathcal{H}_s^\Psi$  and  $\mathcal{H}_s^{\tilde{\Psi}}$ . Thereby, we will drop the index  $\psi$  at  $\mathcal{H}_s$  henceforth, and we consider the space  $\mathcal{H}_s$  as a topological space of smooth  $(1, 1)$ -differentials with compact support.

We will use the space  $\mathcal{H}_s$  for the forward coupling (see Section 5.2). To study the reverse coupling we will use a slightly different space

$$\mathcal{H}_s^* := \left\{ f \in \mathcal{H}_s : \int_{D^\Psi} f^\Psi(z) l(dz) = 0 \right\}. \quad (4.3)$$

where  $l$  is the Lebesgue measure. This space consists of smooth compactly supported functions with the zero mean value in any chart. In Sections 6.3.2, 6.3.3, and 6.3.4, we consider other examples of such spaces. Henceforth, we denote by  $\mathcal{H}$  any of those nuclear spaces  $\mathcal{H}_s$ ,  $\mathcal{H}_s^*$ ,  $\mathcal{H}_{s,b}$ ,  $\mathcal{H}_{s,b}^*$ , or  $\mathcal{H}_{s,b}^\pm$  for shortness.

An important property of  $\mathcal{H}$  is the **nuclearity**, see [GV64, HS08, Pie72] which is necessary and sufficient to admit the uniform Gaussian measure on the dual space  $\mathcal{H}'$  (the GFF).

Constructing such a uniform Gaussian measure on a finite dimensional linear space is a trivial problem, however, it is not possible on an infinite-dimensional Hilbert space. On the other hand, if a space  $\mathcal{H}$  is nuclear as  $\mathcal{H}_s$  or  $\mathcal{H}_s^*$ , then the dual space  $\mathcal{H}'$  admits a uniform Gaussian measure. A general recipe holds not only for Gaussian measures and is given by the following theorem.

**Theorem 4.1. (Bochner-Minols [GV64, SJSS, HS08])**

Let  $\mathcal{H}$  be a nuclear space, and let  $\hat{\mu} : \mathcal{H} \rightarrow \mathbb{C}$  be a functional (non-linear). Then the following 3 conditions

1.  $\hat{\mu}$  is positive definite

$$\forall \{z_1, z_2, \dots, z_n\} \in \mathbb{C}^n, \forall \{f_1, f_2, \dots, f_n\} \in \mathcal{H}^n \Rightarrow \sum_{1 \leq k, l \leq n} z_k \bar{z}_l \hat{\mu}[f_k - f_l] \geq 0; \quad (4.4)$$

2.  $\hat{\mu}(0) = 1$ ;

3.  $\hat{\mu}$  is continuous

are satisfied if and only if there exists a unique probability measure  $P$  on  $(\Omega, \mathcal{F}, P)$  for  $\Omega = \mathcal{H}'$ , which has  $\hat{\mu}$  as a characteristic function

$$\hat{\mu}[f] := \int_{\Phi \in \mathcal{H}'} e^{i\Phi[f]} P_\Phi(d\Phi), \quad \forall f \in \mathcal{H}. \quad (4.5)$$

The corresponding  $\sigma$ -algebra  $\mathcal{F}_\Phi$  is generated by the cylinder sets

$$\{F \in \mathcal{H}' : F[f] \in B\}, \quad \forall f \in \mathcal{H}, \quad \forall \text{ Borel sets } B \text{ of } \mathbb{R}. \quad (4.6)$$

The random law on  $\mathcal{H}'$  is called uniform with respect to a bilinear functional  $B : \mathcal{H} \times \mathcal{H} \rightarrow \mathbb{R}$  if the characteristic function  $\hat{\mu}$  is of the form

$$\hat{\mu}[f] = e^{-\frac{1}{2}B[f,f]}, \quad f \in \mathcal{H}. \quad (4.7)$$

We consider the class of bilinear functionals we work with in Section 4.4. First we study the linear and bilinear functionals over  $\mathcal{H}_s$  and their transformation properties.

## 4.2 Pre-pre-Schwarzian

In Section 1.1 we defined a vector field by considering all charts and a certain transformation rule. Here we define an analogous construction with the same method.

A collection of maps  $\eta^\psi: \psi(\mathcal{D}) \rightarrow \mathbb{C}$ , each of which is given for a global chart map  $\psi: \mathcal{D} \rightarrow \psi(\mathcal{D}) \subset \mathbb{C}$ , is called a **pre-pre-Schwarzian** form of order  $\mu, \mu^* \in \mathbb{C}$  if for any chart map  $\tilde{\psi}$

$$\eta^{\tilde{\psi}}(\tilde{z}) = \eta^\psi(\tau(\tilde{z})) + \mu \log \tau'(\tilde{z}) + \mu^* \log \overline{\tau'(\tilde{z})}, \quad \tau = \psi \circ \tilde{\psi}^{-1}, \quad \tilde{z} \in \tilde{D}, \quad \forall \psi, \tilde{\psi}. \quad (4.8)$$

If  $\eta$  is defined for one chart map, then it is automatically defined for all other chart maps. We borrowed the term ‘pre-pre-Schwarzian’ from [KM11]. In [She10] the analogous object is called ‘AC surface’ and it is used in CFT as well.

Following Section 1.1 we define

$$F_* \eta^\psi(z) := \eta^{\psi \circ F}(z) = \eta^\psi((F^\psi)^{-1}(z)) + \mu \log \left( (F^\psi)^{-1} \right)'(z) + \mu^* \log \overline{\left( (F^\psi)^{-1} \right)'(z)} \quad (4.9)$$

We are interested in two special cases. The first one is  $\mu = \mu^* = \gamma/2 \in \mathbb{R}$ , and

$$F_* \eta^\psi(z) = \eta^\psi((F^\psi)^{-1}(z)) + Q \log \left| \left( (F^\psi)^{-1} \right)'(z) \right|. \quad (4.10)$$

The second is  $\mu = i\chi/2, \mu^* = -i\chi/2, \chi \in \mathbb{R}$ , and

$$F_* \eta^\psi(z) = \eta^\psi((F^\psi)^{-1}(z)) - \chi \arg \left( (F^\psi)^{-1} \right)'(z). \quad (4.11)$$

In both cases  $\eta$  can be chosen real in all charts. Moreover, if the pre-pre-Schwarzian is represented by a real-valued function in all charts it is one of two above forms.

A  $(\mu, \mu^*)$ -pre-pre-Schwarzian can be obtained from a vector field  $v$  by the relation

$$\eta^\psi(z) \equiv -\mu \log v^\psi(z) - \mu^* \log \overline{v^\psi(z)}. \quad (4.12)$$

For the two special cases above we have

$$\eta = -Q \log |v| \quad (4.13)$$

and

$$\eta = \chi \arg v, \quad (4.14)$$

where we dropped the upper index  $\psi$  and the argument  $z$ .

In Section 4.3, we obtain the transformation rules (4.10) by taking logarithm of a  $(1,1)$ -differential. The second type of the real pre-pre-Schwarzian is connected to a sort of an imaginary analog of a metric.

We can define the **Lie derivative** of  $X$ , where  $X$  can be a pre-pre-Schwarzian, a vector field, or even an object with a more general transformation rule (assignment), as

$$\mathcal{L}_v X^\psi(z) := \left. \frac{\partial}{\partial s} H_s^{-1}[v]_* X^\psi(z) \right|_{s=0}, \quad (4.15)$$



see (1.14) for the definition of  $H_s[v]$ . If  $X$  is a vector field  $w$ , then

$$\mathcal{L}_v w^\Psi = v^\Psi(z) \partial w^{\Psi'}(z) - v^{\Psi'}(z) w^\Psi(z) = [v, w]^\Psi(z), \quad (4.16)$$

see (3.1) for the definition of  $[\cdot, \cdot]$ .

If  $X$  is a pre-pre-Schwarzian, then

$$\mathcal{L}_v \eta^\Psi(z) = v^\Psi(z) \partial_z \eta^\Psi(z) + \overline{v^\Psi(z)} \partial_{\bar{z}} \eta^\Psi(z) + \mu v^{\Psi'}(z) + \mu^* \overline{v^{\Psi'}(z)}. \quad (4.17)$$

Here and further, we use notations

$$\partial_z := \frac{1}{2} \left( \frac{\partial}{\partial x} - i \frac{\partial}{\partial y} \right), \quad \partial_{\bar{z}} := \frac{1}{2} \left( \frac{\partial}{\partial x} + i \frac{\partial}{\partial y} \right), \quad (4.18)$$

and  $f' = \partial_z f$  for a holomorphic function  $f$ .

If  $\mu = \mu^* = 0$ , then  $\eta$  is called a **scalar**. It is remarkable that if  $\eta$  is a pre-pre-Schwarzian, then  $\mathcal{L}_v \eta$  is a scalar anyway, which is stated in the following lemma.

**Lemma 4.1.** *Let  $\eta$  be a pre-pre-Schwarzian of order  $\mu, \mu^*$ , let  $v$  be a holomorphic vector field, and let  $G$  be a conformal self-map. Then*

$$F_*^{-1}(\mathcal{L}_v \eta)^\Psi(z) = (\mathcal{L}_v \eta)^\Psi \circ F^\Psi(z), \quad (4.19)$$

or in the infinitesimal form

$$\mathcal{L}_w(\mathcal{L}_v \eta)^\Psi(z) = w^\Psi(z) \partial_z(\mathcal{L}_v \eta)^\Psi(z) + \overline{w^\Psi(z)} \partial_{\bar{z}}(\mathcal{L}_v \eta)^\Psi(z) \quad (4.20)$$

We present two short proves.

*Proof.* (first)

$$\begin{aligned}
F_*^{-1}(\mathcal{L}_v \eta)^\Psi(z) &= F_*^{-1} \left( v^\Psi(z) \partial_z \eta^\Psi(z) + \overline{v^\Psi(z)} \partial_{\bar{z}} \eta^\Psi(z) + \mu v^{\Psi'}(z) + \mu^* \overline{v^{\Psi'}(z)} \right) = \\
&= \frac{v^\Psi \circ F^\Psi(z)}{F^{\Psi'}(z)} \partial_z \left( \eta^\Psi \circ F^\Psi(z) + \mu \log F^{\Psi'}(z) + \mu^* \log \overline{F^{\Psi'}(z)} \right) + \\
&+ \frac{\overline{v^\Psi \circ F^\Psi(z)}}{F^{\Psi'}(z)} \partial_{\bar{z}} \left( \eta^\Psi \circ F^\Psi(z) + \mu \log F^{\Psi'}(z) + \mu^* \log \overline{F^{\Psi'}(z)} \right) + \\
&+ \mu \partial_z \frac{v^\Psi \circ F^\Psi(z)}{F^{\Psi'}(z)} + \mu^* \partial_{\bar{z}} \frac{\overline{v^\Psi \circ F^\Psi(z)}}{F^{\Psi'}(z)} = \\
&= v^\Psi \circ F^\Psi(z) (\partial \eta^\Psi) \circ F^\Psi(z) + \mu \frac{v^\Psi \circ F^\Psi(z)}{F^{\Psi'}(z)} \partial_z \log F^{\Psi'}(z) + 0 + \\
&+ \overline{v^\Psi \circ F^\Psi(z)} (\bar{\partial} \eta^\Psi) \circ F^\Psi(z) + 0 + \mu^* \frac{\overline{v^\Psi \circ F^\Psi(z)}}{F^{\Psi'}(z)} \partial_{\bar{z}} \log \overline{F^{\Psi'}(z)} + \\
&+ \mu v^{\Psi'} \circ F^\Psi(z) - \mu \frac{v^\Psi \circ F^\Psi(z) F^{\Psi''}(z)}{F^{\Psi'}(z)^2} + \mu^* \overline{v^{\Psi'} \circ F^\Psi(z)} - \mu^* \frac{\overline{v^\Psi \circ F^\Psi(z)} F^{\Psi''}(z)}{F^{\Psi'}(z)^2} = \\
&= (v^\Psi \partial \eta^\Psi) \circ F^\Psi(z) + \mu v^{\Psi'} \circ F^\Psi(z) + \\
&+ (\overline{v^\Psi} \bar{\partial} \eta^\Psi) \circ F^\Psi(z) + \mu^* \overline{v^{\Psi'} \circ F^\Psi(z)} = \\
&= \left( v^\Psi \partial \eta^\Psi + \overline{v^\Psi} \bar{\partial} \eta^\Psi + \mu v^{\Psi'} + \mu^* \overline{v^{\Psi'}} \right) \circ F^\Psi(z) = \\
&= (\mathcal{L}_v \eta)^\Psi \circ F^\Psi(z)
\end{aligned} \tag{4.21}$$

□

*Proof.* (second)

Let  $\alpha$  and  $\beta$  be two not necessary holomorphic vector fields such that

$$\eta^\Psi(z) = -\mu \log \alpha^\Psi(z) - \mu^* \log \beta^\Psi(z) \tag{4.22}$$

in some fixed chart  $\psi$ . For example, we can assume that  $\beta^\Psi \equiv 0$  and  $\alpha^\Psi = \mu^{-1} e^{-\eta^\Psi}$  in the chart  $\psi$ . Then, the transformation rules (4.8) are satisfied. □

### 4.3 Linear functionals and change of coordinates

In this section, we consider linear functionals over  $\mathcal{H}_s$  and  $\mathcal{H}$  that transform as pre-pre-Schwarzians.

Let  $\eta^\Psi \in \mathcal{H}_s^\Psi$  be a linear functional over  $\mathcal{H}_s^\Psi$  for a given chart  $\psi$ . The functional is called regular if there exists a locally integrable function  $\eta^\Psi(z)$  such that

$$\eta^\Psi[f] := \int_{\psi(\mathcal{D})} \eta^\Psi(z) f^\Psi(z) l(dz), \tag{4.23}$$

where  $l$  is the Lebesgue measure on  $\mathbb{C}$ . We use the brackets  $[\cdot]$  for functionals and the parentheses  $(\cdot)$  for corresponding functions (kernels).

We assume that  $f$  transforms according to (4.2). If  $\eta^\Psi(z)$  is a scalar, then the number  $\eta^\Psi[f] \in \mathbb{R}$  does not depend on the choice of the chart  $\psi$ . Indeed, for any choice of another chart  $\tilde{\psi}$  we have

$$\begin{aligned} \eta^{\tilde{\psi}}[f] &:= \int_{\tilde{\psi}(\mathcal{D})} \eta^{\tilde{\psi}}(\tilde{z}) f^{\tilde{\psi}}(\tilde{z}) l(d\tilde{z}) = \int_{\tilde{\psi}(\mathcal{D})} \eta^\Psi(\tau(\tilde{z})) f^\Psi(\tau(\tilde{z})) |\tau'(\tilde{z})|^2 l(d\tilde{z}) = \\ &= \int_{\psi(\mathcal{D})} \eta^\Psi(z) f^\Psi(z) l(dz) = \eta^\Psi[f], \end{aligned} \quad (4.24)$$

If  $\eta^\Psi(z)$  is a pre-pre-Schwarzian, we have

$$\begin{aligned} \eta^{\tilde{\psi}}[f] &= \int_{\tilde{\psi}(\mathcal{D})} \eta^{\tilde{\psi}}(\tilde{z}) f^{\tilde{\psi}}(\tilde{z}) l(d\tilde{z}) = \\ &= \int_{\tilde{\psi}(\mathcal{D})} \left( \eta^\Psi(\tau(\tilde{z})) + \mu \log \tau'(z) + \mu^* \overline{\log \tau'(z)} \right) f^\Psi(\tau(\tilde{z})) |\tau'(\tilde{z})|^2 l(d\tilde{z}) = \\ &= \int_{\psi(\mathcal{D})} \left( \eta^\Psi(z) - \mu \log \tau^{-1'}(z) - \mu^* \overline{\log \tau^{-1'}(z)} \right) f^\Psi(z) l(dz) = \\ &= \eta^\Psi[f] - \int_{\psi(\mathcal{D})} \left( \mu \log \tau^{-1'}(z) + \mu^* \overline{\log \tau^{-1'}(z)} \right) f^\Psi(z) l(dz) \end{aligned} \quad (4.25)$$

according to (4.9).

If  $\eta^\Psi$  is not a regular pre-pre-Schwarzian but just a functional from  $\mathcal{H}'_s$  we can consider the last line of (4.25) as a definition of the transformation rules for  $\eta[f]$  from a chart  $\psi$  to a chart  $\tilde{\psi}$ . We denote by  $\mathcal{H}'_s$  the linear space of pre-pre-Schwarzians as above.

The space  $\mathcal{H}^{*'}_s$  dual to  $\mathcal{H}_s^*$  is a quotient space

$$\mathcal{H}^{*'}_s = \mathcal{H}_s' / \sim, \quad \eta \sim \eta + C \quad \Leftrightarrow \quad C \in \mathbb{R}, \quad \eta \in \mathcal{H}_s' \quad (4.26)$$

of functionals over  $\mathcal{H}_s$  defined up to a constant.

Consider now the pushforward operation  $F_*$  on  $(1,1)$ -differentials  $f$  defined by

$$(F_*f)^\Psi(z) := \left| (F^\Psi)^{-1'}(z) \right|^2 f^\Psi \left( (F^\Psi)^{-1}(z) \right). \quad (4.27)$$

For a conformal map  $F: \mathcal{D} \setminus \mathcal{K} \rightarrow \mathcal{D}$  the right-hand side is a finitely supported function and  $F_*$  is a linear homeomorphism  $F_*: \mathcal{H}_s \rightarrow \mathcal{H}_s$  or  $F_*: \mathcal{H}_s^* \rightarrow \mathcal{H}_s^*$ . However, if  $F: \mathcal{D} \rightarrow \mathcal{D} \setminus \mathcal{K}$ , then the right-hand side is well-defined only if  $\text{supp } f \subset \mathcal{D} \setminus \mathcal{K}$ . In this work we define  $F_*$  only on a subset of  $\mathcal{H}_s$  of test functions that are supported in  $\mathcal{D} \setminus \mathcal{K} = F^{-1}(\mathcal{D})$ .

Define the pushforward operation by

$$\begin{aligned} F_*\eta^\Psi[f] &= \eta^{\Psi \circ F}[f] = \\ &= \eta^\Psi[F_*^{-1}f] + \int_{\text{supp } f^\Psi} \left( \mu \log (F^\Psi)^{-1'}(z) + \mu^* \overline{\log (F^\Psi)^{-1'}(z)} \right) f^\Psi(z) l(dz), \end{aligned} \quad (4.28)$$

$$f \in \mathcal{H}_s: \text{supp } f \subset \text{Im}(F).$$

It can be understood as a pushforward  $F_* : \mathcal{H}'_s \rightarrow \mathcal{H}'_s$  in the dual space if  $F : \mathcal{D} \setminus \mathcal{K} \rightarrow \mathcal{D}$ . For  $F : \mathcal{D} \rightarrow \mathcal{D} \setminus \mathcal{K}$  the formula (4.60) is well-defined only for functional  $\eta$  over test functions supported on  $\mathcal{D} \setminus \mathcal{K}$ .

Functionals over the space  $\mathcal{H}_s$  are differentiable infinitely many times. The Lie derivative is defined by

$$\begin{aligned} \mathcal{L}_v \eta[f] &= \left. \frac{\partial}{\partial s} H_s^{-1}[v]_* \eta^\Psi[f] \right|_{s=0} = \\ &= -\eta^\Psi[\mathcal{L}_v f] + \int_{\text{supp } f^\Psi} \left( \mu v^{\Psi'}(z) + \mu^* \overline{v^{\Psi'}(z)} \right) f^\Psi(z) l(dz), \end{aligned} \quad (4.29)$$

where

$$\begin{aligned} \mathcal{L}_v f^\Psi(z) &= \left. \frac{\partial}{\partial s} H_s^{-1}[v]_* f^\Psi \right|_{s=0} = \\ &= v^\Psi(z) \partial_z f^\Psi(z) + \overline{v^\Psi(z)} \partial_{\bar{z}} f^\Psi(z) + v^{\Psi'}(z) f^\Psi(z) + \overline{v^{\Psi'}(z)} f^\Psi(z). \end{aligned} \quad (4.30)$$

#### 4.4 Fundamental solution to the Laplace-Beltrami equation

In this section, we consider linear continuous functionals with respect to each argument in  $\mathcal{H}_s$ . An important example is the Dirac functional

$$\delta_\lambda[f, g] := \int_{\psi(\mathcal{D})} f^\Psi(z) g^\Psi(z) \frac{1}{\lambda^\Psi(z)} l(dz), \quad f, g \in \mathcal{H}_s, \quad (4.31)$$

where  $\lambda(z)l(dz)$  is a differential of some measure on  $\psi(\mathcal{D})$  that is mutually absolutely continuous with respect to the Lebesgue measure  $l(dz)$ . The Radon–Nikodym coefficient  $\lambda^\Psi(z)$  transforms as a  $(1, 1)$ -differential:

$$\lambda^{\tilde{\Psi}}(\tilde{z}) = \tau'(\tilde{z}) \overline{\tau'(\tilde{z})} \lambda^\Psi(\tau(\tilde{z})), \quad \tau := \psi \circ \tilde{\psi}^{-1}. \quad (4.32)$$

It is easy to see that the right-hand side of (4.31). does not depend on the choice of  $\psi$ .

We call the functional regular if there exists a function  $B^\Psi(z, w)$  on  $\psi^{\mathcal{D}} \times \psi^{\mathcal{D}}$  such that

$$B^\Psi[f, g] := \int_{\psi(\mathcal{D})} \int_{\psi(\mathcal{D})} B^\Psi(z, w) f^\Psi(z) g^\Psi(w) l(dz) l(dw), \quad f, g \in \mathcal{H}_s. \quad (4.33)$$

We use the same convention about the brackets and parentheses as for the linear functionals. We consider only scalar regular bilinear functionals and require the transformation rules

$$B^{\tilde{\Psi}}(\tilde{z}, \tilde{w}) = B^\Psi(\tau(\tilde{z}), \tau(\tilde{w})), \quad \tau = \psi \circ \tilde{\psi}^{-1}, \quad z, w \in \tilde{\psi}(\mathcal{D}). \quad (4.34)$$

Thus, the right-hand side of (4.33) does not depend on the choice of the chart  $\psi$  and we can drop the index  $\psi$  in the left-hand side.

The pushforward is defined by

$$F_*B^\Psi(z, w) = B^{\Psi \circ F}(z, w) := B^\Psi((F^\Psi)^{-1}(z), (F^\Psi)^{-1}(w)), \quad z, w \in \text{Im}(F^\Psi). \quad (4.35)$$

and, for an arbitrary functional,

$$F_*B^\Psi[f, g] = B^{\Psi \circ F}[f, g] := B^\Psi[F_*^{-1}f, F_*^{-1}g], \quad f, g \in \mathcal{H}_s: \text{supp } f \subset \text{Im}(F). \quad (4.36)$$

The same remarks as in the previous section for  $\eta$  remain true in this case.

Define now the Lie derivative in the same way as above

$$\begin{aligned} \mathcal{L}_v B^\Psi(z, w) &:= \left. \frac{\partial}{\partial s} H_s[v]_*^{-1} B^\Psi(z, w) \right|_{s=0} = \\ &= v^\Psi(z) \partial_z B^\Psi(z, w) + \overline{v^\Psi(z)} \partial_{\bar{z}} B^\Psi(z, w) + v^\Psi(w) \partial_w B^\Psi(z, w) + \overline{v^\Psi(w)} \partial_{\bar{w}} B^\Psi(z, w). \end{aligned} \quad (4.37)$$

We remark that  $\mathcal{L}_v B$  is also scalar in two variables. Functionals  $\delta_\lambda$  and  $B$  are both scalar and continuous with respect to each variable.

Define the Laplace-Beltrami operator  $\Delta_\lambda$  as

$$\Delta_{\lambda 1} B^\Psi(z, w) := -\frac{4}{\lambda \psi(z)} \partial_z \partial_{\bar{z}} B^\Psi(z, w), \quad (4.38)$$

where the lower index '1' means that the operator acts only with respect to the first argument.

Let a regular bilinear functional  $\Gamma_\lambda$  be a solution to the equation

$$\Delta_{\lambda 1} \Gamma_\lambda[f, g] = 2\pi \delta_\lambda[f, g], \quad \Gamma_\lambda[f, g] = \Gamma_\lambda[g, f], \quad f, g \in \mathcal{H}_s. \quad (4.39)$$

We fix the boundary conditions later. This equation is conformally invariant in the sense that if  $\Gamma_\lambda^\Psi(z, w)$  is a solution on a chart  $\psi$ , then

$$\Gamma_\lambda^\Psi(\tau(\tilde{z}), \tau(\tilde{w})) = \Gamma_\lambda^{\tau^{-1} \circ \Psi}(z, w) \quad (4.40)$$

is a solution in the chart  $\tau^{-1} \circ \psi$ .

The solution  $\Gamma_\lambda^\Psi(z, w)$  is a collection of smooth and harmonic functions on  $\psi(\mathcal{D}) \times \psi(\mathcal{D}) \setminus \{z \times w: z = w\}$  of general form

$$\Gamma_\lambda^\Psi(z, w) = -\frac{1}{2} \log(z - w)(\bar{z} - \bar{w}) + H^\Psi(z, w), \quad (4.41)$$

where  $H^\Psi(z, w)$  is an arbitrary symmetric harmonic function with respect to each variable that is defined by the boundary conditions and will be specified in what follows.

It is straightforward to verify that the function  $\Gamma_\lambda^\Psi(z, w)$  does not depend on the choice of  $\lambda$  because the identity (4.39) in the integral form is

$$\begin{aligned} &\int_{\psi(\mathcal{D})} \int_{\psi(\mathcal{D})} -\frac{4}{\lambda \psi(z)} \partial_z \partial_{\bar{z}} \Gamma^\Psi(z, w) f^\Psi(z) g^\Psi(w) l(dz) l(dw) = \\ &= \int_{\psi(\mathcal{D})} f^\Psi(z) g^\Psi(z) \frac{1}{\lambda \psi(z)} l(dz). \end{aligned} \quad (4.42)$$

The change  $\lambda \rightarrow \tilde{\lambda}$  is equivalent to a change  $f^\Psi(z) \rightarrow \frac{\lambda^\Psi(z)}{\tilde{\lambda}^\Psi(z)} f^\Psi(z)$ . We will drop the lower index  $\lambda$  in  $\Gamma_\lambda$  below. The fundamental solutions of the Laplace equation are also known as **Green's functions** (for free field).

**Example 4.1. Dirichlet boundary conditions.** Let us denote by  $\Gamma_D$  the solution  $\Gamma$  to (4.39) satisfying the zero boundary conditions, namely,

$$\Gamma_D^{\mathbb{H}}(z, w) \Big|_{z \in \mathbb{R}} = 0, \quad \lim_{z \rightarrow \infty} \Gamma_D^{\mathbb{H}}(z, w) = 0, \quad w \in \mathbb{H}. \quad (4.43)$$

Then,  $\Gamma_D$  admits the form

$$\Gamma_D^{\mathbb{H}}(z, w) := -\frac{1}{2} \log \frac{(z-w)(\bar{z}-\bar{w})}{(z-\bar{w})(\bar{z}-w)}, \quad (4.44)$$

and possesses the property of symmetry with respect to all Möbius automorphisms  $H : \mathcal{D} \rightarrow \mathcal{D}$ ,

$$H_* \Gamma_D = \Gamma_D \quad (4.45)$$

or

$$\mathcal{L}_\sigma \Gamma_D(z, w) = 0, \quad \forall \text{ complete vector field } \sigma. \quad (4.46)$$

**Example 4.2. Combined Dirichlet-Neumann boundary conditions.** Let  $\Gamma_{DN}$  denote the solution to (4.39) satisfying the following boundary conditions in the strip chart

$$\begin{aligned} \Gamma_{DN}^{\mathbb{S}}(z, w) \Big|_{z \in \mathbb{R}} = 0, \quad \partial_y \Gamma_{DN}^{\mathbb{S}}(x+iy, w) \Big|_{y=\pi} = 0, \quad x \in \mathbb{R}, \\ \lim_{z \rightarrow \infty \wedge \operatorname{Re} z > 0} \Gamma_{DN}^{\mathbb{S}}(z, w) = 0, \quad \lim_{z \rightarrow \infty \wedge \operatorname{Re} z < 0} \Gamma_{DN}^{\mathbb{S}}(z, w) = 0, \quad w \in \mathbb{H}. \end{aligned} \quad (4.47)$$

We consider this case in Section 6.2.4 and the exact form of  $\Gamma_{DN}$  is given by (6.68). It is not invariant with respect to all Möbius automorphisms but it is invariant if the automorphism preserves the points of change of the boundary conditions, which are  $\pm\infty$  in the strip chart.

The set of bilinear functionals  $\mathcal{H}_s^* \otimes \mathcal{H}_s^* \rightarrow \mathbb{R}$  over  $\mathcal{H}_s^*$  can be obtained from the corresponding set of functionals over  $\mathcal{H}_s$  with the equivalence relation

$$B[f, g] \sim B[f, g] + \beta[f] + \beta[g], \quad \beta \in \mathcal{H}_s'. \quad (4.48)$$

In particular,  $B^\Psi(z, w)$  is defined up to a sum  $\beta^\Psi(z) + \beta^\Psi(w)$ , for any locally integrable real-valued function  $\beta(z)$ .

**Example 4.3.** Let  $\mathcal{H} = \mathcal{H}_s^*$ , define the bilinear functional by the regular expression

$$\Gamma_N^{\mathbb{H}}(z, w) := -\frac{1}{2} \log(z-w)(\bar{z}-\bar{w})(z-\bar{w})(\bar{z}-w) + \beta(z) + \beta(w). \quad (4.49)$$

The functional  $\Gamma_N$  is invariant with respect to Möbius transforms  $H$

$$\Gamma[f, g] = H_* \Gamma[f, g], \quad f, g \in \mathcal{H}_s^* \quad (4.50)$$

as well as  $\Gamma_D$ . Equivalently,

$$\Gamma(z, w) = \Gamma(H^{-1}(z), H^{-1}(w)) + \varepsilon(z) + \varepsilon(w) \quad (4.51)$$

for some locally integrable function  $\varepsilon$ .

If we ignore the term  $\beta(z) + \beta(w)$  the function  $\Gamma_N^{\mathbb{H}}(z, w)$  possesses the Neumann boundary condition

$$\partial_y \Gamma_N^{\mathbb{H}}(x + iy, w) \Big|_{y=0} = 0, \quad x \in (-\infty, +\infty), \quad w \in \mathbb{H}. \quad (4.52)$$

There is a singular point at the infinity, but it can be cancelled by some proper choice of  $\beta$ .

We will consider one more example ( $\Gamma_{tw,b}$ ) in Section 6.3.4.

## 4.5 Gaussian free field

**Definition 4.1.** Let for some nuclear space of smooth functions  $\mathcal{H}$  the linear functional  $\eta$  and some Green's functional  $\Gamma$  are given. Assume in Theorem 4.1

$$\hat{\mu}[f] := \exp\left(-\frac{1}{2}\Gamma[f, f] + i\eta[f]\right), \quad f \in \mathcal{H}. \quad (4.53)$$

Then the  $\mathcal{H}'$ -valued random variable  $\Phi$  is called the **Gaussian free field (GFF)**. We will denote it by  $\Phi(\mathcal{H}, \Gamma, \eta)$ .

For convenience, we change the definition of the characteristic function from (4.5) to

$$\hat{\phi}[f] := \int_{\Phi \in \mathcal{H}'_s} e^{\Phi[f]} P_{\Phi}(d\Phi), \quad \forall f \in \mathcal{H}, \quad (4.54)$$

and (4.53) changes to

$$\hat{\phi}[f] = e^{\left(\frac{1}{2}\Gamma[f, f] + \eta[f]\right)}, \quad (4.55)$$

which is possible for the Gaussian measures.

The **expectation** of a random variable  $X[\Phi]$  ( $X : \mathcal{H}' \rightarrow \mathbb{C}$ ) is defined as

$$\mathbb{E}[X] := \int_{\Phi \in \mathcal{H}'_s} X[\Phi] P(d\Phi). \quad (4.56)$$

An alternative and equivalent (see, for example [HS08]) definition of GFF can be formulated as follows:

**Definition 4.2.** The **Gaussian free field**  $\Phi$  is a  $\mathcal{H}'$ -valued random variable, that is a map  $\Phi : \mathcal{H} \times \Omega \rightarrow \mathbb{R}$  (measurable on  $\Omega$  and continuous linear on the nuclear space  $\mathcal{H}$ ), or a measurable map  $\Phi : \Omega \rightarrow \mathcal{H}'$ , such that  $\text{Law}[\Phi[f]] = N\left(\eta[f], \Gamma[f, f]^{\frac{1}{2}}\right)$ ,  $f \in \mathcal{H}$ , i.e., it possesses the properties

$$\mathbb{E}[\Phi[f]] = \eta[f], \quad \forall f \in \mathcal{H}, \quad (4.57)$$

$$\mathbb{E}[\Phi[f]\Phi[f]] = \Gamma[f, f] + \eta[f]\eta[f], \quad \forall f \in \mathcal{H} \quad (4.58)$$

for Green's bilinear positively defined functional  $\Gamma$ , and for a linear functional  $\eta$ .

The random variable  $\Phi$  introduced this way transforms from one chart to another according to the pre-pre-Schwarzian rule

$$\Phi^{\tilde{\psi}}[f] = \Phi^{\psi}[f] - \int_{\psi(\mathcal{D})} \left( \mu \log \tau^{-1'}(z) + \mu^* \overline{\log \tau^{-1'}(z)} \right) f^{\psi}(z) l(dz), \quad \tau := \psi \circ \tilde{\psi}^{-1}, \quad (4.59)$$

due to the corresponding property (4.25) of  $\eta$ .

The pushforward can also be defined by

$$F_* \Phi^{\psi}[f] = \Phi^{\psi}[F_*^{-1} f] + \int_{\text{supp } f^{\psi}} \left( \mu \log (F^{\psi})^{-1'}(z) + \mu^* \overline{\log (F^{\psi})^{-1'}(z)} \right) f(z) l(dz),$$

$$f \in \mathcal{H}: \text{supp } f \subset \text{Im}(F) \quad (4.60)$$

as well as the Lie derivatives

$$\begin{aligned} \mathcal{L}_v \Phi[f] &= \left. \frac{\partial}{\partial s} H_s^{-1}[v]_* \Phi^{\psi}[f] \right|_{s=0} = \\ &= -\Phi^{\psi}[\mathcal{L}_v f] + \int_{\text{supp } f^{\psi}} \left( \mu v^{\psi'}(z) + \mu^* \overline{v^{\psi'}(z)} \right) f^{\psi}(z) l(dz), \end{aligned} \quad (4.61)$$

**Example 4.4.** Let  $\mathcal{H} := \mathcal{H}_s$ ,  $\Gamma := \Gamma_D$  (as in Example 5.85), let  $\eta^{\psi}(z) := 0$  in all charts  $\psi$  ( $\mu = \mu^* = 0$ ). Then we call  $\Phi(\mathcal{H}_s, \Gamma_D, 0)$  the Gaussian free field with **zero boundary condition**.

**Example 4.5.** Relax the previous example. Let  $\eta^{\psi}$  be a harmonic function in  $D^{\psi}$  continuously extendable to the boundary  $\partial D^{\psi}$  if the chart map  $\psi$  can be extended to  $\partial \mathcal{D}$ . Then we call  $\Phi$  the Gaussian free field with the **Dirichlet boundary condition**.

We can define the Laplace-Beltrami operator  $\Delta_{\lambda}$  over  $\Phi$  as well as the Lie derivative by

$$(\Delta_{\lambda} \Phi)[g] := \Phi[\Delta_{\lambda} g], \quad g \in \mathcal{H}, \quad (4.62)$$

where  $\Delta_{\lambda}$  on a  $(1, 1)$ -differential is defined by

$$\Delta_{\lambda} g^{\psi}(z) := -4 \partial_z \partial_{\bar{z}} \frac{g^{\psi}(z)}{\lambda \psi(z)} \quad (4.63)$$

in any chart  $\psi$ . If  $\eta$  is harmonic the identity

$$\begin{aligned} &\mathbb{E}[(\Delta_{\lambda} \Phi)[g] \Phi[f_1] \Phi[f_2] \dots \Phi[f_n]] = \\ &= \sum_{i=1, 2, \dots, n} \delta_{\lambda}[g, f_i] \mathbb{E}[\Phi[f_1] \Phi[f_2] \dots \Phi[f_{i-1}] \Phi[f_{i+1}] \dots \Phi[f_n]] \end{aligned} \quad (4.64)$$

is satisfied. Thereby, one can write heuristically

$$\Delta_{\lambda} \Phi(z) = 0, \quad z \notin \text{supp } f_1 \cup \text{supp } f_2 \cup \dots \cup \text{supp } f_n. \quad (4.65)$$



It turns out that the characteristic functional  $\hat{\phi}$  is also a derivation functional for the correlation functions. Define the variational derivative over some functional  $\nu$  as a map  $\frac{\delta}{\delta f}: \nu \mapsto \frac{\delta}{\delta f} \nu$  to the set of functionals by

$$\left( \frac{\delta}{\delta f} \nu \right) [g] := \frac{\partial}{\partial \alpha} \nu[g + \alpha f] \Big|_{\alpha=0}, \quad \forall f, g \in \mathcal{H}. \quad (4.66)$$

If  $\nu$  is such that  $\nu[g + \alpha f]$  is an analytic function with respect to  $\alpha$  in a neighbourhood of  $\alpha = 0$  for each  $f$  and  $g$ , like  $\hat{\phi}$ , it is straightforward to see that for each  $g, f_1, f_2, \dots \in \mathcal{H}$

$$\nu[g] = \nu[0], \quad g \in \mathcal{H} \quad \Leftrightarrow \quad \left( \frac{\delta}{\delta f_1} \frac{\delta}{\delta f_2} \dots \frac{\delta}{\delta f_n} \nu \right) [0] = 0, \quad n = 1, 2, \dots \quad (4.67)$$

Define the Schwinger functionals as

$$S_n[f_1, f_2, \dots, f_n] := \mathbb{E}[\Phi[f_1]\Phi[f_2]\dots\Phi[f_n]] = \left( \frac{\delta}{\delta f_1} \frac{\delta}{\delta f_2} \dots \frac{\delta}{\delta f_n} \hat{\phi} \right) [0] \quad (4.68)$$

where  $\hat{\phi}: \mathcal{H} \rightarrow \mathbb{R}$  is defined in (4.55).

The identity (4.64) can be reformulated as

$$\mathbb{E} \left[ (\Delta_\lambda \Phi)[g] e^{\Phi[f]} \right] = (\delta_\lambda [g, f] + \eta[\Delta_\lambda f]) \hat{\phi}[f], \quad f, g \in \mathcal{H}. \quad (4.69)$$

## 4.6 The Schwinger functionals

In this section, we consider the Schwinger functionals defined by (4.68) and their derivation functional  $\hat{\phi}$  in more detail.

For any finite collection  $\{f_1, f_2, \dots, f_n\}$  of functions from  $\mathcal{H}_s$  or  $H_\Gamma$ , the collection of random variables  $\{\Phi[f_1], \Phi[f_2], \dots, \Phi[f_n]\}$  has the multivariate normal distribution. Thus, we have

$$\mathbb{E}[\Phi[f_1]\Phi[f_2]\dots\Phi[f_n]] = \sum_{\text{partitions}} \prod_k \Gamma[f_{i_k}, f_{j_k}], \quad (4.70)$$

for  $\eta(z) \equiv 0$ , where the sum is taken over all partitions of the set  $\{1, 2, \dots, n\}$  into disjoint pairs  $\{i_k, j_k\}$ . In particular, the expectation of the product of an odd number of fields is identically zero. For the general case ( $\eta \neq 0$ ) the Schwinger functionals are

$$S[f_1, f_2, \dots, f_n] := \mathbb{E}[\Phi[f_1]\Phi[f_2]\dots\Phi[f_n]] = \sum_{\text{partitions}} \prod_k \Gamma[f_{i_k}, f_{j_k}] \prod_l \eta[f_{i_l}], \quad (4.71)$$

where the sum is taken over all partitions of the set  $\{1, 2, \dots, n\}$  into disjoint non-ordered pairs  $\{i_k, j_k\}$ , and non-ordered single elements  $\{i_l\}$ . In particular,

$$\begin{aligned} S_1[f_1] &= \eta[f_1], \\ S_2[f_1, f_2] &= \Gamma[f_1, f_2] + \eta[f_1]\eta[f_2], \\ S_3[f_1, f_2, f_3] &= \Gamma[f_1, f_2]\eta[f_3] + \Gamma[f_3, f_1]\eta[f_2] + \Gamma[f_2, f_3]\eta[f_1] + \eta[f_1]\eta[f_2]\eta[f_3], \\ S_4[f_1, f_2, f_3, f_4] &= \Gamma[f_1, f_2]\Gamma[f_3, f_4] + \Gamma[f_1, f_3]\Gamma[f_2, f_4] + \Gamma[f_1, f_4]\Gamma[f_2, f_3] + \\ &\quad + \Gamma[f_1, f_2]\eta[f_3]\eta[f_4] + \Gamma[f_1, f_3]\eta[f_2]\eta[f_4] + \Gamma[f_1, f_4]\eta[f_2]\eta[f_3] + \\ &\quad + \eta[f_1]\eta[f_2]\eta[f_3]\eta[f_4]. \end{aligned} \quad (4.72)$$

Such correlation functionals are called the **Schwinger functionals**. Their kernels

$$S_n(z_1, z_2, \dots, z_n) \quad (4.73)$$

are known as Schwinger functions or  $n$ -point functions. For regular functionals  $\Gamma$  and  $\eta$ , the Schwinger functions are also regular but it is still reasonable to understand  $S_n$  as a functional because the derivatives are not regular. For example,

$$\Delta_{\lambda_1} S_2^\Psi(z, w) = 2\pi\delta_\lambda(z - w). \quad (4.74)$$

The transformation rules for  $S_n$  (the behaviour under the action of  $G_*$ ) are quite complex. We present here only the infinitesimal ones

$$\begin{aligned} \mathcal{L}_v S_n^\Psi[f_1, f_2, \dots] = & - \sum_{1 \leq k \leq n} S_n^\Psi[f_1, f_2, \dots, \mathcal{L}_v f_k, \dots, f_n] - \\ & - \sum_{1 \leq k \leq n} S_{n-1}^\Psi[f_1, f_2, \dots, f_{k-1}, f_{k+1}, \dots, f_{n-1}] \int_{\psi(\mathcal{D})} \left( \mu v^{\Psi'}(z) + \mu^* \overline{v^{\Psi'}(z)} \right) f_k^\Psi(z) l(dz) \end{aligned} \quad (4.75)$$

We prefer to work with the characteristic functional  $\hat{\phi}$ , rather than with  $S_n$ . For instance, for any endomorphism  $F: \tilde{\mathcal{D}} \rightarrow \mathcal{D}$  We can define the pushforward operation  $F_*: \hat{\phi}(\Gamma, \eta) \mapsto \hat{\phi}(F_*\Gamma, F_*\eta)$  which maps functionals on  $\mathcal{D}$  to functionals on  $\tilde{\mathcal{D}}$ . Equivalently,

$$(F_*\hat{\phi}(\Gamma, \eta))[\tilde{f}] := \hat{\phi}(F_*\Gamma, F_*\eta)[\tilde{f}], \quad \tilde{f} \in \mathcal{H}_s[\tilde{\mathcal{D}}]. \quad (4.76)$$

(we need to mark the dependence on the functionals  $\Gamma$  and on  $\eta$  here).

The Lie derivative  $\mathcal{L}_v$  over an arbitrary nonlinear functional  $\rho: \mathcal{H}_s \rightarrow \mathbb{C}$  can also be defined as

$$\mathcal{L}_v \rho[f] := (\mathcal{L}_v \rho)[f] = \frac{\partial}{\partial \alpha} (H_\alpha[v]_*^{-1} \rho)[f] \Big|_{\alpha=0} \quad (4.77)$$

(if the partial derivative over  $\alpha$  is well-defined).

For example,

$$\mathcal{L}_v \exp(\rho[f]) = (\mathcal{L}_v \rho[f]) \exp(\rho[f]), \quad (4.78)$$

$$\mathcal{L}_v^2 \exp(\rho[f]) = (\mathcal{L}_v^2 \rho[f] + (\mathcal{L}_v \rho[f])^2) \exp(\rho[f]). \quad (4.79)$$

In our case  $\rho[f] = \hat{\phi}[f] = \frac{1}{2}\Gamma[f, f] + \eta[f]$ . We remind that the Lie derivative of  $\eta$  and  $\Gamma$  are defined in (4.17) and (4.37) respectively.

The operations  $G_*^{-1}$  and  $\frac{\delta}{\delta f}$  or  $\mathcal{L}$  and  $\frac{\delta}{\delta f}$  commute. Thus, for example, we have

$$\mathcal{L}_v S_n[f_1, f_2, \dots, f_n] = \left( \frac{\delta}{\delta f_1} \frac{\delta}{\delta f_2} \dots \frac{\delta}{\delta f_n} \mathcal{L}_v \hat{\phi} \right) [0]. \quad (4.80)$$

We use this to deduce the martingale properties of  $G_t^{-1} S_n$  and of all their variational derivatives from the martingale property of  $G_t^{-1} \hat{\phi}$ , which will be discussed in the next section.

## 4.7 Gaussian Hilbert space

Define inner product on  $\mathcal{H}$  by

$$(f, g)_\Gamma := \Gamma[f, g], \quad f, g \in \mathcal{H}. \quad (4.81)$$

If the bilinear functional  $\Gamma$  is positively defined, then consider the real Hilbert space

$$H_\Gamma := \overline{\mathcal{H}}^{(\cdot, \cdot)_\Gamma} \quad (4.82)$$

obtained by the completion of  $\mathcal{H}$  with respect to the inner product  $(\cdot, \cdot)_\Gamma$ .

**Proposition 4.1.** *Let  $\eta$  be continuous with respect to the topology of  $H_\Gamma$ , and let consequently  $\eta^\psi \in H'_\Gamma$ . For any  $f \in H_\Gamma$  there exists a Gaussian random variable  $\Phi[f] \in L_2(\Omega)$  with the expectation  $\eta[f]$  and the covariance  $(f, f)_\Gamma^{\frac{1}{2}}$ . Moreover, for any collection of  $f_1, f_2, \dots, f_N \in H_\Gamma$  the set  $\{\Phi[f_1], \Phi[f_2], \dots, \Phi[f_N]\}$  is a collection of jointly Gaussian variables and*

$$\mathbb{E}[(\Phi[f_n] - \eta[f_n])(\Phi[f_m] - \eta[f_m])] = \Gamma[f_n, f_m], \quad n, m = 1, 2, \dots, N. \quad (4.83)$$

*Proof.* Consider a fundamental sequence  $\{g_n\}_{n=1,2,\dots}$  such as

$$g_k \xrightarrow{H_\Gamma} f, \quad k \rightarrow +\infty. \quad (4.84)$$

Then, the sequence  $\Phi[g_k]$ ,  $k = 1, 2, \dots$  converges in  $L_2(\Omega)$  because

$$\mathbb{E}[(\Phi[g_n] - \Phi[g_m])^2] = \Gamma[g_k - g_l, g_k - g_l] = (g_k - g_l, g_k - g_l)_\Gamma \quad (4.85)$$

tends to zero according to the definition of the sequence  $\{g_k\}_{n=1,2,\dots}$  we started from.

To show (4.83) we can consider the limit of characteristic functions

$$\begin{aligned} & \mathbb{E} \left[ e^{\Phi[g_{1,k_1}] + \Phi[g_{2,k_2}] + \dots + \Phi[g_{N,k_N}]} \right] = \\ & = e^{\frac{1}{2}\Gamma[g_{1,k_1} + g_{2,k_2} + \dots + g_{N,k_N}, g_{1,k_1} + g_{2,k_2} + \dots + g_{N,k_N}] + \eta[g_{1,k_1} + g_{2,k_2} + \dots + g_{N,k_N}]} \rightarrow \\ & \rightarrow e^{\frac{1}{2}\Gamma[f_1 + f_2 + \dots + f_N, f_1 + f_2 + \dots + f_N] + \eta[f_1 + f_2 + \dots + f_N]}, \\ & g_{n,k_n} \xrightarrow{H_\Gamma} f_n, \quad k_n \rightarrow +\infty, \quad n = 1, 2, \dots, N. \end{aligned} \quad (4.86)$$

□

We remark that  $\Phi$  can not be understood as a random variable that takes values in  $H'_\Gamma$ , even though  $\Phi[f]$  is a random variable for any  $f \in H_\Gamma$ . However, the functionals  $\Gamma$ ,  $\eta$ ,  $S_n$ , and  $\hat{\phi}$  are defined for  $f \in H_\Gamma$  as well and the machinery from the previous section can be extended from  $f \in \mathcal{H}$  to  $f \in H_\Gamma$

**Definition 4.3.** *Gaussian Hilbert space is subspace  $\Phi[H_\Gamma] \subset L_2(\Omega)$  consisting of vector  $\Phi[f]$  for  $f \in H_\Gamma$ .*

Define the convolution

$$(\Gamma * f)^\Psi(z) := \int_{\psi(\mathcal{D})} \Gamma(z, w) f^\Psi(w) l(dz), \quad f \in \mathcal{H} \quad (4.87)$$

for any chart  $\psi$ . Let

$$\mathcal{H}_\Gamma^1 := \Gamma * \mathcal{H} \quad (4.88)$$

be the image space which is also nuclear with respect to the image topology. It consists of functions

$$h = \Gamma * f \in \mathcal{H}_\Gamma^1, \quad f \in \mathcal{H} \quad (4.89)$$

that transform as scalars

$$F_* h^\Psi = h^\Psi \circ (F^\Psi)^{-1}. \quad (4.90)$$

We remark that  $h$  possess the some boundary conditions as  $\Gamma$ . In particular, if  $\Gamma = \Gamma_{DN}$  is as in Example 4.2 then  $h$  posses Dirichlet and Neumann boundary conditions on corresponding intervals of  $\partial \mathcal{D}$ .

Let

$$(h, f) := \int_{\psi(\mathcal{D})} f^\Psi(z) h^\Psi(z) l(dz), \quad f \in \mathcal{H}, \quad h \in \mathcal{H}_\Gamma^1. \quad (4.91)$$

and

$$(h_1, h_2)_\nabla := 4 \int_{\psi(\mathcal{D})} \overline{\partial h_1^\Psi(z)} \partial h_2^\Psi(z) l(dz) \quad (4.92)$$

be the Dirichlet inner product. We notice that the form (4.92) is chart independent. This property can be called **conformal invariance of the Dirichlet inner form**. It is straightforward to check that

$$(f_1, f_2)_\Gamma = (f_1, h_2) = (h_1, f_2) = \frac{1}{2\pi} (h_1, h_2)_\nabla, \quad h_i = \Gamma * f_i, \quad i = 1, 2, \quad (4.93)$$

if  $\Gamma$  possesses ether Dirichlet or Neumann boundary conditions on each interval of the boundary. This condition is satisfied for all choices of  $\Gamma$  in this text. For the last relation and (4.92) we can conclude that  $(\cdot, \cdot)_\Gamma$  is positively defined.

The separable Hilbert space

$$H_\Gamma^1 := \overline{\mathcal{H}_\Gamma^1}^{(\cdot, \cdot)_\nabla} \quad (4.94)$$

is naturally isomorphic to  $H_\Gamma$  with the convolution map (4.89). As well as  $\mathcal{H}_\Gamma^1$  it consists of functions satisfying the same boundary conditions as  $\Gamma$ .

Due to (4.93) it is natural to associate the Gaussian free field  $\Phi$  with the space  $H_\Gamma^1$ . Let  $\{\xi_n\}_{n=1,2,\dots}$  be a countable collection of independent standard normally distributed random variables, let  $\{e_n\}_{n=1,2,\dots}$  be an orthonormal basis of  $H_\Gamma$ , let  $\{e_n^1\}_{n=1,2,\dots}$  be an orthonormal basis of  $H_\Gamma^1$  such that  $(e_i^1, e_j) = \delta_{i,j}$ ,  $i, j = 1, 2, \dots$ , and let

$$f = \sum_{n=1,2,\dots} f_i e_i. \quad (4.95)$$

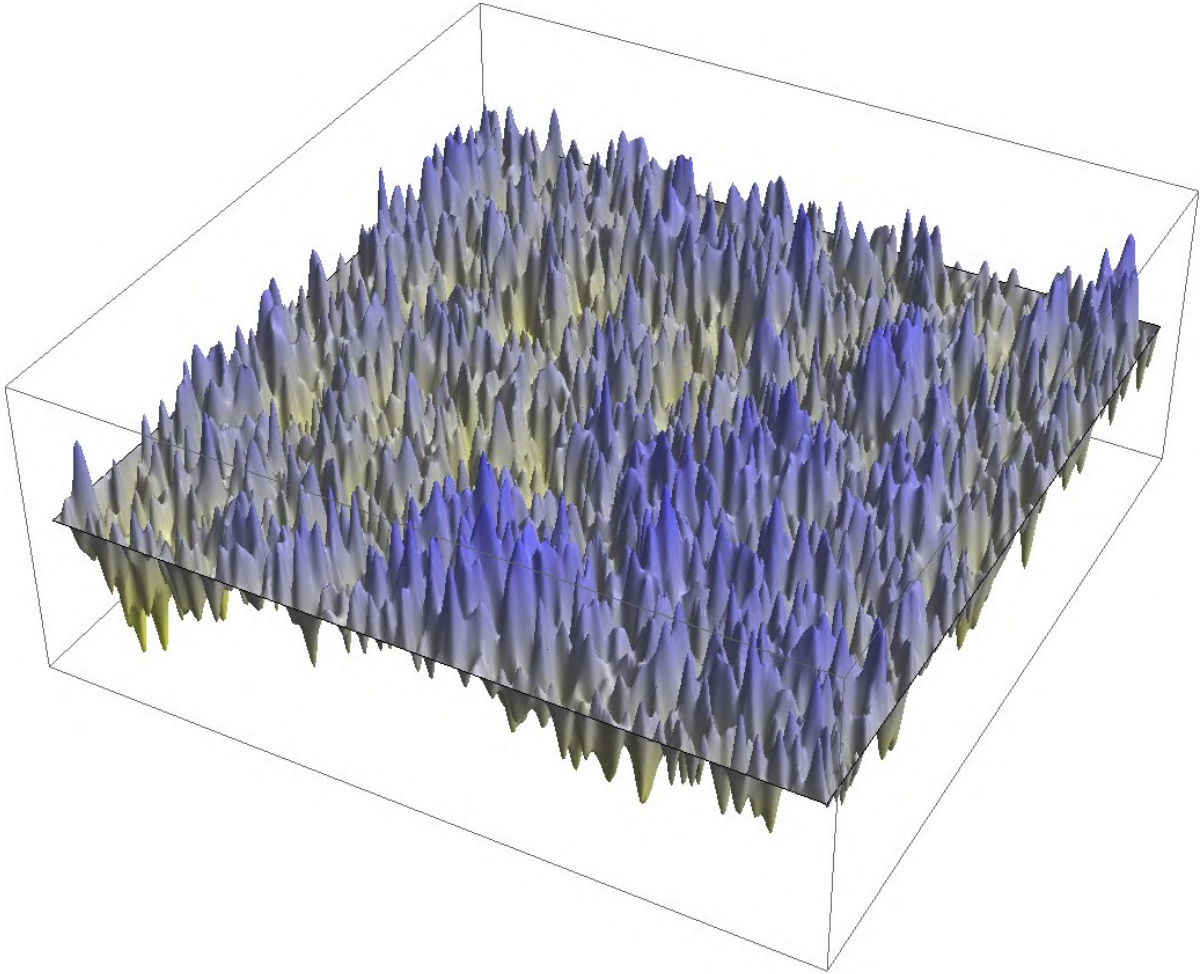


Figure 4.1: Visualisation of a sample of the Gaussian free field with  $\Gamma = \Gamma_D$  on a square  $[0, \pi] \times [0, \pi]$ . The picture is obtained as a sum of first  $10^4$  terms in (4.97). The basis is  $e_{i,j}^1 := \frac{1}{\sqrt{i^2+j^2}} \sin(xi) \sin(xj)$ ,  $i, j = 1, 2, \dots$ . We remark that the series (4.97) does not converge neither uniformly for a.a  $z \in [0, \pi] \times [0, \pi]$ , nor pointwise a.s. Thus, this picture provides only a heuristic visualisation.

Then, the GFF  $\Phi(\mathcal{H}, \Gamma, 0)$  can be equivalently defined by

$$\Phi[f] := \sum_{n=1,2,\dots} \xi_n f_n, \quad f \in H_\Gamma \quad (4.96)$$

and can be understood as formal series

$$\Phi = \sum_{n=1,2,\dots} \xi_n e_n^1. \quad (4.97)$$

We notice that  $(\Phi, \Phi)_\nabla$  diverges a.s.

## 4.8 Stress tensor and the conformal Ward identity

This section is not essential for understanding the next chapter. We explain what can be implied under the **stress tensor** from mathematical point of view in frameworks of

the probabilistic approach to CFT. We also derive the **Ward identities**. This provides a connection between the relations (5.41-5.43) of the coupling in the next chapter and the structure of CFT.

We start from studying the properties of the Dirichlet form  $(\cdot, \cdot)_\nabla$  introduced in the previous section. It is conformally invariant in the sense that the expression on the right-hand side of (4.92) is identical in all charts. It is also invariant with respect to the Möbius transform  $M$ :

$$(M_*h, M_*k)_\nabla = (h, k)_\nabla, \quad h, k \in \mathcal{H}_\Gamma^1. \quad (4.98)$$

Our purpose is to study how the Dirichlet inner product  $(\cdot, \cdot)_\nabla$  transforms with respect to infinitesimal non-conformal automorphisms that are closed to be conformal in the sense that is explained below. Such automorphism can be induced by a vector field  $v$  with the aid of (1.14). In order to induce an automorphism the vector field should be tangent at the boundary, and the automorphisms are conformal if the field is holomorphic. If both conditions are satisfied, then  $v$  is complete, see Section 1.1. The vector field  $\delta$  defined in (1.26) satisfies both conditions except for only one point  $a \in \mathcal{D}$ , where there is a simple pole.

We consider now the Lie derivative with respect to a not necessary holomorphic but continuously differentiable and tangent at the boundary vector field  $v$ . Define

$$\mathcal{L}_v(h, k)_\nabla := (\mathcal{L}_v h, k) + (h, \mathcal{L}_v k), \quad h, k \in \mathcal{H}_\Gamma^1, \quad (4.99)$$

and mention that

$$\begin{aligned} (f_1, \mathcal{L}_v f_2)_\Gamma &= (h_1, \mathcal{L}_v f_2) = -(\mathcal{L}_v h_1, f_2) = -\frac{1}{2\pi} (\mathcal{L}_v h_1, h_2)_\nabla, \\ f_i &\in \mathcal{H}, \quad h_i = \Gamma * f_i, \quad i = 1, 2, \end{aligned} \quad (4.100)$$

due to (4.93) and the integration by parts. We use the relation

$$\partial_{\bar{z}}(\mathcal{L}_v h^\Psi(z)) = \mathcal{L}_v(\partial_{\bar{z}} h^\Psi(z)) + (\partial_{\bar{z}} v^\Psi(z)) \partial_z h^\Psi(z) + \left( \partial_{\bar{z}} \overline{v^\Psi(z)} \right) \partial_{\bar{z}} h^\Psi(z) \quad (4.101)$$

to conclude that

$$\begin{aligned} &\mathcal{L}_v(h, k)_\nabla = (\mathcal{L}_v h, k)_\nabla + (h, \mathcal{L}_v k)_\nabla = \\ &= 4 \int_{\psi(\mathcal{D})} (\partial_{\bar{z}}(\mathcal{L}_v h^\Psi(z)) \partial_z k^\Psi(z) + \partial_{\bar{z}} h^\Psi(z) \partial_z(\mathcal{L}_v k^\Psi(z))) = \\ &= 4 \int_{\psi(\mathcal{D})} \left[ \partial_z(v^\Psi(z)) \partial_{\bar{z}} h^\Psi(z) \partial_z k^\Psi(z) + \partial_{\bar{z}} \left( \overline{v^\Psi(z)} \right) \partial_{\bar{z}} h^\Psi(z) \partial_z k^\Psi(z) \right] + \\ &+ \partial_{\bar{z}} v^\Psi(z) \partial_z h^\Psi(z) \partial_z k^\Psi(z) + \partial_z \overline{v^\Psi(z)} \partial_{\bar{z}} h^\Psi(z) \partial_{\bar{z}} k^\Psi(z) \Big] l(dz) = \\ &= 4 \int_{\psi(\mathcal{D})} \left[ (\partial_{\bar{z}} v^\Psi(z)) \partial_z h^\Psi(z) \partial_z k^\Psi(z) + \left( \partial_z \overline{v^\Psi(z)} \right) \partial_{\bar{z}} h^\Psi(z) \partial_{\bar{z}} k^\Psi(z) \right] l(dz). \end{aligned} \quad (4.102)$$

The last expression equals to zero if  $v$  is a holomorphic vector field, which is possible only if it is complete. Define now a regularized version of the vector field  $\delta$  from (1.26)

by

$$\delta_\varepsilon^{\mathbb{H}}(z) := \begin{cases} \delta^{\mathbb{H}}(z) & \text{if } |z| > \varepsilon \\ \delta_{-2} \left( -\frac{2}{\varepsilon^3} |z|^2 + \frac{3}{\varepsilon^2} |z| \right) e^{-i \arg z} & \text{if } |z| \leq \varepsilon \end{cases}, \quad z \in \mathbb{H}, \quad \varepsilon > 0. \quad (4.103)$$

This vector field is continuously differentiable and tangent at the entire boundary and  $\delta_\varepsilon \xrightarrow{\varepsilon \rightarrow 0} \delta$  pointwise. Besides,

$$\partial_{\bar{z}} \delta_\varepsilon^{\mathbb{H}}(z) = \begin{cases} 0 & \text{if } |z| > \varepsilon \\ 3\delta_{-2} \frac{\varepsilon - |z|}{\varepsilon^3} & \text{if } |z| \leq \varepsilon \end{cases}, \quad z \in \mathbb{H}. \quad (4.104)$$

We substitute now  $v := \delta_\varepsilon$  in (4.102) to calculate

$$\begin{aligned} \lim_{\varepsilon \rightarrow 0} \mathcal{L}_{\delta_\varepsilon}(h, k)_\nabla &= 2\pi \delta_{-2} \left( \partial_z h(z) \partial_z k(z) \Big|_{z=0} + \partial_{\bar{z}} h(z) \partial_{\bar{z}} k(z) \Big|_{z=0} \right) = \\ &= \pi \delta_{-2} \left( \partial_x h(x) \partial_x k(x) \Big|_{x=0} - \partial_y h(iy) \partial_y k(iy) \Big|_{y=0} \right). \end{aligned} \quad (4.105)$$

The geometrical meaning of this relation can be understood as all variations of the conformally invariant inner product  $(h, k)_\nabla$  is concentrated in the point  $a$  where  $\delta$  has a pole.

Let now  $h := \Gamma * f$  and  $k := \Gamma * g$  for some  $f, g \in \mathcal{H}$ . Using (4.39) and (4.100) we obtain

$$\begin{aligned} \lim_{\varepsilon \rightarrow 0} (\mathcal{L}_{\delta_\varepsilon} \Gamma)[f, g] &= - \lim_{\varepsilon \rightarrow 0} \left( \Gamma[\mathcal{L}_{\delta_\varepsilon} f, g] + \Gamma[f, \mathcal{L}_{\delta_\varepsilon} g] \right) = \\ &= \frac{1}{2\pi} \lim_{\varepsilon \rightarrow 0} \mathcal{L}_{\delta_\varepsilon} (\Gamma * f, \Gamma * g)_\nabla = \\ &= \frac{\delta_{-2}}{2} \left( \partial_x (\Gamma * f)^{\mathbb{H}}(x) \partial_x (\Gamma * g)^{\mathbb{H}}(x) \Big|_{x=0} - \partial_y (\Gamma * f)^{\mathbb{H}}(iy) \partial_y (\Gamma * g)^{\mathbb{H}}(iy) \Big|_{y=0} \right) \end{aligned} \quad (4.106)$$

This is a version of the Hadamard's variational formula, which describes the variations of the Green's function under small perturbations of the domain, for the case when the perturbations are concentrated in the point  $\psi^{\mathbb{H}}(a) = 0$ .

We consider first the case  $\Gamma = \Gamma_D$ , and the case  $\Gamma = \Gamma_N$  is considered afterwards. Other cases can be studied analogously, the most essential point is the boundary conditions of  $\Gamma$  at the point  $a$  that are identical for  $\Gamma_D$ ,  $\Gamma_{DN}$ , and  $\Gamma_{\text{tw},b}$ .

In the Dirichlet case,

$$\partial_x (\Gamma_D * f)^{\mathbb{H}}(x) \Big|_{x=0} = 0 \quad (4.107)$$

and the first term in (4.106) cancels. In order to have covariant relations and a convenient connection with the next chapter, we introduce a complete vector field  $\sigma$  such as  $\sigma(a) \neq 0$  and the Lie derivative in a direction orthogonal to a vector field  $v$  by

$$\mathcal{L}_v^\perp := \mathcal{L}_{iv} \quad (4.108)$$

In particular, for a scalar  $s$  we have

$$\mathcal{L}_v^\perp s = (i\mathcal{L}_v^+ - i\mathcal{L}_v^-) s \quad (4.109)$$

and, in a fixed chart  $\psi$ , the same formula is

$$\mathcal{L}_v^\perp s^\Psi(z) = \left( iv^\Psi(z) \partial_z - i\overline{v^\Psi(z)} \partial_{\bar{z}} \right) s^\Psi(z). \quad (4.110)$$

Thus,

$$\partial_y(\Gamma_D * f)^\mathbb{H}(iy) \Big|_{y=0} = \frac{1}{\sigma^\mathbb{H}(0)} \mathcal{L}_\sigma^\perp(\Gamma_D * f)^\mathbb{H}(z) \Big|_{z=0} = \frac{1}{\sigma_{-1}} \mathcal{L}_\sigma^\perp(\Gamma_D * f)(a) \quad (4.111)$$

and

$$\mathcal{L}_\delta \Gamma[f, g] = -\frac{\delta_{-2}}{2\sigma_{-1}^2} \mathcal{L}_\sigma^\perp(\Gamma_D * f)(a) \mathcal{L}_\sigma^\perp(\Gamma_D * g)(a). \quad (4.112)$$

Thereby, the Lie derivative  $\mathcal{L}_\delta \Gamma[f, g]$  is a product of two linear functionals of  $f$  and of  $g$ . This relation plays an important role in coupling that is considered in the next chapter, see (5.42).

Let  $f_{\varepsilon, b} \in \mathcal{H}$ ,  $\varepsilon > 0$  be a delta sequence for the point  $b \in \bar{\mathcal{D}}$ , namely,

$$\int_{\psi(\mathcal{D})} f_{\varepsilon, b}^\Psi(z) l(dz) = 1, \quad \varepsilon > 0, \quad (4.113)$$

$$\lim_{\varepsilon \rightarrow 0} \text{supp } f_{\varepsilon, b} = b \in \bar{\mathcal{D}}$$

We define now the **stress tensor** for Dirichlet type GFF (or CFT) by

$$T_\varepsilon(b) := -\frac{c_1}{2} \left( \Phi[\mathcal{L}_\sigma^\perp f_{\varepsilon, b}] - \eta[\mathcal{L}_\sigma^\perp f_{\varepsilon, b}] \right)^2 + \frac{c_1}{2} \Gamma_D[\mathcal{L}_\sigma^\perp f_{\varepsilon, b}, \mathcal{L}_\sigma^\perp f_{\varepsilon, b}] + \quad (4.114)$$

$$+ c_2 \left( \Phi[\mathcal{L}_\sigma \mathcal{L}_\sigma^\perp f_{\varepsilon, b}] - \eta[\mathcal{L}_\sigma \mathcal{L}_\sigma^\perp f_{\varepsilon, b}] \right),$$

where  $c_1$  and  $c_2$  are some real coefficients that we fix below. For each  $\varepsilon$  we have the following properties

$$\mathbb{E}[T_\varepsilon(b)] = 0, \quad (4.115)$$

$$\mathbb{E}[T_\varepsilon(b) \Phi[g]] = c_2 \Gamma_D[\mathcal{L}_\sigma \mathcal{L}_\sigma^\perp f_{\varepsilon, b}, g], \quad (4.116)$$

$$\mathbb{E}[T_\varepsilon(b) \Phi[g] \Phi[k]] = -c_1 \Gamma_D[\mathcal{L}_\sigma f_{\varepsilon, b}, g] \Gamma_D[\mathcal{L}_\sigma f_{\varepsilon, b}, k] + \quad (4.117)$$

$$+ c_2 \Gamma_D[\mathcal{L}_\sigma \mathcal{L}_\sigma^\perp f_{\varepsilon, b}, g] \eta[k] + c_2 \Gamma_D[\mathcal{L}_\sigma \mathcal{L}_\sigma^\perp f_{\varepsilon, b}, k] \eta[g],$$

and more generally

$$\mathbb{E} \left[ T_\varepsilon(b) e^{\Phi[g]} \right] = \quad (4.118)$$

$$= \left( -\frac{c_1}{2} \Gamma_D[\mathcal{L}_\sigma^\perp f_{\varepsilon, b}, g] \Gamma_D[\mathcal{L}_\sigma^\perp f_{\varepsilon, b}, g] + c_2 \Gamma_D[\mathcal{L}_\sigma \mathcal{L}_\sigma^\perp f_{\varepsilon, b}, g] \right) e^{\frac{1}{2} \Gamma_D[g, g] + \eta[g]}$$

Assume now  $b := a$ , then according to (4.113) we have

$$\lim_{\varepsilon \rightarrow 0} \Gamma_D[\mathcal{L}_\sigma^\perp f_{\varepsilon, a}, g] = -\mathcal{L}_\sigma^\perp(\Gamma_D * g)(a), \quad (4.119)$$

$$\lim_{\varepsilon \rightarrow 0} \Gamma_D[\mathcal{L}_\sigma \mathcal{L}_\sigma^\perp f_{\varepsilon, a}, g] = \mathcal{L}_\sigma \mathcal{L}_\sigma^\perp(\Gamma_D * g)(a).$$



Let us choose  $\eta$  such that

$$\mathcal{L}_\delta \eta[g] = c_2 \mathcal{L}_\sigma \mathcal{L}_\sigma^\perp(\Gamma_D * g)(a) \quad (4.120)$$

and assume

$$c_1 = \frac{\delta_{-2}}{2\sigma_{-1}^2}, \quad (4.121)$$

then, due to (4.112),

$$\begin{aligned} \lim_{\varepsilon \rightarrow 0} \mathbb{E} \left[ T_\varepsilon(a) e^{\Phi[g]} \right] &= \left( \mathcal{L}_\delta \frac{1}{2} \Gamma_D[g, g] + \mathcal{L}_\delta \eta[g] \right) e^{\frac{1}{2} \Gamma_D[g, g] + \eta[g]} = \\ &= \mathcal{L}_\delta e^{\frac{1}{2} \Gamma[g, g] + \eta[g]}, \quad f \in \mathcal{H} \end{aligned} \quad (4.122)$$

In particular,

$$\begin{aligned} \mathcal{L}_\delta \mathbb{E} [\Phi[f_1] \Phi[f_2] \dots \Phi[f_n]] &= \lim_{\varepsilon \rightarrow 0} \mathbb{E} [T_\varepsilon(a) \Phi[f_1] \Phi[f_2] \dots \Phi[f_n]], \\ f_i \in \mathcal{H}, \quad i &= 1, 2, \dots, n. \end{aligned} \quad (4.123)$$

This relation is known as the **conformal Ward identity**. We notice that the limit  $\lim_{\varepsilon \rightarrow 0} T_\varepsilon(a)$  is not well-defined. This is why it cannot be interchanged with the expectation ‘ $\mathbb{E}[\dots]$ ’. It is not just a technical difficulty because, in order to have a non zero commutator of the Lie derivatives

$$\begin{aligned} [\mathcal{L}_\delta, \mathcal{L}_{\delta'}] \mathbb{E} [\Phi[f_1] \Phi[f_2] \dots \Phi[f_n]] &= \\ = \left( \lim_{\varepsilon \rightarrow 0} \lim_{\varepsilon' \rightarrow 0} - \lim_{\varepsilon' \rightarrow 0} \lim_{\varepsilon \rightarrow 0} \right) \mathbb{E} [T_\varepsilon(a) T_{\varepsilon'}(a') \Phi(z_1) \Phi(z_2) \dots \Phi(z_n)] &\neq 0, \end{aligned} \quad (4.124)$$

where  $\delta'$  is some vector field analogous to  $\delta$ , but with the pole at a different point  $a' \in \partial \mathcal{D}$ .

In order to study the Neumann case we consider the Green’s function  $\Gamma = \Gamma_N$  (see (4.49)) for the space of test functions  $\mathcal{H} = \mathcal{H}_s$ . The property (4.93) is satisfied because the singularity of  $\Gamma_N$  at the point  $z = \infty$  in the half-plane chart is logarithmic.

Instead of (4.107) we have the condition

$$\partial_y(\Gamma_N * f)^{\mathbb{H}}(iy) \Big|_{y=0} = 0 \quad (4.125)$$

and we have some other slightly different relations

$$\partial_x(\Gamma_D * f)^{\mathbb{H}}(x) \Big|_{x=0} = \frac{1}{\sigma^{\mathbb{H}}(0)} \mathcal{L}_\sigma(\Gamma_N * f)^{\mathbb{H}}(z) \Big|_{z=0} = \frac{1}{\sigma_{-1}} \mathcal{L}_\sigma(\Gamma_N * f)(a), \quad (4.126)$$

$$\mathcal{L}_\delta \Gamma_N[f, g] = \frac{\delta_{-2}}{2\sigma_{-1}^2} \mathcal{L}_\sigma(\Gamma_N * f)(a) \mathcal{L}_\sigma(\Gamma_N * g)(a). \quad (4.127)$$

We can define

$$\begin{aligned} T_\varepsilon(b) &:= -\frac{c_1}{2} \left( \Phi[\mathcal{L}_\sigma f_{\varepsilon, b}] - \eta[\mathcal{L}_\sigma f_{\varepsilon, b}] \right)^2 + \frac{c_1}{2} \Gamma_N[\mathcal{L}_\sigma f_{\varepsilon, b}, \mathcal{L}_\sigma f_{\varepsilon, b}] + \\ &+ c_2 \left( \Phi[\mathcal{L}_\sigma^2 f_{\varepsilon, b}] - \eta[\mathcal{L}_\sigma^2 f_{\varepsilon, b}] \right), \end{aligned} \quad (4.128)$$

and assume

$$\mathcal{L}_\delta \eta[g] = c_2 \mathcal{L}_\sigma^2(\Gamma_N * g)(a). \quad (4.129)$$

in order to obtain (4.122).

The expression (4.128) is in agreement with the heuristic expression

$$T(z) = -\frac{1}{2} \partial_z \Phi(z) \partial_z \Phi(z) + i\alpha \partial_z^2 \Phi(z) \quad (4.130)$$

for the stress tensor, see, for example [GM93, (1.15)]. We notice that the singular part  $\frac{c_1}{2} \Gamma_N[\mathcal{L}_\sigma f_{\varepsilon,b}, \mathcal{L}_\sigma f_{\varepsilon,b}]$  in (4.128) is added in order to have a finite expression in (4.117) after taking the limit  $\varepsilon \rightarrow 0$ . It is invariant with respect to the choice of chart. However, it can be chosen to be just  $\frac{C}{\varepsilon^2}$  in any chart with some constant  $C$ , as in [KM11] for example. In this case,  $T_\varepsilon(b)$  transforms from one chart to another in a complicated manner (as a Schwarzian), but not as a scalar as it is in our frameworks.

It is straightforward to check that the condition (4.120) or (4.129) is satisfied for all cases considered in this monograph. For example, for the case considered in Section 6.1.2, from (6.21) and (5.85) we have

$$c_1 = 1, \quad c_2 = -\kappa^{-\frac{3}{2}}. \quad (4.131)$$

## 4.9 Vertex operators

In this section, we consider how the so-called vertex operator in CFT can be interpreted from the probabilistic point of view. We specify all limits that usually dropped in the classical literature about CFT and avoid some heuristic notations such as ‘ $\Phi(z)$ ’ and ‘ $\mathcal{V}(z)$ ’. This differs from [KM11], where a similar problem is considered. As well as the previous section, this one is not necessary for further understanding.

We notice first that

$$\mathbb{E} \left[ e^{\Phi[g]} e^{\Phi[f]} \right] = e^{\frac{1}{2}\Gamma[f,f] + \Gamma[f,g] + \frac{1}{2}\Gamma[g,g] + \eta[f] + \eta[g]}, \quad f, g \in H_\Gamma \quad (4.132)$$

due to (4.54). Define now the random variable

$$\mathcal{V}_1[g] := e^{\Phi[g] - \eta[g] - \frac{1}{2}\Gamma[g,g]}, \quad g \in H_\Gamma, \quad (4.133)$$

and notice that inserting it into an expectation is equivalent to the changing

$$\eta[\cdot] \rightarrow \eta[\cdot] + \Gamma[g, \cdot]. \quad (4.134)$$

In other words,

$$\mathbb{E}_{\Gamma, \eta} [\mathcal{V}_1[g] X] = \mathbb{E}_{\Gamma, \eta[\cdot] + \Gamma[g, \cdot]} [X] \quad (4.135)$$

for any random variable  $X$ .

For example, let  $\Gamma = \Gamma_N$ ,  $\eta = 0$ ,  $\mu = \mu^* = 0$ , and assume  $g := -\frac{1}{2}f_{\varepsilon,b}$ , see (4.113). Consider the random variable

$$\mathcal{V}_\varepsilon(b) := e^{-\frac{1}{2}\Phi[f_{\varepsilon,b}] + \frac{1}{2}\eta[f_{\varepsilon,b}] - \frac{1}{8}\Gamma[f_{\varepsilon,b}, f_{\varepsilon,b}]}, \quad \varepsilon > 0, \quad b \in \bar{\mathcal{D}}, \quad (4.136)$$

and the limit  $\varepsilon \rightarrow 0$

$$\lim_{\varepsilon \rightarrow 0} \mathbb{E}_{\Gamma_N, 0} [\mathcal{V}_\varepsilon(a) X] = \mathbb{E}_{\Gamma_N, \eta} [X], \quad \eta^{\text{H}}(z) = \log |z|. \quad (4.137)$$

This combination of  $\Gamma$  and  $\eta$  is similar to the combination considered in Section 6.1.3 for  $\nu = 0$ . The difference is that  $\mu = \mu^* \neq 0$  for all values of  $\kappa$ . Thus, it may be possible to avoid introducing non-zero  $\eta$  in the definition of the GFF and work with the insertion of  $\mathcal{V}_\varepsilon(a)$  instead. However, we did not use this approach due to the following reasons:

1. The term  $\Gamma[g, \cdot]$  in (4.135) is scalar, whereas we need a pre-pre-Schwarzian behaviour of  $\eta$ ;
2. The limit in (4.137) cannot be interchanged with the expectation because  $\lim_{\varepsilon \rightarrow 0} \mathcal{V}_\varepsilon(b)$  does not exist as an element of a reasonable normed space such as  $H_\Gamma$ .

The random variable  $\mathcal{V}_\varepsilon(b)$  can be thought of an analogue of the heuristic vertex operator  $e^{\alpha\Phi(z)}$  frequently used in CFT literature. For the singular part  $-\frac{1}{8}\Gamma[f_{\varepsilon,b}, f_{\varepsilon,b}]$  in (4.137) we made the same remark as for the singular part of  $T_\varepsilon(b)$  in the end of the previous section. If one uses  $C \log \varepsilon$  for some constant  $C$  instead of  $-\frac{1}{8}\Gamma[f_{\varepsilon,b}, f_{\varepsilon,b}]$  in any chart, that leads to a more sophisticated transformation rule of  $\mathcal{V}_\varepsilon$ .

It is also possible to introduce a similar random variable, the insertion of which changes the covariance  $\Gamma$ . Calculate first the expectation

$$\mathbb{E} \left[ e^{\frac{1}{2}\Phi[g]^2} e^{\Phi[f]} \right] = \frac{1}{\sqrt{1 - \Gamma[g, g]}} e^{\frac{1}{2}\Gamma[f, f] + \eta[f] + \frac{1}{2} \frac{(\Gamma[f, g] + \eta[g])^2}{1 - \Gamma[g, g]}}, \quad (4.138)$$

$$f, g \in H_\Gamma, \quad \Gamma[g, g] < 1.$$

This can be done by using a standard finite-dimensional machinery for Gaussina integrals. Define the variable

$$\mathcal{V}_2[g] := \sqrt{1 - \Gamma[g, g]} e^{\frac{1}{2}(\Phi[g] - \eta[g])^2}. \quad (4.139)$$

It possesses the property

$$\mathbb{E} \left[ \mathcal{V}_2[g] e^{\Phi[f]} \right] = e^{\frac{1}{2}\Gamma[f, f] + \frac{1}{2} \frac{\Gamma[f, g]^2}{1 - \Gamma[g, g]} + \eta[f]}. \quad (4.140)$$

Consequently, its insertion leads to

$$\Gamma[\cdot, \cdot] \rightarrow \Gamma[\cdot, \cdot] + \frac{\Gamma[\cdot, g]\Gamma[\cdot, g]}{1 - \Gamma[g, g]}, \quad (4.141)$$

or equivalently,

$$\mathbb{E}_{\Gamma, \eta} [\mathcal{V}_2[g] X] = \mathbb{E}_{\Gamma[\cdot, \cdot] + \frac{1}{2} \frac{\Gamma[\cdot, g]\Gamma[\cdot, g]}{1 - \Gamma[g, g]}, \eta} [X]. \quad (4.142)$$



# Chapter 5

## Coupling of $(\delta, \sigma)$ -SLE and the GFF

### Introduction

In this introduction, we slightly simplify the notation from the previous chapters, drop the chart indices, and use the notation  $\Phi(z)$  instead of  $\Phi[f]$  for the GFF.

The relationships between CFT and both forward and reverse forms of SLE have several aspects. The most important are:

1. For some choice of the covariance  $\Gamma$  and the expectation  $\eta$  of the GFF  $\Phi$  the random laws of  $\Phi(z)$  and  $G_t^{-1} * \Phi(z)$  (in the simplest case  $\Phi(G_t(z))$ ) are identical if GFF  $\Phi(z)$  and SLE map  $G_t(z)$  are sampled independently, [She10].
2. The CFT correlation functions  $S_n(z_1, z_2, \dots, z_n)$  induce SLE (local) martingales

$$G_t^{-1} * S_n(z_1, z_2, \dots, z_n),$$

[BB04b].

3. Two Riemann surfaces equipped with independent random metrics according to the Liouville Theory can be glued together along the boundary segments in a boundary length-preserving-way (conformal welding). The resulting law of the interface between the two surfaces is the SLE, [DS11].
4. Some of CFT correlation functions are related to the probabilities of touching the boundary by the SLE slit, [BB04b, FW03].
5. The heuristic Lie semigroup of conformal endomorphism of  $\mathcal{D}$ , where the SLE map takes values, has a highest weight representation in the CFT space of states. The diffusion operator  $\mathcal{A}$  of the SLE differential equation corresponds to the null vector of this representation which is singular, see Chapter 3 and [BB04b].

The coupling proposition (the first item above) was formulated first in a talk of Scott Sheffield in 2005. A detail proof for the chordal SLE case is presented in [She10] for the chordal SLE  $\kappa < 4$ . The SLE/CFT relation is extended from the chordal equation to the radial one in [BB04a, KM12] and to the dipolar one in [BBH04, KT13, Kan13], see also [IK10] for the SLE- $(\kappa, \rho)$  case. The 5th aspect is considered in Chapter 3.

In this chapter, we discuss only the first two aspects. Thus, in our frameworks, we consider only the SLE/GFF coupling and leave the term ‘SLE/CFT coupling’ for a

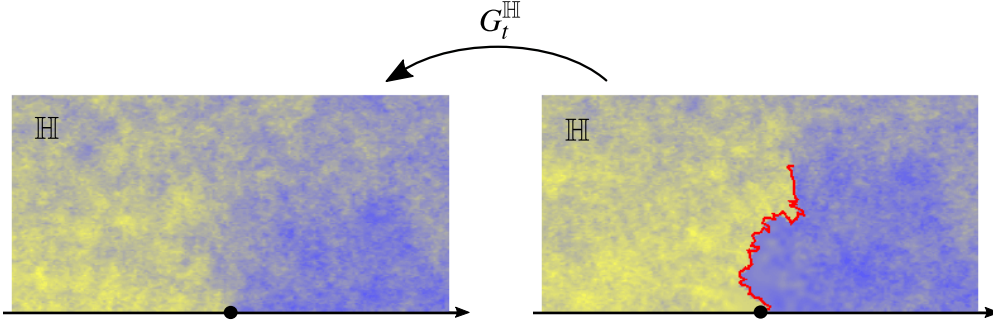


Figure 5.1: This figure illustrates the first aspect of the coupling discussed in the introduction to Chapter 5. On the left-hand side, we present a sample of the GFF  $\Phi(\mathcal{H}_s, \Gamma_D, \chi(-\arg z + \pi/2))$  (see the caption to figure 4.1) in the half-plane chart. The blue color corresponds to positive values of  $\Phi(z)$ , and yellow color corresponds to the negative values of  $\Phi(z)$ . We take the value of the coefficient  $\chi$  bigger than it is supposed to be according to the formula (5.4). This is done in order to make the domination of blue color near  $\mathbb{R}^+$  more visible as well as for the yellow color near  $\mathbb{R}^-$ . The red line on the right-hand side is an independent sample of the chordal SLE slit for some  $t > 0$  and  $\kappa = 2$ . Blue and yellow colors on the right-hand side correspond to the pushforward  $G_t^{-1*}\Phi(z)$  of the GFF  $\Phi(z)$  on the left-hand side. The coupling proposition states that the expectation with respect to the SLE random law gives a sample of GFF  $\Phi(\mathcal{H}_s, \Gamma_D, \chi(-\arg z + \pi/2))$  on the right-hand side.

more general scope. We consider the general case of  $(\delta, \sigma)$ -SLE and the GFF which transforms as a pre-pre-Schwarzian (4.59) and the covariance  $\Gamma$  as in (4.41). To motivate this assumption let us discuss a geometric interpretation of the coupling.

It can be heuristically explained as follows. A properly defined zero-level line started from the origin of GFF  $\Phi(z)$  on the half-plane  $\mathbb{H}$  has the same law as the chordal SLE slit if  $\kappa = 4$ . This proposition can be generalized to other values of  $\kappa < 4$ , see [She10]. In order to explain its geometric meaning, let us associate to  $\Phi$  another field  $J(z)$  of unit vectors  $|J(z)| = 1$  by

$$J(z) := e^{i\Phi(z)/\chi} \quad (5.1)$$

for some  $\chi \in \mathbb{R} \setminus \{0\}$ . We assume that the unit vector field transforms from the domain  $\mathbb{H}$  to  $\mathbb{H} \setminus \gamma$  for some  $\gamma \subset \mathbb{H}$  according to the rule

$$J(z) \rightarrow \arg(G'(z))J(G(z)), \quad (5.2)$$

where  $G$  is a conformal map  $G: \mathbb{H} \setminus \gamma \rightarrow \mathbb{H}$  (which can be understood as a change of coordinates). Thereby,  $\Phi(z)$  transforms according to the rule

$$\Phi(z) \rightarrow G_*^{-1}\Phi(z) := \Phi(G(z)) - \chi \arg G'(z). \quad (5.3)$$

The coupling statement is the agreement in law of  $\Phi(G_t(z)) - \chi \arg G'(z)$  and  $\Phi(z)$ , where

$$\chi = \frac{2}{\sqrt{\kappa}} - \frac{\sqrt{\kappa}}{2}, \quad (5.4)$$

if  $G_t$  is a forward chordal SLE map. Besides, a flow line of  $J(z)$ , starting at the origin, has the same law as the  $\text{SLE}_\kappa$  curve.

For the geometric interpretation of the coupling of the reverse SLE assume that  $e^{\Phi(z)/Q}l(dz)$  is a random measure on  $\mathbb{H}$  for some  $\kappa$ -dependent constant  $Q \in \mathbb{R} \setminus \{0\}$  and for the Lebesgue measure  $l$ . A Riemann surface  $\mathcal{D}$  equipped with such a random measure is actually what is called the Liouville model. Its relation to SLE is explained in the item 3 above if

$$Q = \frac{2}{\sqrt{\kappa}} + \frac{\sqrt{\kappa}}{2}. \quad (5.5)$$

In [DS11], it was shown that the expectation of measure of a subset  $A \subset \mathbb{H}$

$$\mathbb{E} \left[ \int_A e^{\Phi(z)/Q} l(dz) \right] \quad (5.6)$$

is invariant with respect to the conformal change of coordinates  $G$  if the GFF  $\Phi$  transforms according to the rule

$$\Phi(z) \rightarrow G_*^{-1} \Phi(z) := \Phi(G(z)) + Q \log |G'(z)|. \quad (5.7)$$

Both of these interpretations of coupling are related to the fact that the stochastic process

$$G_t^{-1} *_t \mathbb{E}[\Phi(z_1)\Phi(z_2)\dots\Phi(z_n)] \quad (5.8)$$

is a (local) martingale if we assume the rules (5.3) and (5.7) for the forward and reverse SLEs correspondingly. We show in Chapter 1 that the slit of  $(\delta, \sigma)$ -SLE has the same local behaviour as the chordal SLE. Thus, it is reasonable to expect that the general form of  $(\delta, \sigma)$ -SLE can be coupled with some GFF with the same local covariance. Namely, we assumed for  $\Gamma^\Psi(z, w)$  the form (4.41) which corresponds to logarithmic singularity when  $z = w$  with the general harmonic part.

Before the organization part we discuss a technical question regarding the definition of the pushforward operation in the forward case. We discuss in Section 4.3 that the pushforward  $G_t^{-1} *_t \Phi[f]$  of  $\Phi[f]$  is well-defined if  $\text{supp } f \in \text{Im}[G_t^{-1}]$ . This is not a restriction for the reverse SLE  $\{G_t\}_{t \in [0, +\infty)}$ . In order to handle that for the forward SLE, we introduce a stopping time  $T[f]$ , for which the hull  $\mathcal{K}_t$  touches the support of  $f$  for the first time (see (5.10) below) and we consider a stopped process  $\{G_{t \wedge T[f]}\}_{t \in [0, +\infty)}$ . This approach is also used in [IK10]. The most important for us property of the process  $\{G_{t \wedge T[f]}^{-1} *_t \Phi[f]\}_{t \in [0, +\infty)}$  is that it is a local martingale. A stopped local martingale is also a local martingale. This is why a stopping of  $\{G_t\}_{t \in [0, +\infty)}$  does not change our results. However, we lose some information, which makes the proposition of coupling less substantial than one possibly expects. An approach to avoid the stopping for the case when the hull  $\mathcal{K}_t$  is a simple curve ( $\kappa \leq 4$ ) is considered in [She10, SS08]. For the case  $\kappa > 4$ , it is a more complicated and interesting problem. Once someone defines the pushforward  $G_t^{-1} *_t \Phi[f]$  for a bigger stopping time than (5.10) such that the propositions in Section 5.1 are satisfied, the coupling given in the key Theorem 5.1 below can be extended. In the last Section 5.4 we consider without a proof a possible alternative to [She10, SS08] way to define  $G_t^{-1} *_t \Phi[f]$  for  $t \in [0, +\infty)$ .

We remark that the stopping is not essential if  $\kappa \leq 4$  in the following sense. If the Lebesgue measure of the support of the test function tends to zero, then  $P(\{T[f] <$

$+\infty\}$ ) also tends to zero. Together with the fact of regularity of the Schwinger functions  $\mathcal{S}_n$ , we can conclude that

$$\{G_t^{-1} * \mathcal{S}_n(z_1, z_2, \dots, z_n)\}_{t \in [0, +\infty)}, \quad z_1, z_2, \dots, z_n \in \mathcal{D}, \quad (5.9)$$

is a local martingale a.s. for  $\kappa \leq 4$ .

This chapter is organized as follows. After some technical remarks in Section 5.1, we prove Theorem 5.1 in Section 5.2. It states that for  $(\delta, \sigma)$ -SLE a pushforward  $G_t^{-1} * \mathcal{S}_n$  is a local martingale if and only if the system of the partial differential equations (5.41)-(5.43) for  $\delta$ ,  $\sigma$ ,  $\Gamma$ , and  $\eta$  is satisfied. The second equation (5.42) is known as Hadamard's formula, and the third (5.43) states that the covariance  $\Gamma$  must be invariant with respect to the Möbius automorphisms generated by the vector field  $\sigma$ . The same theorem also states that both the local martingale property of  $\{G_t\}_{t \in [0, +\infty)}$  and the system of equations are equivalent to a **local coupling** which is a weaker version of the coupling from [She10] discussed above. We expect, that the local coupling leads to the same property of the flow lines of  $e^{i\Phi(z)/\chi}$  to agree in law with the  $(\delta, \sigma)$ -SLE curves as well as the connection to the welding of the Liouville surfaces.

A general solution to the system (5.41–5.43) gives all possible ways to couple  $(\delta, \sigma)$ -SLEs with the GFF at least in the frameworks of our assumptions of the pre-pre-Schwarzian behaviour of  $\eta$  and of the scalar behaviour of  $\Gamma$ . Theorem 5.2 in Section 5.3 explains why it is natural to couple forward  $(\delta, \sigma)$ -SLE to the GFF with transformation rule (5.3) and the reverse SLE to GFF with the transformation rule (5.7). It also shows that the conditions (5.4) and (5.5) are necessary.

In Section 5.3, we assume the simplest choices of the Dirichlet ( $\Gamma = \Gamma_D$ ) and Neumann ( $\Gamma = \Gamma_N$ ) boundary conditions for the covariance  $\Gamma$  and study all  $(\delta, \sigma)$ -SLEs that can be coupled. It turns out that only the following  $(\delta, \sigma)$ -SLEs are allowed

1. Classical SLEs with the drift  $\mathbf{v} \in \mathbb{R}$ ,  $\kappa > 0$ ;
2. Two one-parametric cases that are reparametrizations of the driftless ( $\mathbf{v} = 0$ ) chordal SLE,  $\kappa > 0$ ;
3. All  $(\delta, \sigma)$ -SLEs with  $\kappa = 6$  and  $\mathbf{v} = 0$  for  $\Gamma = \Gamma_D$ .

The last item makes a bridge to the result of Theorem 1.3, which states that all such  $(\delta, \sigma)$ -SLEs define the same random law on unparametrized curves.

We consider all these cases of the coupling in detail one by one in Chapter 6. Two more examples of the coupling can be obtained if we assume less trivial choices of  $\Gamma$ . We also consider them in Chapter 6, Sections 6.2.4 and 6.3.4.

## 5.1 Some technical propositions

Here we formulate and prove some technical statements that will be used in the proof of Theorem 5.1 below. This section can be skipped if the reader is not interested in the details of the proof.

As we discussed in Section 4.3, we can define  $G_t^{-1} * \eta[f]$  and  $G_t^{-1} * \Gamma[f, f]$  only if  $\text{supp } f \subset \text{Im}(G^{-1})$ . This is why we introduce a stopping time. For  $f \in \mathcal{H}$ , let  $T[f]$  be



the stopping time for which the hull  $\mathcal{K}_t$  of forward  $(\delta, \sigma)$ -SLE touches first some small neighborhood  $U(\text{supp } f)$  of the support of  $f$ :

$$T[f] := \sup\{t > 0: \mathcal{K}_t \cap U(\text{supp } f) = \emptyset\}, \quad f \in \mathcal{H}. \quad (5.10)$$

The neighborhood  $U(\text{supp } f)$  can be defined, for example, as the set of points with Poincaré distance less than some  $\varepsilon > 0$  from  $\text{supp } f$ . Thus,  $T[f] > 0$  a.s. We also define the stopping time  $T(x)$ ,  $x \in \bar{\mathcal{D}}$  analogously using the neighborhood  $U(x)$  of single point  $x \in \mathcal{D}$ . In the reverse case, we set  $T[f] := +\infty$ .

Consider now an Itô process  $\{X_t\}_{t \in [0, +\infty)}$  such that

$$d^{\text{Itô}} X_t = a_t dt + b_t d^{\text{Itô}} B_t, \quad t \in [0, +\infty), \quad (5.11)$$

for some continuous processes  $\{a_t\}_{t \in [0, +\infty)}$  and  $\{b_t\}_{t \in [0, +\infty)}$ . We denote by  $\{X_{t \wedge T}\}_{t \in [0, +\infty)}$  the stopped process by a stopping time  $T$ . It possesses

$$d^{\text{Itô}} X_{t \wedge T} = \theta(T-t) a_t dt + \theta(T-t) b_t d^{\text{Itô}} B_t, \quad t \in [0, +\infty), \quad (5.12)$$

where

$$\theta(t) := \begin{cases} 0 & \text{if } t \leq 0 \\ 1 & \text{if } t > 0. \end{cases} \quad (5.13)$$

If  $\{X_t\}_{t \in [0, +\infty)}$  is a local martingale ( $a_t = 0$ ,  $t \in [0, +\infty)$ ) then  $\{X_{t \wedge T}\}_{t \in [0, +\infty)}$  is also a local martingale.

We consider below the stopped processes  $\{Y(G_{t \wedge T})\}_{t \in [0, +\infty)}$  instead of  $\{Y(G_t)\}_{t \in [0, +\infty)}$  for some functions  $Y: \mathcal{G} \rightarrow \mathbb{R}$  and the Itô differential equations for them. In order to make the relations less cluttered, we usually drop the terms ‘...  $\wedge T[f]$ ’ and  $\theta(T-t)$ . However, in the places where it is essential to remember about them, such as the proof of Theorem 5.1, we specify the stopping times explicitly.

Define the **diffusion operator**

$$A := \mathcal{L}_\delta + \frac{1}{2} \mathcal{L}_\sigma^2. \quad (5.14)$$

and consider how a regular pre-pre-Schwarzian  $\eta$  changes under random evolution  $G_t$ . The functions  $G_t^{-1} * \eta^\Psi(z)$  and  $G_t^{-1} * \Gamma^\Psi(z, w)$  are defined by (4.9) and (4.35) until the stopping times  $T(z)$  and  $\min(T(z), T(w))$  correspondingly.

**Proposition 5.1.** *Let  $\{G_t\}_{t \in [0, +\infty)}$  be a  $(\delta, \sigma)$ -SLE.*

1. *Let  $\eta$  be a regular pre-pre-Schwarzian such that the Lie derivatives  $\mathcal{L}_\sigma \eta$ ,  $\mathcal{L}_\delta \eta$ , and  $\mathcal{L}_\sigma^2 \eta$  are well-defined. Then*

$$d^{\text{Itô}} G_t^{-1} * \eta^\Psi(z) = G_t^{-1} * (A \eta^\Psi(z) dt + \mathcal{L}_\sigma \eta^\Psi(z) d^{\text{Itô}} B_t). \quad (5.15)$$

2. *Let  $\Gamma$  be a scalar ((4.35) is satisfied) bilinear functional such that the Lie derivatives  $\mathcal{L}_\sigma \Gamma$ ,  $\mathcal{L}_\delta \Gamma$ , and  $\mathcal{L}_\sigma^2 \Gamma$  are well-defined. Then*

$$d^{\text{Itô}} G_t^{-1} * \Gamma^\Psi(z, w) = G_t^{-1} * (A \Gamma^\Psi(z, w) dt + \mathcal{L}_\sigma \Gamma^\Psi(z, w) d^{\text{Itô}} B_t). \quad (5.16)$$

This can be proved by the direct calculation but we show a more preferable way, which is valid not only for pre-pre-Schwarzians but, for instance, for vector fields, and even more generally, for assignments whose transformation rules contain an arbitrary finite number of derivatives at a finite number of points. To this end let us prove the following lemma.

**Lemma 5.1.** *Let  $X^i(t)$  ( $i = 1, 2, \dots, n$ ) be a finite collection of stochastic processes defined by the following system of equations in the Stratonovich form*

$$d^S X_t^i = \alpha^i(X_t) dt + \beta^i(X_t) d^S B_t, \quad (5.17)$$

for some fixed functions  $\alpha, \beta: \mathbb{R}^n \rightarrow \mathbb{R}^n$ . Let us define  $Y_s^i, Z_s^i$  as the solutions to the initial value problems

$$\begin{aligned} \dot{Y}_s^i &= \alpha^i(Y_s), & Y_0^i &= 0, \\ \dot{Z}_s^i &= \beta^i(Z_s), & Z_0^i &= 0, \end{aligned} \quad (5.18)$$

defined in some neighbourhood of  $s = 0$ . Let also  $F: \mathbb{R}^n \rightarrow \mathbb{C}$  be a twice-differentiable function. Then, the Itô's differential of  $F(X_t)$  can be written in the following form

$$d^{\text{Itô}} F(X_t) = \frac{\partial}{\partial s} F(X_t + Y_s) dt + \frac{\partial}{\partial s} F(X_t + Z_s) d^{\text{Itô}} B_t + \frac{1}{2} \frac{\partial^2}{\partial s^2} F(X_t + Z_s) dt \Big|_{s=0}. \quad (5.19)$$

*Proof.* The direct calculation of the right-hand side of (5.19) gives

$$F'_i(X_t) \left( \alpha^i(X_t) + \frac{1}{2} \beta_j^{i'}(X_t) \beta^j(X_t) \right) dt + F'_i(X_t) \beta^i(X_t) d^{\text{Itô}} B_t + \frac{1}{2} F''_{ij}(X_t) \beta^i(X_t) \beta^j(X_t) dt, \quad (5.20)$$

which is indeed the Itô's differential of  $F(X_t)$ . We employed summation over repeated indices and used the notation  $F'_i(X) := \frac{\partial}{\partial X^i} F(X)$ .  $\square$

*Proof of Proposition 5.1.* We use the lemma above. Let  $n = 4$ , and let us define a vector valued linear map  $\{\cdot\}$  for an analytic function  $x(z)$  as

$$\{x(z)\} := \{\operatorname{Re} x(z), \operatorname{Im} x(z), \operatorname{Re} x'(z), \operatorname{Im} x'(z)\}. \quad (5.21)$$

For example,

$$X_t := \{G_t^\Psi(z)\} = \{\operatorname{Re} G_t^\Psi(z), \operatorname{Im} G_t^\Psi(z), \operatorname{Re} G_t^{\Psi'}(z), \operatorname{Im} G_t^{\Psi'}(z)\}. \quad (5.22)$$

From (1.104) we have

$$\alpha(X_t) = \{\delta^\Psi(G_t^\Psi(z))\}, \quad \beta(X_t) = \{\sigma^\Psi(G_t^\Psi(z))\}. \quad (5.23)$$

Let also

$$\begin{aligned} F(X_t) &= F(\{G_t^\Psi(z)\}) := G_t^{-1} \eta^\Psi(z) = \\ &= \eta^\Psi(G_t^\Psi(z)) + \mu \log G_t^{\Psi'}(z) + \mu^* \overline{\log G_t^{\Psi'}(z)}. \end{aligned} \quad (5.24)$$

We have

$$Y_s = \{H_s[\delta]^\Psi(z) - z\}, \quad Z_s = \{H_s[\sigma]^\Psi(z) - z\} \quad (5.25)$$

due to (1.104), (5.17), (5.18), and (1.13).

Now we can use Lemma 5.1 in order to obtain (5.15) for  $t = 0$ :

$$\begin{aligned} d^{\text{It}\hat{o}} G_t^{-1} * \eta^\Psi(z) \Big|_{t=0} &= d^{\text{It}\hat{o}} F[X_t] \Big|_{t=0} = \\ &= (\text{right-hand side of (5.19) with } t = 0). \end{aligned} \quad (5.26)$$

But

$$\begin{aligned} \frac{\partial}{\partial s} F(X_t + Y_s) \Big|_{s=0, t=0} &= \frac{\partial}{\partial s} F(\{z + H_s[\delta]^\Psi(z) - z\}) \Big|_{s=0} = \\ &= \frac{\partial}{\partial s} F(\{H_s[\delta]^\Psi(z)\}) \Big|_{s=0} = \frac{\partial}{\partial s} \{H_s[\delta]_*^{-1} \eta^\Psi(z)\} \Big|_{s=0} = \mathcal{L}_\delta \eta^\Psi(z). \end{aligned} \quad (5.27)$$

A similar observation for other terms in (5.26) yields that

$$\begin{aligned} d^{\text{It}\hat{o}} G_t^{-1} * \eta^\Psi(z) \Big|_{t=0} &= \mathcal{L}_\delta \eta^\Psi(z) dt + \mathcal{L}_\sigma \eta^\Psi(z) d^{\text{It}\hat{o}} B_t + \frac{1}{2} \mathcal{L}_\sigma^2 \eta^\Psi(z) dt = \\ &= \mathcal{A} \eta^\Psi(z) dt + \mathcal{L}_\sigma \eta^\Psi(z) d^{\text{It}\hat{o}} B_t. \end{aligned} \quad (5.28)$$

For  $t > 0$  we use the results of Section 1.2.1 to conclude

$$\begin{aligned} d^{\text{It}\hat{o}} G_t^{-1} * \eta^\Psi(z) &= d^{\text{It}\hat{o}} (\tilde{G}_{t-t_0} \circ G_{t_0})_*^{-1} \eta^\Psi(z) = d^{\text{It}\hat{o}} G_{t_0}^{-1} * \tilde{G}_{t-t_0}^{-1} * \eta^\Psi(z) \Big|_{t_0=t} = \\ &= G_t^{-1} * d^{\text{It}\hat{o}} \tilde{G}_s^{-1} * \eta^\Psi(z) \Big|_{s=0} = G_t^{-1} * (\mathcal{A} \eta^\Psi(z) dt + \mathcal{L}_\sigma \eta^\Psi(z) d^{\text{It}\hat{o}} B_t). \end{aligned} \quad (5.29)$$

The proof of 5.16 is analogous. The only difference is that we do not have the pre-Schwarzian terms with the derivatives but there are two points  $z$  and  $w$ . We can assume

$$\{x\} := \{\text{Re}x(z), \text{Im}x(z), \text{Re}x(w), \text{Im}x(w)\} \quad (5.30)$$

instead of (5.21) and the remaining part of the proof is the same.  $\square$

We will obtain below the Itô differential over  $G_t^{-1} * \eta[f]$  and  $G_t^{-1} * \Gamma[f, g]$  for  $(\delta, \sigma)$ -SLE  $\{G_t\}_{t \in [0, +\infty)}$  and  $f, g \in \mathcal{H}$ . To this end we need the Itô formula for nonlinear functionals over  $\mathcal{H}$ . For linear functionals on the Schwartz space this has been shown in [Kry11]. However, the author is not aware of the results for nonlinear functionals. The following propositions are special cases we will need in the next section. They are consequences of the proposition above, the classical Itô formula, and the stochastic Fubini theorem.

**Proposition 5.2.**

*Let the conditions of Proposition 5.1 be satisfied, then:*

1. *The Itô differential is interchangeable with the integration over  $\mathcal{D}$ . Namely,*

$$\begin{aligned} d^{\text{It}\hat{o}} \int_{\psi(\text{supp } f)} G_t^{-1} * \eta^\Psi(z) f^\Psi(z) l(dz) &= \\ &= \int_{\psi(\text{supp } f)} G_t^{-1} * \mathcal{A} \eta^\Psi(z) f^\Psi(z) l(dz) dt + \\ &+ \int_{\psi(\text{supp } f)} G_t^{-1} * \mathcal{L}_\sigma \eta^\Psi(z) f^\Psi(z) l(dz) d^{\text{It}\hat{o}} B_t. \end{aligned} \quad (5.31)$$

An equivalent shorter formulation is

$$d^{It\hat{o}} G_t^{-1} *_\eta[f] = G_t^{-1} *_\mathcal{A} \eta[f] dt + G_t^{-1} *_\mathcal{L}_\sigma \eta[f] d^{It\hat{o}} B_t. \quad (5.32)$$

2. The Itô differential is interchangeable with the double integration over  $\mathcal{D}$ , namely,

$$\begin{aligned} & d^{It\hat{o}} \int_{\psi(\text{supp } f)} \int_{\psi(\text{supp } f)} G_t^{-1} \Gamma(x, y) f^\Psi(x) f^\Psi(y) l(dx) l(dy) = \\ &= \int_{\psi(\text{supp } f)} \int_{\psi(\text{supp } f)} G_t^{-1} *_\mathcal{A} \Gamma(x, y) f^\Psi(x) f^\Psi(y) l(dx) l(dy) dt + \\ &+ \int_{\psi(\text{supp } f)} \int_{\psi(\text{supp } f)} G_t^{-1} *_\mathcal{L}_\sigma \Gamma(x, y) f^\Psi(x) f^\Psi(y) l(dx) l(dy) d^{It\hat{o}} B_t. \end{aligned} \quad (5.33)$$

An equivalent shorter formulation is

$$d^{It\hat{o}} G_t^{-1} *_\Gamma[f, g] = G_t^{-1} *_\mathcal{A} \Gamma[f, g] dt + G_t^{-1} *_\mathcal{L}_\sigma \Gamma[f, g] d^{It\hat{o}} B_t. \quad (5.34)$$

*Proof.* The relation (5.31) in integral form is

$$\begin{aligned} & \int_{\psi(\text{supp } f)} G_t^{-1} *_\eta^\Psi(z) f^\Psi(z) l(dz) = \eta[f] + \\ &+ \int_0^t \int_{\psi(\text{supp } f)} G_\tau^{-1} *_\mathcal{A} \eta^\Psi(z) f^\Psi(z) l(dz) d\tau + \int_0^t \int_{\psi(\text{supp } f)} G_\tau^{-1} *_\mathcal{L}_\sigma \eta^\Psi(z) f^\Psi(z) l(dz) d^{It\hat{o}} B_\tau \end{aligned} \quad (5.35)$$

The order of the Itô and the Lebesgue integrals can be changed using the stochastic Fubini theorem, see, for example [Pro04]. It is enough now to use (5.15) to obtain (5.31).

The proof of 5.34 is analogous.  $\square$

**Proposition 5.3.** *Let*

$$\hat{\phi}[f] = \exp(W[f]), \quad W[f] := \frac{1}{2} \Gamma[f, f] + \eta[f]. \quad (5.36)$$

Then  $G_t^{-1} *_\hat{\phi}[f]$  is an Itô process defined by the integral

$$\begin{aligned} & G_t^{-1} *_\hat{\phi}[f] = \\ &= \int_0^t \exp(G_\tau^{-1} *_W[f]) \left( G_\tau^{-1} *_\mathcal{A} W[f] d\tau + G_\tau^{-1} *_\mathcal{L}_\sigma W[f] d^{It\hat{o}} B_\tau + \frac{1}{2} (G_\tau^{-1} *_\mathcal{L}_\sigma W[f])^2 d\tau \right). \end{aligned} \quad (5.37)$$

*Proof.* The stochastic process  $G_t^{-1} *_W^\Psi[f]$  has the integral form

$$\begin{aligned} G_t^{-1} *_W^\Psi[f] &= \frac{1}{2} G_t^{-1} *_\Gamma^\Psi[f, f] + G_t^{-1} *_\eta^\Psi[f] = \\ &= \int_{\psi(\text{supp } f)} \int_{\psi(\text{supp } f)} G_t^{-1} *_\Gamma^\Psi(z, w) f^\Psi(z) f^\Psi(w) l(dz) l(dw) + \int_{\psi(\text{supp } f)} G_t^{-1} *_\eta^\Psi(z) f^\Psi(z) l(dz). \end{aligned} \quad (5.38)$$

due to the Proposition. 5.2. In terms of Itô differentials it is

$$d^{\text{Itô}} G_t^{-1} *_W^\Psi[f] = G_t^{-1} *_\mathcal{A} W^\Psi[f] dt + G_t^{-1} *_\mathcal{L}_\sigma W^\Psi[f] d^{\text{Itô}} B_t. \quad (5.39)$$

In order to obtain the exponential function we can just use Itô's lemma

$$\begin{aligned} d^{\text{Itô}} G_t^{-1} *_\exp(W^\Psi[f]) &= d^{\text{Itô}} \exp(G_t^{-1} *_W^\Psi[f]) = \\ &= \exp(G_t^{-1} *_W^\Psi[f]) \left( G_t^{-1} *_\mathcal{A} W^\Psi[f] dt + G_t^{-1} *_\mathcal{L}_\sigma W^\Psi[f] d^{\text{Itô}} B_t + \frac{1}{2} (G_t^{-1} *_\mathcal{L}_\sigma W^\Psi[f])^2 dt \right) \end{aligned} \quad (5.40)$$

□

## 5.2 Coupling between SLE and GFF

Let  $(\Omega^\Phi, \mathcal{F}^\Phi, P^\Phi)$  be the probability space for GFF  $\Phi$  and let  $(\Omega^B, \mathcal{F}^B, P^B)$  be the independent probability space for the Brownian motion  $\{B_t\}_{t \in [0, +\infty)}$ , which governs some  $(\delta, \sigma)$ -SLE  $\{G_t\}_{t \in [0, +\infty)}$ . In this section, we consider a coupling between these random laws. Let  $T[f]$  be the stopping time as defined above.

**Definition 5.1.** A GFF  $\Phi(\mathcal{H}, \Gamma, \eta)$  is called **coupled** to forward or reverse  $(\delta, \sigma)$ -SLE, driven by  $\{B_t\}_{t \in [0, +\infty)}$ , if the random variable  $G_{t \wedge T[f]}^{-1} *_\Phi^\Psi[f]$  obtained by independent samplings of  $\Phi$  and  $G_t$  has the same law as  $\Phi^\Psi[f]$  for any test function  $f \in \mathcal{H}$ , chart map  $\psi$ , and  $t \in [0, +\infty)$ .

If the coupling holds for a fixed chart map  $\psi$  and for any  $f \in \mathcal{H}$ , then it also holds for any other chart map  $\tilde{\psi}$ , due to (4.59). We also give a weaker version of the coupling statement that we plan to use here.. To this end, we have to consider a stopped versions of the stochastic process  $\{G_{t \wedge T[f]}\}_{t \in [0, +\infty)}$ .

A collection of stopping times  $\{T_n\}_{n=1,2,\dots}$  is called a **fundamental sequence** if  $0 \leq T_n \leq T_{n+1} \leq \infty$ ,  $n = 1, 2, \dots$  a.s., and  $\lim_{n \rightarrow \infty} T_n = \infty$  a.s. A stochastic process  $\{x_t\}_{t \in [0, +\infty)}$  is called a **local martingale** if there exists a fundamental sequence of stopping times  $\{T_n\}_{n=1,2,\dots}$ , such that the stopped process  $\{x_{t \wedge T_n}\}_{t \in [0, +\infty)}$  is a martingale for each  $n = 1, 2, \dots$ .

Let now the statement of coupling above is valid only for the stopped by  $T_n$  process  $\{G_{t \wedge T[f] \wedge T_n}\}_{t \in [0, +\infty)}$  for each  $n = 1, 2, \dots$ . Namely,  $G_{t \wedge T[f] \wedge T_n}^{-1} *_\Phi^\Psi[f]$  has the same law as  $\Phi^\Psi[f]$  for each  $n = 1, 2, \dots$ . We are ready now to define local coupling.

**Definition 5.2.** A GFF  $\Phi(\mathcal{H}, \Gamma, \eta)$  is called *locally coupled* to forward or reverse  $(\delta, \sigma)$ -SLE, driven by  $\{B_t\}_{t \in [0, +\infty)}$ , if there exist a fundamental sequence  $\{T_n[f, \Psi]\}_{n=1,2,\dots}$  such that the random variable  $G_{t \wedge T_n[f, \Psi]}^{-1} \Phi^\Psi[f]$  obtained by independent samplings of  $\Phi$  and  $G_t$  has the same law as  $\Phi^\Psi[f]$  until stopping time  $T_n[f, \Psi]$  for each  $n = 1, 2, \dots$ , for any test function  $f \in \mathcal{H}$ , and chart map  $\Psi$ .

**Remark 5.1.** If  $\mathbb{T}[f, \Psi] = +\infty$  a.s. for each  $f \in \mathcal{H}$ , then the coupling is not local.

In this subsection, we prove the following theorem.

**Theorem 5.1.** *The following three propositions are equivalent:*

1. GFF  $\Phi(\mathcal{H}, \Gamma, \eta)$  is locally coupled to  $(\delta, \sigma)$ -SLE;
2.  $G_{t \wedge T_n[f, \Psi]}^{-1} \hat{\phi}^\Psi[f]$  is a local martingale for  $f \in \mathcal{H}$  in any chart  $\Psi$ ;
3. The system of the equations

$$\mathcal{L}_\delta \eta[f] + \frac{1}{2} \mathcal{L}_\sigma^2 \eta[f] = 0, \quad f \in \mathcal{H}, \quad (5.41)$$

$$\mathcal{L}_\delta \Gamma[f, g] + \mathcal{L}_\sigma \eta[f] \mathcal{L}_\sigma \eta[g] = 0, \quad f, g \in \mathcal{H}, \quad (5.42)$$

and

$$\mathcal{L}_\sigma \Gamma[f, g] = 0, \quad f, g \in \mathcal{H}. \quad (5.43)$$

is satisfied.

We start the proof after some remarks. Just for clarity (but not for applications) we reformulate the system (5.41–5.43) directly in terms of partial derivatives using (4.17), (4.20), (4.37), and (5.14) as

$$\begin{aligned} & \delta(z) \partial_z \eta(z) + \overline{\delta(z)} \partial_{\bar{z}} \eta(z) + \mu \delta'(z) + \mu^* \overline{\delta'(z)} + \\ & + \frac{1}{2} \sigma^2(z) \partial_z^2 \eta(z) + \frac{1}{2} \overline{\sigma^2(z)} \partial_{\bar{z}}^2 \eta(z) + \sigma(z) \overline{\sigma(z)} \partial_z \partial_{\bar{z}} \eta + \\ & + \frac{1}{2} \sigma(z) \sigma'(z) \partial_z \eta(z) + \frac{1}{2} \overline{\sigma(z) \sigma'(z)} \partial_{\bar{z}} \eta(z) + \mu \sigma(z) \sigma''(z) + \mu^* \overline{\sigma(z) \sigma''(z)} = \beta; \\ & \delta(z) \partial_z \Gamma(z, w) + \delta(w) \partial_w \Gamma(z, w) + \overline{\delta(z)} \partial_{\bar{z}} \Gamma(z, w) + \overline{\delta(w)} \partial_{\bar{w}} \Gamma(z, w) + \\ & + \left( \sigma(z) \partial_z \eta(z) + \overline{\sigma(z)} \partial_{\bar{z}} \eta(z) + \mu \sigma'(z) + \mu^* \overline{\sigma'(z)} \right) \times \\ & \times \left( \sigma(w) \partial_w \eta(w) + \overline{\sigma(w)} \partial_{\bar{w}} \eta(w) + \mu \sigma'(w) + \mu^* \overline{\sigma'(w)} \right) = \beta_1(z) + \beta_1(w); \\ & \sigma(z) \partial_z \Gamma(z, w) + \sigma(w) \partial_w \Gamma(z, w) + \overline{\sigma(z)} \partial_{\bar{z}} \Gamma(z, w) + \overline{\sigma(w)} \partial_{\bar{w}} \Gamma(z, w) = \\ & = \beta_2(z) + \beta_2(w), \end{aligned} \quad (5.44)$$

for  $\mathcal{H} = \mathcal{H}_s^*$ . We drop above the upper index  $\Psi$  for shortness. The right hand side is not zero, but arbitrary real constant  $\beta$  for the first equation and a sum of two real-valued functions  $\beta_i(z) + \beta_i(w)$ ,  $i = 1, 2$  for other two equations because linear functionals over  $\mathcal{H}_s^*$  are defined up to a constant and bilinear ones are defined up to a sum  $\beta(z) + \beta(w)$ ,

see Sections 4.1 and 4.4. For the space  $\mathcal{H} = \mathcal{H}_s$  the right-hand sides in (5.44) are just zeros.

The first equation (5.41) is just a local martingale condition for  $\eta$ . The second one (5.42) is known as Hadamard's formula, see also Section 4.8. The third means that  $\Gamma$  should be invariant under the one-parametric family of Möbius automorphisms generated by  $\sigma$ .

*Proof of Theorem 5.1.* Let us start with showing how the statement 1 about the coupling implies the statement 2 about the local martingality.

**1. $\Leftrightarrow$ 2.** Let  $G_{t \wedge T_f \wedge T_n[f, \psi]}$  be a stopped process  $G_{t \wedge T_f}$  by the stopping times  $T_n[f, \psi]$  forming some fundamental sequence. The coupling statement can be reformulated as an equality of characteristic functions for the random variables  $G_{t \wedge \tilde{T}_n[f, \psi]}^{-1} \Phi^\Psi[f]$  and  $\Phi^\Psi[f]$  for all test functions  $f$ . Namely, the following expectations must be equal

$$\mathbb{E}_B \left[ \mathbb{E}_\Phi \left[ e^{G_{t \wedge T_f \wedge T_n[f, \psi]}^{-1} \Phi^\Psi[f]} \right] \right] = \mathbb{E}_\Phi \left[ e^{\Phi^\Psi[f]} \right], \quad f \in \mathcal{H}, \quad t \in [0, +\infty), \quad n = 1, 2, \dots, \quad (5.45)$$

which, in particular, means the integrability of  $e^{G_{t \wedge \tilde{T}_n[f, \psi]}^{-1} \Phi^\Psi[f]}$  with respect to  $\Omega^B$  and  $\Omega^\Phi$ . We used  $\mathbb{E}_B[\cdot]$  for the expectation with respect to the random law of  $\{B_t\}_{t \in [0, +\infty)}$  (or  $\{G_t\}_{t \in [0, +\infty)}$ ) and  $\mathbb{E}_\Phi[\cdot]$  for the expectation with respect to  $\Phi$ . Let us use Definitions (4.55) and (4.76) to simplify this identity to

$$\mathbb{E}_B \left[ G_{t \wedge T_f \wedge T_n[f, \psi]}^{-1} \hat{\phi}^\Psi[f] \right] = \hat{\phi}^\Psi[f], \quad f \in \mathcal{H}, \quad t \in [0, +\infty), \quad n = 1, 2, \dots. \quad (5.46)$$

After the change  $f \rightarrow \tilde{G}_{s \wedge T[f]} * f$  for some independently sampled  $\tilde{G}_s$  and  $s \in [0, +\infty)$ , we obtain

$$\mathbb{E}_B \left[ G_{t \wedge T[\tilde{G}_{s \wedge T[f]} * f]}^{-1} \hat{\phi}^\Psi[\tilde{G}_{s \wedge T[f]} * f] \right] = \hat{\phi}^\Psi[\tilde{G}_{s \wedge T[f]} * f], \quad (5.47)$$

$$f \in \mathcal{H}, \quad t \in [0, +\infty), \quad n = 1, 2, \dots.$$

Multiplying both sides on

$$e^{\int_{\text{supp } f} \Psi \left( \mu \log(\tilde{G}_{s \wedge T[f]}^\Psi)'(z) + \mu^* \overline{\log(\tilde{G}_{s \wedge T[f]}^\Psi)'(z)} \right) f(z) l(dz)} \quad (5.48)$$

and using (4.60) and (4.55) we conclude that

$$\mathbb{E}_B \left[ \tilde{G}_{s \wedge T[f]}^{-1} G_{t \wedge T[\tilde{G}_{s \wedge T[f]} * f]}^{-1} \hat{\phi}^\Psi[\tilde{G}_{s \wedge T[f]} * f] \right] = \tilde{G}_{s \wedge T[f]}^{-1} \hat{\phi}^\Psi[f], \quad (5.49)$$

$$f \in \mathcal{H}, \quad t \in [0, +\infty), \quad n = 1, 2, \dots.$$

Defined now the process

$$\tilde{\tilde{G}}_{t+s} := G_t \circ \tilde{G}_s, \quad s, t \in [0, +\infty), \quad (5.50)$$

which has the law of  $(\delta, \sigma)$ -SLE. Its stopped version possesses

$$\tilde{\tilde{G}}_{t+s \wedge T[f]} = G_{t \wedge T[\tilde{G}_{s \wedge T[f]} * f]} \circ \tilde{G}_{s \wedge T[f]}, \quad s, t \in [0, +\infty), \quad f \in \mathcal{H}. \quad (5.51)$$

The left-hand side of (5.49) equals to

$$\begin{aligned} & \mathbb{E}_B \left[ \left( G_{t \wedge T[\tilde{G}_{s \wedge T[f]^* f}]} \wedge T_n[\tilde{G}_{s \wedge T[f]^* f, \psi}]^{-1} \circ \tilde{G}_{s \wedge T[f]} \right)_*^{-1} \hat{\phi}^\psi[f] \right] = \\ & = \mathbb{E}_B \left[ \left( \tilde{G}_{t+s \wedge T[f] \wedge T_n[\tilde{G}_{s \wedge T[f]^* f, \psi} + s]}^{-1} \right)_*^{-1} \hat{\phi}^\psi[f] \mid \mathcal{F}_{s \wedge T[f]}^B \right]. \end{aligned} \quad (5.52)$$

We use now the Markov property of  $(\delta, \sigma)$ -SLE and conclude that  $T'_n[f, \psi] := T_n[\tilde{G}_{s \wedge T[f]^* f, \psi}^{-1} + s]$  is a fundamental sequence for the pair of  $f$  and  $\psi$ . Thus, (5.49) simplifies to

$$\mathbb{E}_B \left[ G_{t+s \wedge T[f] \wedge T'_n[f, \psi]}^{-1} \hat{\phi}^\psi[f] \mid \mathcal{F}_{s \wedge T[f] \wedge T'_n[f, \psi]}^B \right] = G_{t+s \wedge T[f] \wedge T'_n[f, \psi]}^{-1} \hat{\phi}[f], \quad (5.53)$$

hence,  $\{G_{t \wedge T[f]^*}^{-1} \hat{\phi}[f]\}_{t \in [0, +\infty)}$  is a local martingale.

The inverse statement can be obtained by the same method in the reverse order.

**2. $\Leftrightarrow$ 3.** According to Lemma 5.3, the drift term, the coefficient at  $dt$ , vanishes identically when

$$\mathcal{A}W[f] + \frac{1}{2}(\mathcal{L}_\sigma W[f])^2 = 0, \quad f \in \mathcal{H}. \quad (5.54)$$

The left-hand side is a functional polynomial of power four. We use the fact that a regular symmetric functional  $P[f] := \sum_{k=1,2,\dots,n} p_k[f, f, \dots, f]$  of power  $n$  over such spaces as  $\mathcal{H}_s$ ,  $\mathcal{H}_s^*$ ,  $\mathcal{H}_{s,b}$  (see Sections 6.3.2),  $\mathcal{H}_{s,b}^*$  (see Section 6.3.3), or  $\mathcal{H}_{s,b}^{\pm}$  (see Section 6.3.4) is identically zero if and only if

$$p_k[f_1, f_2, \dots, f_n] = 0, \quad k = 1, 2, \dots, n, \quad f \in \mathcal{H}. \quad (5.55)$$

Thus, each of the following functions must be identically zero:

$$\begin{aligned} \mathcal{A}\eta[f] &= 0, \quad \frac{1}{2}\mathcal{A}\Gamma[f, g] + \frac{1}{2}\mathcal{L}_\sigma \eta[f] \mathcal{L}_\sigma \eta[g] = 0, \\ \mathcal{L}_\sigma \eta[f] \mathcal{L}_\sigma \Gamma[g, h] &+ \text{symmetric terms} = 0, \\ \mathcal{L}_\sigma \Gamma[f, g] \mathcal{L}_\sigma \Gamma[h, l] &+ \text{symmetric terms} = 0, \\ f, g, h, l &\in \mathcal{H}. \end{aligned} \quad (5.56)$$

We can conclude that  $\mathcal{L}_\sigma \Gamma[f, g] = 0$ ,  $\mathcal{A}\Gamma[f, g] = \mathcal{L}_\delta \Gamma[f, g]$  for any  $f, g \in \mathcal{H}$ , and this system is equivalent to the system (5.41–5.43). For the case  $\mathcal{H} = \mathcal{H}_s$  we can write (5.56) in terms of functions on  $\psi(\mathcal{D})$ :

$$\begin{aligned} \mathcal{A}\eta(z) &= 0, \quad \frac{1}{2}\mathcal{A}\Gamma(z, w) + \frac{1}{2}\mathcal{L}_\sigma \eta(z) \mathcal{L}_\sigma \eta(w) = 0, \\ \mathcal{L}_\sigma \eta(z) \mathcal{L}_\sigma \Gamma(w, u) &+ \text{symmetric terms} = 0, \\ \mathcal{L}_\sigma \Gamma(z, w) \mathcal{L}_\sigma \Gamma(u, v) &+ \text{symmetric terms} = 0, \\ z, w, u, v &\in \psi(\mathcal{D}), \quad z \neq w, u \neq v, \dots \end{aligned} \quad (5.57)$$



**Remark 5.2.** Fix a chart  $\psi$ . The coupling and the martingales are not local if in addition to the proposition 3 in Theorem 5.1 the relation

$$\mathbb{E}_B \left[ \left| \int_0^t \exp \left( G_{\tau \wedge T[f]*}^{-1} W^\psi[f] \right) G_{\tau \wedge T[f]*}^{-1} \mathcal{L}_\sigma W^\psi[f] d^{It\hat{\delta}} B_\tau \right| \right] < \infty, \quad t \geq 0, \quad (5.58)$$

holds. This is the condition that the diffusion term at  $d^{It\hat{\delta}} B_t$  in (5.37) is in  $L_1(\Omega^B)$ . However, this may not be true, in general, in another chart  $\tilde{\psi}$ . Meanwhile, if the local martingale property of  $G_{t \wedge T[f]*}^{-1} \hat{\phi}^\psi[f]$  is satisfied in one chart  $\psi$  for any  $f \in \mathcal{H}$ , then it is also true in any other chart due to the invariance of the condition (5.54) in the proof.

The studying of the general solution of (5.41-5.43) is an interesting and complicated problem. Take the Lie derivative  $\mathcal{L}_\sigma$  over the second equation, the Lie derivative  $\mathcal{L}_\delta$  over the third equation, and consider the difference of the resulting equations. It is an algebraically independent equation

$$\mathcal{L}_{[\delta, \sigma]} \Gamma[f, g] = -\mathcal{L}_\sigma^2 \eta[f] \mathcal{L}_\sigma \eta[g] \mathcal{L}_\sigma^2 \eta[f] \mathcal{L}_\sigma^2 \eta[g]. \quad (5.59)$$

Continuing by induction we obtain an infinite system of a priori algebraically independent equations because the Lie algebra  $\mathcal{U}[\delta, \sigma]$ , induced by  $\delta$  and  $\sigma$  and introduced in Section 3.1, is infinite dimensional. Thereby, the existence of the solution on the system (5.41-5.43) is a special event that is strongly related to the properties of  $\mathcal{U}[\delta, \sigma]$ . A geometric interpretation of the second equation (5.42) and a hint to solve this equation are discussed in Section 4.8.

Before studying special solutions to the system (5.41–5.43), let us consider some of its general properties. We also reformulate it in terms of the analytic functions  $\eta^+$ ,  $\Gamma^{++}$  and  $\Gamma^{+-}$ , which is technically more convenient.

**Theorem 5.2.** Let  $\delta$ ,  $\sigma$ ,  $\eta$ , and  $\Gamma$  be such that the system (5.41–5.43) is satisfied, let  $\Gamma$  be a fundamental solution to the Laplace equation (see (4.41)), and which transforms as a scalar, see (4.35), and let  $\eta$  be a pre-pre-Schwazian. Then,

- For the forward case and  $\mathcal{H} = \mathcal{H}_s$ :
  1.  $\eta$  is a  $(i\chi/2, -i\chi/2)$ -pre-pre-Schwarzian (4.11) given by a harmonic function in any chart with  $\chi$  given by

$$\chi = \frac{2}{\sqrt{\kappa}} - \frac{\sqrt{\kappa}}{2}. \quad (5.60)$$

2. The boundary value of  $\eta$  undergoes a jump  $2\pi/\sqrt{\kappa}$  at the source point  $a$ , namely, its local behaviour in the half-plane chart is given by (5.80) up to a sign;
3. The system (5.41–5.43) is equivalent to the system (5.62), (5.69), (5.70), (5.75), and (5.74).

- For the reverse case and  $\mathcal{H} = \mathcal{H}_s^*$ :

1.  $\eta$  is a  $(Q/2, Q/2)$ -pre-pre-Schwarzian (4.10) given by a harmonic function in any chart with  $Q$  given by

$$Q = \frac{2}{\sqrt{\kappa}} + \frac{\sqrt{\kappa}}{2}. \quad (5.61)$$

2. The value of  $\eta$  possesses a logarithmic singularity at the source point  $a$ , namely, its local behaviour in the half-plane chart is given by (5.81) up to a sign;
3. The system (5.41–5.43) is equivalent to the system (5.62), (5.69), (5.70), (5.75), and (5.74).

*Proof.* The system (5.41–5.43) defines  $\eta$  only up to an additive constant  $C$  that we keep writing in the formulas for  $\eta$  below. The condition for the pre-pre-Schwarzian  $\eta$  to be real leads to only two possibilities:

1.  $\mu = -\mu^*$  and is pure imaginary as in (4.11);
2.  $\mu = \mu^*$  and is real as in (4.10).

The equation (5.42) shows that functional  $\mathcal{L}_\sigma \eta$  has to be given by a harmonic function as well as  $\mathcal{L}_\sigma^2 \eta$  in any chart. On the other hand, (5.41) implies that  $\mathcal{L}_\delta \eta$  is also harmonic. The vector fields  $\delta$  and  $\sigma$  are transversal almost everywhere. We conclude that  $\eta$  is harmonic. We used also the fact that the additional  $\mu$ -terms in (4.17) are harmonic.

The harmonic function  $\eta^\psi(z)$  can be represented as a sum of an analytic function  $\eta^{+\psi}(z)$  and its complex conjugate in any chart  $\psi$

$$\eta^\psi(z) = \eta^{+\psi}(z) + \overline{\eta^{+\psi}(z)}. \quad (5.62)$$

Below in this proof, we drop the chart index  $\psi$ , which can be chosen arbitrarily.

We can define  $\eta^+$  and  $\overline{\eta^+}$  to be pre-pre-Schwarzians of orders  $(\mu, 0)$  and  $(0, \mu^*)$  correspondingly due to (4.17). Thus,  $\eta^+$  is defined up to a complex constant  $C^+$ . We denote

$$j^+ := \mathcal{L}_\sigma \eta^+. \quad (5.63)$$

and

$$j := \mathcal{L}_\sigma \eta = \mathcal{L}_\sigma \eta^+ + \overline{\mathcal{L}_\sigma \eta^+}. \quad (5.64)$$

The reciprocal formula is

$$\eta^+(z) := \int \frac{j^+(z) - \mu \sigma'(z)}{\sigma(z)} dz. \quad (5.65)$$

This integral can be a ramified function if  $\sigma(z)$  has a zero inside of  $\mathcal{D}$  (the elliptic case). We consider how to handle this technical difficulty in Sections 6.3.2 and 6.3.3.

Let us reformulate now (5.41) in terms of  $j^+$ . Using the fact that

$$\mathcal{L}_v^2(\eta^+ + \overline{\eta^+}) = \mathcal{L}_v^2 \eta^+ + \mathcal{L}_v^2 \overline{\eta^+}, \quad (5.66)$$

we conclude that

$$\mathcal{L}_\delta \eta^+ + \frac{1}{2} \mathcal{L}_\sigma^2 \eta^+ = C^+. \quad (5.67)$$

Here  $C^+ = i\beta$  for some  $\beta \in \mathbb{R}$  for the forward case. For the reverse case,  $C^+ = -\beta + i\beta'$  for some  $\beta, \beta' \in \mathbb{R}$  because (5.67) is an identity in sense of functionals over  $\mathcal{H}_s^*$ .

The relation (5.67) is equivalent to

$$\begin{aligned} \frac{\delta}{\sigma} \mathcal{L}_\sigma \eta^+ + \frac{\sigma \mathcal{L}_\delta \eta^+ - \delta \mathcal{L}_\sigma \eta^+}{\sigma} + \frac{1}{2} \mathcal{L}_\sigma^2 \eta^+ = C^+ &\Leftrightarrow \\ \frac{\delta}{\sigma} j^+ + \frac{\sigma \delta \partial \eta^+ + \mu \sigma \delta' - \delta \sigma \partial \eta^+ - \mu \delta \sigma'}{\sigma} + \frac{1}{2} \mathcal{L}_\sigma j^+ = C^+ &\Leftrightarrow \end{aligned} \quad (5.68)$$

$$\frac{\delta}{\sigma} j^+ + \mu \frac{[\sigma, \delta]}{\sigma} + \frac{1}{2} \mathcal{L}_\sigma j^+ = C^+. \quad (5.69)$$

We used (4.17) and (4.16).

Consider now the function  $\Gamma^{\mathbb{H}}(z, w)$ . It is harmonic with respect to both variables with the only logarithmic singularity. Hence, it can be split as a sum of four terms

$$\Gamma^{\mathbb{H}}(z, w) := \Gamma^{++\mathbb{H}}(z, w) + \overline{\Gamma^{++\mathbb{H}}(z, w)} \mp \Gamma^{+-\mathbb{H}}(z, \bar{w}) \mp \overline{\Gamma^{+-\mathbb{H}}(z, \bar{w})}, \quad (5.70)$$

where  $\Gamma^{++\mathbb{H}}(z, w)$  and  $\Gamma^{+-\mathbb{H}}(z, w)$  are analytic with respect to both variables except the diagonal  $z = w$  for  $\Gamma^{++\mathbb{H}}(z, w)$ . We use the upper sign in the pairs  $\mp$  for the forward case and the lower sign for the reverse case.

So, e.g.,  $\overline{\Gamma^{+-\mathbb{H}}(z, \bar{w})}$  is anti-analytic with respect to  $z$  and analytic with respect to  $w$ . We can assume that both  $\Gamma^{++}(z, w)$  and  $\Gamma^{+-}(z, w)$  transform as scalars represented by analytic functions in all charts and symmetric with respect to  $z \leftrightarrow w$ . Observe that these functions are defined at least up to the transform

$$\begin{aligned} \Gamma^{++\mathbb{H}}(z, w) &\rightarrow \Gamma^{++\mathbb{H}}(z, w) + \varepsilon^{\mathbb{H}}(z) + \varepsilon^{\mathbb{H}}(w), \\ \Gamma^{+-\mathbb{H}}(z, w) &\rightarrow \Gamma^{+-\mathbb{H}}(z, w) + \varepsilon^{\mathbb{H}}(z) + \varepsilon^{\mathbb{H}}(w) \end{aligned} \quad (5.71)$$

for any analytic function  $\varepsilon^{\mathbb{H}}(z)$  such that

$$\overline{\varepsilon^{\mathbb{H}}(z)} = \varepsilon^{\mathbb{H}}(\bar{z}). \quad (5.72)$$

In the forward case, these additional terms are canceled due to the choice of minus in the pairs ' $\mp$ ' in (5.70). In the reverse case, the contribution of these functions is equivalent to zero bilinear functional over  $\mathcal{H}_s^*$ .

Consider the equation (5.43). It leads to

$$\mathcal{L}_\sigma \Gamma^{++\mathbb{H}}(z, w) = \beta_2^{\mathbb{H}}(z) + \beta_2^{\mathbb{H}}(w), \quad \mathcal{L}_\sigma \Gamma^{+-\mathbb{H}}(z, w) = \beta_2^{\mathbb{H}}(z) + \beta_2^{\mathbb{H}}(w) \quad (5.73)$$

for any analytic function  $\beta_2^{\mathbb{H}}(z)$  such that  $\overline{\beta_2^{\mathbb{H}}(z)} = \beta_2^{\mathbb{H}}(\bar{z})$ . One can fix this freedom, the function  $\beta_2^{\mathbb{H}}$ , by the conditions

$$\mathcal{L}_\sigma \Gamma^{++\mathbb{H}}(z, w) = 0, \quad \mathcal{L}_\sigma \Gamma^{+-\mathbb{H}}(z, w) = 0. \quad (5.74)$$

Thus,  $\Gamma^{++\mathbb{H}}(z, w)$  and  $\Gamma^{+-\mathbb{H}}(z, w)$  are fixed up to a non-essential constant.

The second equation (5.42) can be reformulated now as

$$\begin{aligned} \mathcal{L}_\delta \Gamma^{++\mathbb{H}}(z, w) + \mathcal{L}_\sigma \eta^{+\mathbb{H}}(z) \mathcal{L}_\sigma \eta^{+\mathbb{H}}(w) &= \beta_1^{\mathbb{H}}(z) + \beta_1^{\mathbb{H}}(w), \\ \mathcal{L}_\delta \Gamma^{+-\mathbb{H}}(z, \bar{w}) + \mathcal{L}_\sigma \eta^{+\mathbb{H}}(z) \overline{\mathcal{L}_\sigma \eta^{+\mathbb{H}}(w)} &= \beta_1^{\mathbb{H}}(z) + \beta_1^{\mathbb{H}}(\bar{w}) \end{aligned} \quad (5.75)$$

for any analytic function  $\beta_1^{\mathbb{H}}(z)$  such that  $\overline{\beta_1^{\mathbb{H}}(z)} = \beta_1^{\mathbb{H}}(\bar{z})$  analogous to (5.73). We can conclude now that the system (5.41–5.43) is equivalent to the system (5.62), (5.69), (5.70), (5.75), and (5.74).

Use now the fact

$$\Gamma^{++\mathbb{H}}(z, w) = -\frac{1}{2} \log(z - w) + \text{analytic terms} \quad (5.76)$$

to obtain a singularity of  $j^{+\mathbb{H}}$  about the origin in the half-plane chart. Relation (1.122) yields

$$\pm \frac{2}{z} \partial_z \left( -\frac{1}{2} \log(z - w) \right) \pm \frac{2}{w} \partial_w \left( -\frac{1}{2} \log(z - w) \right) = \pm \frac{1}{zw}, \quad (5.77)$$

hence,

$$\begin{aligned} j^{+\mathbb{H}}(z) &= \frac{-i}{z} + \text{holomorphic part}, & \text{for the forward case;} \\ j^{+\mathbb{H}}(z) &= \frac{-1}{z} + \text{holomorphic part}, & \text{for the reverse case.} \end{aligned} \quad (5.78)$$

The choice of the sign of  $j^{+\mathbb{H}}(z)$  is irrelevant. We made this choice just to be consistent with [She10]. The analytic terms in (5.76) can give a term with the sum of simple poles at  $z$  and  $w$  but in the form of the product  $1/zw$ .

From (5.65) we conclude that the singular part of  $\eta^{+\mathbb{H}}$  is proportional to the logarithm of  $z$ :

$$\begin{aligned} \eta^{+\mathbb{H}}(z) &= \frac{i}{\sqrt{\kappa}} \log z + \text{holomorphic part}, & \text{for the forward case;} \\ \eta^{+\mathbb{H}}(z) &= \frac{1}{\sqrt{\kappa}} \log z + \text{holomorphic part}, & \text{for the reverse case.} \end{aligned} \quad (5.79)$$

Thus, we have

$$\eta^{\mathbb{H}}(z) = \frac{-2}{\sqrt{\kappa}} \arg z + \text{non-singular harmonic part}, \quad \text{for the forward case;} \quad (5.80)$$

$$\eta^{\mathbb{H}}(z) = \frac{2}{\sqrt{\kappa}} \log |z| + \text{non-singular harmonic part}, \quad \text{for the reverse case.} \quad (5.81)$$

We can chose the additive constant such that, in the half-plane chart, we have

$$\eta^{\mathbb{H}}(+0) = -\eta^{\mathbb{H}}(-0) = \frac{\pi}{\sqrt{\kappa}} \quad (5.82)$$

in the forward case. This provides the jump  $2\pi/\sqrt{\kappa}$  of the value of  $\eta$  at the boundary near the origin, which is exactly the same behaviour of  $\eta$  needed for the flow line construction in [MS12] and [She10]. However, the form (5.82) is not chart independent, and only the jump  $2\pi/\sqrt{\kappa} = \eta^\Psi(+0) - \eta^\Psi(-0)$  does not change its value if the boundary of  $\psi(\mathcal{D})$  is not singular in the neighbourhood of the source  $\psi(a)$ . In the reverse case, such constant has no meaning also because  $\eta$  is a functional over  $\mathcal{H}_s^*$ .

Substitute now (5.78) in (5.69) in the half-plane chart, use (1.122), and consider the corresponding Laurent series. We are interested in the coefficient near the first term  $\frac{1}{z^2}$ :

$$\frac{2}{z} \frac{1}{-\sqrt{\kappa}} \frac{-i}{z} + \mu \frac{-2}{z^2} + \frac{1}{2} (-\sqrt{\kappa}) \frac{i}{z^2} + o\left(\frac{1}{z^2}\right) = C^+ \quad (5.83)$$

for the forward case and we have the same expression but without  $i$  in the reverse case. We can conclude that

$$\begin{aligned} \mu &= i \frac{4 - \kappa}{4\sqrt{\kappa}}, & \text{for the forward case;} \\ \mu &= \frac{4 + \kappa}{4\sqrt{\kappa}}, & \text{for the reverse case.} \end{aligned} \quad (5.84)$$

Thus, the pre-pre-Schwarzians (4.11) with  $\chi$  given by (5.60) is only one that can be realized in the forward case. The same is true for the pre-pre-Schwarzians (4.10),  $Q$  given by (5.61), and the reverse case.  $\square$

### 5.3 Coupling in the case of the Dirichlet and Neumann boundary conditions

In this section, we consider some special solutions to the system (5.41–5.43) with the help of Theorem 5.2. We assume the Dirichlet and Neumann boundary condition for  $\Gamma$  (see Examples 4.1 and 4.3) and find the general solution in these cases. In other words, we systematically study which of  $(\delta, \sigma)$ -SLE can be coupled to GFF if  $\Gamma = \Gamma_D$  and  $\Gamma = \Gamma_N$ .

**Theorem 5.3.** *Let a forward  $(\delta, \sigma)$ -SLE be coupled to the GFF with  $\mathcal{H} = \mathcal{H}_s$ ,  $\Gamma = \Gamma_D$ , and let  $\eta$  be a pre-pre-Schwartzian (4.11) of order  $\chi$ . Then only the special combinations of  $\delta$  and  $\sigma$  summarized in Table 5.1, and all combinations with  $\kappa = 6$  and  $\nu = 0$  are possible.*

The table consists of 6 cases, 3 of which are classical. Each case is a one-parametric family of  $(\delta, \sigma)$ -SLEs parametrized by the drift  $\nu \in \mathbb{R}$ , or by the parameter  $\xi \in \mathbb{R}$ . The cases may intersect for vanishing values of  $\nu$  or  $\xi$ . Different combinations of  $\delta$  and  $\sigma$  can correspond to essentially the same process in  $\mathcal{D}$  but written in different coordinates as we studied in Section 1.3.2. In the columns of  $\delta$  and  $\sigma$ , we present only one example of such choices in each case.

Some special cases of the forward coupling presented here have been considered before. The chordal SLE without drift (case 1 from the table with  $\nu = 0$ ) was considered

	Name	$\delta =$	$\sigma =$	$\alpha =$	$\beta =$
1	Chordal with drift	$\pm 2\ell_{-2} - \nu\ell_{-1}$	$-\sqrt{\kappa}\ell_{-1}$	$-\frac{\nu}{2}$	$\frac{-\nu^2}{2\sqrt{\kappa}}$
2	Chordal with fixed time change	$\pm 2\ell_{-2} + 2\xi\ell_0$	$-\sqrt{\kappa}\ell_{-1}$	0	$-\frac{\xi(\pm\kappa-8)}{2\sqrt{\kappa}}$
3	Dipolar with drift	$\pm 2(\ell_{-2} - \ell_0) - \nu(\ell_{-1} - \ell_1)$	$-\sqrt{\kappa}(\ell_{-1} - \ell_1)$	$-\frac{\nu}{2}$	$\frac{4-\nu^2}{2\sqrt{\kappa}}$
4	One right fixed boundary point	$\pm 2\ell_{-2} + (\kappa \mp 6)\ell_{-1} + 2(\pm 3 - \kappa \pm \xi)\ell_0 + (\mp 2 + \kappa \mp 2\xi)\ell_1$	$-\sqrt{\kappa}(\ell_{-1} - \ell_1)$	$+\frac{1}{2}(\kappa \mp 6)$	$\frac{\xi(\mp\kappa+8)}{2\sqrt{\kappa}}$
5	One left fixed boundary point	$\pm 2\ell_{-2} - (\kappa \mp 6)\ell_{-1} + 2(\pm 3 - \kappa \pm \xi)\ell_0 - (\mp 2 + \kappa \mp 2\xi)\ell_1$	$-\sqrt{\kappa}(\ell_{-1} - \ell_1)$	$-\frac{1}{2}(\kappa \mp 6)$	$\frac{\xi(\mp\kappa+8)}{2\sqrt{\kappa}}$
6	Radial with drift	$\pm 2(\ell_{-2} + \ell_0) - \nu(\ell_{-1} + \ell_1)$	$-\sqrt{\kappa}(\ell_{-1} + \ell_1)$	$-\frac{\nu}{2}$	$\frac{4-\nu^2}{2\sqrt{\kappa}}$

Table 5.1: The list of  $(\delta, \sigma)$ -SLE types that can be coupled with GFF with the Dirichlet boundary conditions  $\Gamma = \Gamma_D$  (the upper sign in the ‘ $\pm$ ’ and ‘ $\mp$ ’ pairs) and with the Neumann boundary conditions  $\Gamma = \Gamma_N$  (the lower sign).

in [KM11], the radial SLE without drift (case 6 from the table with  $\nu = 0$ ) in [KM12], and the dipolar SLE without drift (case 4 from the table with  $\nu = 0$ ) appeared in [KT13]. The case 2 actually corresponds to the same measure as the chordal SLE but stopped at time  $t = \frac{1}{4}\xi$  if  $\xi > 0$  (see section 6.4). The cases 4 and 5 are mirror images of each other. They are discussed in Section 6.5. The reverse coupling of the chordal SLE with zero drift is considered in [She10].

*Proof of Theorem 5.3.* Let us use Theorem 5.1 and assume the Dirichlet boundary conditions for  $\Gamma = \Gamma_D$ .

$$\Gamma^{++\mathbb{H}}(z, w) = -\frac{1}{2} \log(z - w), \quad \Gamma^{+-\mathbb{H}}(z, \bar{w}) = -\frac{1}{2} \log(z - \bar{w}) \quad (5.85)$$

in Theorem 5.2. The condition (5.73) is satisfied for any complete vector field  $\sigma$  and some  $\sigma$ -dependent  $\beta_2$  which is irrelevant.

In order to obtain  $j^+$  we remark first that due to the Möbius invariance (4.46) we can ignore the polynomial part of  $\delta^{\mathbb{H}}(z)$

$$\mathcal{L}_\delta \Gamma^{\mathbb{H}}(z, w) = \left( \frac{2}{z} \partial_z + \frac{2}{\bar{z}} \partial_{\bar{z}} + \frac{2}{w} \partial_w + \frac{2}{\bar{w}} \partial_{\bar{w}} \right) \Gamma^{\mathbb{H}}(z, w). \quad (5.86)$$

Using (5.75), (5.85), and (5.77) we obtain that

$$j^{+\mathbb{H}}(z) = \frac{-i}{z} + i\alpha, \quad \alpha \in \mathbb{C}, \quad (5.87)$$

with

$$\beta_1(z) = \frac{\alpha}{z} - \frac{\alpha^2}{2}. \quad (5.88)$$

In order to satisfy all conditions formulated in Theorem 5.2 we need to check (5.69). Substituting (5.87) to (5.69) gives

$$\begin{aligned} \frac{\delta}{\sigma} j^+ + \mu \frac{[\sigma, \delta]}{\sigma} + \frac{1}{2} \mathcal{L}_\sigma^+ j^+ &= i\beta \Leftrightarrow \\ \delta j^+ + \mu [\sigma, \delta] + \frac{1}{2} \sigma \mathcal{L}_\sigma^+ j^+ - i\beta \sigma &= 0 \Leftrightarrow \\ \delta^{\mathbb{H}}(z) \left( \frac{-i}{z} + i\alpha \right) + \mu [\sigma, \delta]^{\mathbb{H}}(z) + \frac{1}{2} \left( \sigma^{\mathbb{H}}(z) \right)^2 \partial \left( \frac{-i}{z} + i\alpha \right) - i\beta \sigma^{\mathbb{H}}(z) &= 0. \end{aligned} \quad (5.89)$$

In what follows, we will use the half-plane chart in the proof. With the help of (1.2.3) and (1.2.3) we can assume without loss of generality that  $\sigma^{\mathbb{H}}$  is one of three possible forms:

1.  $\sigma^{\mathbb{H}}(z) = -\sqrt{\kappa}$ ,
2.  $\sigma^{\mathbb{H}}(z) = -\sqrt{\kappa}(1 - z^2)$ ,
3.  $\sigma^{\mathbb{H}}(z) = -\sqrt{\kappa}(1 + z^2)$ .

Let us consider these cases turn by turn.

1.  $\sigma(z) = -\sqrt{\kappa}$ .

Inserting (1.122) the relation (5.89) reduces to

$$\begin{aligned} \frac{-2 + \frac{\kappa}{2} - 2i\sqrt{\kappa}\mu}{z^2} + \frac{2\alpha - \delta_{-1}}{z} + (\beta\sqrt{\kappa} + \alpha\delta_{-1} - \delta_0 + i\sqrt{\kappa}\mu\delta_0) + \\ + z(\alpha\delta_0 - \delta_1 + 2i\sqrt{\kappa}\mu\delta_1) + z^2\alpha\delta_1 \equiv 0 \Leftrightarrow \end{aligned} \quad (5.90)$$

$$(5.84), \quad 2\alpha - \delta_{-1} = 0, \quad \beta\sqrt{\kappa} + \alpha\delta_{-1} - \delta_0 + i\sqrt{\kappa}\mu\delta_0 = 0, \\ \alpha\delta_0 - \delta_1 + 2i\sqrt{\kappa}\mu\delta_1 = 0, \quad \alpha\delta_1 = 0.$$

There are three possible cases:

- 1.

$$\delta_{-1} = 2\alpha, \quad \delta_0 = 0, \quad \delta_1 = 0, \quad \kappa > 0, \quad \beta = \frac{-2\alpha^2}{\sqrt{\kappa}}. \quad (5.91)$$

It is convenient to use the drift parameter (1.126), Thus,

$$v = -2\alpha, \quad (5.92)$$

that is related to the drift in the chordal equation. This case is presented in the first line of Table 5.1.

- 2.

$$\delta_{-1} = 0, \quad \delta_0 = -\frac{4\beta\sqrt{\kappa}}{\kappa - 8}, \quad \delta_1 = 0, \quad \kappa > 0, \quad \alpha = 0. \quad (5.93)$$

This case is presented in the second line of Table ( $\xi \in \mathbb{R}$ ) and discussed in details in Section 6.4.

3.

$$\delta_{-1} = 0, \quad \delta_0 = 2\sqrt{5}\beta, \quad \delta_1 \in \mathbb{R}, \quad \kappa = 6, \quad \alpha = 0. \quad (5.94)$$

This is a general case of  $\delta$  with  $\kappa = 6$  and  $\nu = 0$ .

2.  $\sigma^{\mathbb{H}}(z) = -\sqrt{\kappa}(1 - z^2)$ .

Relation (5.89) reduces to

$$\begin{aligned} & \frac{-2 + \frac{\kappa}{2} + 2i\mu\sqrt{\kappa}}{z^2} + \frac{2\alpha - \delta_{-1}}{z} + (\beta\sqrt{\kappa} - \kappa + 6i\sqrt{\kappa}\mu + \alpha\delta_{-1} - \delta_0 + i\sqrt{\kappa}\mu\delta_0) + \\ & + z(2i\sqrt{\kappa}\mu\delta_{-1} + \alpha\delta_0 - \delta_1 + 2i\sqrt{\kappa}\mu\delta_1) + z^2\left(-\beta\sqrt{\kappa} + \frac{\kappa}{2} + i\sqrt{\kappa}\mu\delta_0 + \alpha\delta_1\right) = 0 \quad \Leftrightarrow \\ & (5.84), \quad 2\alpha - \delta_{-1} = 0, \quad \beta\sqrt{\kappa} - \kappa + 6i\sqrt{\kappa}\mu + \alpha\delta_{-1} - \delta_0 + i\sqrt{\kappa}\mu\delta_0 = 0, \\ & 2i\sqrt{\kappa}\mu\delta_{-1} + \alpha\delta_0 - \delta_1 + 2i\sqrt{\kappa}\mu\delta_1 = 0, \quad -\beta\sqrt{\kappa} + \frac{\kappa}{2} + i\sqrt{\kappa}\mu\delta_0 + \alpha\delta_1 = 0. \end{aligned} \quad (5.95)$$

There are four solutions each of which is a two-parameter family. The first one corresponds to the dipolar SLE with the drift  $\nu$ , line 3 in Table 5.1. The second and the third equations are ‘mirror images’ of each other, as it can be seen from the lines 4 and 5 in the table. They are parametrized by  $\xi := \frac{2\beta\sqrt{\kappa}}{8-\kappa}$  and discussed in details in Section 6.5. The fourth case is when

$$\delta_{-1} = 0, \quad \delta_0 = 2(\sqrt{6}\beta - 3), \quad \delta_1 \in \mathbb{R}, \quad \kappa = 6, \quad \alpha = 0. \quad (5.96)$$

This is a general form of  $\delta$  with  $\kappa = 6$  and  $\nu = 0$ .

3.  $\sigma^{\mathbb{H}}(z) = -\sqrt{\kappa}(1 + z^2)$ .

Relation (5.89) reduces to

$$\begin{aligned} & \frac{-2 + \frac{\kappa}{2} - 2i\sqrt{\kappa}\mu}{z^2} + \frac{2\alpha - \delta_{-1}}{z} + \\ & + (\beta\sqrt{\kappa} - \kappa + 6i\sqrt{\kappa}\mu + \alpha\delta_{-1} - \delta_0 + i\sqrt{\kappa}\mu\delta_0) + \\ & + z(2i\kappa\mu\delta_{-1} + \alpha\delta_0 - \delta_1 + 2i\sqrt{\kappa}\mu\delta_1) + \\ & + z^2\left(-\beta\sqrt{\kappa} + \frac{\kappa}{2} + i\sqrt{\kappa}\mu\delta_0 + \alpha\delta_1\right) = 0 \quad \Leftrightarrow \\ & (5.84), \quad 2\alpha - \delta_{-1} = 0, \quad \beta\sqrt{\kappa} - \kappa + 6i\sqrt{\kappa}\mu + \alpha\delta_{-1} - \delta_0 + i\sqrt{\kappa}\mu\delta_0 = 0, \\ & 2i\kappa\mu\delta_{-1} + \alpha\delta_0 - \delta_1 + 2i\sqrt{\kappa}\mu\delta_1 = 0, \quad -\beta\sqrt{\kappa} + \frac{\kappa}{2} + i\sqrt{\kappa}\mu\delta_0 + \alpha\delta_1 = 0. \end{aligned} \quad (5.97)$$

The first solution is presented in the line 6 of Table 5.1, where it is again convenient to introduce the parameter  $\nu$  related to the drift in the radial equation. The second solution is

$$\delta_{-1} = 0, \quad \delta_0 = 2(\sqrt{6}\beta - 3), \quad \delta_1 \in \mathbb{R}, \quad \kappa = 6, \quad \alpha = 0. \quad (5.98)$$

This is a general form of  $\delta$  with  $\kappa = 6$  and  $\nu = 0$ .  $\square$

The following theorem is an analogue of the previous one.

**Theorem 5.4.** *Let a reverse  $(\delta, \sigma)$ -SLE be coupled to a the GFF with  $\Gamma = \Gamma_N$  and  $\mathcal{H} = \mathcal{H}_s^*$ , and let  $\eta$  be a pre-pre-Schwartzian (4.10) of order  $Q$ . Then only the combinations of  $\delta$  and  $\sigma$  summarized in Table 5.1 are possible.*



*Proof.* We use the same method as in the proof of the previous theorem. The difference is in using the space  $\mathcal{H}_s^*$  instead of  $\mathcal{H}_s$ . We still have (5.85), but instead of (5.87) we have

$$j^{+\mathbb{H}}(z) = \frac{-1}{z} - \alpha, \quad \alpha \in \mathbb{C}. \quad (5.99)$$

This definition of  $\alpha$  makes formulas more similar to the previous case. We also have

$$\delta^{\mathbb{H}}(z) \left( \frac{-1}{z} - \alpha \right) + \mu[\sigma, \delta]^{\mathbb{H}}(z) + \frac{1}{2} \left( \sigma^{\mathbb{H}}(z) \right)^2 \partial \left( \frac{-1}{z} - \alpha \right) + (\beta - i\beta') \sigma^{\mathbb{H}}(z) \equiv 0. \quad (5.100)$$

instead of (5.89). We obtain that  $\beta' = 0$ , the same relations for  $\beta$ , and the same set of solutions from Table 5.1 with slightly different signs (the lower ones in all pairs ‘ $\pm$ ’ and ‘ $\mp$ ’). We do not have the special case  $\kappa = 6$  as before, because the analogous solutions give the negative value  $\kappa = -6$ .  $\square$

## 5.4 Alternative definition of $G_t^{-1} *_\eta[f]$

This section is actually the beginning of the conclusion/perspective part. We briefly consider how one can solve the difficulties in the definition of  $G_t^{-1} *_\eta[f]$ ,  $G_t^{-1} *_\Gamma[f, f]$ , and other such quantities, which appears when  $\text{Im } G_t^{-1} \cap \text{supp } f \neq \emptyset$ .

Consider the initial value problem

$$d^S G_{t,\varepsilon} = \delta_\varepsilon \circ G_{t,\varepsilon} dt + \sigma \circ G_{t,\varepsilon} d^S B_t, \quad t \in [0, +\infty), \quad \varepsilon > 0, \quad (5.101)$$

where the vector field  $\delta_\varepsilon$  is defined by (4.103). The solution  $\{G_{t,\varepsilon}\}_{t \in [0, +\infty)}$  is a family of automorphisms of  $\mathcal{D}$  that are not conformal but continuously differentiable. It can be understood as a regularized version of  $\{G_t\}_{t \in [0, +\infty)}$  because

$$G_{t,\varepsilon} \xrightarrow{\varepsilon \rightarrow 0} G_t, \quad t \in [0, +\infty), \quad (5.102)$$

pointwise.

We remark that for a non-conformal map  $F$  the definition of the pre-pre-Schwarzian (4.10) should be generalized to

$$F_* \eta^\Psi(z) = \eta^\Psi(\tau(z)) + Q \log \left( \partial_z \tau(z) \partial_{\bar{z}} \overline{\tau(z)} - \partial_{\bar{z}} \tau(z) \partial_z \overline{\tau(z)} \right), \quad \tau(z) = (F^\Psi)^{-1}(z). \quad (5.103)$$

Random variables such as  $G_{t,\varepsilon}^{-1} *_\eta[f]$  and  $G_{t,\varepsilon}^{-1} *_\Gamma[f, f]$  are defined for  $t \in [0, +\infty)$  because  $G_{t,\varepsilon}$  is an automorphism. Thus, we can define

$$G_t^{-1} *_\eta[f] := \lim_{\varepsilon \rightarrow 0} G_{t,\varepsilon}^{-1} *_\eta[f], \quad t \in [0, +\infty). \quad (5.104)$$

If  $t \leq T[f]$  this definition coincides with the standard one. We expect it to be equivalent to the approach described in [SS10] if the hull  $\mathcal{K}_t$  is a simple curve ( $\kappa \leq 4$ ). If  $\mathcal{K}_t$  is

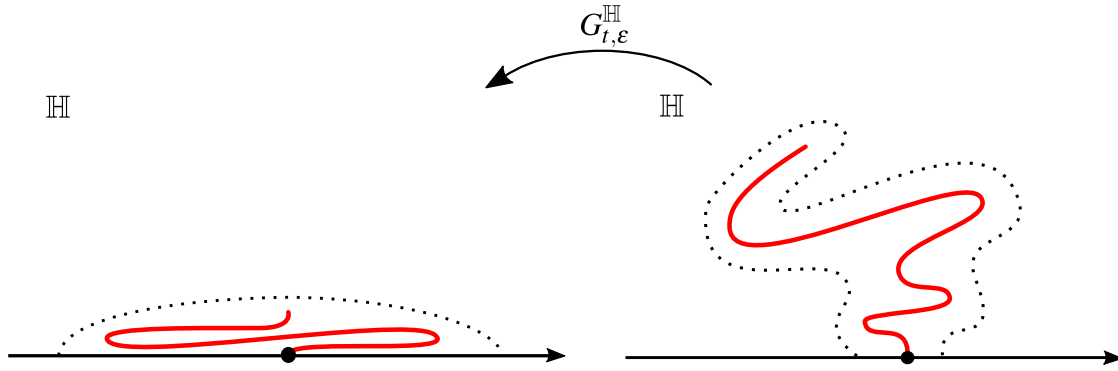


Figure 5.2: Schematic illustration of how the map  $G_{t,\epsilon}^{\mathbb{H}}$  acts in the case when the slit  $\gamma_t$  of  $G_t^{\mathbb{H}}$  is a simple curve. It is denoted by the red line on the right-hand side. On the left-hand side, the red line is the corresponding image  $G_{t,\epsilon}^{\mathbb{H}}(\gamma_t)$ . The map  $G_{t,\epsilon}^{\mathbb{H}}$  is conformal outside the dashed line.

generated by a curve with self-touches, than the pushforward  $G_t^{-1} * \eta[f]$  depends also on the chain  $\{G_s\}_{s \in [0,t]}$ , or equivalently, on the driving function  $\{u_s\}_{s \in [0,t]}$ , but not only on the final map  $G_t$ .

Let us now consider how the limit in (5.104) works in this case, see Fig. (5.3). Let the hull  $\mathcal{K}_t$  be generated by the curve  $\gamma_t$  with self-touches. It can be represented as union of the curve  $\gamma_t$  and the connected open components  $U_n^+$  and  $U_n^-$ ,  $n = 1, 2, \dots$ , bounded by  $\gamma_t$ :

$$\mathcal{K}_t = \gamma_t \cup \bigcup_{n=1,2,\dots} U_n^+ \cup \bigcup_{n=1,2,\dots} U_n^- \tag{5.105}$$

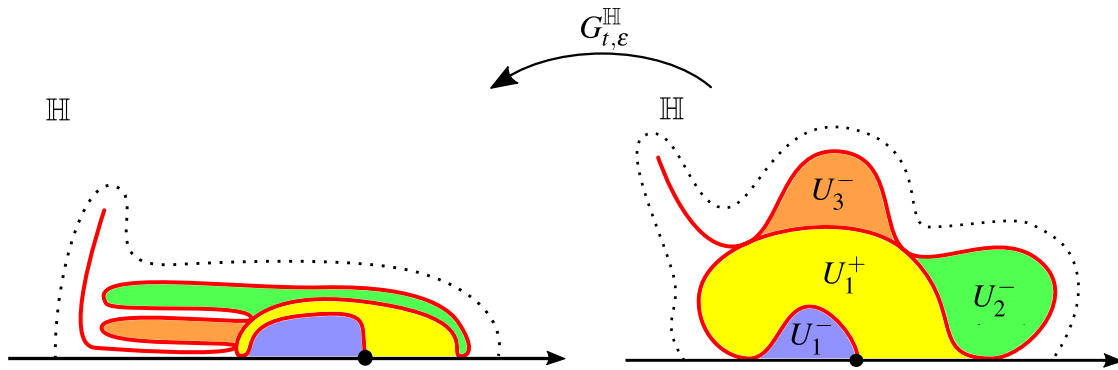


Figure 5.3: This is a schematic illustration of how the map  $G_{t,\epsilon}^{\mathbb{H}}$  acts in the case of self-touching curve  $\gamma_t$ . The red line on the right-hand side is the slit  $\gamma$  of  $G_t^{\mathbb{H}}$ , on the left-hand side, the red line is the image  $G_{t,\epsilon}^{\mathbb{H}}(\gamma_t)$ . The map  $G_{t,\epsilon}^{\mathbb{H}}$  is conformal beyond the dashed line.

We denote by the upper indexes ‘+’ and ‘-’ the components bounded by  $\gamma_t$  passing clockwise and counterclockwise correspondingly. We state without a proof that

$$\lim_{\epsilon \rightarrow 0} G_{t,\epsilon}^{\mathbb{H}}(U_n^+) \subset [0, +\infty), \quad \lim_{\epsilon \rightarrow 0} G_{t,\epsilon}^{\mathbb{H}}(U_n^-) \subset (-\infty, 0], \quad n = 1, 2, \dots \tag{5.106}$$

In other words, the sets  $U_n^+$ ,  $n = 1, 2, \dots$  are ‘pressed’ to the positive real axis and  $U_n^-$  to the negative one. Consider, for instance, the case from Section 6.1.2 with  $\kappa = 4$ ,  $\nu = 0$ ,

when  $\eta$  is a scalar and

$$\eta^{\mathbb{H}}(z) = -\arg z + \pi/2, \quad z \in \mathbb{H}. \quad (5.107)$$

We use the results of Section 4.3 to conclude that

$$\begin{aligned} G_t^{-1} *_\eta[f] = & \int_{\psi^{\mathbb{H}}(\mathcal{D} \setminus \mathcal{K}_t)} \eta^{\mathbb{H}}(G_t^{\mathbb{H}}(z)) f^{\mathbb{H}}(z) l(dz) + \\ & + \frac{\pi}{2} \sum_{n=1,2,\dots} \left[ \int_{\psi^{\mathbb{H}}(U_n^+)} f^{\mathbb{H}}(z) l(dz) - \int_{\psi^{\mathbb{H}}(U_n^-)} f^{\mathbb{H}}(z) l(dz) \right], \quad f \in \mathcal{H}_s. \end{aligned} \quad (5.108)$$

Equivalently, we can define  $\eta^{\mathbb{H}}(G_t^{\mathbb{H}}(z))$  for  $z \in \mathcal{K}_t$  to be equal to  $+\pi/2$  and  $-\pi/2$  on  $U_n^+$  and  $U_n^-$  correspondingly.

In order to see that the proposed definition of the pushforward gives the extension of Theorem 5.1 for  $t > T[f]$ , one can apply the following method. Let  $\eta_\varepsilon$  and  $\Gamma_\varepsilon$  be the solution of (5.41–5.43) with  $\delta_\varepsilon$  instead of  $\delta$ . Then

$$\hat{\phi}_\varepsilon[f] = e^{\frac{1}{2}\Gamma_\varepsilon[f,f] + \eta_\varepsilon[f]} \quad (5.109)$$

induces the local martingales as well as  $\hat{\phi}$ . The last part of the method is to show that  $\eta_\varepsilon \xrightarrow{\varepsilon \rightarrow 0} \eta$ ,  $\Gamma_\varepsilon \xrightarrow{\varepsilon \rightarrow 0} \Gamma$ , and consequently,  $\hat{\phi}_\varepsilon \xrightarrow{\varepsilon \rightarrow 0} \hat{\phi}$ .

## Conclusions and perspectives

1. We did not prove it in this monograph, but our experience shows that we listed all possible ways of coupling of GFF with  $(\delta, \sigma)$ -SLE if we assume that  $\Gamma$  transforms as a scalar, see (4.35), and that  $\eta$  is a pre-pre-Schwarzian. It would be useful to prove this as well as to understand what should be relaxed in our frameworks to couple all  $(\delta, \sigma)$ -SLEs.
2. The pre-pre-Schwarzian rule (4.9) is motivated by the local geometry of SLE curve [She10]. In principle, one can consider alternative rules. Moreover, the scalar behaviour of  $\Gamma$  can also be relaxed because the harmonic part  $H^\Psi(z, w)$  in (4.41) can transform in many ways. Such more general coupling is intrinsic and can be thought of as a generalization of the coupling in Sections 6.2.4 and 6.3.4 for arbitrary  $\kappa$ .
3. We considered only the simplest case of one GFF. It would be interesting to examine tuples of  $\{\Phi_i\}_{i=1,2,\dots,n}$ .
4. The Bochner-Minols Theorem 4.1 suggests to consider not only free fields, but for example, some polynomial combinations in the exponential of (4.53). In particular, the quartic functional

$$\hat{\phi}[f] = e^{\eta[f] + \frac{1}{2}\Gamma[f,f] + \frac{1}{6}W_3[f,f,f] + \frac{1}{24}W_4[f,f,f,f]}, \quad (5.110)$$

for some symmetric cubic  $W_3$  and quartic  $W_4$  functionals with some transformation properties (not necessary scalar), corresponds to conformal field theories related

to 2-to-2 scattering of particles in dimension two. Then, the generalization of the system (5.41–5.43) is

$$\begin{aligned}
\mathcal{L}_\delta \eta[f] + \frac{1}{2} \mathcal{L}_\sigma^2 \eta[f] &= 0, \\
\mathcal{L}_\delta \Gamma[f, g] + \mathcal{L}_\sigma \eta[f] \mathcal{L}_\sigma \eta[g] + \frac{1}{2} \mathcal{L}_\sigma^2 \Gamma[f, g] &= 0, \\
\mathcal{L}_\delta W_3[f, g, h] + \mathcal{L}_\sigma \Gamma[f, g] \mathcal{L}_\sigma \eta[h] + \text{symmetric terms} &= 0, \\
\mathcal{L}_\delta W_4[f, g, h, l] + \mathcal{L}_\sigma \Gamma[f, g] \mathcal{L}_\sigma \Gamma[h, l] + \text{symmetric terms} &= 0, \\
\mathcal{L}_\sigma W_3[f, g, h] = 0, \quad \mathcal{L}_\sigma W_4[f, g, h, l] &= 0, \\
f, g, h, l \in \mathcal{H}.
\end{aligned} \tag{5.111}$$

Any nontrivial solution of this system (which corresponds to positive definite  $\hat{\phi}$ ) gives a new type of coupling which is particularly interesting because it is related to a field theory with a self-interaction.

For the general form of the the Schwinger functionals  $S_n$  the necessary and sufficient condition for the coupling is

$$\left( \mathcal{L}_\delta + \frac{1}{2} \mathcal{L}_\sigma^2 \right) S_n(z_1, z_2, \dots, z_n) = 0, \quad n = 1, 2, \dots, \tag{5.112}$$

which can be understood as a version of BPZ formula form [BPZ84].

# Chapter 6

## Important spacial cases

In this chapter, we collect the most important special cases of  $(\delta, \sigma)$ -Löwner equations and couplings. Each section starts from some special choice of  $\delta$  and  $\sigma$  with the corresponding motivation. We continue with discussion of properties of deterministic and stochastic versions that are specific for given  $\delta$  and  $\sigma$ . The last part of each section is dedicated to the coupling to GFF. We consider all known types of couplings related to the given  $\delta$  and  $\sigma$ .

To compare different cases we have to consider them in the same chart. We use two charts for this purpose: the half-plane  $\mathbb{H}$  chart and the unit disk  $\mathbb{D}$  chart. The advantage of the first one is the simplicity of formulas. The unit disk is sometimes more convenient because it is a compact domain with smooth boundary. It is the chart on which we compared the global behaviour of the slits. Numerical simulations of all  $(\delta, \sigma)$ -SLEs are also presented in the unit disk chart.

We discuss in details only the chordal case. The analogous comments for other cases are dropped in order to avoid repetitions.

### 6.1 Chordal case

#### 6.1.1 Chordal Löwner equation

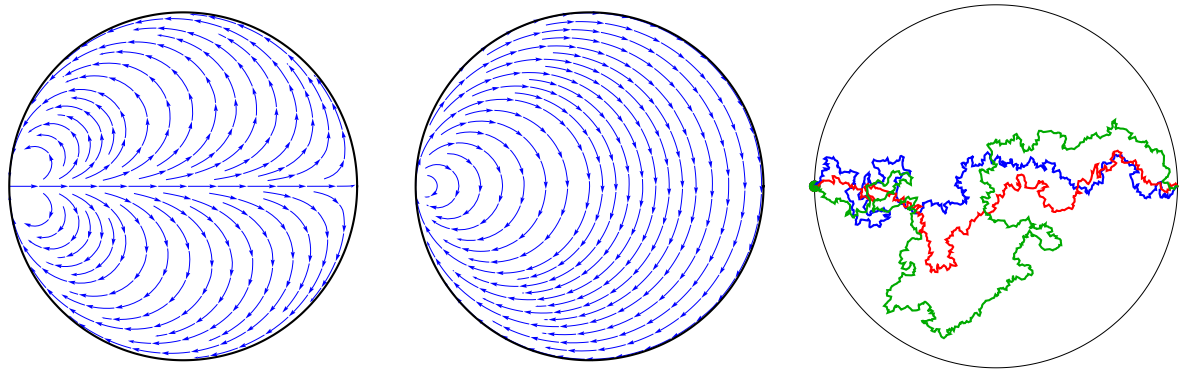
The chordal version of Löwner equation is the most known and well-studied. The ordinary equation was discovered by Charles Löwner in 1923. Its stochastic version was introduced by Schramm [Sch00] in 2000.

Assume that both of the holomorphic vector fields  $\delta$  and  $\sigma$  have second order zero at a boundary point  $b \in \mathcal{D}$ . This point can always be mapped to  $\psi^{\mathbb{D}}(b) = 1$  in the unit disk chart, or equivalently, to  $\psi^{\mathbb{H}}(b) = \infty$  in the half-plane chart. Thus, without loss of generality we can assume that

$$\begin{aligned}\sigma &= \sigma_{-1}\ell_{-1}, & \sigma_{-1} &\in \mathbb{R}, \\ \delta &= \delta_{-2}\ell_{-2} + \delta_{-1}\ell_{-1}, & \delta_{-2} &> 0, \quad \delta_{-1} \in \mathbb{R},\end{aligned}\tag{6.1}$$

where we restrict ourselves to the forward case. Using the transforms  $\mathcal{V}$ ,  $\mathcal{T}$ , and  $\mathcal{D}$  we can normalize

$$\delta_c = 2\ell_{-2}, \quad \sigma_c = -\ell_{-1}.\tag{6.2}$$



(a) Flow lines of vector field  $\delta_c$ . (b) Flow lines of vector field  $\sigma_c$ . (c) Three samples of chordal SLE slits for  $\kappa = 2$ . All slits tend to the point  $\phi^{\mathbb{D}}(b) = -1$ .

Figure 6.1: flow lines of the chordal vector field  $\delta_c$ ,  $\sigma_c$ , and corresponding slit samples in the unit disk chart.

This normalization is motivated by historical reasons, because the chordal Löwner equation in the half-plane chart has usually the form

$$\dot{G}_t^{\mathbb{H}}(z) = \frac{2}{G_t^{\mathbb{H}}(z)} - \dot{u}_t. \quad (6.3)$$

This corresponds to the vector fields

$$\delta_c^{\mathbb{H}}(z) = \frac{2}{z}, \quad \sigma_c^{\mathbb{H}}(z) = -1. \quad (6.4)$$

that are the relations (6.2) in the half-plane chart.

To obtain a more traditional form of the chordal Löwner equation which is valid also for not differentiable driving functions we can apply the procedure from the beginning of Section 1.2.1. The one parametric group of Möbius automorphisms  $H[\sigma]_s$  can be found in the half-plane chart from the equation (1.14), which in our case takes the form

$$\dot{H}_s[\sigma_c]^{\mathbb{H}}(z) = -1, \quad H_0[\sigma_c]^{\mathbb{H}}(z) = z, \quad z \in \mathbb{H}, \quad (6.5)$$

has the solution

$$H_s[\sigma_c]^{\mathbb{H}}(z) = z - s, \quad z \in \mathbb{H}. \quad (6.6)$$

We define

$$g_t^{\mathbb{H}}(z) := (H_{u_t}[\sigma_c]^{-1} \circ G_t)^{\mathbb{H}}(z) = G_t^{\mathbb{H}}(z) + u_t, \quad (6.7)$$

which is a form of (1.33). Taking into account that

$$(H_s[\sigma_c]_*^{-1} \delta)^{\mathbb{H}}(z) = \frac{2}{z - s} \quad (6.8)$$

we derive the equation for  $g_t^{\mathbb{H}}(z)$

$$\dot{g}_t^{\mathbb{H}}(z) = \frac{2}{g_t^{\mathbb{H}}(z) - u_t}, \quad (6.9)$$

which is known as the chordal Löwner equation.

We remark that the maps  $G_t^{\mathbb{H}}$  and  $g_t^{\mathbb{H}}$  possess the normalization conditions

$$G_t^{\mathbb{H}}(z) = z - u_t + O(z^{-1}) \quad (6.10)$$

and

$$g_t^{\mathbb{H}}(z) = z + O(z^{-1}). \quad (6.11)$$

These conditions uniquely fix the maps  $G_t$  and  $g_t$  for given  $\mathcal{K}_t$  if  $\psi^{\mathbb{H}}(\mathcal{K}_t)$  is compact.

In the unit disk chart, the relations above have the form

$$\delta_c^{\mathbb{D}}(z) = \frac{(1+z)^3}{1-z}, \quad \sigma_c^{\mathbb{D}}(z) = -\frac{i}{2}(1+z)^2. \quad (6.12)$$

The analogue of (6.3) is

$$\dot{G}_t^{\mathbb{D}}(z) = \frac{(1+G_t^{\mathbb{D}}(z))^3}{1-G_t^{\mathbb{D}}(z)} - \frac{i}{2}(1+G_t^{\mathbb{D}}(z))^2 \dot{u}_t. \quad (6.13)$$

The equation (6.9) in the unit disk chart is

$$\dot{g}_t^{\mathbb{D}}(z) = \frac{-4i(1+g_t^{\mathbb{D}}(z))^3}{(2i+u_t+u_t g_t^{\mathbb{D}}(z))(i+u_t-i g_t^{\mathbb{D}}(z)+u_t g_t^{\mathbb{D}}(z))}. \quad (6.14)$$

To define the stochastic version of chordal Löwner equation (chordal SLE) we can substitute  $u_t = \sqrt{\kappa}B_t + \nu t$  in (6.3) or (6.9). In the first case we thus obtain in the chordal SLE in Stratonovich form

$$d^S G_t^{\mathbb{H}}(z) = \frac{2}{G_t^{\mathbb{H}}(s)} dt - \sqrt{\kappa} d^S B_t - \nu dt \quad (6.15)$$

The Itô form of the same equation in the half-plane chart is

$$d^{\text{Itô}} G_t^{\mathbb{H}}(z) = \frac{2}{G_t^{\mathbb{H}}(s)} dt - \sqrt{\kappa} d^{\text{Itô}} B_t - \nu dt. \quad (6.16)$$

The last two equations are identical, because  $\sigma^{\mathbb{H}'}(z) \equiv 0$ . In other charts,  $\sigma^{\psi'}(z) \neq 0$ , and the Stratonovich and Itô forms differ.

Thereby, we define  $\delta$  and  $\sigma$  for stochastic case by

$$\delta = \pm \delta_c + \nu \sigma_c = \pm 2\ell_{-2} - \ell_{-1} \nu, \quad \sigma = \sqrt{\kappa} \sigma_c = -\sqrt{\kappa} \ell_{-1}, \quad \kappa > 0, \quad \nu \in \mathbb{R}, \quad (6.17)$$

where we add parameters  $\kappa$  and  $\nu$ , see comments in Section 1.3.2 and ‘ $\pm$ ’ corresponds to the forward and reverse cases.

The chordal SLE without drift has a specific property that is only hold for this case. The random laws of  $\{G_t\}_{t \in [0, +\infty)}$  and  $\{\mathcal{K}_t\}_{t \in [0, +\infty)}$  are invariant with respect to the transform  $\mathcal{P}$ , see Section 1.3.2. In other words, this is the only  $(\delta, \sigma)$ -SLE whose law is scale invariant. This property makes the chordal case special, see also the end of Section 3.1. This is why it is natural to use chordal equation to study local properties of the slit.

### 6.1.2 Coupling of forward chordal SLE and Dirichlet GFF

This is the simplest type of coupling considered in [She10]. A another aspect is discussed in In [KM11]. We consider here a generalization with a nonzero drift  $\nu \in \mathbb{R}$ . It is a special case of Theorem 5.1 and Theorem 5.3 (the 1st string of Table 5.1 and sing ‘+’ in the ‘ $\pm$ ’ pair).

We assume

$$\delta = \delta_c + \nu \sigma_c, \quad \sigma = \sqrt{\kappa} \sigma_c, \quad \mathcal{H} = \mathcal{H}_s, \quad \Gamma = \Gamma_D. \quad (6.18)$$

The pre-pre-Schwarzian  $\eta$ , can be obtained directly form the Hadamard formula (5.42).

We show here how to calculate  $\eta$  from the relations (5.63) by substituting (5.87) and (5.92). In the half-plane chart, we have

$$-\kappa^{\frac{1}{2}} \partial_z \eta^{+\mathbb{H}}(z) + \mu \cdot 0 = \frac{-i}{z} + i\alpha. \quad (6.19)$$

Then

$$\eta^{+\mathbb{H}}(z) = \frac{i}{\sqrt{\kappa}} \log z - \frac{i\alpha z}{\sqrt{\kappa}} + C^+, \quad C^+ \in \mathbb{C}. \quad (6.20)$$

and taking into account that  $\alpha = -\frac{\nu}{2}$  (see (5.92)) and (5.62) we obtain finally

$$\eta^{\mathbb{H}}(z) = \frac{-2}{\sqrt{\kappa}} \arg z - \frac{\nu}{\sqrt{\kappa}} \operatorname{Im} z + C, \quad C \in \mathbb{R}. \quad (6.21)$$

We present here an explicit form of the time evolution  $M_{1_t}$  of the one-point function  $S_1(z) = \eta(z)$

$$M_{1_t}^{\mathbb{H}}(z) = (G_t^{-1} * \eta)^{\mathbb{H}}(z) = \frac{-2}{\sqrt{\kappa}} \arg G_t^{\mathbb{H}}(z) - \frac{\nu}{\sqrt{\kappa}} \operatorname{Im} G_t^{\mathbb{H}}(z) + \frac{\kappa - 4}{2\sqrt{\kappa}} \arg G_t^{\mathbb{H}'}(z) + C. \quad (6.22)$$

When  $\nu = 0$  this expression coincides (up to a constant) with the analogous one from [KM11, Section 8.5].

### 6.1.3 Coupling of reverse chordal SLE and Neumann GFF

We assume

$$\delta = -\delta_c + \nu \sigma_c, \quad \sigma = \sqrt{\kappa} \sigma_c, \quad \mathcal{H} = \mathcal{H}_s^*, \quad \Gamma = \Gamma_N. \quad (6.23)$$

This type of the coupling is also considered in [She10]. It corresponds to the first string of the Table 5.1 and the sign ‘-’ in the ‘ $\pm$ ’ pairs. We use the space  $\mathcal{H}_s^{*}$  for the GFF, which means that  $\Phi$  is a linear functional defined up to a constant over the space of smooth functions with compact support. The covariance  $\Gamma = \Gamma_N$  is defined in (4.49).

Following the same way as in the previous section we obtain

$$j^{\mathbb{H}}(z) = -\operatorname{Re} \frac{1}{z} + \nu, \quad \nu \in \mathbb{R}, \quad (6.24)$$

$$\eta^{+\mathbb{H}}(z) = \frac{1}{\sqrt{\kappa}} \log z + \frac{\alpha}{\sqrt{\kappa}} z, \quad (6.25)$$



$$\eta^{\mathbb{H}}(z) = \frac{2}{\sqrt{\kappa}} \log |z| - \frac{\nu}{\sqrt{\kappa}} \operatorname{Re} z, \quad (6.26)$$

$$\eta = \frac{2}{\sqrt{\kappa}} \log \left| \frac{\sigma_c^{\frac{\kappa}{4}}}{\delta_c} \right| + \frac{2\nu}{\sqrt{\kappa}} \operatorname{Re} \frac{\sigma_c}{\delta_c} + C = \frac{2}{\sqrt{\kappa}} \log \left| \frac{\sigma^{\frac{\kappa}{4}}}{\delta - \frac{\nu}{\sqrt{\kappa}} \sigma} \right| - \frac{2\nu}{\kappa} \operatorname{Re} \frac{\sigma}{\delta - \frac{\nu}{\sqrt{\kappa}} \sigma} + C. \quad (6.27)$$

The one point local martingale in the half-plane chart is

$$\begin{aligned} M_{1_t}^{\mathbb{H}}(z) &= G_t^{-1} \ast \eta^{\ast \mathbb{H}}(z) = \\ &= \frac{2}{\sqrt{\kappa}} \log \left| G_t^{\mathbb{H}}(z) \right| - \frac{\nu}{\sqrt{\kappa}} \operatorname{Re} \left( G_t^{\mathbb{H}}(z) \right) + \frac{\kappa+4}{2\sqrt{\kappa}} \log \left| \left( G_t^{\mathbb{H}} \right)'(z) \right| + C \end{aligned} \quad (6.28)$$

## 6.2 Dipolar Case

### 6.2.1 Dipolar Löwner equation

The dipolar version of the Löwner equation was considered first in [BB03b].

Assume that both of the vector fields  $\delta$  and  $\sigma$  have zero at the same two different points  $b_1$  and  $b_2$  on the boundary  $\partial \mathcal{D}$ . Namely,

$$\delta(b_1) = \sigma(b_1) = \delta(b_2) = \sigma(b_2) = 0, \quad b_1 \neq b_2 \in \partial \mathcal{D}. \quad (6.29)$$

With the help of the of the transforms  $\mathcal{R}$  and  $\mathcal{P}$  we can always normalize such that

$$\begin{aligned} \sigma &= \sigma_{-1}(\ell_{-1} - \ell_1), \quad \sigma_{-1} \in \mathbb{R} \setminus \{0\}, \\ \delta &= \delta_{-2}(\ell_{-2} - \ell_0) + \delta_{-1}(\ell_{-1} - \ell_1), \quad \delta_{-2} > 0, \quad \delta_{-1} \in \mathbb{R}. \end{aligned} \quad (6.30)$$

This corresponds to  $\psi^{\mathbb{D}}(b_1) = i$  and  $\psi^{\mathbb{D}}(b_2) = -i$  in the unit disk chart and  $\psi^{\mathbb{H}}(b_1) = 1$  and  $\psi^{\mathbb{H}}(b_2) = -1$  in the half plane chart. Using the transforms  $\mathcal{V}$ ,  $\mathcal{D}$ , and  $\mathcal{T}$  we can normalize further and assume

$$\sigma = \ell_{-1} - \ell_1, \quad \delta = 2(\ell_{-2} - \ell_0). \quad (6.31)$$

It is natural to consider the dipolar Löwner equation in the chart defined by the following transition map

$$\tau_{\mathbb{H}, \mathbb{S}}(z) = \operatorname{th} \frac{z}{2} : \mathbb{S} \rightarrow \mathbb{H}. \quad (6.32)$$

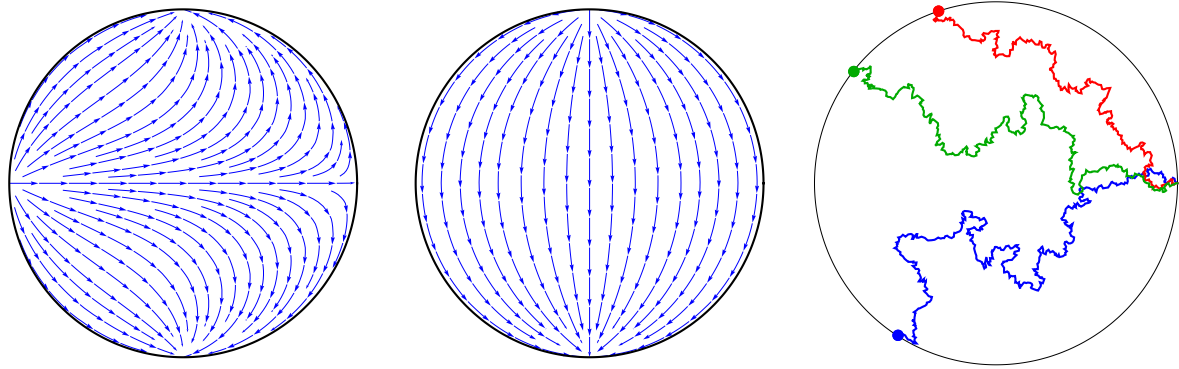
This domain  $\mathbb{S}$  is called **strip**

$$\mathbb{S} := \psi^{\mathbb{S}}(\mathcal{D}) = \{z \in \mathbb{C} : 0 < \operatorname{Im} z < \pi\} \quad (6.33)$$

and the chart  $\psi^{\mathbb{S}}$  we call **strip chart**. We denote vector fields, conformal maps a pre-Schwarzians in this coordinates with the upper index  $\mathbb{S}$  analogous to  $\mathbb{D}$  and  $\mathbb{H}$ . In this coordinates  $\psi^{\mathbb{S}}(b_1) = \text{'right infinity'}$ ,  $\psi^{\mathbb{S}}(b_2) = \text{'left infinity'}$ , and  $\psi^{\mathbb{S}}(a) = 0$ .

The vector fields have the form

$$\delta^{\mathbb{S}}(z) = 4 \operatorname{cth} \frac{z}{2}, \quad \sigma^{\mathbb{S}}(z) = -2. \quad (6.34)$$



(a) Flow lines of vector field  $\delta_d$ . (b) Flow lines of vector field  $\sigma_d$ . (c) 3 samples for dipolar SLE slits for  $\kappa = 2$ . The slits tend to a random points (big color dots) on the left arc between  $\psi^{\mathbb{D}}(b_1) = i$  and  $\psi^{\mathbb{D}}(b_2) = -i$ .

Figure 6.2: Flow lines of the dipolar field  $\delta_d$ ,  $\sigma_d$ , and corresponding slit samples in the unit disk chart.

The Löwner equation can be written as

$$\dot{G}_t^{\mathbb{S}}(z) = 4 \operatorname{cth} \frac{G_t^{\mathbb{S}}(z)}{2} - 2\dot{u}_t. \quad (6.35)$$

A more frequently used normalization is

$$\dot{g}_t^{\mathbb{S}}(z) = \operatorname{cth} \frac{G_t^{\mathbb{S}}(z)}{2} - \dot{u}_t, \quad (6.36)$$

which can be obtained from (6.35) by the transform  $\mathcal{P}_c$  with  $c = 2$ .

We prefer the normalization only for universality (the invariant coefficients  $\delta_{-2} = 2$  and  $\sigma_{-1} = -1$  are the same in all cases).

We obtain the following form of the Löwner equation

$$\dot{g}_t^{\mathbb{S}}(z) = 4 \operatorname{cth} \left( \frac{g_t^{\mathbb{S}}(z)}{2} - u_t \right) \quad (6.37)$$

with

$$g_t^{\mathbb{S}}(z) = G_t^{\mathbb{S}}(z) + 2u_t \quad (6.38)$$

in the same way as in the previous section.

We define  $\delta_c$  and  $\sigma_c$  for the stochastic case by

$$\delta_d = 2\ell_{-2} - \ell_{-1}\mathbf{v}, \quad \sigma_d = -(\ell_{-1} - \ell_{-1}), \quad \mathbf{v} \in \mathbb{R}, \quad (6.39)$$

where we add parameters  $\kappa$  and  $\mathbf{v}$ , see comments in Section 1.3.2. The dipolar SLE can be expressed as

$$d^{\mathbb{S}} G_t^{\mathbb{S}}(z) = 4 \operatorname{cth} \frac{G_t^{\mathbb{S}}(z)}{2} dt - 2\sqrt{\kappa} d^{\mathbb{S}} B_t - \frac{\mathbf{v}}{2} dt \quad (6.40)$$

in the Stratonovich form and as

$$d^{\text{It}\hat{o}} G_t^{\mathbb{S}}(z) = 4 \operatorname{cth} \frac{G_t^{\mathbb{S}}(z)}{2} dt - 2\sqrt{\kappa} d^{\text{It}} B_t - \frac{\nu}{2} dt \quad (6.41)$$

in terms of the Itô differentials, because  $\sigma^{\mathbb{S}}(z)$  is a constant.

Consider now the same relations for the stochastic case in the half-plane chart. They are

$$\delta_d^{\mathbb{H}}(z) = 2 \left( \frac{1}{z} - z \right) - \nu(1 - z^2), \quad \sigma_d^{\mathbb{H}}(z) = -(1 - z^2), \quad \kappa > 0, \quad \nu \in \mathbb{R}, \quad (6.42)$$

$$d^{\mathbb{S}} G_t^{\mathbb{S}}(z) = 2 \left( \frac{1}{G_t^{\mathbb{S}}(z)} - G_t^{\mathbb{S}}(z) \right) dt - \nu \left( 1 - G_t^{\mathbb{S}}(z)^2 \right) dt - \sqrt{\kappa} \left( 1 - G_t^{\mathbb{S}}(z)^2 \right) d^{\mathbb{S}} B_t \quad (6.43)$$

$$d^{\text{It}\hat{o}} G_t^{\mathbb{S}}(z) = 2 \left( \frac{1}{G_t^{\mathbb{S}}(z)} - G_t^{\mathbb{S}}(z) - \kappa G_t^{\mathbb{S}}(z) \left( 1 - G_t^{\mathbb{S}}(z)^2 \right) \right) dt - \nu \left( 1 - G_t^{\mathbb{S}}(z)^2 \right) dt - \sqrt{\kappa} \left( 1 - G_t^{\mathbb{S}}(z)^2 \right) d^{\text{It}\hat{o}} B_t, \quad (6.44)$$

where we used (1.106).

We remark that the maps  $G_t^{\mathbb{S}}$  and  $g_t^{\mathbb{S}}$  possess the normalization conditions

$$\begin{aligned} G_t^{\mathbb{S}}(z) &= z - 2u_t + O(z^{-1}), \quad \operatorname{Re} z > 0, \\ G_t^{\mathbb{S}}(z) &= z - 2u_t + O(z^{-1}), \quad \operatorname{Re} z < 0, \end{aligned} \quad (6.45)$$

and

$$\begin{aligned} g_t^{\mathbb{S}}(z) &= z + O(z^{-1}), \quad \operatorname{Re} z > 0, \\ g_t^{\mathbb{S}}(z) &= z + O(z^{-1}), \quad \operatorname{Re} z < 0. \end{aligned} \quad (6.46)$$

Besides  $G_t(z_{\text{tip}}) = a$  and  $g_t^{\mathbb{S}}(z_{\text{tip}}) = u_t$  in the forward case and  $G_t(a) = z_{\text{tip}}$  in the reverse case. These conditions uniquely fix the maps  $G_t$  and  $g_t$  for given  $\mathcal{K}_t$  if  $\psi^{\mathbb{S}}(\mathcal{K}_t)$  is compact and does not touch the upper boundary of the strip  $\mathbb{S}$ .

The unit disk chart is also reasonable to consider.

$$\delta_d^{\mathbb{D}}(z) = 2 \frac{(1+z)(1+z^2)}{1-z} - \nu(1 - z^2), \quad \sigma_d^{\mathbb{D}}(z) = -i(1 + z^2), \quad \kappa > 0, \quad \nu \in \mathbb{R}, \quad (6.47)$$

$$d^{\mathbb{S}} G_t^{\mathbb{D}}(z) = 2 \frac{(1 + G_t^{\mathbb{D}}(z))(1 + G_t^{\mathbb{D}}(z)^2)}{1 - G_t^{\mathbb{D}}(z)} dt - i\nu(1 + G_t^{\mathbb{D}}(z)^2) dt - i\sqrt{\kappa}(1 + G_t^{\mathbb{D}}(z)^2) d^{\mathbb{S}} B_t \quad (6.48)$$

$$\begin{aligned} d^{\text{It}\hat{o}} G_t^{\mathbb{D}}(z) &= 2 \left( \frac{(1 + G_t^{\mathbb{D}}(z))(1 + G_t^{\mathbb{D}}(z)^2)}{1 - G_t^{\mathbb{D}}(z)} - \kappa G_t^{\mathbb{D}}(z)(1 + G_t^{\mathbb{D}}(z)^2) \right) dt - \\ &\quad - i\nu(1 + G_t^{\mathbb{D}}(z)^2) dt - i\sqrt{\kappa}(1 + G_t^{\mathbb{D}}(z)^2) d^{\text{It}\hat{o}} B_t. \end{aligned} \quad (6.49)$$

We define  $\delta$  and  $\sigma$  for the stochastic case by

$$\begin{aligned} \delta &= \pm \delta_d + \nu \sigma_d = \pm 2(\ell_{-2} - \ell_0) - \nu(\ell_{-1} - \ell_1), \\ \sigma &= \sqrt{\kappa} \sigma_d = -\sqrt{\kappa}(\ell_{-1} - \ell_1), \quad \kappa > 0, \quad \nu \in \mathbb{R}, \end{aligned} \quad (6.50)$$

where ‘ $\pm$ ’ corresponds to the forward and reverse cases.

## 6.2.2 Coupling of forward dipolar SLE and Dirichlet GFF

We assume

$$\delta = \delta_d + \nu \sigma_d, \quad \sigma = \sqrt{\kappa} \sigma_d, \quad \mathcal{H} = \mathcal{H}_s, \quad \Gamma = \Gamma_D. \quad (6.51)$$

This case corresponds to the third string in the Table 5.1 and sign ‘+’ in the pairs  $\pm$ . With  $\nu = 0$  it is also considered in [KT13].

We obtain first  $\eta^+$ ,  $\eta$  and  $M_{1t}$  in the half-plane chart. The same way as in the previous subsection we calculate

$$-\sqrt{\kappa}(1-z^2) \partial_z \eta^{+\mathbb{H}}(z) + \mu (-\sqrt{\kappa}(1-z^2))' = \frac{-i}{z} + i\alpha. \quad (6.52)$$

Taking into account (5.84) and  $\alpha = -\nu/2$  we obtain

$$\eta^{+\mathbb{H}}(z) = \frac{i}{\sqrt{\kappa}} \log z + \frac{i(\kappa-6)}{4\sqrt{\kappa}} \log(1-z^2) + \frac{i\nu}{2\sqrt{\kappa}} \operatorname{arcthz} + C^+. \quad (6.53)$$

$$\eta^{\mathbb{H}}(z) = \frac{-2}{\sqrt{\kappa}} \arg z - \frac{(\kappa-6)}{2\sqrt{\kappa}} \arg(1-z^2) - \frac{\nu}{\sqrt{\kappa}} \operatorname{Im} \operatorname{arcthz} + C. \quad (6.54)$$

$$\begin{aligned} M_{ct}^{\mathbb{H}}(z) &= (G_t^{-1} \ast \eta)^{\mathbb{H}}(z) = \\ &= \frac{-2}{\sqrt{\kappa}} \arg G_t^{\mathbb{H}}(z) - \frac{(\kappa-6)}{2\sqrt{\kappa}} \arg(1-G_t^{\mathbb{H}}(z)^2) - \\ &\quad - \frac{\nu}{\sqrt{\kappa}} \operatorname{Im} \operatorname{arcth} G_t^{\mathbb{H}}(z) + \frac{\kappa-4}{2\sqrt{\kappa}} \arg G_t^{\mathbb{H}\prime}(z) + C. \end{aligned} \quad (6.55)$$

The corresponding relations in the strip chart are

$$\delta_d^{\mathbb{S}}(z) = 4 \operatorname{cth} \frac{z}{2} - 2\nu, = -2, \quad \nu \in \mathbb{R}, \quad (6.56)$$

$$j^{\mathbb{S}}(z) = -i \operatorname{cth} \frac{z}{2} + i\alpha, \quad (6.57)$$

The function  $\eta^{\mathbb{S}}(z)$  can be found as the solution to (5.63) in the strip chart

$$\eta^{\mathbb{S}}(z) = \frac{-2}{\sqrt{\kappa}} \arg \operatorname{sh} \frac{z}{2} - \frac{\nu}{2\sqrt{\kappa}} \operatorname{Im} z + C, \quad (6.58)$$

$$\begin{aligned} M_{1t}^{\mathbb{S}}(z) &= (G_t^{-1} \ast \eta)^{\mathbb{S}}(z) = \\ &= \frac{-2}{\sqrt{\kappa}} \arg \operatorname{sh} \frac{G_t^{\mathbb{S}}(z)}{2} - \frac{\nu}{2\sqrt{\kappa}} \operatorname{Im} G_t^{\mathbb{S}}(z) + \frac{\kappa-4}{2\sqrt{\kappa}} \arg \left( G_t^{\mathbb{S}} \right)'(z) + C. \end{aligned} \quad (6.59)$$

The expression for  $\Gamma_D$  in the strip chart is

$$\Gamma_D^{\mathbb{S}}(z, w) = \Gamma_D^{\mathbb{H}}(\tau_{\mathbb{H},\mathbb{S}}(z), \tau_{\mathbb{H},\mathbb{S}}(w)) = -\frac{1}{2} \log \frac{\operatorname{sh}(\frac{z-w}{2}) \operatorname{sh}(\frac{\bar{z}-\bar{w}}{2})}{\operatorname{sh}(\frac{\bar{z}-w}{2}) \operatorname{sh}(\frac{z-\bar{w}}{2})}. \quad (6.60)$$

### 6.2.3 Coupling of reverse dipolar SLE and Neumann GFF

We assume

$$\delta = -\delta_d + \nu\sigma_d, \quad \sigma = \sqrt{\kappa}\sigma_d, \quad \mathcal{H} = \mathcal{H}_s^*, \quad \Gamma = \Gamma_N. \quad (6.61)$$

This case corresponds to the third string in the Table 5.1 and sign ‘-’ in the pairs  $\pm$ . We have

$$\eta^{+\mathbb{H}}(z) = \frac{1}{\sqrt{\kappa}} \log z - \frac{(\kappa+6)}{4\sqrt{\kappa}} \log(1-z^2) - \frac{\nu}{2\sqrt{\kappa}} \operatorname{arcth} z + C^+, \quad (6.62)$$

$$\eta^{\mathbb{H}}(z) = \frac{2}{\sqrt{\kappa}} \log |z| - \frac{(\kappa+6)}{2\sqrt{\kappa}} \log |1-z^2| - \frac{\nu}{\sqrt{\kappa}} \operatorname{Re} \operatorname{arcth} z + C, \quad (6.63)$$

and

$$\begin{aligned} M_{1_t^{\mathbb{H}}}(z) &= G_t^{-1} \eta^{\mathbb{H}}(z) = \\ &= \frac{2}{\sqrt{\kappa}} \log |G_t^{\mathbb{H}}(z)| - \frac{(\kappa+6)}{2\sqrt{\kappa}} \log \left| 1 - \left( G_t^{\mathbb{H}}(z) \right)^2 \right| - \frac{\nu}{\sqrt{\kappa}} \operatorname{Re} \operatorname{arcth} G_t^{\mathbb{H}}(z) + \\ &+ \frac{\kappa+4}{2\sqrt{\kappa}} \log \left| \left( G_t^{\mathbb{H}} \right)'(z) \right| + C, \end{aligned} \quad (6.64)$$

in the half-plane chart. In the strip chart the covariance  $\Gamma_N$  and  $\eta$  are of the form

$$\begin{aligned} \Gamma_N^{\mathbb{S}}(z, w) &= \\ &= -\frac{1}{2} \log \left( \left( \operatorname{th} \frac{z}{2} - \operatorname{th} \frac{w}{2} \right) \left( \operatorname{th} \frac{z}{2} - \operatorname{th} \frac{\bar{w}}{2} \right) \left( \operatorname{th} \frac{\bar{z}}{2} - \operatorname{th} \frac{w}{2} \right) \left( \operatorname{th} \frac{\bar{z}}{2} - \operatorname{th} \frac{\bar{w}}{2} \right) \right) + \\ &+ \beta(z) + \beta(w), \end{aligned} \quad (6.65)$$

and

$$\eta^{\mathbb{S}}(z) = \frac{2}{\sqrt{\kappa}} \log \left| \operatorname{sh} \frac{z}{2} \right| + \frac{\nu}{2\sqrt{\kappa}} \operatorname{Re} z + C. \quad (6.66)$$

### 6.2.4 Coupling of forward dipolar SLE and combined Dirichlet-Neumann GFF

We assume

$$\delta = \delta_d + \nu\sigma_d, \quad \sigma = \sqrt{\kappa}\sigma_d, \quad \mathcal{H} = \mathcal{H}_s, \quad \Gamma = \Gamma_{DN} \quad (6.67)$$

(see Example 4.2). Below we conclude that the coupling is possible if and only if  $\kappa = 4$  and  $\nu = 0$ . This case is considered in [Kan13] and it is also a special case in [IK10].

In the strip chart, the covariance  $\Gamma_{DN}$  is of the form

$$\Gamma_{DN}^{\mathbb{S}}(z, w) = -\frac{1}{2} \log \frac{\operatorname{th} \frac{z-w}{4} \operatorname{th} \frac{\bar{z}-\bar{w}}{4}}{\operatorname{th} \frac{\bar{z}-w}{4} \operatorname{th} \frac{z-\bar{w}}{4}}, \quad z, w \in \mathbb{S} := \{z : 0 < \operatorname{Im} z < \pi\}. \quad (6.68)$$

The function  $\Gamma_{DN}^{\mathbb{S}}(z, w)$  satisfies the boundary conditions

$$\Gamma_{DN}^{\mathbb{S}}(x, w) \Big|_{x \in \mathbb{R}} = 0, \quad \partial_y \Gamma_{DN}^{\mathbb{S}}(x + iy, w) \Big|_{x \in \mathbb{R}, y = \pi} = 0, \quad (6.69)$$

and the symmetry property

$$\mathcal{L}_\sigma \Gamma_{DN}(z, w) = 0. \quad (6.70)$$

The coupling of GFF with this  $\Gamma$  and the dipolar SLE is geometrically motivated. Both zeros of  $\delta$  and  $\sigma$  are at the same boundary points where  $\Gamma_{DN}$  changes the boundary conditions from Dirichlet to Neumann. In the strip chart these points are  $-\infty$  and  $+\infty$ .

**Proposition 6.1.** *Let (6.67) is satisfied and let  $\eta$  be a pre-pre-Schwarzian (4.11). Then the coupling is possible only for  $\kappa = 4$  and  $\nu = 0$ .*

*Proof.* We use Theorem 5.2 and the strip chart. From (6.68) we obtain

$$\Gamma_{DN}^{++\mathbb{S}}(z, w) = -\frac{1}{2} \log \operatorname{th} \frac{z-w}{4}, \quad \Gamma_{DN}^{+-\mathbb{S}}(z, \bar{w}) = -\frac{1}{2} \log \operatorname{th} \frac{z-\bar{w}}{4}. \quad (6.71)$$

The relations (5.73) are satisfied. From (5.75) we find that

$$(\mathcal{L}_\sigma \eta^+)^{\mathbb{S}}(z) = j^{+\mathbb{S}}(z) = \frac{-i}{\operatorname{sh} \frac{z}{2}} + i\alpha, \quad \alpha \in \mathbb{R}. \quad (6.72)$$

Substituting in (5.69) gives

$$-i \frac{(\beta \sqrt{\kappa} - \alpha \nu) \operatorname{sh}^2 \frac{z}{2} + \nu \operatorname{sh} \frac{z}{2} - 2i\sqrt{\kappa} \mu \operatorname{ch} \frac{z}{2} (4 \operatorname{sh} \frac{z}{2} \alpha + (\kappa - 4))}{2\sqrt{\kappa} \operatorname{sh}^2 \frac{z}{2}} \equiv 0, \quad (6.73)$$

which is possible only if  $\kappa = 4$ ,  $\nu = 0$ ,  $\beta = 0$  and  $\mu = 0$  (the latter agrees with (5.84)).  $\square$

From (5.63) we obtain that

$$\eta^{+\mathbb{S}}(z) = \frac{i}{2} \log \operatorname{th} \frac{z}{4} + C^+, \quad (6.74)$$

and

$$\eta^{\mathbb{S}}(z) = -\arg \operatorname{cth} \frac{z}{4} + C. \quad (6.75)$$

We also present here the relations in the half-plane chart

$$\eta^{\mathbb{H}}(z) = -\arg \frac{z}{1 + \sqrt{1 - z^2}} + C, \quad (6.76)$$

$$\begin{aligned} \Gamma_{DN}^{\mathbb{H}}(z) &= \\ &= -\frac{1}{2} \log \frac{(z-w)(\bar{z}-\bar{w})(1-\bar{z}w + \sqrt{1-\bar{z}^2}\sqrt{1-w^2})(1-z\bar{w} + \sqrt{1-z^2}\sqrt{1-\bar{w}^2})}{(\bar{z}-w)(z-\bar{w})(1-zw + \sqrt{1-z^2}\sqrt{1-w^2})(1-\bar{z}\bar{w} + \sqrt{1-\bar{z}^2}\sqrt{1-\bar{w}^2})}. \end{aligned} \quad (6.77)$$

## 6.3 Radial Case

### 6.3.1 Radial Löwner equation

The radial Löwner equation was studied together with the chordal Löwner version.

Assume that both of the vector fields  $\delta$  and  $\sigma$  have zero at the same point  $b \in \mathcal{D}$  at the interior of  $\mathcal{D}$ :

$$\delta(b) = \sigma(b) = 0, \quad b \in \mathcal{D}. \quad (6.78)$$

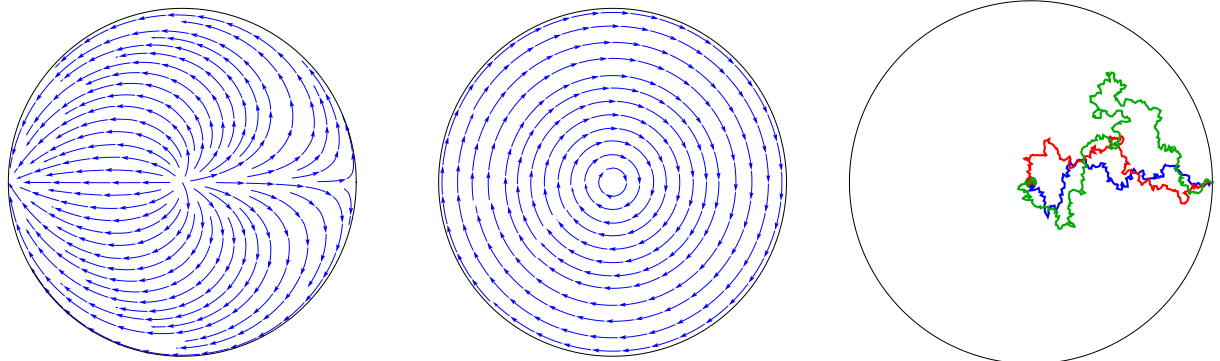
With the aid of the transforms  $\mathcal{R}$  and  $\mathcal{S}$  it is always possible to normalize  $\psi^{\mathbb{D}}(b) = 0$  in the unit disc chart or, equivalently,  $\psi^{\mathbb{H}}(b) = i$  in the half-plane chart. Thereby, in terms of basis vectors  $\ell_n$  we have

$$\begin{aligned} \sigma &= \sigma_{-1}(\ell_{-1} + \ell_1), \quad \sigma_{-1} \in \mathbb{R} \setminus \{0\}, \\ \delta &= \delta_{-2}(\ell_{-2} + \ell_0) + \delta_{-1}(\ell_{-1} + \ell_1), \quad \delta_{-2} \neq 0, \quad \delta_{-1} \in \mathbb{R}, \end{aligned} \quad (6.79)$$

Using the transforms  $\mathcal{V}$ ,  $\mathcal{D}$ , and  $\mathcal{T}$  we can normalize further and assume

$$\delta_r = 2(\ell_{-2} + \ell_0), \quad \sigma_r = -\ell_{-1} - \ell_1 \quad (6.80)$$

for the forward case.



(a) Flow lines of vector field  $\delta_r$ . (b) Flow lines of vector field  $\sigma_r$ . (c) 3 samples for radial SLE slits for  $\kappa = 2$  in the unit disk chart. The slits tend to the fixed point  $\psi^{\mathbb{D}}(b) = 0$ .

Figure 6.3: Flow lines of the radial vector field  $\delta_r$ ,  $\sigma_r$ , and corresponding slit samples in the unit disk chart.

It is natural to consider radial Löwner equation in the unit disk and logarithmic charts. We will define the logarithmic chart later and present first the relations in the unit disk chart. The vector fields have the form

$$\delta_r^{\mathbb{D}}(z) = 4z \frac{1+z}{1-z}, \quad \sigma_r^{\mathbb{D}}(z) = -2iz. \quad (6.81)$$

The Löwner equation in terms of  $G_t$  can be written as

$$\dot{G}_t^{\mathbb{D}}(z) = 4G_t^{\mathbb{D}}(z) \frac{1 + G_t^{\mathbb{D}}(z)}{1 - G_t^{\mathbb{D}}(z)} - 4iG_t^{\mathbb{D}}(z)\dot{u}_t. \quad (6.82)$$

The equation for  $H_s[\sigma]$  in the unit disk chart is

$$\dot{H}_s[\sigma]^{\mathbb{D}}(z) = -2iH_s[\sigma]^{\mathbb{D}}(z), \quad H_0[\sigma]^{\mathbb{D}}(z) = z, \quad z \in \mathbb{D}. \quad (6.83)$$

The solution is

$$H_s[\sigma]^{\mathbb{D}}(z) = e^{-2is}z. \quad (6.84)$$

Thus, the equation for  $g_t$  is

$$\begin{aligned} \dot{g}_t^{\mathbb{D}}(z) &= \left( \frac{1}{H_{u_t}[\sigma]^{\mathbb{D}'}} \left( 4H_{u_t}[\sigma]^{\mathbb{D}} \frac{1 + H_{u_t}[\sigma]^{\mathbb{D}}}{1 - H_{u_t}[\sigma]^{\mathbb{D}}} \right) \right) \circ g_t^{\mathbb{D}}(z) = \\ &= \frac{1}{e^{-2iu_t}} \left( e^{-2iu_t} g_t^{\mathbb{D}}(z) \frac{1 + e^{-2iu_t} g_t^{\mathbb{D}}(z)}{1 - e^{-2iu_t} g_t^{\mathbb{D}}(z)} \right) \end{aligned} \quad (6.85)$$

or

$$\dot{g}_t^{\mathbb{D}}(z) = 4g_t^{\mathbb{D}}(z) \frac{e^{2iu_t} + g_t^{\mathbb{D}}(z)}{e^{2iu_t} - g_t^{\mathbb{D}}(z)}. \quad (6.86)$$

We remark that the maps  $G_t^{\mathbb{D}}$  and  $g_t^{\mathbb{D}}$  possess the normalization conditions

$$G_t^{\mathbb{D}}(z) = ze^{4t-2iu_t} + O(z^2), \quad (6.87)$$

and

$$g_t^{\mathbb{D}}(z) = ze^{4t} + O(z^2). \quad (6.88)$$

These conditions uniquely fix the maps  $G_t$  and  $g_t$  for given  $\mathcal{K}_t$  if  $\psi^{\mathbb{D}}(\mathcal{K}_t)$  does not touch the origin  $\psi^{\mathbb{D}}(b) = 0$ .

The stochastic version is given in the Stratanovich form by

$$d^S G_t^{\mathbb{D}}(z) = 4G_t^{\mathbb{D}}(z) \frac{1 + G_t^{\mathbb{D}}(z)}{1 - G_t^{\mathbb{D}}(z)} dt - 2i\sqrt{\kappa} G_t^{\mathbb{D}}(z) d^S B_t. \quad (6.89)$$

The same equation in the Itô form is

$$d^{\text{Itô}} G_t^{\mathbb{D}}(z) = 4 \left( G_t^{\mathbb{D}}(z) \frac{1 + G_t^{\mathbb{D}}(z)}{1 - G_t^{\mathbb{D}}(z)} - \frac{1}{2} \kappa G_t^{\mathbb{D}}(z) \right) dt - 2i\sqrt{\kappa} G_t^{\mathbb{D}}(z) d^{\text{Itô}} B_t. \quad (6.90)$$

As well as for the dipolar case, in a more frequently used normalization, the same realations are

$$\delta^{\mathbb{D}}(z) = z \frac{1+z}{1-z} - ivz, \quad \sigma^{\mathbb{D}}(z) = -iz, \quad (6.91)$$

$$\dot{g}_t^{\mathbb{D}}(z) = g_t^{\mathbb{D}}(z) \frac{e^{iu_t} + g_t^{\mathbb{D}}(z)}{e^{iu_t} - g_t^{\mathbb{D}}(z)}, \quad (6.92)$$

$$d^S G_t^{\mathbb{D}}(z) = G_t^{\mathbb{D}}(z) \frac{1 + G_t^{\mathbb{D}}(z)}{1 - G_t^{\mathbb{D}}(z)} dt - i\sqrt{\kappa} G_t^{\mathbb{D}}(z) d^S B_t. \quad (6.93)$$



That can be obtained from (6.35) by the transform  $\mathcal{P}_c$  with  $c = 2$ .

We prefer the normalization only for universality (the invariant coefficients  $\delta_{-2} = 2$  and  $\sigma_{-1} = -1$  are the same in all cases in our frameworks).

In the half-plane chart, we have

$$\delta^{\mathbb{H}}(z) = 2 \left( \frac{1}{z} + z \right) - \nu(1 + z^2), \quad \sigma^{\mathbb{H}}(z) = -(1 + z^2), \quad (6.94)$$

$$H_s[\sigma]^{\mathbb{H}}(z) = \frac{z - \operatorname{tg} s}{1 + z \operatorname{tg} s}, \quad (6.95)$$

$$\dot{g}_t^{\mathbb{H}}(z) = \left( 1 + g_t^{\mathbb{H}}(z)^2 \right) \frac{2 + 2(\operatorname{tg} u_t) g_t^{\mathbb{H}}(z) + \nu(\operatorname{tg} u_t - g_t^{\mathbb{H}}(z))}{g_t^{\mathbb{H}}(z) - \operatorname{tg} u_t} \quad (6.96)$$

$$d^{\mathbb{S}} G_t^{\mathbb{H}}(z) = \left( \frac{1}{G_t^{\mathbb{H}}(z)} + G_t^{\mathbb{H}}(z) \right) dt - \nu(1 + G_t^{\mathbb{H}}(z)^2) dt - \sqrt{\kappa}(1 + G_t^{\mathbb{H}}(z)^2) d^{\mathbb{S}} B_t. \quad (6.97)$$

In a chart where the complete vector field  $\sigma$  is a constant, the relations are always specially simple. We see that for the examples of chordal case (the half-plane chart) and dipolar case (strip chart) in the previous two sections. The chart where radial field  $\sigma_r$  is a constant is called **logarithmic**. We denote it by  $\mathbb{L}$  and define by the transition map

$$\tau_{\mathbb{D},\mathbb{L}}(z) := e^{iz} : \mathbb{H} \rightarrow \mathbb{D}, \quad \tau_{\mathbb{L},\mathbb{D}}(z) = \tau_{\mathbb{D},\mathbb{L}}^{-1}(z) = -i \log z. \quad (6.98)$$

Thereby,

$$\tau_{\mathbb{H},\mathbb{L}}(z) = \tau_{\mathbb{H},\mathbb{D}} \circ \tau_{\mathbb{D},\mathbb{L}}(z) = \operatorname{tg} \frac{z}{2} : \mathbb{H} \rightarrow \mathbb{H}, \quad \tau_{\mathbb{L},\mathbb{H}}(z) = \tau_{\mathbb{H},\mathbb{L}}^{-1}(z) = 2 \operatorname{arctg} z, \quad (6.99)$$

The chart maps  $\psi^{\mathbb{H}}$ ,  $\psi^{\mathbb{D}}$ , and  $\psi^{\mathbb{S}}$ , we considered above, are global. It means that the maps are defined on entire  $\mathcal{D}$  and are single-valued. The map  $\psi^{\mathbb{L}}$  is not defined in a point of  $\mathcal{D}$  that is  $b$  in our normalization of the radial equation. Besides, the function  $\log$  is multivalued (ramified) and the upper half-plane (the image of  $\tau_{\mathbb{H},\mathbb{L}}$ ) contains infinite number of identical copies of the radial slit because

$$\tau_{\mathbb{L},\mathbb{H}}(z + 2\pi) = \tau_{\mathbb{L},\mathbb{H}}(z), \quad z \in \mathbb{H}. \quad (6.100)$$

The advantage of this chart is that the automorphisms  $H_t[\sigma_r]^{\mathbb{L}}$  induced by  $\sigma_r$  (see (1.13)) are horizontal translations because  $\sigma_r^{\mathbb{L}}(z)$  is a real constant. In the logarithmic char, we also have

$$\delta_r^{\mathbb{L}}(z) = 4 \operatorname{ctg} \frac{z}{2}, \quad \sigma_r^{\mathbb{L}}(z) = -2. \quad (6.101)$$

From this and the relations below it is observable that if one replace formally all hyperbolic functions in the dipolar case in the strip chart  $\mathbb{S}$  to the corresponding trigonometric functions then he obtain the relations for the radial equation in the logarithmic chart  $\mathbb{L}$ .

$$\dot{G}_t^{\mathbb{L}}(z) = 4 \operatorname{ctg} \frac{G_t^{\mathbb{L}}(z)}{2} - 2\dot{u}_t, \quad (6.102)$$

$$\dot{g}_t^{\mathbb{L}}(z) = 4 \operatorname{ctg} \left( \frac{g_t^{\mathbb{L}}(z)}{2} - u_t \right) \quad (6.103)$$

### 6.3.2 Coupling of forward radial SLE and Dirichlet GFF

We assume

$$\delta = \delta_r + \nu \sigma_r, \quad \sigma = \sqrt{\kappa} \sigma_r, \quad \mathcal{H} = \mathcal{H}_{s,b}, \quad \Gamma = \Gamma_D. \quad (6.104)$$

We define  $\mathcal{H}_{s,b}$  below. This case of the coupling with  $\nu = 0$  is considered in [KM12].

A naive calculation in this case gives a ramified function for  $\eta^\Psi(z)$  due a zero value of  $\sigma_r(z)$  in the denominator of (5.65) in a point inside  $\mathcal{D}$ . To handle this we have to step aside from working with the test functions from the space  $\mathcal{H}_s$ . We define the space  $\mathcal{H}_{s,b}$  as the image of  $\mathcal{H}_s$  with respect to the Lie derivative  $\mathcal{L}_{\sigma_r}$

$$\mathcal{H}_{s,b} := \mathcal{L}_{\sigma_r}(\mathcal{H}_s). \quad (6.105)$$

Equivalently, it consist of all function from  $\mathcal{H}_s$  that have the integral of  $f^{\mathbb{D}}(z)$  along all concentric circles in the unit disk chart equal to zero. Thereby, the dual space is bigger then  $\mathcal{H}'_s$  ( $\mathcal{H}'_s \subset \mathcal{H}'_{s,b}$ ) and in addition contains, for example,

$$\arg z \in \mathcal{H}'_{s,b}{}^{\mathbb{D}}. \quad (6.106)$$

In the logarithmic chart, the same functional can be represented as

$$\operatorname{Re} z \in \mathcal{H}'_{s,b}{}^{\mathbb{L}}. \quad (6.107)$$

Thus, the meaning of ramified expressions for  $\eta^\Psi(z)$  below can be understood in sense of elements of  $\mathcal{H}'_{s,b}$ .

We present here the expressions for  $\delta$ ,  $\sigma$ ,  $\Gamma_D$ ,  $\eta$  and  $M_{1_t}$  in three different charts: half-plane, the unit disk, and logarithmic, using the same method as before. The calculation are similar to the dipolar case. In fact, it is enough to change some signs and replace the hyperbolic functions by trigonometric. In contrast to the dipolar case,  $\eta$  is multiply defined in the half-plane and the unit disk-charts. From the heuristic point of view this is not an essential problem. In any chart  $\eta^\Psi(z)$  just changes its value only up to an irrelevant constant after the harmonic continuation around the point  $b$ .

In the half-plane chart, we have

$$-\sqrt{\kappa}(1+z^2) \partial_z \eta^{+\mathbb{H}}(z) + \mu (-\sqrt{\kappa}(1+z^2))' = \frac{-i}{z} + i\alpha, \quad (6.108)$$

$$\eta^{\mathbb{H}}(z) = \frac{-2}{\sqrt{\kappa}} \arg z - \frac{(\kappa-6)}{2\sqrt{\kappa}} \arg(1+z^2) - \frac{\nu}{\sqrt{\kappa}} \operatorname{Im} \operatorname{arctg} z + C, \quad (6.109)$$

$$\begin{aligned} M_{1_t}^{\mathbb{H}}(z) &= (G_t^{-1} * \eta)^{\mathbb{H}}(z) = \\ &= \frac{-2}{\sqrt{\kappa}} \arg G_t^{\mathbb{H}}(z) - \frac{(\kappa-6)}{2\sqrt{\kappa}} \arg(1+G_t^{\mathbb{H}}(z)^2) - \\ &\quad - \frac{\nu}{\sqrt{\kappa}} \operatorname{Im} \operatorname{arctg} z + \frac{\kappa-4}{2\sqrt{\kappa}} \arg G_t^{\mathbb{H}'}(z) + C \end{aligned} \quad (6.110)$$

analogously to (6.20).

The unit disk chart is defined in (1.4), and

$$\eta^{\mathbb{D}}(z) = \frac{-2}{\sqrt{\kappa}} \arg(1-z) - \frac{\kappa-6}{2\sqrt{\kappa}} \arg z + \frac{\nu}{2\sqrt{\kappa}} \log |z| + C, \quad (6.111)$$

$$\begin{aligned}
M_{1_t}^{\mathbb{D}}(z) &= (G_t^{-1} \ast \eta)^{\mathbb{D}}(z) = \\
&= \frac{-2}{\sqrt{\kappa}} \arg(1 - G_t^{\mathbb{D}}(z)) - \frac{\kappa - 6}{2\sqrt{\kappa}} \arg G_t^{\mathbb{D}}(z) + \frac{\nu}{2\sqrt{\kappa}} \log |G_t^{\mathbb{D}}(z)| + \frac{\kappa - 4}{2\sqrt{\kappa}} \arg G_t^{\mathbb{D}'}(z) + C,
\end{aligned} \tag{6.112}$$

$$\Gamma_D^{\mathbb{D}}(z, w) = \Gamma_D^{\mathbb{H}}(\tau_{\mathbb{H}, \mathbb{D}}(z), \tau_{\mathbb{H}, \mathbb{D}}(w)) = -\frac{1}{2} \log \frac{(z-w)(\bar{z}-\bar{w})}{(\bar{z}-w)(z-\bar{w})}. \tag{6.113}$$

The relations for the radial SLE in the logarithmic chart can be easily obtained from the dipolar SLE in the strip chart just by replacing the hyperbolic functions by their trigonometric analogs

$$\Gamma_D^{++\mathbb{L}}(z, w) = -\frac{1}{2} \log \sin \frac{z-w}{2}, \quad \Gamma_D^{+-\mathbb{L}}(z, \bar{w}) = -\frac{1}{2} \log \sin \frac{z-\bar{w}}{2}, \tag{6.114}$$

$$\Gamma_D^{\mathbb{L}}(z, w) = -\frac{1}{2} \log \frac{\sin(\frac{z-w}{2}) \sin(\frac{\bar{z}-\bar{w}}{2})}{\sin(\frac{\bar{z}-w}{2}) \sin(\frac{z-\bar{w}}{2})}, \tag{6.115}$$

$$\eta^{\mathbb{L}}(z) = \frac{-2}{\sqrt{\kappa}} \arg \sin \frac{z}{2} - \frac{\nu}{2\sqrt{\kappa}} \operatorname{Im} z + C, \tag{6.116}$$

$$\begin{aligned}
M_{1_t}^{\mathbb{L}}(z) &= (G_t^{-1} \ast \eta)^{\mathbb{L}}(z) = \\
&= \frac{-2}{\sqrt{\kappa}} \arg \sin \frac{G_t^{\mathbb{L}}(z)}{2} - \frac{\nu}{2\sqrt{\kappa}} \operatorname{Im} G_t^{\mathbb{L}}(z) + \frac{\kappa - 4}{2\sqrt{\kappa}} \arg G_t^{\mathbb{L}'}(z) + C.
\end{aligned} \tag{6.117}$$

This relations above coincide up to a constant with the analogous ones established in [KM12].

We remark that for  $\kappa = 6$  we can use the usual space  $\mathcal{H}_s$  instead of  $\mathcal{H}_{s,b}$ .

### 6.3.3 Coupling of reverse radial SLE and Neumann GFF

We assume

$$\delta = -\delta_r + \nu \sigma_r, \quad \sigma = \sqrt{\kappa} \sigma_r, \quad \mathcal{H} = \mathcal{H}_{s,b}^*, \quad \Gamma = \Gamma_D, \tag{6.118}$$

where

$$\mathcal{H}_{s,b}^* := \left\{ f \in \mathcal{H}_{s,b} : \int_{D^\psi} f^\psi(z) l(dz) = 0 \right\}. \tag{6.119}$$

We use the space  $\mathcal{H}_{s,b}^*$  but not  $\mathcal{H}_s^*$  because of the same reasons as in the previous subsection.

Analogous to the previous cases we have in the half-plane chart

$$\eta^{+\mathbb{H}}(z) = \frac{1}{\sqrt{\kappa}} \log z - \frac{(\kappa + 6)}{4\sqrt{\kappa}} \log(1 + z^2) - \frac{\nu}{2\sqrt{\kappa}} \operatorname{arctg} z + C^+, \tag{6.120}$$

$$\eta^{\mathbb{H}}(z) = \frac{2}{\sqrt{\kappa}} \log |z| - \frac{(\kappa + 6)}{2\sqrt{\kappa}} \log |1 - z^2| - \frac{\nu}{\sqrt{\kappa}} \operatorname{Re} \operatorname{arctg} z + C, \tag{6.121}$$

$$\begin{aligned}
M_{1_t}^{\mathbb{H}}(z) &= G_t^{-1} * \eta^{\mathbb{H}}(z) = \\
&= \frac{2}{\sqrt{\kappa}} \log |G_t^{\mathbb{H}}(z)| - \frac{(\kappa+6)}{2\sqrt{\kappa}} \log \left| 1 - \left( G_t^{\mathbb{H}}(z) \right)^2 \right| - \frac{\nu}{\sqrt{\kappa}} \operatorname{Re} \operatorname{arctg} G_t^{\mathbb{H}}(z) + \\
&+ \frac{\kappa+4}{2\sqrt{\kappa}} \log \left| G_t^{\mathbb{H}'}(z) \right| + C.
\end{aligned} \tag{6.122}$$

In the logarithmic chart the same expressions are

$$\Gamma_N^{\mathbb{L}}(z, w) = -\frac{1}{2} \log \left( \sin \frac{z-w}{2} \sin \frac{z-\bar{w}}{2} \sin \frac{\bar{z}-w}{2} \sin \frac{\bar{z}-\bar{w}}{2} \right) + \beta(z) + \beta(w), \tag{6.123}$$

$$\eta^{+\mathbb{L}}(z) = \frac{1}{\sqrt{\kappa}} \log \sin \frac{z}{2} - \frac{\nu}{4\sqrt{\kappa}} z, \tag{6.124}$$

$$\eta^{\mathbb{L}}(z) = \frac{2}{\sqrt{\kappa}} \log \left| \sin \frac{z}{2} \right| - \frac{\nu}{2\sqrt{\kappa}} \operatorname{Re} z. \tag{6.125}$$

The function  $\eta^{\mathbb{L}}(z)$  possesses the Neumann boundary condition along all the boundary

$$\left. \partial_y \eta^{\mathbb{L}}(x+iy, w) \right|_{y=0} = -\frac{\nu}{2\sqrt{\kappa}}, \quad x \in \mathbb{R}, \quad w \in \mathbb{C}, \tag{6.126}$$

In the unit disc chart  $\eta$  takes the form:

$$\eta^{\mathbb{D}}(z) = \frac{2}{\sqrt{\kappa}} \log |1-z| + \frac{\kappa+6}{2\sqrt{\kappa}} \log |z| - \frac{\nu}{2\sqrt{\kappa}} \arg z + C, \tag{6.127}$$

If  $\nu = 0$  we do not need to introduce the space  $\mathcal{H}_{s,b}$  and can use  $\mathcal{H}_s^*$  because there is no branch point at  $b$ .

### 6.3.4 Coupling with twisted GFF

We assume

$$\delta = \delta_r + \nu \sigma_r, \quad \sigma = \sqrt{\kappa} \sigma_r, \quad \mathcal{H} = \mathcal{H}_{s,b}^{\pm}, \quad \Gamma = \Gamma_{\text{tw},b}. \tag{6.128}$$

We define  $\mathcal{H}_{s,b}^{\pm}$  and  $\Gamma_{\text{tw}}$  below.

This model is similar to the one from Section 6.2.4. At the algebraic level, as it will be shown below, it is enough to replace formally all hyperbolic functions in the dipolar case in the strip chart  $\mathbb{S}$  to the corresponding trigonometric functions in order to obtain the relations for the radial SLE in the logarithmic chart  $\mathbb{L}$ . But at the analytic level, we have to consider the correlation functions which are doubly defined on  $\mathcal{D}$  and change their sign to the opposite while being turned once around the interior point  $b$ . This construction was considered before and called ‘twisted CFT’ as we were informed by Num-Gyu Kang.

Let  $\mathcal{D}_b^{\pm}$  be the double cover of  $\mathcal{D} \setminus \{b\}$  and let  $\mathcal{H}_{s,b}^{\pm}$  be the space of test functions  $f: \mathcal{D}_b^{\pm} \rightarrow \mathbb{R}$  as in Section 4.1 with an extra condition  $f(z_1) = -f(z_2)$ , where  $z_1$  and  $z_2$  are two points of  $\mathcal{D}_b^{\pm}$  corresponding to the same point of  $\mathcal{D} \setminus \{b\}$ . Thus, in the logarithmic chart, we have

$$f^{\mathbb{L}}(z) = f^{\mathbb{L}}(z+4\pi k) = -f^{\mathbb{L}}(z+2\pi k), \quad k \in \mathbb{Z}, \quad z \in \mathbb{H}. \tag{6.129}$$

Such functions are  $4\pi$ -periodic and  $2\pi$ -antiperiodic. In particular,  $f^{\mathbb{L}}$  is not of compact support in the logarithmic chart, but we require that the support is compact in  $\mathcal{D}_b^{\pm}$ . The dual space  $\mathcal{H}_{s,b}^{\pm}$  also consist of  $4\pi$ -periodic and  $2\pi$  untiperic functions.

We define the covariance functional by

$$\Gamma_{\text{tw},b}^{\mathbb{L}}(z, w) = -\frac{1}{2} \log \frac{\text{tg} \frac{z-w}{4} \text{tg} \frac{\bar{z}-\bar{w}}{4}}{\text{tg} \frac{\bar{z}-w}{4} \text{tg} \frac{z-\bar{w}}{4}}, \quad z, w \in \mathbb{H}, \quad z \neq w + 2\pi k, \quad k \in \mathbb{Z}. \quad (6.130)$$

in the logarithmic chart. Observe that

$$\Gamma_{\text{tw},b}^{\mathbb{L}}(z, w) = \Gamma_{\text{tw},b}^{\mathbb{L}}(z + 4\pi k, w) = -\Gamma_{\text{tw},b}^{\mathbb{L}}(z + 2\pi k, w), \quad k \in \mathbb{Z}, \quad z, w \in \mathbb{H}. \quad (6.131)$$

In the unit disk chart the covariance  $\Gamma_{\text{tw}}^{\mathbb{D}}$  is of the form

$$\Gamma_{\text{tw},b}^{\mathbb{D}}(z, w) = -\frac{1}{2} \log \frac{(\sqrt{z} - \sqrt{w})(\sqrt{\bar{z}} - \sqrt{\bar{w}})(\sqrt{z} + \sqrt{\bar{w}})(\sqrt{\bar{z}} - \sqrt{w})}{(\sqrt{z} + \sqrt{w})(\sqrt{\bar{z}} + \sqrt{\bar{w}})(\sqrt{z} - \sqrt{\bar{w}})(\sqrt{\bar{z}} + \sqrt{w})}, \quad (6.132)$$

or in the half-plane chart it is of the form

$$\Gamma_{\text{tw},b}^{\mathbb{H}}(z) = -\frac{1}{2} \log \frac{(z-w)(\bar{z}-\bar{w})(1+\bar{z}w + \sqrt{1+\bar{z}^2}\sqrt{1+w^2})(1+z\bar{w} + \sqrt{1+z^2}\sqrt{1+\bar{w}^2})}{(\bar{z}-w)(z-\bar{w})(1+z\bar{w} + \sqrt{1+z^2}\sqrt{1+w^2})(1+\bar{z}\bar{w} + \sqrt{1+\bar{z}^2}\sqrt{1+\bar{w}^2})}. \quad (6.133)$$

It is doubly defined because of the square root and the analytic continuation around the center changes its sign.

The covariance  $\Gamma_{\text{tw},b}^{\mathbb{L}}$  satisfies the Dirichlet boundary conditions and tends to zero as one of the variables tends to the center point  $b$  ( $\infty$  in the  $\mathbb{L}$  chart)

$$\Gamma_{\text{tw},b}^{\mathbb{L}}(x, w) \Big|_{x \in \mathbb{R}} = 0, \quad \lim_{y \rightarrow +\infty} \Gamma_{\text{tw}}^{\mathbb{L}}(x + iy, w) = 0, \quad x \in \mathbb{R}, \quad w \in \mathbb{H}; \quad (6.134)$$

$$\Gamma_{\text{tw},b}^{\mathbb{D}}(z, w) \Big|_{|z|=1} = 0, \quad \lim_{z \rightarrow 0} \Gamma_{\text{tw}}^{\mathbb{D}}(z, w) = 0, \quad w \in \mathbb{D}. \quad (6.135)$$

The  $\sigma$ -symmetry property

$$\mathcal{L}_{\sigma_r} \Gamma_{\text{tw}}(z, w) = 0 \quad (6.136)$$

holds.

We call the GFF  $\Phi(\mathcal{H}_{s,b}^{\pm}, \Gamma_{\text{tw},s})$  **twisted Gaussian free field**  $\Phi_{\text{tw}}$ . Similarly to the dipolar case in Section 6.2.4 the following proposition can be proved.

**Proposition 6.2.** *With the assumptions as in (6.128) the twisted GFF  $\Phi_{\text{tw}}$  can be coupled if and only if  $\kappa = 4$  and  $\nu = 0$ .*

The *proof* in the logarithmic chart actually repeats the proof of Proposition 6.1.

We give here the expressions for  $\eta$  in the logarithmic, unit-disk and half-plane charts:

$$\eta^{\mathbb{L}}(z) = -2 \arg \text{tg} \frac{4}{z} + C. \quad (6.137)$$

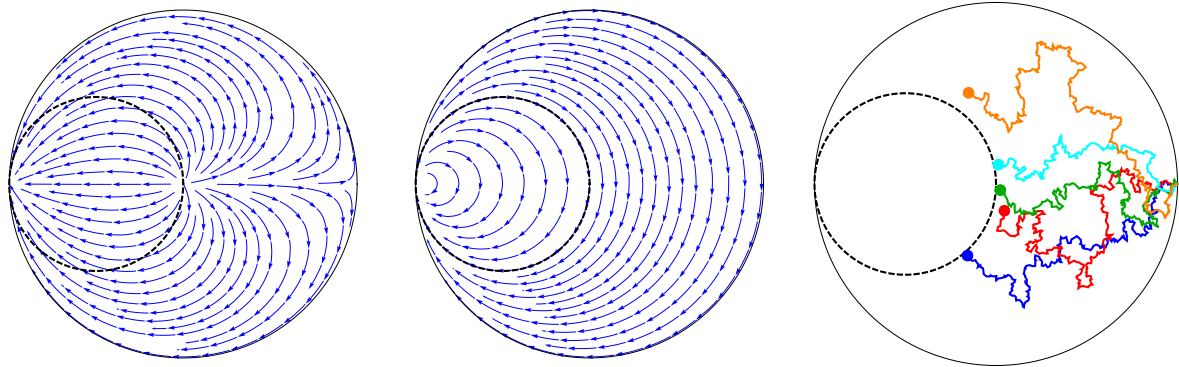
$$\eta^{\mathbb{D}}(z) = -2 \arg \frac{1 - \sqrt{z}}{1 + \sqrt{z}} + C = 4 \text{Im} \text{arctgh} \sqrt{z} + C. \quad (6.138)$$

$$\eta^{\mathbb{H}}(z) = -2 \arg \frac{z}{1 + \sqrt{1 + z^2}} + C. \quad (6.139)$$

From this relation it is clear that  $\eta$  is antiperiodic.

Established  $\eta^{\mathbb{L}}$  also possesses the property (6.129). Thus, the construction of the level (flow) lines, which we discussed in the introduction to Chapter 5, can be performed for both layers simultaneously and the lines will be identical. In particular, this means that the line can turn around the central point and appears in the second layer but can not intersect itself. This agrees with the property of the SLE slit which avoids self-intersections.

## 6.4 Chordal case with a fix time change



(a) Flow lines of vector field  $\delta$ . (b) Flow lines of vector field  $\sigma$ . (c) 5 samples for the SLE slits for  $\kappa = 2$  in the unit disk chart. The slits tend to a random point not far from the boundary of the invariant domain  $\mathcal{J}$ .

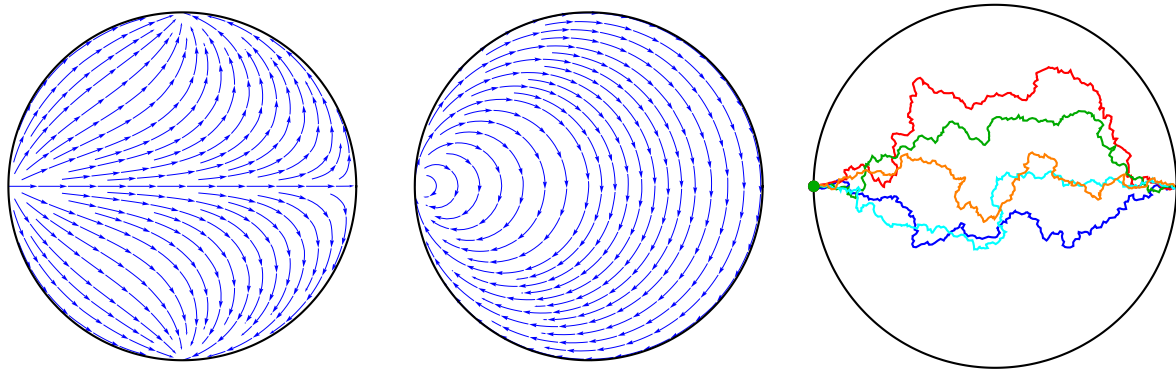
Figure 6.4: Flow lines of the vector fields  $\delta$  and  $\sigma$  from (6.140), and corresponding  $(\delta, \sigma)$ -SLE slit samples for  $\xi = 1$  in the unit disk chart. The dashed line in the boundary of the invariant domain  $\mathcal{J}$ .

We assume

$$\delta = \pm 2\ell_{-2} + 2\xi\ell_0, \quad \sigma = -\sqrt{\kappa}\ell_{-1}, \quad \xi \in \mathbb{R} \setminus \{0\}. \quad (6.140)$$

We consider the forward case ('+' in ' $\pm$ ' pair) first. The stochastic equation with such parameters appeared in Theorem 1.4 and Theorem 5.3. We do not consider deterministic Löwner chain, because only stochastic version is motivated by these theorems. According to the Theorem 1.4 this choice of  $\delta$  and  $\sigma$  is equivalent to the chordal for any  $\kappa > 0$  if we do a fixed time reparametrization and a scale transform. But this and chordal cases are not essentially equivalent in sense described in Section 1.2.3. The stochastic equation in the half-plane chart is

$$d^{\mathbb{S}} G_t^{\mathbb{H}}(z) = \frac{2}{G_t^{\mathbb{H}}(z)} dt + 2\xi G_t^{\mathbb{H}}(z) dt - \sqrt{\kappa} 1 d^{\mathbb{S}} B_t. \quad (6.141)$$



(a) Flow lines of vector field  $\delta$ . (b) Flow lines of vector field  $\sigma$ . (c) 5 samples for the SLE slits for  $\kappa = 2$ . The slits are of the same law as chordal in Fig. 6.1.

Figure 6.5: Vector fields (6.140) and corresponding  $(\delta, \sigma)$ -SLE slit samples for  $\xi = -1$  in the unit disk chart.

We explain now the relation to the chordal case described in Section 6.1.1. Let  $\xi \in \mathbb{R} \setminus \{0\}$  and let  $\{\tilde{G}_{\tilde{t}}\}_{t \in [0, +\infty)}$  is the chordal stochastic flow (chordal SLE (6.50)). Define

$$\tilde{G}_{\tilde{t}}^{\mathbb{H}}(z) = e^{2\xi\tilde{t}} G_{\lambda(\tilde{t})}^{\mathbb{H}}(z) \tag{6.142}$$

in the half-plane chart and assume that

$$\begin{aligned} \lambda(\tilde{t}) &:= \frac{1 - e^{-4\xi\tilde{t}}}{4\xi}; \\ \lambda : [0, +\infty) &\rightarrow [0, (4\xi)^{-1}), \quad \xi > 0; \\ \lambda : [0, +\infty) &\rightarrow [0, +\infty), \quad \xi < 0. \end{aligned} \tag{6.143}$$

This choice of  $\lambda$  corresponds to  $c_{\tilde{t}} = -2\xi\tilde{t}$  in Theorem 1.4. We notice that the time reparametrization is not random.

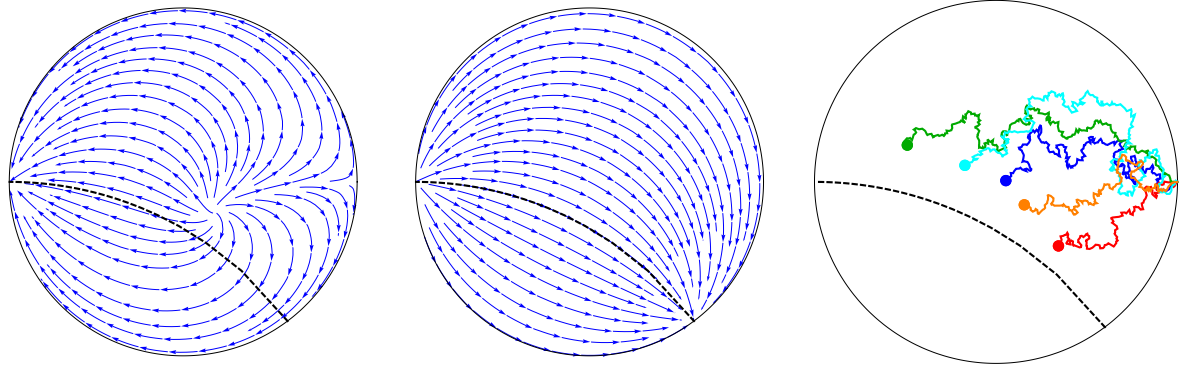
The flow  $\{\tilde{G}_{\tilde{t}}\}_{t \in [0, +\infty)}$  satisfies the autonomous equation (1.104) with  $\delta$  and  $\sigma$  from (6.140), that are vector fields from the second string of Table 5.1 and a special case of (1.144) with  $x_{\tilde{t}} = -4\xi e^{2c_{\tilde{t}}}$  and  $y_{\tilde{t}} = 0$ .

There is a common zero of  $\delta$  and  $\sigma$  at infinity in the half-plane chart and at  $z = -1$  in the unit disk chart, so the infinity is a stable point:  $\tilde{G}_{\tilde{t}}^{\mathbb{H}} : \infty \rightarrow \infty$ . But in contrast to the chordal case the coefficient at  $z^1$  in the Laurent series is not 1 but  $e^{2\xi\tilde{t}}$ .

The vector field  $\delta$  is of radial type if  $\xi > 0$ , and of dipolar type if  $\xi < 0$ . In the second case the equation induces exactly the same measure as the chordal stochastic flow but with a different time parametrization. If  $\xi > 0$  the measures also coincide when the chordal stochastic flow is stopped at the time  $t = (4\xi)^{-1}$ .

Due to this this observation it is reasonable to expect that the Dirichlet GFF ( $\mathcal{H} = \mathcal{H}_S$  and  $\Gamma = \Gamma_D$ ) coupled with such kind of  $(\delta, \sigma)$ -SLE is the same as in the chordal case, because it is supposed to induce the same random law of the flow lines. Indeed,  $\sigma$  from (6.140) coincides with that from the chordal case, hence,  $\eta$ , defined by (5.64), with  $\alpha = 0$  (see the table) also coincides with (6.21) with  $\nu = 0$ . Thus, the martingales are the same as in the chordal case. The same observation can be made in the reverse case ('-' in ' $\pm$ ' pair) and Neumann GFF ( $\mathcal{H} = \mathcal{H}_S^*$  and  $\Gamma = \Gamma_N$ ).

## 6.5 The case with one fixed point



(a) Flow lines of vector field  $\delta$ . (b) Flow lines of vector field  $\sigma$ . (c) 5 slits samples for  $(\delta, \sigma)$ -SLE. The slits tends to a random point inside the disk not far from the boundary of  $\tilde{\mathcal{J}}$

Figure 6.6: Flow lines of vector field  $\delta$ ,  $\sigma$  from (6.144) and corresponding slit samples in the unit disk chart. The dashed line is the boundary of the invariant domain  $\tilde{\mathcal{J}}$ .

We assume

$$\delta = \pm 2\ell_{-2} + \kappa\ell_{-1} \pm 2\xi\ell_0, \quad \sigma = -\sqrt{\kappa}(\ell_{-1} + 2\ell_0), \quad \xi \in \mathbb{R}, \quad \kappa > 0. \quad (6.144)$$

These vector fields have a common zero  $b$  at the infinity,  $\psi^{\mathbb{H}}(b) = \infty$ , in the half-plane chart. Thereby,  $b$  is a fixed point ( $G_t(b) = b$ ) of the map  $G_t$  for  $t \in [0, +\infty]$ .

As well as in the previous section we, consider the forward case ('+' in ' $\pm$ ' pair) first. There is also a mirror case

$$\delta = \pm 2\ell_{-2} - \kappa\ell_{-1} \pm 2\xi\ell_0, \quad \sigma = -\sqrt{\kappa}(\ell_{-1} - 2\ell_0), \quad \xi \in \mathbb{R}, \quad \kappa > 0. \quad (6.145)$$

that can be considered analogously.

The stochastic equation with such parameters appeared at the third case in Theorem 1.4. The corresponding stochastic equation

$$d^S G_t^{\mathbb{H}}(z) = \left( \frac{2}{G_t^{\mathbb{H}}(z)} + \kappa + 2\xi G_t^{\mathbb{H}}(z) \right) dt - \sqrt{\kappa} \left( 1 + 2G_t^{\mathbb{H}}(z) \right) d^S B_t, \quad (6.146)$$

Can be obtained for the chordal equation after a time change  $\lambda_{\tilde{t}} = e^{4\xi\tilde{t} - 4\sqrt{\kappa}\tilde{B}_{\tilde{t}}}$  and a multiplication on  $e^{2\xi\tilde{t} - 2\sqrt{\kappa}\tilde{B}_{\tilde{t}}}$ .

On the other hand, the case form the 4th string in Table 5.1 is essentially equivalent to this. Indeed, let is apply a transform  $\mathcal{R}_c$  with  $c = -1$  which corresponds to the Möbious automorphism

$$H_{-1}[\ell_1]: \mathcal{D} \rightarrow \mathcal{D} \quad (6.147)$$

having the form

$$H_{-1}[\ell_1]^{\mathbb{H}}(z) = \frac{z}{1+z}. \quad (6.148)$$



in the half-plane chart. It maps the fixed point  $z = \infty$  to  $z = 1$  in the half-plane chart and keeps the origin and the normalization (6.10) unchanged. It results in

$$\begin{aligned}\tilde{G}_t &:= H_{-1}[\ell_1] \circ G_t \circ H_{-1}[\ell_1]^{-1}, \\ \tilde{\delta}^{\mathbb{H}}(z) &:= H_{-1}[\ell_1]_* \delta^{\mathbb{H}}(z) = \frac{2}{z} + \kappa - 6 + 2(3 - \kappa + \xi)z + (-2 + \kappa - 2\xi)z^2, \\ \tilde{\sigma}^{\mathbb{H}}(z) &:= H_{-1}[\ell_1]_* \sigma^{\mathbb{H}}(z) = -\sqrt{\kappa}(1 - z^2).\end{aligned}\quad (6.149)$$

That corresponds to

$$\begin{aligned}\tilde{\delta} &= 2\ell_{-2} + (\kappa - 6)\ell_{-1} + 2(3 - \kappa + \xi)\ell_0 + (-2 + \kappa - 2\xi)\ell_1, \quad \xi \in \mathbb{R}, \\ \tilde{\sigma} &= -\sqrt{\kappa}(\ell_{-1} - \ell_1),\end{aligned}\quad (6.150)$$

which is exactly the vector fields  $\delta$  and  $\sigma$  from the 4th string in Table 5.1. The 5th string corresponds to the mirror case, for which the point  $z = 1$  is fixed.

We do not consider deterministic Löwner chain for (6.144), because only stochastic version is motivated by Theorems 5.3 and 1.4. We notice that the subsurface  $\tilde{\mathcal{J}} \subset \mathcal{D}$  defined in the half-plane chart by

$$\psi^{\mathbb{H}}(\tilde{\mathcal{J}}) = \{z \in \mathbb{H} : \operatorname{Re}(z) > -\frac{1}{2}\} \quad (6.151)$$

is invariant ( $G_t^{-1}(\tilde{\mathcal{J}}) \subset \tilde{\mathcal{J}}$ ) if and only if  $\xi \geq \kappa - 4$ . In order to see this, it is enough to calculate the real part of

$$\delta^{\mathbb{H}}(z) = \frac{2}{z} + \kappa + 2\xi z, \quad \sigma^{\mathbb{H}}(z) = -\sqrt{\kappa}(1 + 2z), \quad (6.152)$$

which are actually the horizontal components of the vector fields on the boundary of  $\psi^{\mathbb{H}}(\tilde{\mathcal{J}})$  in  $\mathbb{H}$ ,  $\{z \in \mathbb{H} : \operatorname{Re}(z) = -\frac{1}{2}\}$ ,

$$\begin{aligned}\operatorname{Re}\left(\tilde{\delta}^{\mathbb{H}}\left(-\frac{1}{2} + ih\right)\right) &= \operatorname{Re}\left(\frac{2}{-\frac{1}{2} + ih} + \kappa + 2\xi\left(-\frac{1}{2} + ih\right)\right) = \\ &= -\frac{1}{h^2 + \frac{1}{4}} + \kappa - \xi,\end{aligned}\quad (6.153)$$

$$\operatorname{Re}\left(\tilde{\sigma}^{\mathbb{H}}\left(-\frac{1}{2} + ih\right)\right) = \operatorname{Re}\left(\sqrt{\kappa}\left(1 + 2\left(-\frac{1}{2} + ih\right)\right)\right) = 0, \quad h > 0.$$

The first number is negative for all values of  $h$  if and only if  $\xi \geq \kappa - 4$ .

We remark that the  $H_{-1}[\ell_1]$ -transform has the invariant subsurface  $\tilde{\mathcal{J}} := H_{-1}[\ell_1](\tilde{\mathcal{J}}) \subset \mathcal{D}$  for the  $(\delta, \sigma)$ -SLE above, which is an upper half of the unit disk

$$\psi^{\mathbb{H}}(\tilde{\mathcal{J}}) = \{z \in \mathbb{H} : |z| < 1\} \quad (6.154)$$

Similarly to the previous section it is reasonable to expect that  $\eta$  for the coupling with the Dirichlet GFF is the same as in the chordal case, because it is supposed to induce the same random law of the flow lines. Indeed, the solution to (5.63), with  $\sigma$  and  $\alpha$  as in the 5<sup>th</sup> string of the table, is

$$\eta^{+\mathbb{H}}(z) = \frac{i}{\sqrt{\kappa}} \log z + i \frac{\kappa - 6}{2\sqrt{\kappa}} \arg(1 - z) + C^+. \quad (6.155)$$

Thus,

$$\eta^{\mathbb{H}}(z) = \frac{-2}{\sqrt{\kappa}} \arg z - \frac{\kappa - 6}{\sqrt{\kappa}} \arg(1 - z) + C. \quad (6.156)$$

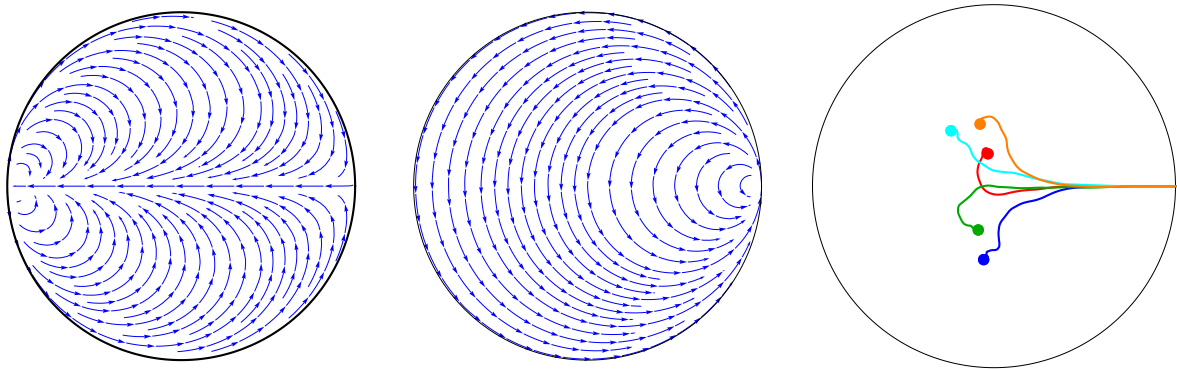
After the  $r_{-1}$ -transform for  $\tilde{\delta}$  and  $\tilde{\sigma}$ , we have

$$\tilde{\eta}^{\mathbb{H}}(z) = \frac{-2}{\sqrt{\kappa}} \arg z + C. \quad (6.157)$$

The last relation coincides with (6.21) with  $\nu = 0$ . We remind that  $\Gamma_D$  is invariant under Möbius transforms, in particular, under  $r_{-1}$ .

The analogous propositions are true for the reverse case and Neumann GFF.

## 6.6 Degenerate case



(a) Flow lines of vector field  $\delta$ . (b) Flow lines of vector field  $\sigma$ . (c) 5 samples for the degenerate SLE slits. The slits look smooth and tend to a random point inside the disk. All slits are closed to the trivial straight line for small  $t$ .

Figure 6.7: Vector fields (6.160) and corresponding  $(\delta, \sigma)$ -SLE slit samples in the unit disk chart.

In this section, we consider a special case when  $\sigma(a) = 0$ :

$$\begin{aligned} \delta &= \delta_{-2}l_{-2} + \delta_{-1}l_{-1} + \delta_0l_0 + \delta_1l_1, & \delta_{-2}, \delta_{-1}, \delta_0, \delta_1 &\in \mathbb{R}, & \delta_{-2} &\neq 0 \\ \sigma &= \sigma_0l_0 + \sigma_1l_1, & \sigma_0, \sigma_1 &\in \mathbb{R}, & \sigma_{-1} &\neq 0, \end{aligned} \quad (6.158)$$

We call this choice **degenerate Löwner equation**. This case was excluded above because the most part of propositions such as Theorem 1.1 and 1.3 fails and we can not construct a bridge from well-studied classical Löwner equations to this one as above. In particular, it is not possible to show that the hulls  $\{\mathcal{K}_t\}_{t \in [0, +\infty)}$  are curve generated using the same methods. However, we expect that the hulls are smooth curves for continuous driving functions. We do not present here any systematic investigation of degenerate case. Instead, we consider some special cases and force the methods of numerical simulation considered in Chapter 2 for the stochastic version.

If we assume, for example,

$$\delta = -2\ell_{-2}, \quad \sigma = \ell_0 \tag{6.159}$$

then the chain is a composition of  $H_t[-2\ell_{-2}]$  and some Möbious automorphism. Thus, the hull is trivial, it is just a vertical straight line segment from the origin in the half-plane chart.

A more interesting case is

$$\delta = -2\ell_{-2}, \quad \sigma = \ell_1. \tag{6.160}$$

A numerical simulation for  $u_t = B_t$  is given in the fig. 6.7.

**Remark 6.1.** *The  $(\delta, \sigma)$ -SLE with (6.160) induces a random law on **smooth** planar curves that possesses the property of conformal invariance and a version of Markov property. There is no contradiction with the known fact that conformal invariance and Markov property necessary leads to fractional SLE curves because we relaxed the condition that fixes the end of the curve.*

For other choices of degenerate  $\delta$  and  $\sigma$  gives similar pictures or trivial (not random) slits.



# Appendix A

## Some relations from stochastic calculus

We refer to [Oks14], [Pro04], [Gar82] for the definition of Itô and Stratonovich integrals and others for details.

Stochastic differential equations in Stratonovich of the form

$$d^S X_t = a_t dt + b_t d^S B_t \quad (\text{A.1})$$

is by the definition a shorter version of the Stratonovich integral equations

$$\int_0^T d^S X_t = \int_0^T a_t dt + \int_0^T b_t d^S B_t. \quad (\text{A.2})$$

And the same for Itô differential and integral. We use notations  $d^S$  and  $d^{\text{Itô}}$  for these cases correspondingly. The advantage of the Stratonovich form is that the usual rules of differentiation are satisfied. The advantage of the Itô form appears in the working with martingales.

We do not use differential equations that contain both Itô and Stratonovich differential in this paper. Instead, we use the following relation between the integrals

$$\int_0^T F(X_t, t) d^S B_t = \int_0^T F(X_t, t) d^{\text{Itô}} B_t + \frac{1}{2} \int_0^T b_t \partial_1 F(X_t, t) dt. \quad (\text{A.3})$$

The last term can also be expressed in terms of covariance

$$\int_0^T b_t \partial_1 F(X_t, t) dt = \langle F(X_T), B_T \rangle. \quad (\text{A.4})$$

For example to obtain (1.106) from 1.104 we assume

$$X_t := G_t(z), \quad b_t := \sigma(G_t(z)), \quad F(x_t, t) := \sigma(X_t) = \sigma(G_t(z)). \quad (\text{A.5})$$

Then

$$\partial_1 F(X_t, t) = \sigma'(G_t(z)), \quad (\text{A.6})$$

and

$$\int_0^T \sigma(G_t(z)) d^S B_t = \int_0^T \sigma(G_t(z)) d^{\text{It}\hat{o}} B_t + \frac{1}{2} \int_0^T \sigma(G_t(z)) \sigma'(G_t(z)) dt. \quad (\text{A.7})$$

It is enough now to add  $\int_0^T \delta(G_t(z)) dt$  to both parts to obtain the right-hand sides of the integral forms of (1.106) and (1.104).

We also used in this paper that for any monotonic continuously differentiable function  $\lambda : [0, \tilde{T}] \rightarrow [0, T]$

$$\tilde{B}_{\tilde{T}} := \int_0^{\tilde{T}} \dot{\lambda}_{\tilde{t}}^{\frac{1}{2}} d^{\text{It}\hat{o}} B_{\lambda_{\tilde{t}}} = \int_0^{\lambda_{\tilde{T}}} \dot{\lambda}_{\lambda_{\tilde{t}}^{-1}}^{\frac{1}{2}} d^{\text{It}\hat{o}} B_t \quad (\text{A.8})$$

has the same law as  $B_{\tilde{T}}$ . In differential form this relation is

$$d^{\text{It}\hat{o}} \tilde{B}_{\tilde{t}} = \dot{\lambda}_{\tilde{t}}^{\frac{1}{2}} d^{\text{It}\hat{o}} B_{\lambda_{\tilde{t}}}. \quad (\text{A.9})$$

We need to reformulate the relation (A.9) in the Stratonovich form. Let now  $\lambda$  satisfies

$$d^S \lambda_{\tilde{t}} = x_{\tilde{t}} d\tilde{t} + y_{\tilde{t}} d^S \tilde{B}_{\tilde{t}}. \quad (\text{A.10})$$

$$\begin{aligned} \int_0^{\tilde{T}} d^S \tilde{B}_{\tilde{t}} &= \int_0^{\tilde{T}} d^{\text{It}\hat{o}} \tilde{B}_{\tilde{t}} = \int_0^{\lambda_{\tilde{T}}} \dot{\lambda}_{\lambda_{\tilde{t}}^{-1}}^{\frac{1}{2}} d^{\text{It}\hat{o}} B_t = \int_0^{\lambda_{\tilde{T}}} \dot{\lambda}_{\lambda_{\tilde{t}}^{-1}}^{\frac{1}{2}} d^S B_t - \frac{1}{2} \langle \dot{\lambda}_{\tilde{T}}^{\frac{1}{2}}, B_{\lambda_{\tilde{T}}} \rangle = \\ &= \int_0^{\tilde{T}} \dot{\lambda}_{\tilde{t}}^{\frac{1}{2}} d^S B_{\lambda_{\tilde{t}}} - \frac{1}{2} \langle \dot{\lambda}_{\tilde{T}}^{\frac{1}{2}}, \int_0^{\tilde{T}} \lambda_{\tilde{t}}^{-\frac{1}{2}} d\tilde{B}_{\tilde{t}} \rangle = \int_0^{\tilde{T}} \dot{\lambda}_{\tilde{t}}^{\frac{1}{2}} d^S B_{\lambda_{\tilde{t}}} - \frac{1}{2} \int_0^{\tilde{T}} \frac{1}{2} \dot{\lambda}_{\tilde{t}}^{-\frac{1}{2}} y_{\tilde{t}} \dot{\lambda}_{\tilde{t}}^{-\frac{1}{2}} d\tilde{t} = \\ &= \int_0^{\tilde{T}} \dot{\lambda}_{\tilde{t}}^{\frac{1}{2}} d^S B_{\lambda_{\tilde{t}}} - \frac{1}{4} \int_0^{\tilde{T}} \frac{y_{\tilde{t}}}{\dot{\lambda}_{\tilde{t}}} d\tilde{t}. \end{aligned} \quad (\text{A.11})$$

Thus we conclude that

$$d^S \tilde{B}_{\tilde{t}} = \dot{\lambda}_{\tilde{t}}^{\frac{1}{2}} d^S B_{\lambda_{\tilde{t}}} - \frac{1}{4} \frac{y_{\tilde{t}}}{\dot{\lambda}_{\tilde{t}}} d\tilde{t}. \quad (\text{A.12})$$

# List of Figures

1.1	Examples of three types of complete vector field in the unit disk chart. . . . .	7
1.2	Examples of three types of vector field $\delta$ defined by (1.26) in the unit disk chart. Each field has a simple pole at $\psi^{\mathbb{D}}(a) = 1$ . The attracting zeros of order one correspond to singular points with divergent arrows. . . . .	9
1.3	This is how a typical conformal map $G_t$ acts in the unit disk chart $\mathbb{D}$ for some choice of $\delta$ , $\sigma$ , the driving function $u$ , and $t$ in the forward case. The red line is the hull $\mathcal{K}_t$ , which is a simple curve (slit) in this case. In the reverse case, the map $G_t$ acts in the opposite direction, see Proposition 1.3. . . . .	11
1.4	This figure illustrates how a slit curve $\gamma_t$ (the red line ) generates a hull $\mathcal{K}_t$ (the red line and the pink interior) which is not a curve. The time $t$ increases from left to right. The slit touches itself at the green point and swallows up the pink connected component of $\mathbb{H} \setminus \gamma_t$ . . . . .	18
1.5	Samples of the $(\delta, \sigma)$ -SLE slits (in the right column) for different choices of $\delta$ (the left column) and $\sigma$ (the central column). We use the normalization from Section 1.3.2 and $\kappa = 2$ . Each of the four strings corresponds to some choice of $\delta$ and $\sigma$ . We pick these four combinations just for illustration, they do not have any special properties. Some other combinations are studied in Chapter 6. . . . .	27
1.6	Schematic illustration of the qualitative behaviour of the SLE slit for different values of $\kappa$ in the half-plane chart. . . . .	31
1.7	This is an illustration of the domain Markov property of $(\delta, \sigma)$ -SLE. The three color lines on the left-hand side are samples of the $(\delta, \sigma)$ -SLE slit $\gamma$ . The corresponding color lines on the right-hand side are the preimages with respect to an independently sampled forward $(\delta, \sigma)$ -SLE map $G_t$ , which has the slit denoted by the black line $\gamma_{\sim}$ . The domain Markov property states that the union of the black line and any of the color lines has the same law as the $(\delta, \sigma)$ -SLE slit. For this figure we made the slit simulation for $\delta = 2\ell_{-2}$ and $\sigma = -\sqrt{2}(\ell_{-1} + \ell_1)$ . in the unit disk chart . . . . .	35

- 2.1 We show the slit (the blue line) of the approximation map  $\bar{G}_t^N$ . We denote the points  $\bar{\gamma}_{i,a}^N$  with yellow color and the points  $\bar{\gamma}_{i,b}^N$  with blue color. We also demonstrate the convergence of  $\bar{\gamma}_t^N$  to  $\gamma_t$  when  $N \rightarrow +\infty$ . This figure shows how the slit  $\bar{\gamma}_t^N$  of  $\bar{G}_t^N$  looks for different values of  $N$ . For illustration we consider the chordal case, half-plane chart, the driving function  $u_s := -4s^2(s-1)(s-2)$ ,  $t = 1.8$ , and use the partition (2.3). The black line is the exact slit  $\gamma_t$ , the blue, green, and red lines are the slits  $\bar{\gamma}_t^N$  for  $N = 10$ ,  $N = 20$ , and  $N = 80$  correspondingly. . . . 40
- 2.2 An approximation of the slit of a chordal Löwner chain with the driving function given by a sample of Brownian motion (SLE slit) in the half-plane chart. The partition of the time interval is uniform. The parameters are chosen to be  $\kappa = 6$  and  $N = 10000$ . ([Ken09]) . . . . . 41
- 2.3 Simulation of chordal SLE slit in the half-plane chart for  $\kappa = 4$  ( $10^5$  points,  $d_{\max} = 10^{-3}$ , and  $d_{\min} = 0.5 \cdot 10^{-3}$ ). . . . . 46
- 2.4 Simulation of the chordal SLE slit for  $\kappa = 7$  in the half-plane chart (38793 points),  $d_{\max} = 10^{-3}$ , and  $d_{\min} = 0.5 \cdot 10^{-3}$ . The method gives only an approximation of the curve that generates the hull  $\mathcal{K}_t$ . This approximate curve  $\bar{\gamma}_t^N$  never touches itself, but passes close to itself. We fill the regions that are numerically close to be bounded by the curve with pink color by hand in a graphics editor. . . . . 47
- 2.5 The histograms illustrate the distribution of the length of the intervals  $t_n - t_{n-1}$ ,  $n = 1, 2, \dots, N$  in the partitions of time that are used for the simulations in Fig.2.3 and 2.3. We used the logarithmic scale on the horizontal axis. The left histogram demonstrates that the length of the time intervals varies from  $10^{-12}$  to  $10^{-4}$ , which corresponds to a difference of eight orders of magnitude between the typical smallest and typical biggest time interval. The right histogram demonstrates the same variation, but from  $10^{-15}$  to  $10^{-5}$ . . . . . 48
- 2.6 Samples of the stable Levy process  $\{L_t^\alpha\}_{t \in [0, +\infty)}$  for different values of  $\alpha$ . . . . . 49
- 4.1 Visualisation of a sample of the Gaussian free field with  $\Gamma = \Gamma_D$  on a square  $[0, \pi] \times [0, \pi]$ . The picture is obtained as a sum of first  $10^4$  terms in (4.97). The basis is  $e_{i,j}^1 := \frac{1}{\sqrt{i^2+j^2}} \sin(xi) \sin(xj)$ ,  $i, j = 1, 2, \dots$ . We remark that the series (4.97) does not converge neither uniformly for a  $z \in [0, \pi] \times [0, \pi]$ , nor pointwise a.s. Thus, this picture provides only a heuristic visualisation. . . . . 79



5.1 This figure illustrates the first aspect of the coupling discussed in the introduction to Chapter 5. On the left-hand side, we present a sample of the GFF  $\Phi(\mathcal{H}_s, \Gamma_D, \chi(-\arg z + \pi/2))$  (see the caption to figure 4.1) in the half-plane chart. The blue color corresponds to positive values of  $\Phi(z)$ , and yellow color corresponds to the negative values of  $\Phi(z)$ . We take the value of the coefficient  $\chi$  bigger then it is supposed to be according to the formula (5.4). This is done in order to make the domination of blue color near  $\mathbb{R}^+$  more visible as well as for the yellow color near  $\mathbb{R}^-$ . The red line on the right-hand side is an independent sample of the chordal SLE slit for some  $t > 0$  and  $\kappa = 2$ . Blue and yellow colors on the right-hand side correspond to the pushforward  $G_t^{-1} * \Phi(z)$  of the GFF  $\Phi(z)$  on the left-hand side. The coupling proposition states that the expectation with respect to the SLE random law gives a sample of GFF  $\Phi(\mathcal{H}_s, \Gamma_D, \chi(-\arg z + \pi/2))$  on the right-hand side. . . . . 88

5.2 Schematic illustration of how the map  $G_{t,\varepsilon}^{\mathbb{H}}$  acts in the case when the slit  $\gamma_t$  of  $G_t^{\mathbb{H}}$  is a simple curve. It is denoted by the red line on the right-hand side. On the left-hand side, the red line is the corresponding image  $G_{t,\varepsilon}^{\mathbb{H}}(\gamma_t)$ . The map  $G_{t,\varepsilon}^{\mathbb{H}}$  is conformal outside the dashed line. . . . 108

5.3 This is a schematic illustration of how the map  $G_{t,\varepsilon}^{\mathbb{H}}$  acts in the case of self-touching curve  $\gamma_t$ . The red line on the right-hand side is the slit  $\gamma$  of  $G_t^{\mathbb{H}}$ , on the left-hand side, the red line is the image  $G_{t,\varepsilon}^{\mathbb{H}}(\gamma_t)$ . The map  $G_{t,\varepsilon}^{\mathbb{H}}$  is conformal beyond the dashed line. . . . . 108

6.1 low lines of the chordal vector field  $\delta_c, \sigma_c$ , and corresponding slit samples in the unit disk chart. . . . . 112

6.2 Flow lines of the dipolar field  $\delta_d, \sigma_d$ , and corresponding slit samples in the unit disk chart. . . . . 116

6.3 Flow lines of the radial vector field  $\delta_r, \sigma_r$ , and corresponding slit samples in the unit disk chart. . . . . 121

6.4 Flow lines of the vector fields  $\delta$  and  $\sigma$  from (6.140), and corresponding  $(\delta, \sigma)$ -SLE slit samples for  $\xi = 1$  in the unit disk chart. The dashed line in the boundary of the invariant domain  $\mathcal{J}$ . . . . . 128

6.5 Vector fields (6.140) and corresponding  $(\delta, \sigma)$ -SLE slit samples for  $\xi = -1$  in the unit disk chart. . . . . 129

6.6 Flow lines of vector field  $\delta, \sigma$  from (6.144) and corresponding slit samples in the unit disk chart. The dashed line is the boundary of the invariant domain  $\tilde{\mathcal{J}}$ . . . . . 130

6.7 Vector fields (6.160) and corresponding  $(\delta, \sigma)$ -SLE slit samples in the unit disk chart. . . . . 132



# Bibliography

- [App09] David Applebaum. *Lévy processes and stochastic calculus*. Cambridge University Press, 2009.
- [BB03a] Michel Bauer and Denis Bernard. Conformal Field Theories of Stochastic Loewner Evolutions. *Communications in Mathematical Physics*, 239(3):493–521, aug 2003.
- [BB03b] Michel Bauer and Denis Bernard. SLE, CFT and zig-zag probabilities. *arXiv:math-ph/0401019v1*, (July 2003), 2003.
- [BB04a] Michel Bauer and Denis Bernard. CFTs of SLEs: the radial case. *Physics Letters B*, 583(3-4):324–330, mar 2004.
- [BB04b] Michel Bauer and Denis Bernard. Conformal transformations and the SLE partition function martingale. *Annales Henri Poincaré*, pages 1–41, 2004.
- [BBH04] Michel Bauer, Denis Bernard, and J. Houdayer. Dipolar SLEs. *J.Stat.Mech.0503:P03001,2005*, 2004.
- [BP78] Earl Berkson and Horacio Porta. Semigroups of analytic functions and composition operators. *Michigan Math. J.*, 25(1):101–115, 1978.
- [BP09] Ralph Blumenhagen and Erik Plauschinn. *Introduction to Conformal Field Theory With Application to String Theory*. Springer-Verlag Berlin Heidelberg, 2009.
- [BPZ84] A. A. Belavin, A. M. Polyakov, and A. Zamolodchikov. Infinite conformal symmetry in two-dimensional quantum field theory. *Nuclear Physics B*, 241:333–380, 1984.
- [Car06] John Cardy. Boundary Conformal Field Theory. *Encyclopedia of Mathematical Physics*, 2006.
- [CDMG11] Manuel D. Contreras, Santiago Díaz-Madriral, and Pavel Gumenyuk. Local duality in Loewner equations. *arXiv:1202.2334v2*, 2011.
- [CR09] Zhen Qing Chen and Steffen Rohde. Schramm-Loewner equations driven by symmetric stable processes. *Communications in Mathematical Physics*, 2009.
- [DS11] Bertrand Duplantier and Scott Sheffield. Liouville quantum gravity and KPZ. *Inventiones mathematicae*, 2011.

- [Dub05] Julien Dubédat. SLE( $\kappa, \rho$ ) martingales and duality. *Annals of Probability*, 33(1):223–243, 2005.
- [Dub07] Julien Dubédat. Commutation relations for SLE. *Comm. Pure Applied Mathematics*. 60 (12), pages 1792–1847, 2007.
- [FMS97] Philippe Di Francesco, Pierre Mathieu, and David Senechal. *Conformal Field Theory*. Springer-Verlag, New York, 1997.
- [FW03] Roland Friedrich and Wendelin Werner. Conformal restriction, highest-weight representations and SLE. *Communications in mathematical physics*, pages 1–23, 2003.
- [Gar82] Crispin Gardiner. *Handbook of stochastic methods*. Springer, 3rd edition, 1982.
- [GM93] P Ginsparg and Gregory Moore. Lectures on 2D gravity and 2D string theory. *arXiv:hep-th/9304011v1*, 1993.
- [GV64] I. M. Gel’fand and N. Ya. Vilenkin. *Applications of Harmonic Analysis*. Academic Press, 1964.
- [HS08] T Hida and S Si. *Lectures on white noise functionals*. World Scientific Publishing Company, 2008.
- [IK10] Konstantin Izyurov and Kalle Kytola. Hadamard’s formula and couplings of SLEs with free field. *arXiv:1006.1853v1*, 2010.
- [ITV14] Georgy Ivanov, Alexey Tochin, and Alexander Vasil’ev. General slit Löwner chains. *arXiv:1404.1253v1*, 2014.
- [IV12] Georgy Ivanov and Alexander Vasil’ev. Löwner evolution driven by a stochastic boundary point. *Analysis and Mathematical Physics*, 1(4):387–412, jan 2012.
- [Kan13] Nam-gyu Kang. Conformal field theory of dipolar SLE(4) with mixed boundary condition. *arXiv:1306.6705v1*, 2013.
- [Ken07] Tom Kennedy. A fast algorithm for simulating the chordal Schramm-Loewner Evolution. *Journal of Statistical Physics*, 2007.
- [Ken09] Tom Kennedy. Numerical computations for the schramm-loewner evolution. *Journal of Statistical Physics*, 2009.
- [KM11] Nam-gyu Kang and Nikolai Makarov. Gaussian free field and conformal field theory. *arXiv:1101.1024v3*, jan 2011.
- [KM12] Nam-gyu Kang and Nikolai Makarov. Radial sle martingale-observables. *arXiv:1208.2789v1*, 2012.
- [Kna02] Anthony W. Kna. *Lie Groups: Beyond an Introduction*. Springer Science & Business Media, 2002.

- [KNK04] Wouter Kager, Bernard Nienhuis, and Leo P. Kadanoff. Exact Solutions for Loewner Evolutions. *J. Stat. Phys.* 115:805-822, 2004.
- [KR87] V. G. Kac and A. K. Raina. Bombay Lectures on Highest Weight Representations of Infinite Dimensional Lie Algebras. *Advanced Series in Mathematical Physics*, 2:xii+145, 1987.
- [Kry11] N. V. Krylov. On the Itô-Wentzell formula for and related topics. *Probability Theory and Related Fields*, 150(1):295–319, jun 2011.
- [KT13] Nam-gyu Kang and Hee-joon Tak. Conformal field theory of dipolar SLE with the Dirichlet boundary condition. *arXiv:1307.4424v1*, 2013.
- [Kuf43] P. P. Kufareff. On one-parameter families of analytic functions. *Matematicheskii Sbornik*, 13(1):87–118, 1943.
- [Kyt07] Kalle Kytola. Virasoro Module Structure of Local Martingales of SLE Variants. *arXiv:math-ph/0604047v4*, 2007.
- [Kyt09] Kalle Kytola. SLE local martingales in logarithmic representations. *J.Stat.Mech.0908:P08005,2009*, 2009.
- [Law08] F. Gregory Lawler. *Conformally invariant processes in the plane*. American Mathematical Society, 2008.
- [Loe] K. Loewner. Untersuchungen über schlichte konforme Abbildungen des Einheitskreises. I. *Mathematische Annalen*, 89:103–121.
- [LSW01a] F. Gregory Lawler, Oded Schramm, and Wendelin Werner. Values of Brownian intersection exponents I: Half-plane exponents. *ActaMath*, 187:237–273, 2001.
- [LSW01b] F. Gregory Lawler, Oded Schramm, and Wendelin Werner. Values of Brownian intersection exponents II: Plane exponents. *ActaMath*, 187:275–308, 2001.
- [MR07] Donald E. Marshall and Steffen Rohde. Convergence of a Variant of the Zipper Algorithm for Conformal Mapping. *SIAM Journal on Numerical Analysis*, 45(6):2577–2609, 2007.
- [MS89] Gregory Moore and Nathan Seiberg. Classical and quantum conformal field theory. *Commun. Math. Phys.*, 123(2):177–254, 1989.
- [MS12] Jason Miller and Scott Sheffield. Imaginary Geometry I : Interacting SLEs. *arXiv:1201.1496v1*, 2012.
- [Nel73] Edward Nelson. Probability theory and euclidean field theory. In *Constructive quantum field theory*, pages 94–124. Springer Berlin Heidelberg, 1973.
- [Oks14] Bernt Oksendal. *Stochastic Differential Equations*. Springer, 6th edition, 2014.

- [ORGK08] P. Oikonomou, I. Rushkin, Ilya A. Gruzberg, and Leo P. Kadanoff. Global properties of stochastic Loewner evolution driven by Lévy processes. *Journal of Statistical Mechanics: Theory and Experiment*, 2008(01):P01019, jan 2008.
- [OS75] Konrad Osterwalder and Robert Schrader. Axioms for Euclidean Green's functions II. *Communications in Mathematical Physics*, 42(3):281–305, oct 1975.
- [Pie72] Albrecht Pietsch. *Nuclear locally convex spaces*. Springer-Verlag Berlin Heidelberg, 1972.
- [Pom75] C. Pommerenke. *Univalent functions*. Vandenhoeck & Ruprecht, Göttingen, 1975.
- [Pro04] Philip E Protter. *Stochastic integration and differential equations*, volume 21. 2004.
- [ROKG06] I. Rushkin, P. Oikonomou, Leo P. Kadanoff, and Ilya A. Gruzberg. Stochastic Loewner evolution driven by Lévy processes. *J. Stat. Mech. (2006) P01001*, 2006.
- [RS05] Steffen Rohde and Oded Schramm. Basic properties of SLE. *Annals of Mathematics*, 161(2):883–924, 2005.
- [Sch00] Oded Schramm. Scaling limits of loop-erased random walks and uniform spanning trees. *Israel Journal of Mathematics*, 118(1):221–288, dec 2000.
- [Sch08] M. Schottenloher. A mathematical introduction to conformal field theory. *Lecture Notes in Physics*, 2008.
- [She10] Scott Sheffield. Conformal weldings of random surfaces : SLE and the quantum gravity zipper. *arXiv:1012.4797v2*, 2010.
- [Sho01] David Shoikhet. *Semigroups in Geometrical Function Theory*. Springer Science & Business Media, Dordrecht, 2001.
- [Sim04] Barry Simon. *Functional Integration and Quantum Physics*. Chelsea Pub Co, 2nd edition, 2004.
- [SJSS] Sergio Albeverio, Jurgen Jost, Sylvie Paycha, and Sergio Scarlatti. *A Mathematical Introduction to String Theory: Variational Problems, Geometric and Probabilistic Methods*. Cambridge university press, London.
- [SS08] Oded Schramm and Scott Sheffield. Contour lines of the two-dimensional discrete Gaussian free field. *arXiv:math/0605337v3*, (4), 2008.
- [SS10] Oded Schramm and Scott Sheffield. A contour line of the continuum Gaussian free field. *arXiv:1008.2447v1*, 2010.
- [Sum12] Stephen J Summers. A Perspective on Constructive Quantum Field Theory. *arXiv:1203.3991v1*, 2012.

- 
- [SW05] Oded Schramm and David B Wilson. SLE Coordinate Changes. *New York J. Math.*, 11:659–669, 2005.
- [Tra14] Huy V. Tran. *The regularity of Loewner curves Huy*. A dissertation submitted in partial fulfillment of the requirements for the degree of doctor of philosophy, University of Washington, 2014.
- [Vas98] A.N. Vasiliev. *Functional methods in quantum field theory and statistical physics*. CRC Press, 1st edition, 1998.